DOCTOR OF PHILOSOPHY

Model-based gear ratio and gear shift map optimisation

Fofana, Adama

Award date:
2016

Awarding institution:
Coventry University

Link to publication

Model-Based Gear Ratio and Gear Shift Map Optimisation

By

Adama Fofana

BEng European Engineering

MSc Control Engineering

January 2016

Coventry University

Contents

List of Figures

Summary

In the West, the current political roadmap aims to move to a low carbon economy and, in particular, to reduce pollution associated with transportation systems. This has resulted in increased pressure on manufacturers to reduce their vehicle fleets harmful emissions. This work focuses on the use of advanced control and optimisation to reduce vehicle emissions whilst taking into account the desire for an enjoyable driving experience. The vehicle systems considered are the gear ratio and the gear shift map.

A new efficient and effective problem formulation has been developed to optimise gear ratio and gear selection, first independently and then in combination. Traditional as well as two novel objectives have been developed to capture engineering requirements such as reducing emission, maintaining or improving the vehicle driveability, promoting the durability of transmission components whilst simultaneously meeting problem specific constraints. The first novel objective formulation rewards fuel efficient engine operating points and the second objective rewards the time spent in higher gears to reduce fuel consumption. A Pareto based multi objective optimisation strategy has been adopted to identify the relative trade-off between the different objectives.

A new problem specific operator was designed, to reduce CO_2 emissions by shifting, towards the left side to promote rapid gear shifting.

Three nature inspired optimisation algorithms have been developed and critically evaluated against the Interior-Point Optimization (*Fmincon*), and the Multi-Objective Genetic Algorithm (MOGA) from the MATLAB toolbox. Multi-Objective hybrid Cuckoo Search (MOCS) is used to optimise gear ratio. MOGA combined with the new problem specific operator and constraint handling optimised gear shift map. Finally MOGA was combined with MOCS operator for gear shift map optimisation. Optimised gear shift maps were implemented on a vehicle and tested on a rolling road, following an NEDC cycle. The benefit of the optimisation procedure being developed was demonstrated and resulted in reduction of CO_2 emissions by 2.5%.

Acknowledgement

All the praises and gratefulness due to Allah Subhanahu wa Taala and peace be upon the beloved final Prophet Muhammad Salallahu alaihi wa salam. I thank Allah SWT for His guidance and mercy that are always given to me along my life. Only because of His help and blessing that have given me strength and taught me patience.

I would like to thank and express my gratitude to Prof. Keith J. Burnham, Dr. Olivier Haas and Dr. Vincent Ersanilli for supervising me throughout this enjoyable research project and the overall PhD candidature. Prof. Keith J. Burnham introduced me to this project, while Dr. Olivier Haas provided me with optimisation expertise, patient assistance and guidance, and Dr. Vincent Ersanilli guided me with the automotive expertise.

Additionally thanks to my other supervisors Dr. Karen Vithanage for her support and the competent discussions to guide my studies.

Further thanks are due to Mr. Chris Woolley, Mr. Joe Mahtani and Mr. Ian Entwistle for their technical support, which added valuable information to my project. Additionally, I want to thank Dr. Dina Shona Laila for her support during my write up.

I am grateful for the financial support from the Knowledge Transfer Partnerships (KTP) funding through CTAC that has sponsored my research. I want to also thank Prof. Elena Gaura for giving a year bursary for the completion of my PhD.

I wish to thank my fellow students, colleagues and friends (Othman, Toheed, Oluwaleke, Susan, Jenifer, Wallid, George, Stephane) at Coventry University and Control Theory and Application Centre (CTAC) for the friendly and pleasant working atmosphere.

I would like to thank Andreea whose patience enabled the completion of this work.

Last but not least I would like to thank my family (Maman (Bintou), Papa (Ibrahima), Tonton (Yacouba), Amadou, Mina, Fati, Anita, Ba-doussou) for their continuous support throughout my journey of life that has made it possible for me to reach this achievement.

Nomenclature

Abbreviations

CO_2	Carbon dioxide
IRP	Inverse Reserve Power
BSFC	Brake specific fuel consumption
KD	Kick Down
UDDS	Urban Dynamometer Driving Schedule
WTLP	World Harmonised Light vehicle Test Procedures
NEDC	New European Driving Cycle
FTP	Federal Test Procedure
TCT	Triple Clutch Transmission
DCT	Dual Clutch Transmission
AT	Automatic Transmission
MT	Manual Transmission
AMT	Automated Manual Transmission
kph	Kilometre Per Hour
EA	Evolutionary Algorithm
MOOP	Multi-Objective Optimisation Problem
GES	Gear Early Shifting
FA	Firefly Algorithm
VCT	Variable Camshaft Timing
VCR	Variable Compression Ratio
VVT	Variable Valve Timing
KTP	Knowledge Transfer Partnerships
GA	Genetic Algorithm
MOGA	Multi-objective Genetic Algorithm
MOCS	Multi-objective Cuckoo Search
$MOGA_{Op}$	MOGA with operator from Cuckoo Search
$MOGA_{Toolbox}$	MOGA from MATLAB toolbox
BA	Bat Algorithm
ECU	Engine Control Unit
TCU	Transmission Control Unit

Variables

The following table gives an overview of the used variables:

F_{roll}	rolling resistance force	[N]
F_{aeroDy}	aerodynamic drag force	[N]
F_{Climb}	acceleration force	[N]
F_{trac}	traction force	[N]
J_e	engine flywheel inertia	[kg.m^2]
J_i	transmission ratio inertia	[kg.m^2]
v	vehicle speed	[km/h]
P_e	engine power	[W]
T_e	engine torque	[Nm]
P_e	engine power	[W]
C_D	air resistance coefficient	[-]
Up_{RPM}	upshift point as engine speed	[RPM]
i_g	gear ratio number	[-]
i_F	final gear ration	[-]
R_W	wheel radius	[m]
g	gear number	[-]
t_k	range of throttle position	[-]
$VDw_{g,g-1,t_k}$	velocity increment for the Downshift	[Km/h]
VUp_{g-1,g,t_k}	velocity increment for the Upshift	[Km/h]
V_{hyst,t_k}	minimum velocity between Downshift & Upshift	[Km/h]
d_{cycle}	total distance of a driving cycle	[m]
$d\dot{G}$	gear change frequency	[m]
$G_u\%$	time spent on higher gear	[-]
α_u	ratio of time spent on targeted gear	[-]
ψ_a	gear ratio design variable 1	[-]
ψ_b	gear ratio design variable 2	[-]
ψ_c	gear ratio design variable 3	[-]
ψ_d	gear ratio design variable 4	[-]
θ_0	constant uses in Levy Flight function	[-]
$i^L_{Fact,\tau}$	lower percentage Underreving/Overreving	[-]
$i^U_{Fact,\tau}$	upper percentage Underreving/Overreving	[-]
d_{g,t_k}	distance for each Upshift set	[-]
$Up_{Slope_{k+1}}$	minimum time of gear change Up/Down	[-]
β_{BA}	uniform distribution for BA wavelength	[-]

Q_{min}	bat minimum wavelength frequency	[mm]
Q_{max}	bat maximum wavelength frequency	[mm]
Q_i	bat current wavelength frequency	[mm]
i_{ind}	denoting each individual solution defined by GES	[-]
I_i	firefly i light intensity	[-]
I_j	firefly j light intensity	[-]
$J_{Pare_{rank}}$	modified Pareto rank	[-]
x_i^t	design variables representing the position	[-]
v_i^t	deferred as velocity for Cuckoo hybrid operators	[-]
$x_{cur_{best1}}^t$	the most desirable solution of the current population	[-]
n_{host}	current population size of Cuckoo Search	[-]
β_{ffly}	variation of a Firefly attractiveness	[-]
r_{ffly}	distance of a Firefly light intensity	[-]
g_i	inequality function	[-]
h_j	equality function	[-]
L_l	lower bound	[-]
U_l	upper bound	[-]
x_l	variables	[-]
x_0	initial design variable	[-]
Tw_k	weights coefficient for objective function kth	[-]
J_{N1}	initial objective function for gear shift map based on x_0	[-]
J_{N2}	initial objective function for gear ratio based on x_0	[-]
ζ_k	normalisation factor for objective function kth	[-]
S	search space	[-]
F_r	feasible region	[-]
$f(\mathbf{x})$	represent set of objective functions	[-]
J_{CO2}	objective function of CO2 emissions	[-]
J_{IRP}	objective function of inverse reserve power	[-]
$J_{G_j\%}$	objective function of time spent on each individual gear	[-]
$J_{G_{ch}}$	objective function gear change frequency	[-]
J_{Dist}	objective function of Upshift map distance on BSFC map	[-]
J_{z_1}	objective function of zone 1	[-]
J_{z_2}	objective function of zone 2	[-]
J_{z_3}	objective function of zone 3	[-]
J_{Bwd}	objective function of gear ratio step bandwidth	[-]
W_{GSM_1}	weight associates to J_{CO2} for gear shift map	[-]
W_{GSM_2}	weight associates to J_{IRP} for gear shift map	[-]

W_{GSM_3}	weight associates to J_{G_j} for gear shift map	[-]
W_{GSM_4}	weight associates to $J_{G_{ch}}$ for gear shift map	[-]
W_{GSM_5}	weight associates to J_{Dist} for gear shift map	[-]
W_{GSM_6}	weight associates to J_{z_1} for gear shift map	[-]
W_{GSM_7}	weight associates to J_{z_2} for gear shift map	[-]
W_{GSM_8}	weight associates to J_{z_3} for gear shift map	[-]
W_{GR_1}	weight associates to J_{CO2} for gear shift map	[-]
W_{GR_2}	weight associates to J_{IRP} for gear shift map	[-]
W_{GR_3}	weight associates to J_{Bwd} for gear shift map	[-]
GSM	initial optimised gear shift map before repair	[-]
GSM_R	optimised gear shift map with repair	[-]
$GSM_{GES_{init}}$	initial optimised gear shift map before GES	[-]
$GSM_{GES_{25\%}}$	optimised gear shift map with GES at 25%	[-]
$GSM_{GES_{50\%}}$	optimised gear shift map with GES at 50%	[-]
$GSM_{GES_{75\%}}$	optimised gear shift map with GES at 75%	[-]
S_{sprd}	spacing on Pareto optimal set	[-]
$\overline{d}$	mean value	[-]
M_{p1}	stand for MOGA in tables	[-]
M_{p2}	stand for $MOGA_{Op}$ in tables	[-]
M_{p3}	stand for $MOGA_{Toolbox}$ in tables	[-]
M_{p4}	stand for GES_{Ag} in tables	[-]
M_{p5}	stand for $GES_{Ag/Op}$ in tables	[-]
M_{p6}	stand for $Fmincon$ in tables	[-]
M_{p7}	stand for GA in tables	[-]
Par	pareto-based	[-]
W_{Sum}	weighted sum	[-]
$Group_1$	objective representing emissions	[-]
$Group_2$	objective representing driveability	[-]
$Group_3$	objective representing durability	[-]

Chapter 1

Introduction

1.1 Introduction

This chapter introduces an overview of the research and defines its aim and objectives. It then describes the research methodology, outlines the novelties and finally, gives a high level description of the chapters and thesis organisation.

1.2 Context and problem statement

Government initiatives, legislation (Siskos et al. 2015) as well as the socio political (Yao et al. 2015) prompted vehicles original equipment manufacturers (OEM) and tier one suppliers to make significant investment in research and technology to reduce vehicle emissions.

In the European market, vehicles are tested for fuel consumption and hence emissions production according to the United Nations Economic Community for Europe (UNECE) regulation 101 (Mahlia et al. 2012), (Bielaczyc et al. 2014). Therefore, whilst the approach developed in this thesis is applicable to any drive cycle, the implementation and practical verification employs only the New European Drive Cycle (NEDC) (Barlow et al. 2009*a*), (Tzirakis et al. 2006).

The most significant CO_2 emissions saving at the point of use arises from the adoption of hybrid technologies (25%). However, significant savings can also be gained from novel hardware design and software solutions applied to conventional engine and transmission systems. Improved fuel economy can be achieved by moving the engine towards its most efficient regions on the Brake Specific Fuel consumption (BSFC) map in terms of both emission and performance through optimised gear ratio and gear shift map (B. Mashadi 2012).

Applying a control strategy on gear shift map can achieve an improved performance, especially an Automated Manual Transmission (AMT) (Lucente et al. 2007) and Dual Clutch Transmission (DCT) (Henrique et al. 2006) are both semi-automatic transmissions, as they have the advantage of manual transmission, however their clutches and gearbox mechanism are electronically controlled. Therefore, improving clutch and gear shift software control can results in better fuel economy. André & Hugot (2003) has investigated the impact of gear shift strategy on emissions test, which is mainly influenced by the driver, vehicle type and driving conditions. Ivarsson et al. (2013) designed an optimal gear shift control to minimise fuel consumption for an AMT, Qin et al. (2004) has proposed a gear shift indicator to improve fuel economy based on the environment and driver intention. Fuel economy can be realised through software modification, especially gear shifting strategies from 0.5% to 2% (Sovran & Blaser 2003).

This PhD research was initially started as part of a Knowledge Transfer Partnership (KTP[1]) project, a collaboration research between SAIC Motor UK Technical Centre (SMTC UK) at Longbridge, and Control Theory and Applications Centre (CTAC), Coventry University. This research programme was targeted to be implemented on their new vehicle programme ROEWE 950.

[1]Knowledge Transfer Partnership (KTP) is European leading programme helping businesses to improve their competitiveness and productivity through the use of knowledge, technology and skills that reside within the UK knowledge base. Through KTP, academics can develop business relevant teaching and research, apply knowledge and expertise to important business challenges to identify and develop new research themes & student projects.

1.3 Aim & objectives

The fundamental aim of this project was to reduce CO_2 emissions while maintaining a good dynamic response of the vehicle by optimising gear ratio and gear shift map. To achieve this aim, the following objectives were addressed:

- Implement and validate proprietary powertrain model, prior to its use to predict the effect of different gear ratio and gear shift maps design.
- Formulate mathematically, from a multiple objective optimisation perspective, the gear ratio and gear shift map design problems. Such problem formulation involves:
    1. Formulate the design variables taking into consideration physical bounds and requirements.
    2. Quantify the quality of the solution produced, through the optimisation of the design variable, by adopting and developing appropriate criteria or key performance indicators.
    3. Identify the constraints and develop approaches to prevent them from occurring or automatically adjust the design variables to meet the constraints.
- Investigate the performance of optimisation algorithms and develop a new optimisation approach to exploit problem specific features.
- Optimise gear ratio (hardware).
- Optimise gear shift map (software).
- Combine gear ratio and gear shift map optimisation.
- Evaluate and analyse the results obtained using the validated simulation model.

- Publish or patent the method.

1.4 Research methodologies

Following an initial state of the art survey identifying potential means to save CO_2 it was decided to focus research on software means to achieve CO_2 emissions through gear shift map optimisation. Subsequently, means to achieve further CO_2 savings through hardware optimisation in terms of gear ratio were investigated. To determine optimal or near optimal solutions to a particular problem it is necessary to be able to evaluate alternative solutions in a safe, cost effective and controlled environment. This is usually realised using a computer simulation of the actual system to be optimised. Therefore, a comprehensive proprietary simulation model of a ROEWE 950 prototype vehicle, equipped with a Dual Clutch transmission, was tuned and initially validated against rolling road data.

To carry out the optimisation, a number of criteria were developed. These criteria included CO_2, as well as problem specific criteria to evaluate the quality of the solutions. All criteria considered in the optimisation problem were normalised to obtain values of the same magnitude for each criterion. The review of normalisation techniques is given in Section 2.3.5, in Chapter 2. In this work, the normalisation was carried out with respect to the criteria values obtained from the manufacturer's current gear shift map and gear ratios. The relative importance of each criterion was then realised by associating a weighting to each normalised criterion.

The model validation provided the necessary confidence upon which to evaluate alternative gear shift mappings and gear ratios. The model was realised using the commercial software environment MATLAB/Simulink, which is the tool of choice in the automotive control sector, and provided a convenient platform to evaluate the alternative optimisation strategies developed in this work. Model based optimisation minimises the requirement for vehicle testing and calibration. However, to determine the viability and appropriateness of the solutions developed, the author liaised with SMTC China for the testing of various optimised gear shift maps on a rolling road. The latter provided useful qualitative information as to the nature of a good gear shift map and demonstrated the effectiveness of the approach with quantifiable improvement compared to the standard gear shift map used in the ROEWE 950.

1.5 Contributions and deliverable

The work carried out during this project has led to a number of contributions and adaptations of existing ideas. These are ranked in terms of significance:

- A problem specific repair mechanism has been developed to enable engineers to determine the smallest possible adjustment to an existing gear shift map to ensures that it meets minimum requirements. These minimum requirements can be adjusted post optimisation to favour solutions based on CO_2 saving or performance. This represent a unique application to gear shift map optimisation.

- Problem specific design variables formulations for both gear shift map and gear ratio optimisation. These formulations are applicable to any optimisation technique. The proposed variable formulation maps a set of independent variables to a set of relative increments. Such formulation for the gear shift map enforces the following engineering constraints: i) prevent crossing between downshift and upshift, ii) maintain a minimum hysteresis between downshift and upshift to avoid frequent gear changes for small velocity variations.

- Similarly the gear ratio problem specific design variables formulation are defined to facilitate the optimiser to find the optimal design variables from which the gear ratio can be reconstructed and simulate their effect. Additionally, this formulation impose the following engineering constraints: i) keep a minimum spacing between two adjacent gear ratios, ii) define a set of gear ratio in descending order.

- A gear shift map problem specific local search strategy, named gear early shifting (GES) operator, was developed and combined with the aforementioned hybrid GA. It reduces the CO_2 emissions by promoting an earlier upshift gear change.
- A problem specific contribution is the implementation of the rate of change constraints to restrict the relative values of the gear shift points compared to their neighbours.
- Developed a hybrid optimisation algorithm combining genetic algorithm with the Levy flight operator as well operators used in the Bat, Firefly and Flower pollination algorithms.
- Developed a hybrid Cuckoo search algorithm which includes the Levy flight operator as well operators used in the Bat, Firefly and Flower pollination algorithms for gear ratio optimisation to improve the algorithm exploration and convergence.
- Proposed problem specific objective formulations to offer alternatives or add additional information to facilitate the selection of the most appropriate solutions. These new criteria aim to allow engineers to quantify the relative merit of candidate gear shift maps in terms of:

  (i) time spent on each gear ratio during a drive cycle.

  (ii) time spent within the most efficient zones within the engine fuel map (Brake Specific Fuel Consumption (BSFC)).

(iii) distance between a key reference point within the BSFC map and each engine operating point.

- Developed a combined Gear ratio and gear shift map optimisation strategy based on genetic algorithm and Cuckoo search.

- The work has led to one publication presented at the 14-th IFAC Symposium on Control in Transportation Systems (Fofana et al. 2016).

  Fofana, A., Haas, O., Ersanilli, V., Burnham, K., Mahtani, J., Woolley, C., and Vithanage, K. (2016) Multi-Objective Genetic Algorithm for Automatic Transmission Gear Shift Map Optimisation. 14-th IFAC Symposium on Control in Transportation Systems, May 18-20, 2016, Istanbul Technical University, Taksim, Istanbul, Turkey.

1.6 Outline of the thesis

Chapter 2 provides a literature review relating to powertrain systems. It presents an overview of gear ratio and gear shift map design and reviews software tools used by industry for gear ratio and shift map design. It reviews problem formulation for numerical optimisation techniques, including design variables, objective function and normalisation, constraints handling, single and multi-objective formulation. It reviews the various Evolutionary Algorithm and swarm intelligence algorithm applications to industrial project. It concludes with a justification of the optimisation criteria and algorithms investigated in this thesis.

Chapter 3 gives a description of the ROEWE 950 powertrain model and its validation against rolling road data. The model is used in subsequent chapters to implement and evaluate alternative optimisation strategies. Standard methodologies to design gear ratio and gear shift map are also presented in view to provide sensible starting point to the optimisation carried out in Chapter 4 and 5.

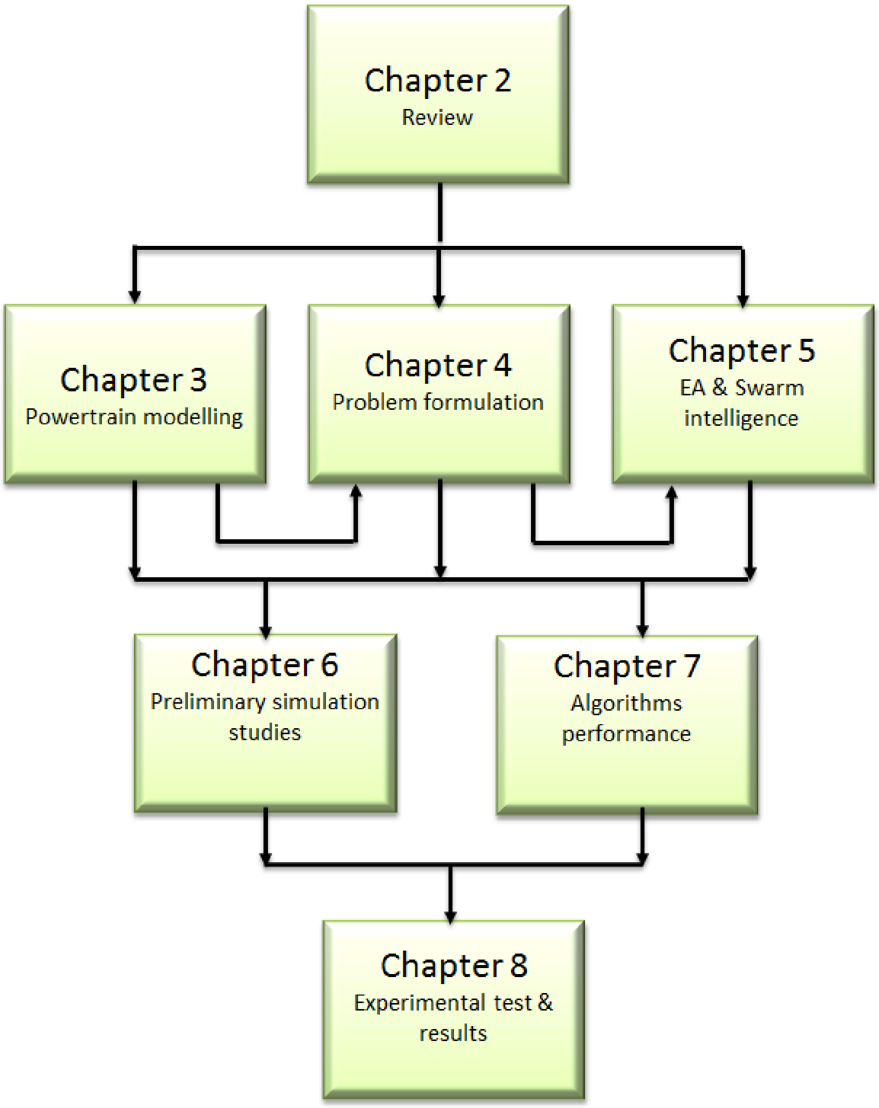

Figure 1.1: Outline schematic flow of logical connection between different chapters of this thesis

Chapter 4 presents the problem formulation, which is one of the major novelty of the work. It converts the engineering requirements for the gear shift map and the gear ratio design into a mathematical framework.

Chapter 5 describes Evolutionary Algorithm (EA) and swarm intelligence with multiple objective functions combined with problem specific operator. Additionally a repair mechanism application is proposed to correct an optimised gear shift map with a given limited reserve power. Chapter 6 describes preliminary simulation studies with a description of parameters selection, weighted coefficients associated with different objective functions. Chapter 7 demonstrates and compares EA and swarm intelligence algorithm against various optimisation techniques from MATLAB toolbox. Chapter 8 completes the work by implementing an initial and optimised gear shift map for a vehicle on the rolling road with the New European Driving Cycle (NEDC) and demonstrates the effectiveness of the algorithm and quantifies the benefit in term of CO_2 saving.

Chapter 2

Background and literature research

2.1 Introduction

The main focus of the thesis is on automating the determination of the most appropriate set of gear ratios and accompanying gear shift map. This chapter presents a critical review of the state of the art in both the theoretical/technical domain and the application domain. The first part focuses on the application domain, namely the powertrain description with emphasis on the gear shift and gear ratio design. The second part describes the key performance indicators or objectives that have been used to evaluate the performance of alternative gear shift and gear ratio designs. The third part reviews current approaches in numerical optimization, with particular attention given to nature inspired constrained multi-objective optimization algorithms and associated methods, to formulate the engineering problem to be solved. The chapter concludes with a justification of the methods and algorithms adopted in this work.

2.2 Powertrain system

This section describes powertrain system (see Figure 2.1). A powertrain system is composed of an internal combustion engine and a transmission. A connector is used to join the crankshaft of the engine to the input shaft. The connector can either be a torque converter or a frictional clutch. A differential unit and an ultimate drive gear is used to connect the output shaft of the transmission to the wheels of the vehicle. A transmission has several speed, torque and gear ratios. Speed ratio is being calculated following the similar way ratio of input speed and transmission output speed are calculated, whereas torque ratio is measured following the ratio of input torque and transmission output torque respectively.

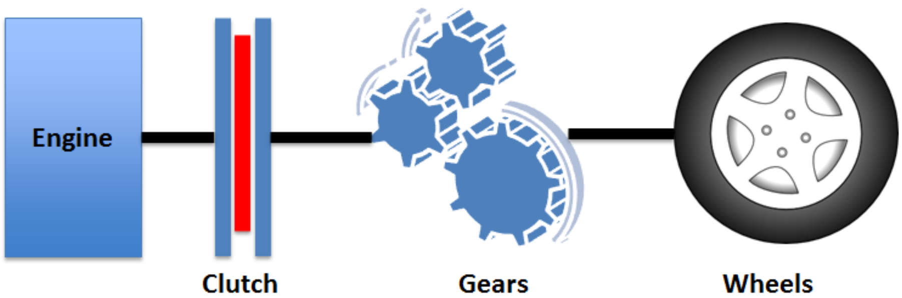

Figure 2.1: Powertrain system

In this thesis, the focus is on Dual Clutch Transmission (DCT), as it is the main concern to optimise gear ratio and gear shift map. In literature, there are many simplified models of DCT utilised for different simulation purposes. Xuexun et al. (2007) has proposed a DCT model based on a Fuzzy Controller to select the appropriate gear upon the driver intention. Galvagno et al. (2011) has described a more detailed mathematical model of DCT, including clutch mechanism synchronisers dynamics, therefore this particular model is suitable to study a control algorithm.

2.3 Problem formulation

In most industrial applications, the optimal product is based on a posteriori knowledge by comparing different design variables. In many cases, this method is applied because of a lack of knowledge of optimisation formulation procedure. This section reviews optimisation procedures to describe efficient and analytical ways of defining and comparing new solutions in order to satisfy an optimal design. The general mathematical formulation is given as follows (Taboada et al. 2008):

$$\begin{cases} \textit{minimise } f(\mathbf{x}) \\ \textit{Subject to } g_j(\mathbf{x}) \geq 0, \quad j = 1, ..., J \\ h_k(\mathbf{x}) = 0, \quad k = 1, ..., K \end{cases} \tag{2.1}$$

where,

$f(\mathbf{x})$ $(f_1(\mathbf{x}), ..., f_n(\mathbf{x}))$ $for\ i = 1, 2, ..., n.$

$g_j(\mathbf{x})$ j-th inequality constraint evaluate at $\mathbf{x}$.

$h_k(\mathbf{x})$ k-th equality constraint evaluate at $\mathbf{x}$.

$f_i(\mathbf{x})$ i-th objective function evaluate at $\mathbf{x}$.

$\mathbf{x}$ $\{x_1, ..., x_p\}$ is a vector of decision variables.

n number of objectives or criteria to be optimised.

p number of decision variables.

The constraints define the feasible region $\mathbf{x}$, where any point $\mathbf{x} \in \mathbb{R}^n$ presents a feasible solution. The vector $f(\mathbf{x})$ presents the values of objective functions to be minimised or maximised. Note that in this thesis, only inequality constraints are considered.

2.3.1 Design variables

The control variables modified by the optimiser is referred to as design variables. When the design variables can take any numerical value within their specified range, the problem is named *continuous-variable*. When there is only discrete/integer values, it is defined as *discrete/integer-variable*. Finally when the problem includes both discrete and continuous variables, it is then named as *mixed-variables* (Statnikov et al. 2009). Discrete variables take a finite set of values, thereby limiting the search space for the optimisation algorithm. Continuous variables can take all possible values between the lower and upper boundary. Whilst the solution space is larger for continuous variables problem optimisation, their solutions are easier to solve than discrete variables optimisation problems. This is due to issues associated with discrete variables optimisation that offer inherently disjoint design and solution space as well as in some cases non convex cost function (Arora et al. 1994).

2.3.2 Objective functions

The main goal of optimising is that there are some merit functions which need to be minimised or maximised, and can be used as quantitative criteria to assess the effectiveness of each design variable. One of the main driving objectives in this thesis is CO_2 emissions. However, minimising CO_2 emissions can deteriorate the car dynamics response. The main objective functions used for powertrain optimisation can be classified as follows:

Fuel consumption and emissions

The primary objective function is the fuel consumption (Mammetti et al. 2013), where emissions are a by-product of fuel. CO_2, carbon monoxide (CO), nitrogen oxides (NO_x), hydrocarbons (HC) emissions Wallington et al. (2008) are mainly dominated the objective functions to assess the performance of engines usage, Yin et al. (2013) have used a combined objective function with CO, NO_x and HC to optimise a gear shift map, therefore this method is limited. It only focuses on emissions, and not the vehicle dynamic response.

Driveability

Reducing fuel consumption or CO_2 emissions can also results the car to poor driving condition, therefore a line must be drawn to limit the reduction of fuel or emissions. A poor driving condition can be defined as driveability, Ngo, Colin Navarrete, Hofman, Steinbuch & Serrarens (2013) have defined the driveability by the car responsiveness, operating smoothness. Therefore, it was expressed that the driveability was the remainder acceleration capability after a certain gear shift, which can be represented by the engine reserve power defined as follows:

$$\Delta P = (T_{e,max} - T_e)\omega_e \tag{2.2}$$

where ω_e denotes the engine speed, $T_{e,max}$ the maximum torque and T_e the engine torque defined as:

$$T_e = F_{trac}\frac{R_w}{i_g\eta} \tag{2.3}$$

where i_g and R_w are the gear ratio and wheel radius, respectively. The engine speed ω_e, is defined as follows (Liu et al. 2009):

$$\omega_e = v\frac{i_g 60}{2\pi 3.6 R_w} \tag{2.4}$$

where v denotes for vehicle speed. To achieve good driveability, ΔP must be maximised, therefore a minimisation expression can be defined by the inverse reserve power (IRP):

$$IRP = (\Delta P)^{-1}. \tag{2.5}$$

2.3.3 Constraint

In any engineering applications, there are always limited resources or certain physical phenomena which can be considered as constraints. Meaning that each design variable must satisfies certain constraints imposed by the design limitation. In the case of gear shift map, an early shifting of gear can result in to a low engine speed, consequently generates Noise, vibration, and Harshness (NVH) (Le Guen et al. 2011). Therefore a minimum engine speed can be defined as constraint. In fact, there is no explicit way to describe the constraints, as it depends on the user. However the mathematical expression of constraint to be considered for any optimisation is based on two formulations, which can be either inequality or equality type. In general, inequality type is mostly used as it is more simpler than equality type.

2.3.4 Bounds

In practice, the design variables are in most cases constrained by the physical limit of the system, therefore considering continuous variables, a minimum and maximum bound must be set on each design variables. In this condition the research space is restricted.

2.3.5 Single-objective versus Multi-objective

Most engineering designs have either one single objective function or more than one objective functions. In general, a single objective function, is often represented by a single scalar, where the optimiser will have only one objective to focus on. However for multi-objective functions, the task becomes more complex, as the aim is to optimise the simultaneously as many defined objective functions as possible. A decision maker is then defined to select one or more solutions, Chiandussi et al. (2012) have classified and surveyed various decision makers. The following statement better summarises the review in brief:

Weighted sum method

In this method, multiple objective functions are converted into one single objective using a weighted sum:

$$F(x) = \sum_{k=1}^{n} w_k f_k(x) \tag{2.6}$$

where x, $F(x)$, k denotes a set of design variables, single objective function after conversion and number of objective functions, respectively. w_k, $k = 1...n$, are the fractional weighting coefficients where the solutions selected will forcibly depend on them. The weighting coefficients must be positive and satisfy:

$$\sum_{i=1}^{k} w_i = 1, \quad w_i \in (0, 1). \tag{2.7}$$

The method has the advantage of combining all objective functions, i.e Yin et al. (2013) used a weighted sum to combine power, fuel and emissions in one objective function in order to optimise a gear shift using GA. However the drawback is that weighting for each objective function must be known in advance (Vachhani et al. 2015). Also in order to obtain several solutions, the algorithm must be run multiple times, which is time consuming (Odu & Charles-Owaba 2013).

e-Constraint

In this method, only one objective function is considered, presumably the most significant on and considering the other objective functions as constraints bounds. It is very easy to implement, however it might require high computational cost

(Mavrotas 2009).

Pareto Optimality

The Pareto optimality concept is frequently used in multi-objective function. The mathematical definition is defined as follows (Van Veldhuizen & Lamont 1998):

A solution $x_d \in S$ is said to be Pareto optimal set, if and only if there is no $x_h \in S$ for which $h = f(x_h) = (h_1, h_2,\cdots,h_p)$ dominates $d = f(x_d) = (d_1, d_2,\cdots,d_p)$.

Usually, they are also called *non-dominated* vector set, considered as acceptable solutions. In literature, various types of Pareto have been proposed. Deb & Saxena (2005) have defined a method of dealing with large dimensional multi-objective functions, where he applied principle component analysis procedure to reduce the number of dimension. The same author has also proposed a Pareto method based on a fixed reference point, where the aim is to target the reference point by converging the Pareto optimal set towards it. Haas et al. (1998) have proposed a modified Pareto ranking that focuses the search on specific regions of the solution space. The main drawback of Pareto approaches is the computational effort (Chiandussi et al. 2012).

The objective functions corresponding to the different criteria expressed in Section 4.4.1, in Chapter 4 can have different magnitude. A normalisation process is therefore required prior to weighting the relative importance of each objective using a set of weights defined as $w_k = Tw_k\zeta_k$, where Tw_k are the weights coefficient, and ζ_k are the normalisation factors. The most relevant normalisation methods are described in (Halevy et al. 2006) and reproduces as follows:

- The first method is to normalise each objective function by the magnitude of its objective function at the initial point x_0

$$\zeta_k = \frac{1}{f_k(x_0)} \tag{2.8}$$

- The second is to normalise each objective by the minimum of the objective function

$$\zeta_k = \frac{1}{f_k(x^{(k)})} \tag{2.9}$$

where x^k solves $min_x\ f_k : x \in \mathrm{F}_r$.

- Normalise based on Nadir and Utopia points

One of the best method is to normalise the objectives based on Nadir and Utopia points. The Nadir and Utopia represent the length of the intervals where the optimal objective functions vary within the Pareto optimal set. Nadir and Utopia points are described as follows: The Utopia point f^{Utopia} is defined as,

$$f_i^{Utopia} = \left[f_1(x^{(1)})\ f_2(x^{(2)})\ ...\ f_k(x^{(k)}) \right] \tag{2.10}$$

where $x^{(k*)}$ is the optimal point solution vector for the single objective function of the $k-$th objective function f_k, and the Nadir point f_i^{Nadir} for each component is defined as,

$$f_i^{Nadir} = max \left[f_1(x^{(1*)})\ f_2(x^{(2*)})\ ...\ f_k(x^{(k*)}) \right] \tag{2.11}$$

The $i-$th anchor point f_i is presented as,

$$f_{i*} = \left[f_i(x^{(1*)})\ f_i(x^{(2*)})\ ...\ f_i(x^{(k*)}) \right] \tag{2.12}$$

where the normalised objective function $\overline{f_i}$ is obtained as,

$$\overline{f_i} = \frac{f_i - f_i^{Utopia}}{f_i^{Nadir} - f_i^{Utopia}}. \tag{2.13}$$

The first method was selected for convenience as it is easier to compare solutions with the baseline. Investigation of alternative normalisation methods is beyond the scope of this thesis.

2.4 Nature-inspired algorithm

The Most important inventions were designed by observing the nature, i.e, submarines have been designed by observing fish, or radar system by adopting bats behaviour. These algorithms can be classified by Evolutionary Algorithm and Swarm intelligence (Binitha & Sathya 2012). This section describes and gives an insight definition on them, also a more detail survey can be find in (Nanda & Panda 2014).

2.4.1 Genetic algorithm

Definition

Evolutionary Algorithm (EA) can be defined as a process of training to adapt to the environment by improving the fitness of the species as they evolve. The so-called Genetic Algorithm (GA) was the adaptation from Darwin Origin of species (Bennett 1872), which was later computerised by Holland (1992). It can be characterised in three main parts: i) it is a population-based, ii) each individual is assessed based on its fitness function, iii) every individual will be modified to mimic the natural evolution by changing their genes, which results in them looking for new solution space. The core of GA can be summarised as follows:

Selection method

Selection method mimics the natural selection of species, where the fittest individuals have a better chance to be selected as parents for reproduction. The most known are the Roulette Wheel Selection and Stochastic Universal Selection (SUS)

(Baker 1987), meaning that the fittest individuals are not necessarily guaranteed to be selected, however they have a better probability to be selected (Reeves 2010). Various selection methods can be found in (Goldberg & Deb 1991). Jebari & Madiafi (2013) have implemented and compared the performance of different selection methods and concluded that RWS and SUS maintain a good diversity among the population and prevent a premature convergence to the local optimal.

Real code versus binary code

A solution can be represented ether by binary code or real code. GA was originally created using binary code as it was to represent the biological gene. The binary can be used to represent small real values and cannot represent exact real number, which means a scaling factor must be considered (Wright 1990). A lot of research has proven that the application of real code outperforms the binary code (Tsutsui & Ghosh 1998), (Raghuwanshi & Kakde 2007). In this thesis real code has been preferred to binary because of the difficulty and exact conversion from binary to real numbers.

Crossover

After selecting individuals to produce new solutions, there are various operators which can be used to modify information of each individual. These process is called crossover or recombination, which is a genetic operator that combines two individuals (parents) to form a new individual (Chromosome). This are many variants of crossover which can be found Kaya et al. (2011). For real code crossover implementation, Single-point, Multipoint-point and Uniform crossover are more suitable due to difficulty of binary conversion to real code, also in Kita et al. (1999) the rational reason of using real code for crossover has been debated

.

Mutation

Mutation can be considered as a random process, which aims to find new solutions in search space by randomly modifying one or several values of the chromosome. One of the interesting properties of mutation is that preserves diversity among the population by searching in an unknown search space. A usual method is the uniform mutation, where a random number is added to each value of the individual. Deb & Goyal (1996) have discussed the binary coded over real coded mutation, and has summarised that real coded in mutation was more efficient.

Elitist

One more important task in GA is the application of elitist. As GA is mainly based on stochastic method, meaning that there is no guarantee of finding a global solution. Consequently the best individual will proceed to the next generation without applying any operators.

Local search

In GA, the use of local search is often applied to solutions in order to improve them. However, the use of local search must be taken carefully as it can lead to a premature convergence (Pandey et al. 2014).

Constraints handling

The most simple way to handle constraint is to penalise invalid solutions by imposing a penalty function, where this penalty might prevent the faulty individual contribution to the next generation. Coello Coello (1999) proposed a survey on different constraints handling, where one of the most extreme is the death penalty, which removes invalid solutions from the population. However, the major problem of this method, is assuming that at least one solution is valid among the population. The next penalty is static penalty, which gradually reduces the fitness values of solutions disobeying the constraints, meaning the penalty is severed for many constraints violations, and soft for low constraints violations. Another penalty, increase the penalty function over generation referred to as dynamic penalty, meaning that the constraints in earlier generations are less penalised than the constraints in later generation, therefore, the drawback is, if the penalty factor is badly selected, the solutions could converge to a non-optimal solution space.

Furthermore, in the same survey, the author has also proposed a method called Co-evolutionary penalty, where two penalty values are used to distinguish the number of violated constraints, and the corresponding amount of violations. They are also two sub-populations, where the first contains the individuals, while the second implements the set of weighted combinations used to calculate the fitness function and also contains the penalty factors. The drawback of this method is the addition of extra-parameters, also the requirement of initialising them. Additionally, Mani & Patvardhan (2009) has proposed an improved version of Co-evolutionary, by using a self determining and regulating penalty factor, however this method still required two sub-populations and it is expensive in computational time.

Another interesting constraint handling, unlike the previous constraint, is based on penalty functions. This method proposes to repair invalid solutions in order to turn them into valid solutions. It means that the encoding design variable is then modified to suit the constraint. Salcedo-Sanz (2009) proposed a review of the main repair mechanism used to handle constraint, where he described the procedure and applications of different repair mechanisms. One of the interesting repair mechanisms mentioned, was applied to gene permutation due to cross-over procedure, where additional operators were used to modify the crossover operator referred to as partially mapped operator (Goldberg & Lingle

1985) and tie breaking crossover. Mitchell et al. (2003) proposed a combined repair operator named *GeneRepair* with crossover and mutation operators, where it is based on two tasks, one is for fault detection and the second is for correction. Repair operators increase the valid search space, however they do not necessarily improve the performance of the algorithm. In this thesis, a problem specific repair mechanism was proposed to modify solutions obtained by the optimisation algorithm to produce new solutions with specific minimum value for the reserve power (see Section 5.2.2, in Chapter 5). This repair mechanism can also be applied during the design process to quickly obtain solutions that meet specific performance based on a set of existing solutions.

The literature on EA is expanding (Zhou et al. 2011), (Khajehzadeh et al. 2011). In Vachhani et al. (2015) an excellent survey on EA handling multi-objective problem is provided, where various optimisation algorithms are compared more particularly in terms of diversity and convergence. The following section will describe Swarm Intelligence algorithm.

2.4.2 Swarm Intelligence algorithm

Swarm Intelligence is a promising search area of optimisation, which is mainly based on understanding and computerising the behaviour of various swarm of animals and insects, like fish, birds, bees or ants (Karaboga & Akay 2009). Researchers have focused their attention to them, because of their intelligence of self-organisation to solve problems (Martens et al. 2011). The same rules defined above in EA, can also be applied to Swarm Intelligence algorithm. The rest of this section will review some relevant Swarm Intelligence algorithms for the interest of this thesis.

Cuckoo Search (CS) was originally created by Xin-She Yang, where it is based on the behaviour of the broad parasitism of certain CS (Yang & Deb 2009). The algorithm is integrated with Levy Flight as a random walk to enhance its performance, and it only requires two parents (Pavlyukevich 2007), however its disadvantage is to select the value of its step (Gopal Dhal et al. 2015). CS is population based, where CS lays eggs in communal nests of other birds, with the eggs considered to be the solution of the objective function.

There are hybrid CS, which combine different algorithms, i.e Kanagaraj et al. (2013) have proposed CS integrated with genetic operator to solve the reliability and redundancy allocation problem. It was confirmed based on experimental tests, that the proposed method was efficient in terms of balance between exploration and exploitation (Kanagaraj et al. 2013), as crossover maintain the parent cuckoo birds identity and at the same time creating diversity in the search space, while the mutation of CS is considered as local search by making small changes in the design variables. Rani et al. (2012) proposed hybrid of modified CS by integrating it with two evolutionary algorithms, Particle Swarm Optimisation (PSO) and GA, where it was applied as multi-objective optimisation to the location of amplitude and phase of symmetric linear array element. The results achieved good improvement in comparison to original CS.

Bat algorithm (BA) was created by Yang (2011*a*). The main idea of the algorithm is based on the echolocation of micro-bats, where micro-bat used echolocation to detect their prey, and avoid obstacles. Additionally BA can be more effective as it uses frequency tuning and parameters control to influence exploration and exploitation (Yang 2010). Different variants of the algorithm have been published. Algorithm proposed by Yang (2011*b*) was applied to solve Multi-objective functions in design of structure, and results shows that BA is an efficient optimiser. Fister et al. (2013) have proposed an hybrid BA integrated with Differential Evolution (DE) algorithm, where different experiments were realised on test functions. It was shown that hybrid BA outstandingly improved the results.

Firefly algorithm is based on the flashing patterns and behaviour of tropical fireflies (Goel & Panchal 2014). This algorithm is mainly a mutation based. Two iterative loops are used to compare each firefly brightness (objective functions), and the firefly with the strongest brightness is attracted by the firefly with weakest brightness. Consequently, the fireflies can be subdivided into various groups, and each group can swarm around a local mode dominated by the firefly with the strongest brightness. The drawback of firefly algorithm, in the case of multi-objective problem is that weighted sum method must be applied to reduce them into one single scalar, as the only concern is the attractiveness of fireflies. Liu et al. (2012) have demonstrated the effectiveness of Firefly algorithm applied to path planning problems. Arora & Singh (2013) have proposed a conceptual study, by comparing Firefly algorithm, Bat algorithm and Cuckoo Search, where it was concluded that FA was better in terms of finding optimum solution, as well as performing local search.

Flower Pollination algorithm is a new type of optimisation developed by Yang (2012), where the main concept of the algorithm is based on the flower pollination process of flowering plants. In this algorithm, there are no explicit crossovers. Additionally, it uses the current best solution among the population to make the next move. Consequently, the algorithm can possibly be trapped in a local mode. Flower Pollination algorithm has been extended to multi-objective function in Yang et al. (2013), where it is applied to solve a disc brake design problem.

2.4.3 Deterministic algorithm

The main concept of the algorithm evoked in this thesis is stochastic-based. There are also deterministic-based algorithms, where they are designed to search for global best solution (Arora 2011). The basic deterministic algorithms are Steepest Descent method, the quasi Newton method, the Newton-Raphson method or the Levenberg-Marquandt method (Colaço & Dulikravich 2011). These type of algorithms are mainly used for non-linear minimisation problems. Their function is based on an iterative process, where after a certain number of iterations, the objective function converges to its minimum value. A more general form describing the iterative process can be defined as follows:

$$Y^{k+1} = Y^k + \xi^k E^k \tag{2.14}$$

where Y, ξ, E and k, denote for the vector of design variables, the search step size, the direction of descent and the number of iterations, respectively. The following statement summarises some of the deterministic algorithms:

- Steepest Descent (Fletcher & Powell 1963): this method is based on basic gradient method, where the principle is to focus the search on the opposite direction of the locally highest variation of the objective function, such that to locate its minimum value .

- Newton-Raphson (Polyak 2007): this method is similar to gradient method. It is a powerful technique of solving equations numerically. It was originally formulated by Newton, and later on the idea was applied into polynomial by Raphson. It is mainly based on linear approximation, where the extension broad by Raphson is the usage of the second derivative.

- Quasi Newton (Shanno 1970): This is another Newton based, except there is no need of second derivative. However, it utilises the Hessian based on the first derivative. This method is computationally faster, but it had a slower convergence.

- Levenberg-Marquandt (Lourakis 2005): this method is based on an iterative process that locates the minimum of the ordinary least square norm. It has the futures of both Steepest Descent and Gauss-Newton. When the current solution is far from the true solution, it follows the steepest descent method, however when it is closed, it behaves as Gauss-Newton method.

The drawback of deterministic algorithm is that the complexity can increase with the number of design variables (Talbi 2009). For the purpose of this thesis, interior-point algorithm (Coleman & Li 1996) from Matlab toolbox *Fmincon* will be used as benchmark. Interior point algorithm can be considered as linear or non nonlinear programming, where optimisation is realised by going through the middle of the solid space defined by the problem rather than around its surface (Forsgren et al. 2002). Further variant of *Fmincon* algorithm are Trust-Region-Reflective Optimization (Byrd et al. 2000) and Active-Set Optimization (Gill et al. 1981).

Having reviewed alternative optimisation algorithm, the next two sections present their application to gear ratio and gear shift map design.

2.4.4 Gear ratio design

The main components of a vehicle transmission are represented by clutch and gearbox, as they connect kinematically the engine to wheel drive. The gear ratio design is a complex process, as it is based on vehicle dynamics and must be robust enough. This design problem has been addressed in a number of text books e.g. Naunheimer et al. (2010), as well as in scientific journals and conferences publications. A process to design intermediate gears ratios design based on traditional geometric and progression methods for a 6 speed AMT was implemented in Singh et al. (2012). It describes the two methods for intermediate gears ratios design based on geometric and progression methods. Newman & Dekraker (2016) used gear ratio progressive method to analyse carbon emissions, driveability and performance for a given transmission. It was concluded that the variation of progression method parameters were fairly insensitive to emissions, however the final drive variation have a bigger impact on emissions.

Gear ratio performance can be analysed by using various road conditions, maximum vehicle speed, intermediate gear ratio selection, engine speed versus vehicle speed characteristic curve, tractive effort and maximum vehicle speed of each gear ratio (Kasseris & Heywood 2007). In design criteria for gear ratio, the weight is considered to be one of the most important aspect in terms of cost and fuel consumption, as well as the bending and wear strength of the gear tooth (Chen & Usman 2001).

Shamekhi et al. (2014) presented a gear ratio optimisation, where a neural network was used to obtain a model of the transmission system which was fast to execute. It was observed that such an approach required a massive set of training data to obtain an accurate model. The model was subsequently exploited by a genetic algorithm (GA) to optimise the gear ratio parameters. Shariatpanahi et al. (2004) have combined GA with neural network to optimised gear ratio. Two models were defined using neural network and used in parallel during optimisation. The first model was used to calculate the acceleration, maximum vehicle speed, and gradability, while the second model was applied to calculate fuel consumption and emissions. The reason of using two models based on neural network was to obtain two simplified accurate models. However the computational time can be costly by running the two models during optimisation. Casavola et al. (2010) have proposed gear ratios optimisation, where a fuzzy logic was used to defined a gear shifting strategy based on engine speed, engine torque, vehicle speed, brake pedal and throttle position. This simplified model was used to minimise fuel consumption by optimising gear ratios. Therefore, this model and optimal gear ratios are only used for benchmark, however they cannot be used for commercial vehicles as their driveability is poor.

Yokota et al. (1998) proposed a GA optimisation and a nonlinear integer programming (NIP) problem formulation for gears weigh reduction based on gear dimension, bending and torsional strength. 44.8% reduction of weigh and 18.5% reduction in mean radius were achieved. Whilst such results were promising, the authors required to carry out additional simulation to ensure that the solutions were realistic. Golabi et al. (2014) have proposed a gear ratio optimisation for volume and weight reduction, where the optimisation algorithm was implemented within the MATLAB function *Fmincon*. The optimisation methods described are used to improve the existing results or to meet the design requirements. There is a lack of benchmark comparison in terms of algorithm. In addition, the gear ratio bandwidth is missing in most cases. The latter is however a requirement according to the technical standard of SAIC Motor and BorgWarner Design for Dual Clutch Transmission (see Section 3.4.5, in Chapter 3).

In literature, several approaches have been applied to optimise vehicle powertrain system. Hu et al. (2010) have applied GA to optimise the shift quality of a DCT, where a trade-off was made between jerk and friction as objective function. Ye et al. (2004) have applied GA to minimise fuel consumption and emissions of a four cylinder engine. The main objective was to find the speed-load point with the minimum Brake Specific Fuel Consumption (BSFC) when using Variable Valve Timing (VVT) and Variable Compression Ratio (VCR) engine. It was noticed that the improvement of fuel economy and emissions was occurred at low speed and mid load region.

Having reviewed the gear ratio design and optimisation methods, it can be observed that the most important design criteria are fuel consumption and emissions as well as gears weight, with driveability mentioned in only a few publications. In addition, the optimisation algorithms are often used without modifications and the problem formulation consider the variables to optimise directly. There is therefore an opportunity to develop more efficient problem formulation as well as introduce problem specific features in the optimisation algorithms to improve the coverage and convergence of the algorithms.

2.4.5 Gear shift map design

Gear shift map design methodologies are complex. The first shift maps are determined using design based-software. Initially the shift points are obtained from vehicle dynamic characteristic by determining the intersection between two acceleration curves of two adjacent gears (Xi et al. 2009), (Liu et al. 2009) and (Kirtane n.d.). Most of the methods developed have not focused on ensuring that gear shift map results in good vehicle's driveability. Such task is traditionally reserved to calibration engineers. Ngo, Hofman, Steinbuch & Serrarens (2013) have proposed alternative gear shift map design, which alleviates the issue of driveability, where the shift points are obtained from statistical data of various driving cycles, also showing an acceptable driveability by comparing different acceleration profiles.

Gear shifting strategy is a very important aspect of reducing fuel consumption, as it can be adapted to driver behaviour as well as the vehicle's environment. Santiciolli et al. (2015) described a gear shift strategy optimisation over the drive cycle FTP-72 (Barlow et al. 2009*b*), using a multi-objective genetic algorithm (MOGA), where the trade-off was to maximise performance and fuel economy. The optimisation results demonstrated a good trade-off between performance and fuel economy using a gear shift strategy. This method is only based on a known driving cycle, and use the current driving cycle shift position to shift earlier. Ha & Jeon (2013) described an adaptive gear shifting strategy based on torque and traffic condition, where the constraints are limited to the maximum and minimum engine rotation and engine torque. Dovgan et al. (2012) used throttle, brake and gear management as decision variables to improve performance and fuel consumption over a known drive cycle, however the optimum solutions were exhibiting an uncomfortable jerk, which can compromise the vehicle driveability. Kim et al. (2007*a*) proposed an integrated transmission control algorithm to assist the driver power demand via throttle pedal acceleration. This method was based on dynamic programming (DP). It was demonstrated that the transmission shift map produced by the algorithm was drivable. However this method was based on an online tuning of the transmission shift map. Modifying the transmission shift map online required additional validation on road testing in order to be fully accepted by manufacturers.

Work directly relevant to this thesis include GA application to optimise a gear shift map. it has been used in Yin et al. (2013) to optimise the gear shift map of an automated manual transmission (AMT), where the objective functions were performance, fuel and emissions. A weighted sum method was used to combine the multiple objective functions into one single scalar. The only design variable was the vehicle speed, assuming a given throttle position, while the constraints were simply minimum and maximum engine speed, and engine output torque. A simple GA was then used to optimise the velocity of a given shift schedule. Details omitted from Yin et al. (2013) work include the design variables formulation and the type of normalisation procedure adopted. Combining all objective functions into one single scalar does not necessarily reflect fully the qualitative criteria of an optimised shift map. Considering a multi-objective genetic algorithm (Konak et al. 2006) can be more beneficial at observing the trade-of between competing objective functions.

For gear shift map optimisation, other techniques have been applied and can be found in the literature. In Le Guen et al. (2011), a gear shift map optimisation method was proposed based on AVL Cruise in built software *Cruise GSP Optimization*. This method gives only an indication to obtain an optimal gear sequence on a given driving cycle. A combined weighted sum was used to combine objectives expressing fuel consumption and CO_2 emissions into one single scalar.

The main concept of this method was to focus on moving the engine operating point towards the most efficient area of the engine fuel map. Thereafter, the gear shift point were then reflected on the gear shift pattern to form various optimum zones for each gear ratio. Then, *Cruise GSP Optimization* was used to adjust the upshift and downshift points around the optimum zones, which in fact reflects the optimum gear shifting point. This method gave good optimised gear shift map. However the problem formulation was not detailed.

Various techniques have been applied to optimise gear shift map. Li & Hu (2010) have proposed a fuzzy neural network to define an optimum gear shifting decision maker. Kim et al. (2007*b*) have proposed an optimum decision maker for gear shift and throttle position using dynamic programming (DP), where fuel consumption is considered as a cost function to be minimised. Fu & Bortolin (2012) have proposed a model predictive controller combined with DP to find an optimum gear shift sequence, considering fuel consumption as cost function. These method are mainly designed for real time driving, where an indicator can advise the driver, when to change gear.

Having reviewed the algorithms used to solve the problems considered in this work, has highlighted research opportunities in applying other evolutionary algorithms such as cuckoo search and variants of multi objective genetic algorithms. Most optimisation strategies presented do not exploit problem specific features nor design variable formulation to improve both solution coverage and speed of convergence. Finally, whilst normalisation procedures are used, there is little mention of the details of these normalisation procedures. The main objectives considered or gear shift map optimisation relate to fuel/CO_2 and driveability/reserve power. There is therefore an opportunity to investigate alternative objective formulation to help quantify the differences between alternative solutions with similar objective values for fuel/CO_2 and driveability/reserve power. The next section reviews the software tools used by industry and academia to support the design, optimisation and calibration of gear shift map and gear ratio.

2.4.6 Software tools used for gear ratio and gear shift map

Simulation tools are extensively used in the automotive industry to model, reduce the cost and speed up the vehicle systems development. Simulation tools are used as part of the design process, to predict and understand specific vehicle systems behaviour and performance, as well as for testing, systems improvement (or optimisation), validation and calibration before the vehicle can be put into production.

They are many simulations tools in the automotive area. This review focuses on software tools associated with gear ratio and gear shift map design and optimisation. These includes: AVL Cruise, MATLAB/Simulink, dSPACE, CATIA, AMESim, GT-Suite, ADAMS, ADVISOR, veDYNA, Modellica, ROMAX.

MATLAB/Simulink is the main environment used in the automotive industry from an electrical and software perspective for vehicle simulation, algorithm development, optimisations and research (Xi et al. 2009).

For example MATLAB/Simulink was used in General Motor to analyse and determine transmission gear content required to minimise fuel consumption for various powertrain system developed (Robinette 2014). These tools can be applied to a variety of vehicle simulation applications. More specifically, AVL has developed a simulation package (Le Guen et al. 2011) to optimise gear shift pattern.

dSPACE (Lucente et al. 2007) is mostly used for rapid prototyping, designing and testing of mechatronic systems. AMESim is used to simulate vehicle dynamics for design and optimisation before integration. More specifically it has been used in Song et al. (2014) to analyse the effect of gear shift characteristics when developing an electric oil pump for automatic transmission and in Xiang et al. (2013) to study the shifting schedule for a speed electric vehicle.

CATIA is well known for optimising and analysing gears. Rajan & Usmansha

(2014) have optimised an automotive transmission gear box for weight reduction and improve fuel consumption. GT-Suite (Ortiz-Soto et al. 2012) was used to model combustion and heat transfer of an engine, in order to optimised fuel consumption over various drive cycles. Lin et al. (2009) have used ROMAX package to assess gearbox optimisation based on design specification.

Simulations packages have played an integral part in the development of tools for fuel economy, Argonne National Laboratory had developed various simulation to study fuel efficiency for electric drive vehicle technologies (Moawad & Rousseau 2014), and gear reduction study to improve energy management strategy (Kim et al. 2012).

Ford Motor has described a simulation study to design a gear shift map for a Dual Clutch Transmission (Liu et al. 2009), where Downshift and Upshift point are initially defined using a vehicle dynamic model. FEV has developed a tool referred to as ShiftAnalyzer (Kirschstein et al. 2009), for online calibration of vehicle powertrain. It has been used to optimise and calibrate the shift quality of the BMW mini Cooper automatic gearbox.

The software tools have a massive advantages, as they can be used to reduce vehicle development cost, reduce weight, and optimise software applications, resulting in reduced fuel consumption. However software usage had some limitation as it cannot give accurate and uniform views onto systems based on theories (Broy 2006).

There are various industry standards used for the design and optimisation of gearbox such as, AGMA standards for gears as well as the ISO6336. ANSI, JIS and DIN standards are also used for gear teeth.

2.4.7 Motivation to use Evolutionary Algorithm & Swarm Intelligence

Considering the analysis above, the use of EA and swarm intelligence is quite simple to justify the motivation of their applications. Firstly, avoiding the formulation into a specific mathematical framework, as it can be costly and time consuming and some of the constraints do not need to be reformulated in a predefined mathematical structure. Secondly, reducing CO_2 emissions, is the main objective in this thesis. However, diminishing CO_2 emissions can conduct to deterioration of different aspects of vehicle good response. Very often, driveability is the measure delimiting how far the optimisation can produce solutions to reduce CO_2 emissions. Additionally, different objective functions are considered to precisely measure qualitatively an obtained gear shift map or gear ratio from the optimiser.

In order to achieve these goals, the use of EA and swarm intelligence appears to be a promising alternative to traditional approaches. These algorithms can consider any objective functions and constraints, regardless of their mathematical framework.

EA and swarm intelligence have been used in many applications, with multi-objective functions. GA has been applied across many fields, as per number of publications (Khajehzadeh et al. 2011). Shariatpanahi et al. (2004) have applied a GA with neural network to optimise gear ratio, Yin et al. (2013) have used aggregation weighted sum to combine several objective functions in attempt to optimise gear shift map. Swarm intelligence have gained enormous attentions, due to their successful applications, CS has been applied to welded beam design and disc brake design (Yang & Deb 2013).

In particular, all these methods do not require any gradient evaluation, which means that the reformulation of objective functions is not necessary any more.

EA and swarm intelligence have also got a drawback. They cannot guarantee the actual optimality of the solution for a given problem. Several arguments can be raised to tackle this issue:

- An algorithm having the ability to find a good gear shift map or gear ratio, by satisfying all constraints, and considerably better than the initial one, is a massive gain for the industry and environment.
- EA and swarm intelligence can permit to solve the initial problem, by obtaining satisfactory results within a reasonable time.

2.5 Concluding remarks

This chapter has given an overview of traditional analytical gear shift map and gear ratio design. Amongst these, the methods adopted by SAIC motors will be used in Chapter 3 to create the initial solutions that will be further refined by the optimisation approaches described in Chapters 4 and 5.

Both deterministic and stochastic methods are applicable to this constrained multi-objective optimisation problem. This work will develop methods based on the most appropriate stochastic algorithms, namely genetic algorithms and cukoo search, as well as deterministic algorithm, namely the interior-point algorithm. Common to all the optimisation approaches considered is the need to evaluate the appropriateness of candidate solutions. The validated model required to evaluatealternative gear shift map and gear ratio is described in chapter 3.

The criteria traditionally used to differentiate between alternative solutions have been reviewed. The adopted criteria as well as the additional criteria developed to help quantify the benefits of alternative solutions are formulated in Chapter 4. These criteria have been combined using both weighted sum and Pareto approaches, see Chapter 4.

Chapter 3

Powertrain modelling

3.1 Introduction

This chapter describes the models and algorithms exploited in subsequent chapter to optimise gear ratio as well as gear shift map. The chapter starts with a description of the ROEWE 950 characteristics and the validation of its proprietary transmission model. It is followed by a technical description of the traditional methods adopted to design gear shift map and gear ratio based on technical standard of SAIC Motor and BorgWarner Design for Dual Clutch Transmission. These methods have been included to provide an understanding of the process which is to be complemented by the optimisation strategies developed in Chapters 4 and 5.

3.2 Vehicle model

In order to study and validate the optimisation algorithms in this thesis, a DCT model has been made available by SAIC Transmission team. This section presents the model description of ROEWE 950, a conventional style saloon car, equipped with 2 litre turbocharged 4 cylinder engine featuring variable camshaft timing

(VCT) and a start-stop system. The engine is mated to a 6 speed Dual Clutch Transmission (DCT 360 variant). Within the Transmission Control Unit (TCU) resides the so-called shift map. This mapping is designed with respect to the engines operating range so that the transmission is in the right gear at the right time e.g. when the driver requires maximal torque, depending on the prevailing conditions, typically the transmission will select a lower gear moving the engine further into maximum torque producing range (high RPM combined with a wide open throttle).

The DCT 360 essentially comprises two transmission units that are independent of each other. Each transmission unit is constructed in the same way as a manual gearbox. Allocated to each transmission unit is a multi-plate clutch. Both multi-plate clutches are of the wet type (operating in oil) and hydraulically actuated. They are regulated, opened and closed by the mechatronics system using hydraulic oil depending on the gear to be selected.

1st, 3rd, 5th and reverse gear are selected via multi-plate clutch 1. 2nd, 4th and 6th gears are selected via multi-plate clutch 2. One transmission unit is always in gear and the other transmission unit has the next gear selected in preparation but with the clutch still in the open position. Every gear is allocated a conventional manual gearbox synchronisation and selector element (Kulkarni et al. 2007). The following section describes the vehicle model including the DCT and engine model.

3.2.1 Description of the vehicle

The vehicle model with DCT was implemented using the commercial software MATLAB/Simulink, which is the standard package of modelling uses in industry. The vehicle model is divided in four subsystems (see Figure 3.1) which are:

- Vehicle speed: in this optimisation process, the main objective is to reduce CO2 emissions by using the well-known NEDC drive cycle, approved among and homologue by the United Nations Economic Community for Europe (ECE) regulation 101 (United Nations 2006). The vehicle model is designed to consider as input a drive cycle. By default, the NEDC in implemented, however the model also include different drive cycle such as WLTP, ARTEMIS Urban, JAPANESE 10-15 Drive cycle. A more detail of these drive cycle can be found in Barlow et al. (2009*a*).

- Transmissions output torque calculation: upon the vehicle speed, an estimated engine torque is calculated. This allows to define the driver requirement in terms of engine torque.

- Transmission model: considering an estimated engine speed and driver demand, a transmission control unit (TCU) is used to define the corresponding gear ratio, and calculates the engine speed.

- Engine model: knowing the driver demand (torque and throttle position) and engine speed, the engine fuel map BSFC is then utilised to estimate fuel consumption, where the CO_2 emission can be derived. Noticed that, this task is crucial in this thesis, as the optimisation is mainly aimed to reduce CO_2 emissions.

The above vehicle model specification is given in Appendix A. The following section gives a comparative vehicle model with the reference data obtained from rolling road.

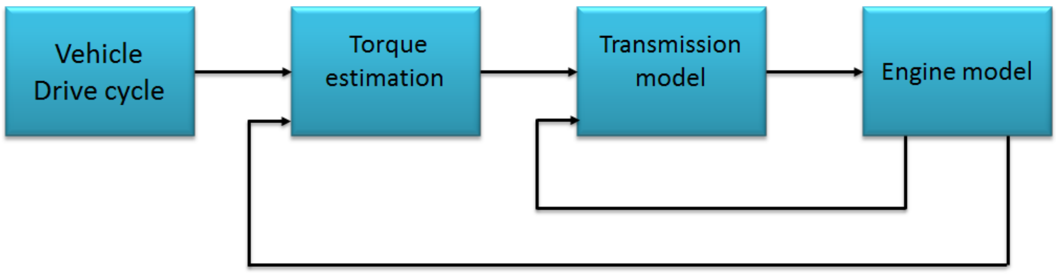

Figure 3.1: Representation of vehicle model implementation in Simulink

3.2.2 Model validation

Having described the vehicle model in Simulink, a verification of the model must be realised in order to validate and accepted it as an abstract representation of the real system. This is achieved by comparing vehicle model against approved data made available from rolling road data. Measured data were obtained from rolling road over the NEDC, then converted into excel spreadsheet, which made easier to extract the data using MATLAB/Simulink environment for comparison studies. The original data runs over a 1250s period with sample interval at 1ms and 10ms. For practical use, the simulation and experimental data were re-sampled at the same rate at 10 ms. Figures 3.2 and 3.2 represent a comparison between simulation and experimental results on rolling road, where both considered initial shift map (see Appendix B) and the NEDC.

The vehicle speeds are almost comparatively similar, except the driver data included a maximum error of magnitude $\pm$ 2 km/h for set of data. Therefore, both engine speed show a good compromise in both dynamic and steady state, with some minor error difference. Regarding the gear shift map, a minor difference can be noticed on the first set of data at higher speed, which could be due to driver throttle position and vehicle speed variation.

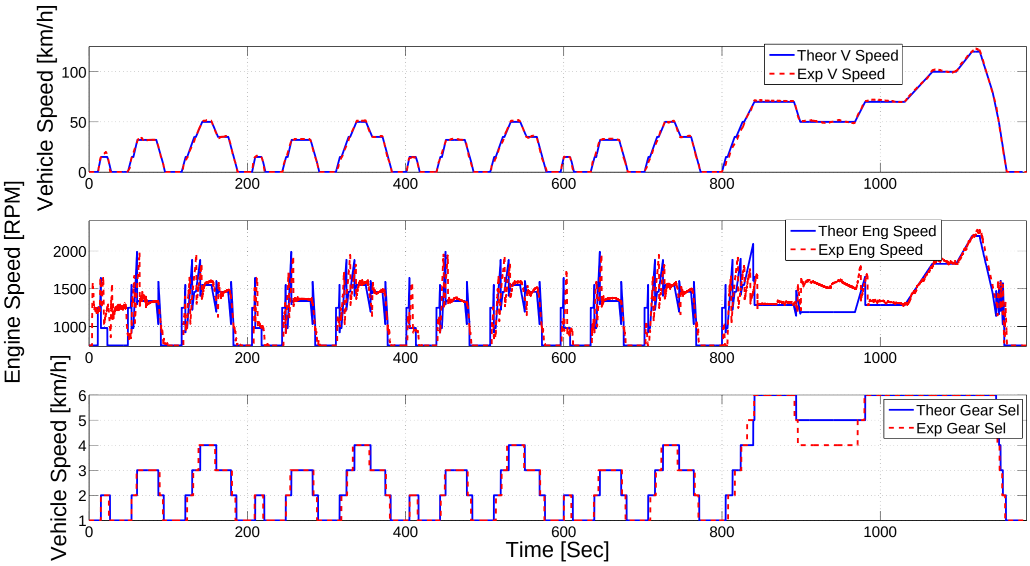

Figure 3.2: First set of validation data representing comparison between simulation and experimental results from rolling road over the NEDC. Theor V Speed, Exp V Speed, Theor Eng Speed, Exp Eng Speed, Theor Gear Sel and Exp Gear Sel denote for vehicle speed, engine speed and gear selection used in simulation and rolling road, respectively.

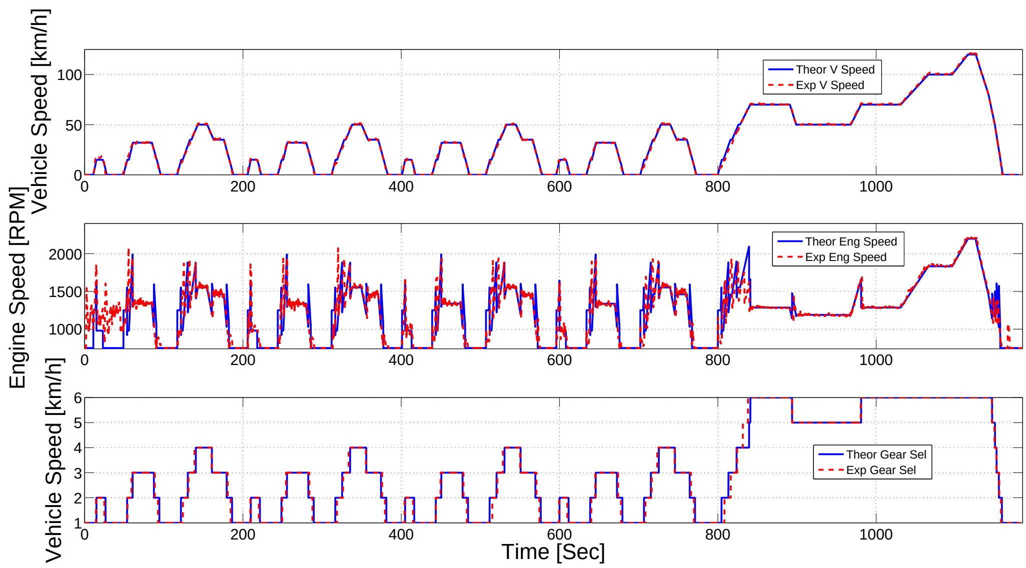

Figure 3.3: Second set of validation data representing comparison between simulation and experimental results from rolling road over the NEDC. Theor V Speed, Exp V Speed, Theor Eng Speed, Exp Eng Speed, Theor Gear Sel and Exp Gear Sel denote for vehicle speed, engine speed and gear selection used in simulation and rolling road, respectively.

3.2.3 Fuel consumption and CO_2 emissions calculation

This subsection describes fuel consumption (Mashadi & Crolla 2012), and CO_2 emissions (US EPA 1999) calculation use in this thesis.

- Fuel consumption

  Fuel consumption represents the engineering measure to determine the amount of fuel required to travel a given distance. It is obtained from the engine power and engine BSFC map. It is described as follows:

$$Fuel_{(g/s)} = P_e \times BSFC. \tag{3.1}$$

  where $\mathrm{Fuel}_{(g/s)}$ denotes the fuel mass. P_e is the engine power expressed by the product of engine speed and torque that are also used to define the BSFC from the engine map.

  The total fuel map of an entire cycle is defined by summing the individual fuel masses:

$$Fuel_{(g)} = \sum_{i=1}^{N} Fuel_{(g/s)}(i). \tag{3.2}$$

  where N denotes the number of sampled data over the driving cycles considered.

  The fuel consumption can be derived a given distance as follows:

$$FC(l/100km) = \frac{Fuel_{(g)}}{d_{cycle} \times \rho_{fuel}} \times 100. \tag{3.3}$$

  where d_{cycle} and ρ_{fuel} denotes for a given driving cycle distance, and the density of the fuel respectively. The factor 100 is used as the fuel consumption is defined by $l/100$km.

- CO_2 emissions

The estimation of CO_2 emissions from fuel consumption is determined from the carbon content of fuel and then applied to the amount of fuel burned redundant. When the fuel is burned, 87% is carbon contents, where the total mass of carbon is obtained. In order to determine the total CO_2 emissions, the carbon emissions is multiplied by the molecule weight ratio of CO_2 (44.01 g/mol) and carbon (12.01 grams).

$$CO_2 emissions = Fuel_{(g)} C_{c,c(\%)} \times \frac{CO_{2(g/mol)}}{C_{(grams)}}. \tag{3.4}$$

where $C_{c,c(\%)}$, $CO_{2(g/mol)}$ and $C_{(grams)}$ denote for percentage of carbon content from fuel, molecular weight of CO_2 and molecular weight of carbon respectively.

3.3 Gear shift schedule design

An automatic transmission gear shift schedule represents the vehicle speed at which each gear shift shall occur. It is usually described as a function of pedal position for a given gear ratio change. The aim of this section is to describe gear shift schedule design based on vehicle dynamic. The shift schedule design is predominated by two objectives which are the vehicle dynamic performance and fuel economy. However a good compromise must be applied between performance and economy to ensure that vehicle driveability is not detrimentally affected. The approaches to establish these two methods are expressed in the following subsystems:

3.3.1 Equation of motion

The longitudinal vehicle dynamic equation defining the equilibrium relation, between drive forces and resistance forces is applied to determine the vehicle acceleration, speed, traction forces, rolling resistance force, and aerodynamic force. The characteristics of engine torque map alongside with fuel consumption map (see Figures 3.4 and 3.5) are required to design the shift schedule. The engine torque map was modelled using the so-called Magic Torque formulae (Mashadi & Crolla 2012), where the fuel map was created using MATLAB handle function.

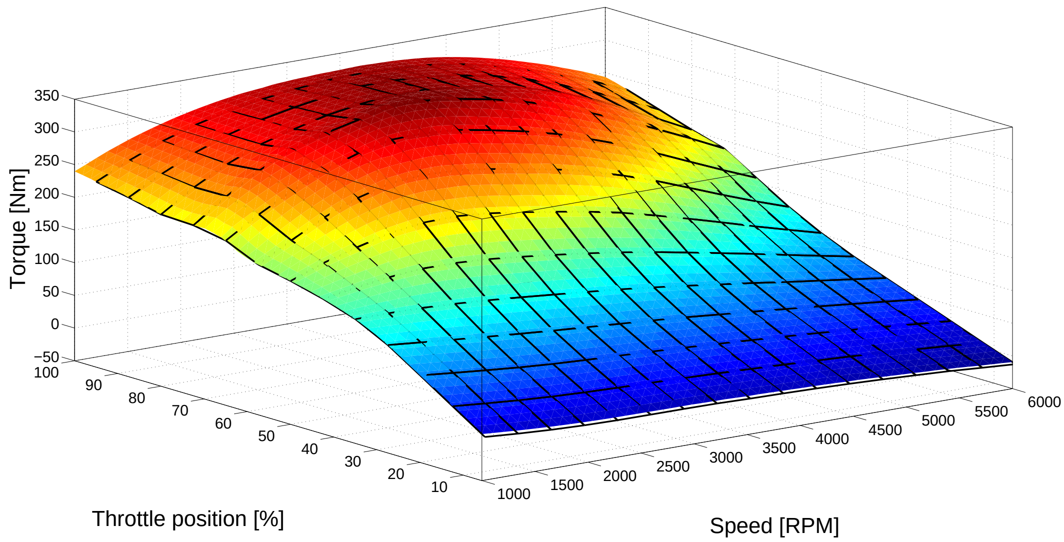

Figure 3.4: Engine speed-torque-throttle 3D map

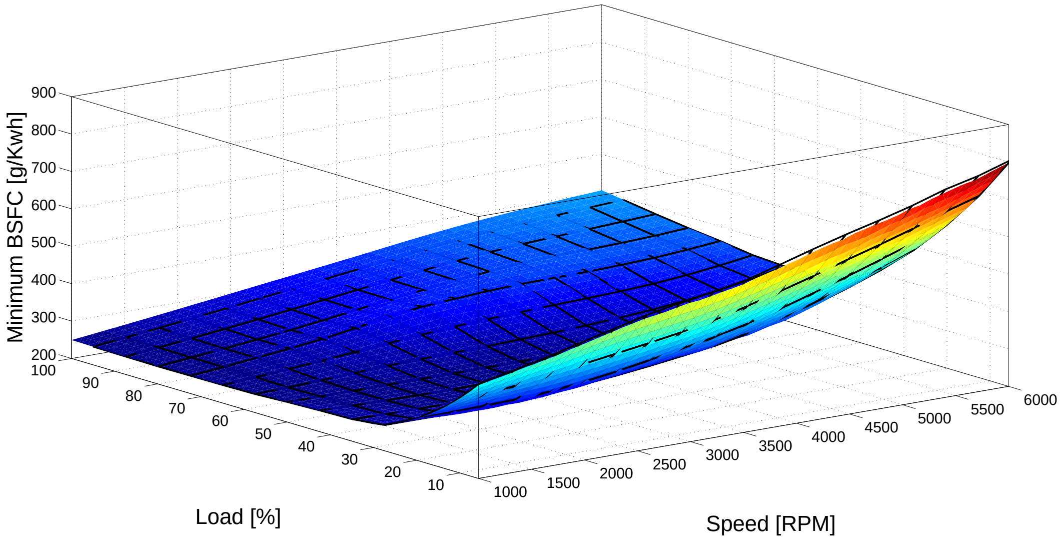

Figure 3.5: Engine speed-BSFC-throttle 3D map

The driving forces developed by engine must overcome the rolling resistance (F_{roll}), aerodynamic drag (F_{aeroDy}), climbing resistance (F_{Climb}) and acceleration resistance (F_{ac}) as describes in Xi et al. (2009) and Kirtane (n.d.).

$$F_{TF} = F_{roll} + F_{aeroDy} + F_{Climb} + F_{ac}\,(\mathrm{N})\,. \tag{3.5}$$

The vehicle acceleration is expressed as:

$$Acc = \frac{F_{TF} - F_{roll} + F_{aeroDy} + F_{Climb} + F_{ac}}{\delta_n M_v}. \tag{3.6}$$

where Acc is the acceleration of the vehicle, M_v is the vehicle mass, δ_n is the equivalent mass of rotary mass of vehicle, influenced by the inertia of the engine flywheel (J_e), vehicle wheels (J_i) and transmission ratio (J_i), which is expressed as follows:

$$\delta_n = 1 + \frac{J_W J_i i_g^2 i_F^2 J_e}{R_W^2 M_v}. \tag{3.7}$$

The vehicle traction force is expressed as:

$$F_{TF} = \frac{T_e i_g i_F \eta_T}{R_W}. \tag{3.8}$$

where T_e is the engine output torque, i_g is the gear ratio of transmission, i_F is the final gear ratio, η_T is the transmission efficiency, and R_W is the radius of wheel.

The air resistance force is expressed as:

$$F_{aeroDy} = \frac{C_D A V^2}{21.15}. \tag{3.9}$$

where C_D is air resistance coefficient, A is frontal area of vehicle, and V (km/h) is the vehicle speed.

The rolling resistance force is expressed as:

$$F_{roll} = 0.01(1 + V/147)M_v g. \tag{3.10}$$

where g is the gravitational acceleration.

The vehicle speed is mainly related to the engine and gear ratio, where it is expressed as:

$$V_i = \frac{2\pi R_W \omega_e}{60 i_g i_F}. \tag{3.11}$$

where V_i and ω_e is the vehicle speed at given gear position and engine speed respectively.

3.3.2 Design principle based acceleration

The vehicle longitudinal acceleration is calculated by Equation (3.6). The engine torque map is a function of engine speed and throttle position, where the engine speed was varied from the minimum (1000 RPM) to the maximum (6000 RPM), and at different throttle angles from 10% to 100%. The relationship between vehicle acceleration and speed (see Equation (3.11)) can be calculated at different gear position with different throttle pedal angle. The shift schedule design for dynamic performance (see Figure 3.6) is to drive at the maximum vehicle acceleration. However, the shifting point is selected at the intersection point of two acceleration curves adjacent gear at the same throttle angle.

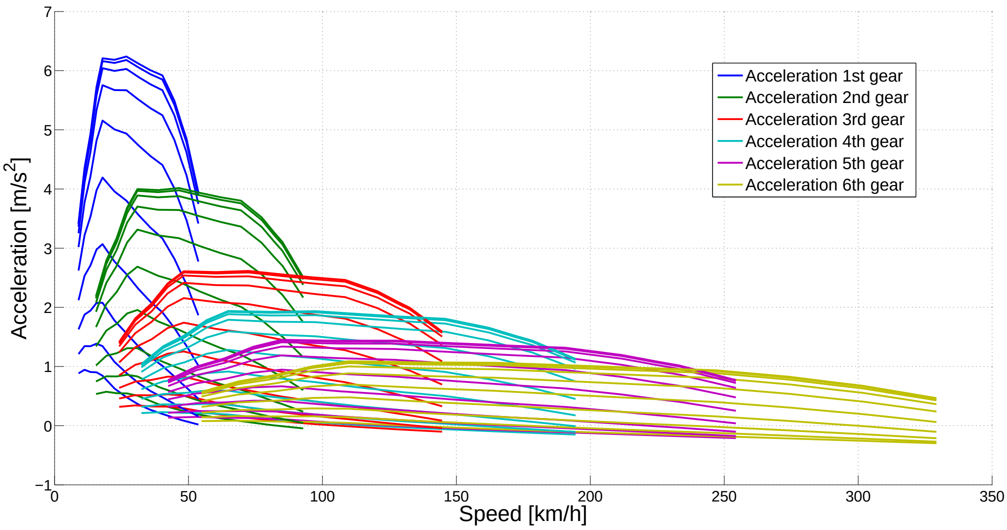

Figure 3.6: Vehicle dynamic performance curves with different gear position and throttle pedal angle

$$g_{(i)\to(i+1)} = Acc_{(i)} \cap Acc_{(i+1)}. \tag{3.12}$$

where $g_{(i)\to(i+1)}$ is the gear shift at a same throttle position from $g_{(i)}$ to gear $g_{(i+1)}$ at the intersection of acceleration curves $Acc_{(i)}$ and $Acc_{(i+1)}$. If there is no intersection between acceleration curves $Acc_{(i)}$ and $Acc_{(i+1)}$, then the maximum speed of the gear $g_{(i)}$ is considered. The Upshift schedule is obtained by connecting together shift point of the same gear between different throttle positions (see Figure 3.7).

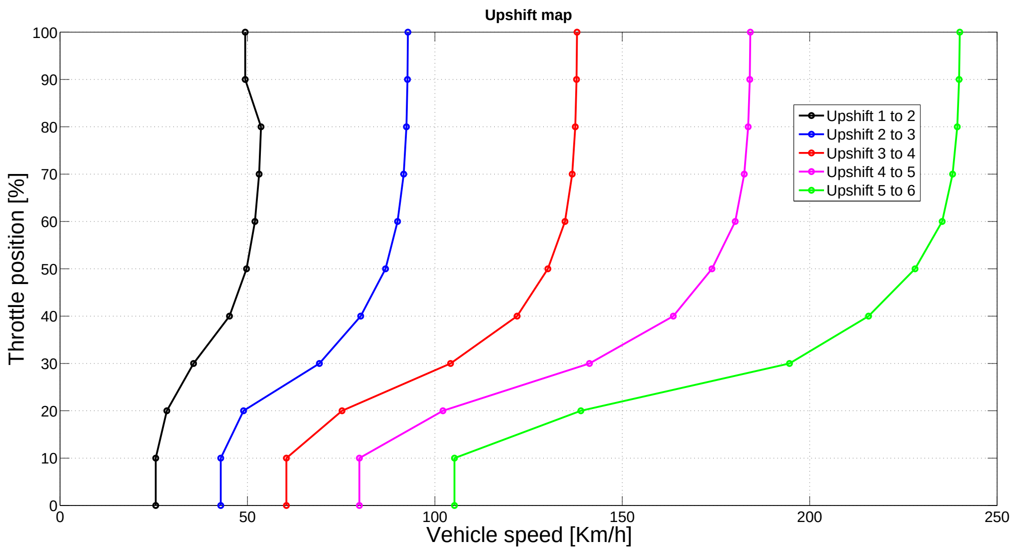

Figure 3.7: Upshift gear shift map based on acceleration curves

3.3.3 Design principle based traction force

Shift schedule based traction force is similar to the acceleration curves, however the Equation (3.8) which is derived from the vehicle longitudinal is used to establish the shift point (see Figure 3.8).

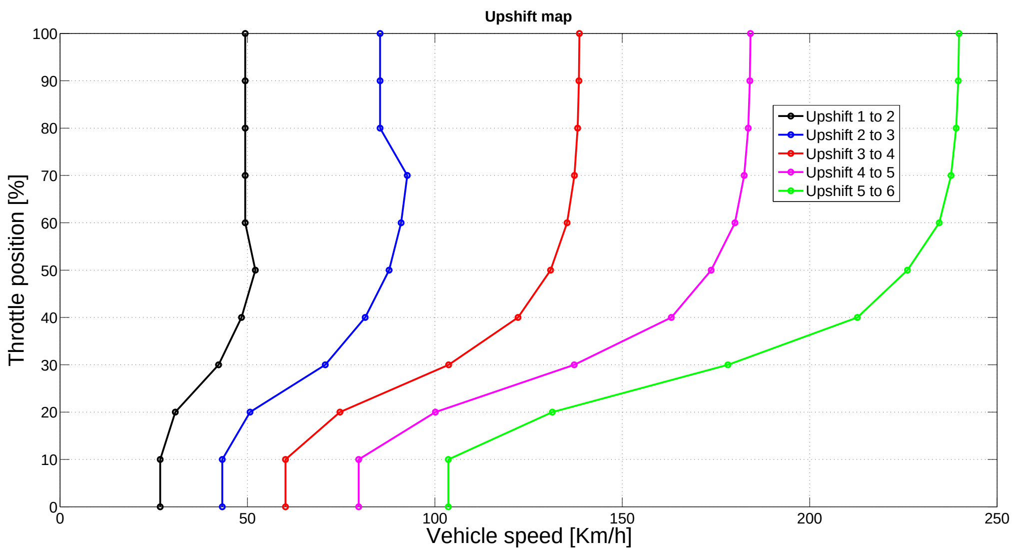

Figure 3.8: Upshift gear shift map based on traction force curves

3.3.4 Design principle based minimum fuel, BSFC

Shift schedule based brake specific fuel consumption (BSFC) map is based on the minimum fuel consumption (see Figure 3.9), where the shift point is following the same as the acceleration shift point.

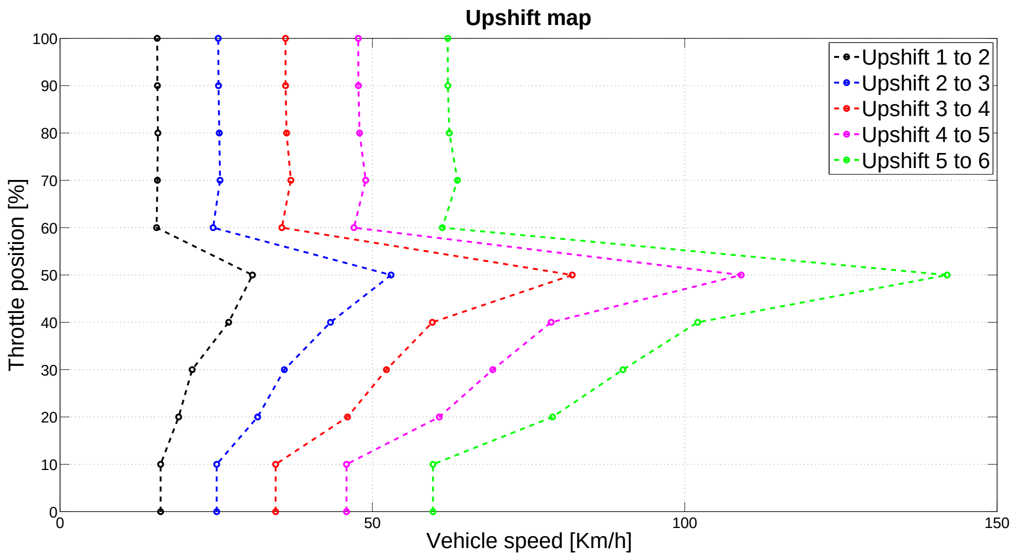

Figure 3.9: Upshift gear shift map based on BSFC curves

Figure 3.11 is to compare different methods to define an initial gear shift map. It is noticed that the ideal fuel consumption for a gear shift map is converging toward the left side of the map which corresponds to the most efficient area of the BSFC map. It might be ideal for fuel consumption to consider a shift map design based on BSFC map, however the driveability might be worst. The gear shift map should be design based on a compromise of fuel consumption and performance. The next of this study will be to design an algorithm capable to select a shift map in order to satisfy the vehicle driveability as well as fuel consumption and vehicle performance.

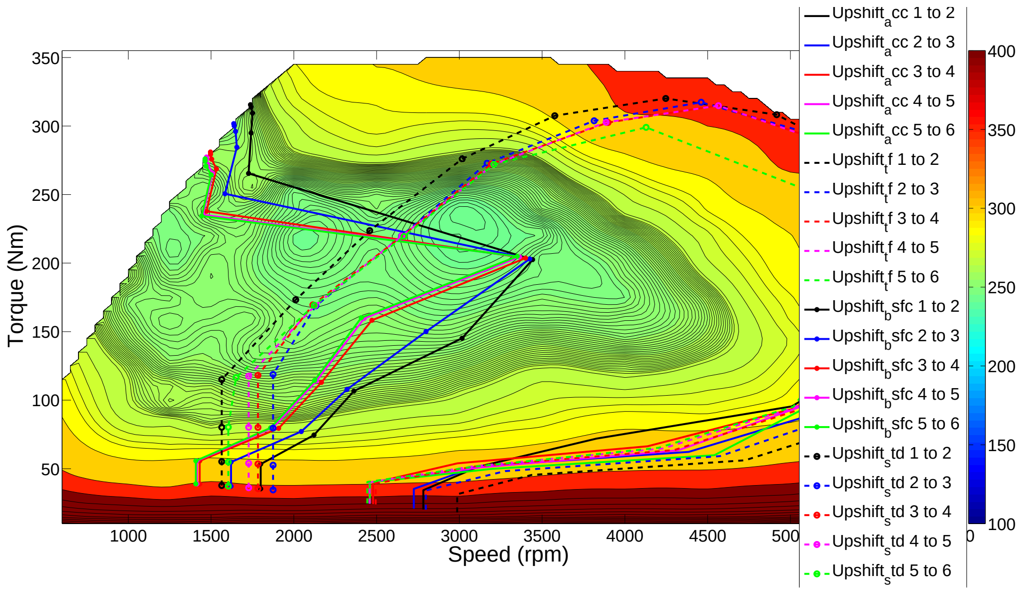

Figure 3.10: Upshift gear shift map on BSFC map

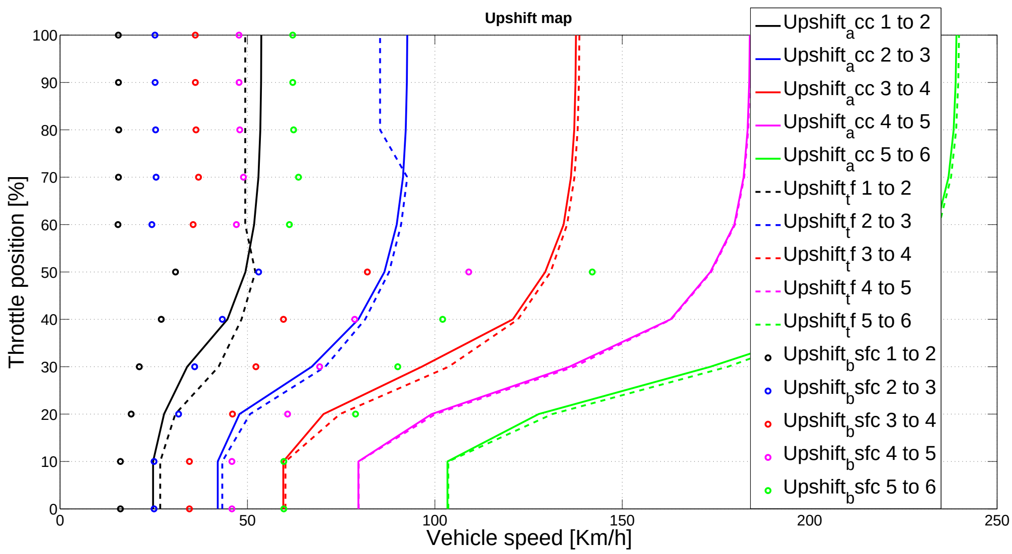

Figure 3.11: Upshift gear shift map, based on acceleration, traction force, BSFC

3.3.5 Criteria of gear shift map

This section discussed different criteria use to qualify a Dual Clutch Transmission gear shift-map. Also, simulation results of different design described in Subsection 3.3.2, 3.3.3 and 3.3.4 are compared with a standard gear shift map. In order to compare different results against each other, every shift were converted as a traction point (see Figure 3.12), and the following expression describes the conversion from gear shift point (in km/h) to traction force:

$$F_{t_{std}} = T_{e(\omega_e)} \frac{i_g \eta}{R_w}. \tag{3.13}$$

where i_g and R_w are the gear ratio and wheel radius respectively. T_e is the engine torque expressed a function of engine speed ω_e (see Subsection 2.4, and Subsection 2.3.2, in Chapter 2).

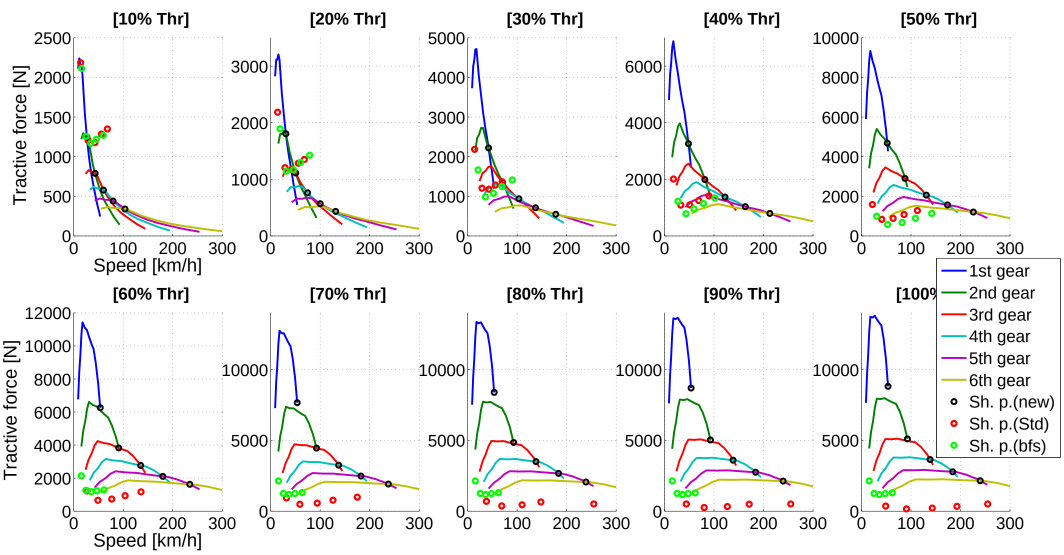

Figure 3.12: Traction force curves with shift point between two adjacent gears compare with standard and minimum BSFC shift map

Figure 3.13 represents the minimum fuel consumption curve for each gear and the intersection between two adjacent curves (black circle). The red circle represents the standard shift point, while the green is BSFC traction force shift point. It can be noticed that both shift points, traction and BSFC shift point start almost at the same point for lower throttle position, however at higher throttle position, traction force are significantly reducing.

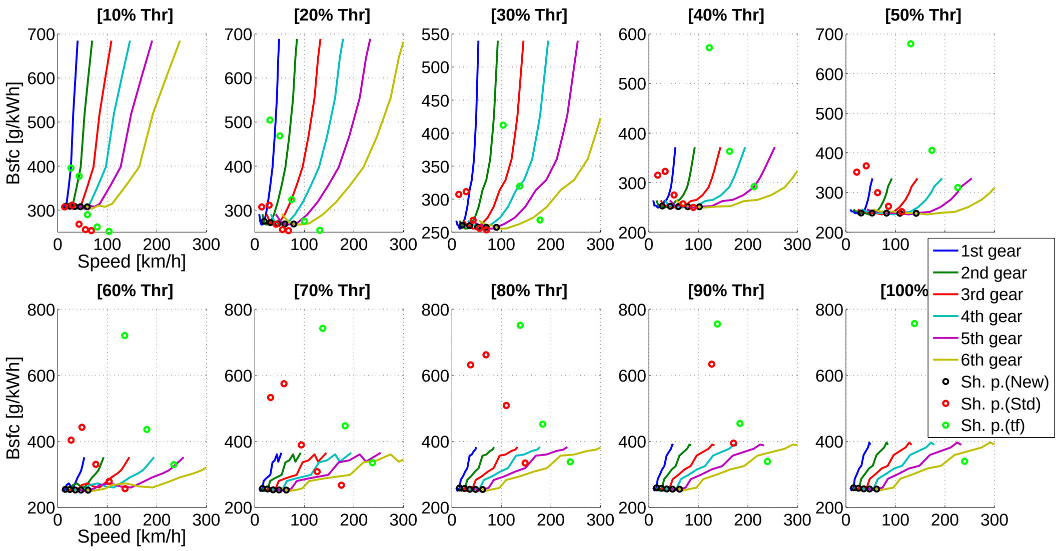

Figure 3.13: BSFC curves with shift point between two adjacent gears compare with standard and traction BSFC shift map

The Figure 3.12 was also defined in the same manner as Figure 3.13, the conversion from gear shift point to BSFC values is described as follows:

$$BSFC_t = bsfcFN\left(T_e, \omega_e\right). \tag{3.14}$$

where $BSFC_t$ is an handle function in MATLAB used to model the BSFC map as a look up table, where it is a function of engine torque and speed. It can be noticed at lower throttle position, the BSFC shift point for standard gear are very low, while the value increased at higher throttle position.

Table 3.1 is to compare standard gear shift map to gear shift map design based on tractive force and BSFC map. It can be remarked that the minimum BSFC design gear shift does not guaranty a good CO_2 emission over the NEDC.

Table 3.1: Zone on BSFC map and CO_2 emission over the NEDC

Shift map	CO_2 $[g/km]$	$Zone1$	$Zone2$	$Zone3$
Standard	198	0.052896	0.11239	0.013851
Traction	228	1.0929	0.13322	0.01092
Standard	202	0.18389	0.14378	0.011415

3.3.6 Final gear shift map design

Downshift schedule

The Downshift schedule is based on a linear convergence or shift buffer zone (Liu et al. 2009), (Xi et al. 2009). Lower shift point are defined using the minimum consumption, meaning from 0% to 30% throttle position. From 30% to 100%, a linear convergence based on engine RPM is used to define the rest of the gear shift map. Notice that the range of engine is covered by the throttle position.

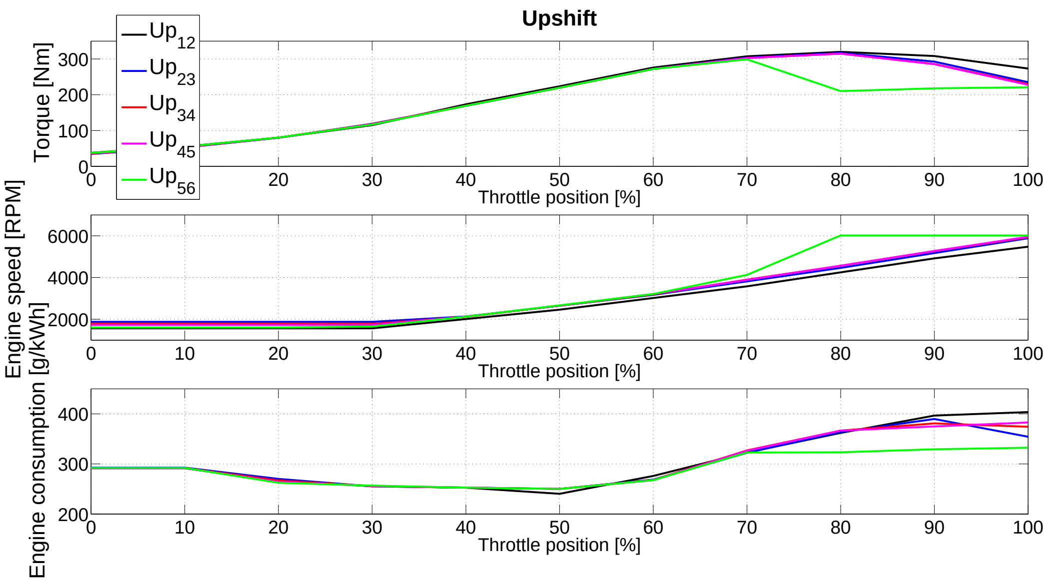

Figure 3.14: Initial shift map study

3.4 Gear ratio design

This section describes different methods for selecting transmission gear ratio. For a given vehicle and engine specification, gear ratios are designed to satisfy performance requirement, gradability, fuel economy and acceleration. At first the low and high gears are defined based on vehicle, engine characteristics and road condition, after the intermediate gear are calculated.

3.4.1 Main formulas for gear ratio design

The starting point to calculate gear ratio is based on longitudinal vehicle dynamic formulas.

The total resistive acting against the vehicle is expressed as follow:

$$F_{RR_{Total}} = F_{roll} + F_{Air} + F_{Clim} + F_{Acc}. \tag{3.15}$$

where:

- F_{roll}: Rolling resistance. The rolling resistance is the resistance force acting on the rolling wheel

$$F_{roll} = Fr_{cof} m_{Total} g \cos(\alpha). \tag{3.16}$$

  where Fr_{cof}, m_{Total}, g and α denote the rolling resistance coefficient, the whole vehicle mass, gravitational force and road gradient, respectively.

- F_{Air}: Air resistance. The air resistance is made up of the pressure drag including induced drag, surface resistance and internal resistance.

$$F_{Air} = \frac{1}{2}\rho C_w A v^2. \tag{3.17}$$

  where ρ, C_w, A and v denote the air density, drag coefficient, front area and vehicle speed.

- F_{Clim}: Climbing resistance. The climbing resistance represents the gradient resistance or downhill force relates to the slope descending force and it is calculated from the weight acting at the centre of gravity:

$$F_{Climb} = m_{Total} g \sin(\alpha). \tag{3.18}$$

- F_{Acc}: Acceleration resistance. The vehicle acceleration:

$$F_{Acc} = m_{Total} a. \tag{3.19}$$

The diving resistance also called tractive force developed by the engine power is described as:

$$F_{drive} = T_e \frac{i_{tot}}{R_w} \eta_{tot}. \tag{3.20}$$

where T_e, i_{tot}, R_w and η_{tot} denote the engine torque, total gear ratio, wheel dynamic radius and transmission efficiency, respectively.

The engine power is expressed as follows:

$$P_e = T_e \omega_e. \tag{3.21}$$

Alternatively, the engine speed can also be expressed as a function of driving force and vehicle speed:

$$P_e = \frac{F_{drive} v}{\eta_{tot}}. \tag{3.22}$$

The equilibrium relation between drive forces and running resistance is naturally obtained from the driving force and total force resistance, using Newton second law:

$$F_{Acc} = F_{drive} - F_{roll} + F_{Air} + F_{Clim} + F_{Acc}. \tag{3.23}$$

The main contribution of the powertrain is to offer ratio between engine speed and road wheel speed enabling the vehicle to move under difficult condition and reasonably operate in the fuel efficient ranges of the engine performance map. The following section describes the maximum ratio required $i_{A,max}$, the smallest gear ratio and finally the intermediate ratio.

3.4.2 The largest gear ratio selection

The largest gear ratio (LGR) is the starter gear, which is mainly used for slow driving and starting up the vehicle. A climbing performance (gradeability) α greater than 50% is normally required for an unladen passenger car. This is to ensure that the vehicle can tow a trailer and overcome ramp easily, however the acceleration and aerodynamic are ignored as the vehicle speed is low. The lower the weigh of the vehicle, the longer the LGR should be (smaller ratio value). The higher the weight of the vehicle, the shorter the LGR should be (smaller value). For low torque engines the LGR must be shorter (higher ratio value). The main driven equation to determine the largest gear ratio is described as follow:

$$i_{A_{max}} = \frac{R_w m_{vehicle+trailer} g \left(Fr_{cof} cos(\alpha) + sin(\alpha)\right)}{Te_m ax\eta_t}. \tag{3.24}$$

where $m_{vehicle+trailer}$ represents the vehicle mass with a trailer. This is to ensure that a trailer can be towed and climb a ramp with ease.

3.4.3 The smallest gear ratio selection

The final or the smallest gear ratio will depend on the maximum engine power delivered to wheels, and the resistive power based on rolling and air resistance.

The smallest gear ratio is defined as follows:

$$i_{A,min} = \omega_e \frac{R_w}{V_{max}} \tag{3.25}$$

where V_{max} is the maximum vehicle speed delivered by the maximum engine power. The theoretical maximum speed is defined at the balance point, which represents the intersection between the resistive power and the engine maximum power (see Figure 3.15).

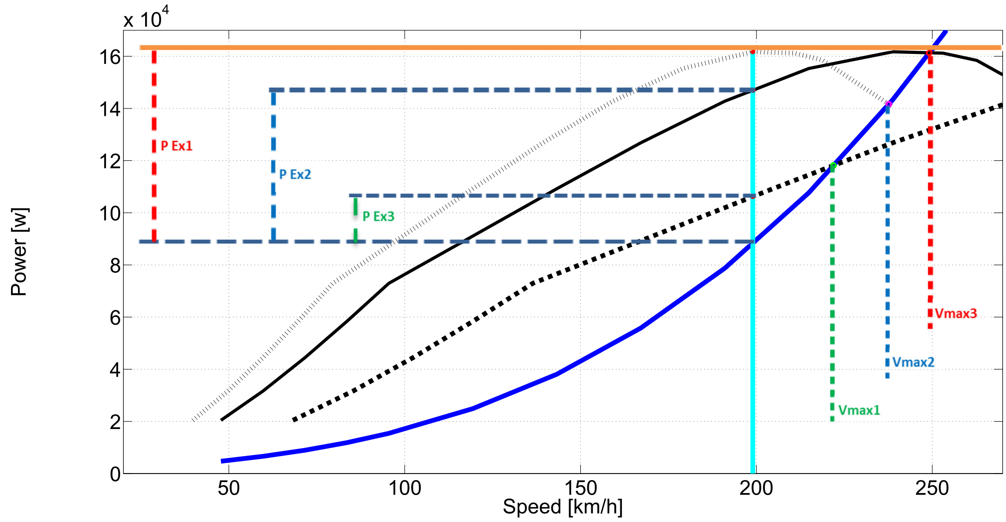

Figure 3.15: Performance power curves, where P Ex1, P Ex2 and P Ex3 are the excess power of Over-revving (racing car), optimality and Under-revving (passenger car) with their respective maximum vehicle speed Vmax1, Vmax2 and Vmax3

The maximum engine power is given by Equation (3.21), where T_e in this case is the maximum engine torque at full throttle position and it is modelled as follows:

$$T_{e_{max}} = a\omega_e^5 + b\omega_e^4 + c\omega_e^3 + d\omega_e^2 + e\omega_e + f. \tag{3.26}$$

where ω_e is the engine speed, and a, b, c, d, e, f are the coefficients of a 5th order polynomial function. A simple least square fitting was used to find the coefficients and the values are written in Table 3.2.

Table 3.2: Engine torque full throttle position coefficients

a	b	c	d	e	f
$3.0986e-16$	$-8.2934e-12$	$7.9418e-08$	-0.00036171	0.78985	-309.89

Consequently, the maximum engine power can be derived as follows:

$$P_{e_{max}} = T_{e_{max}} \omega_e \tag{3.27}$$

Substituting (3.27) into (3.26), results in the following equation:

$$P_{e_{max}} = \left(a\omega_e^5 + b\omega_e^4 + c\omega_e^3 + d\omega_e^2 + e\omega_e + f \right) \omega_e \frac{\pi}{30}. \tag{3.28}$$

By differentiating (3.28) and equating to zero, the maximum engine power with its corresponding engine speed can be defined by solving the following equation :

$$\frac{dP_e}{d\omega_e} \left(a\omega_e^5 + b\omega_e^4 + c\omega_e^3 + d\omega_e^2 + e\omega_e + f \right) \omega_e \frac{\pi}{30} = 0. \tag{3.29}$$

After defining the maximum engine power and speed, the maximum vehicle speed is naturally derived at the balance point of the maximum tractive force (F_{rTot}) and resistive force. The resistive force is expressed as follows:

$$F_{RR} = \left(F_r M g + \frac{1}{2} C_w A \rho_{Air} V^2 \right). \tag{3.30}$$

Alternatively, the maximum tractive force can be defined as a function of the maximum engine power as follows:

$$F_{rTot} = \frac{P_{max} \eta_t}{V_{max}}. \tag{3.31}$$

By equating both tractive and resistive forces, the following equation is derived:

$$P_{max} = \frac{\left(F_r M g + \frac{1}{2} C_w A \rho_{Air} V_{max}^2\right) V_{max}}{\eta_t}. \tag{3.32}$$

By manipulating the maximum power equation (3.32), a third order equation is defined, where the maximum vehicle speed can be derived:

$$F_r M g V_{max} + \frac{1}{2} C_w A \rho_{Air} V_{max}^3 - P_{max} \eta_t = 0. \tag{3.33}$$

The smallest gear ratio is influenced by the trade-off between the vehicle fuel economy and performance. The optimum gear ratio can be either modified for fuel consumption or for vehicle performance. If the gear ratio $i_{A,min}$ increases, the engine power curve will move to the left of the optimum engine power, and the vehicle is over geared (Over-revving), which is good for fuel economy. However if the gear ratio $i_{A,min}$ decreases, the engine power curve will move to the right of the optimum engine power, and the vehicle is under geared (Under-revving), which is good for performance. The following equation expressed over geared and under geared:

$$V_{max} = \omega_e \frac{R_w}{i_{A,min} \times Fact_{gear}}. \tag{3.34}$$

where $Fact_{gear}$ is a factor to increase or decrease the optimum gear ratio. When $Fact_{gear}$ is less than 1, the vehicle is over geared, however if $Fact_{gear}$ greater than 1 the vehicle is under geared.

3.4.4 The intermediate gear selection

The intermediate gears also called discrete gears ratio are linked kinematically the vehicle and engine speed. The gear shifting is realised through the intermediate gears. The intermediate gears should be large enough to allows the next lower gears to be engaged when the engine torque is reached, without outreaching the maximum engine speed. The greater the number of gear ratio, the better the engine can exploits the efficiency of the fuel map, however the gear change frequency will increase. There are standard methods (Naunheimer et al. 2010), (Mashadi & Crolla 2012) to determine initial intermediate gears knowing the high and low gears that will be discussed in the coming section.

Geometric progression design

The geometric progression method is considered as an ideal case, where the gear is changed at a uniform speed, which results in an engine working range ω_H and ω_L (see Figure 3.21). This method requires the engine to operate within the same speed range, which is naturally selected for best fuel consumption.

After defining the high and low gears ratio, for example for a 6 speeds gearbox design, the constant step ratio (K_{step}) for a geometric progression method. This can be defined as follows:

$$\frac{i_{g1}}{i_{g2}} = \frac{i_{g2}}{i_{g3}} = \frac{i_{g3}}{i_{g4}} = \frac{i_{g4}}{i_{g5}} = \frac{i_{g5}}{i_{g6}} = \frac{\omega_H}{\omega_L} = K_{step}. \tag{3.35}$$

where i_{g1}, i_{g2}, i_{g3}, i_{g4}, i_{g5} and i_{g6} are the gear ratios for a 6 speeds gearbox.

Also, multiplying the equalities results in:

$$\frac{i_{g1}}{i_{g2}} \times \frac{i_{g2}}{i_{g3}} \times \frac{i_{g3}}{i_{g4}} \times \frac{i_{g4}}{i_{g5}} \times \frac{i_{g5}}{i_{g6}} = \frac{i_{g1}}{i_{g6}} = K_{step}^5. \tag{3.36}$$

which can be also written as follows:

$$K_{step} = \sqrt[5]{\frac{i_{g1}}{i_{g6}}}. \tag{3.37}$$

In a more general form, for an N-speed gearbox:

$$K_{step} = \sqrt[N-1]{\frac{n_L}{n_H}}. \tag{3.38}$$

Finally each intermediate gear is defined as follows:

$$i_{g_i} = i_{g_{i+1}} \times K_{step}, i = 1, 2, ..., N-1. \tag{3.39}$$

Progression design

It can be noticed that the geometrical method produces smaller speed ranges (δV) for lower speed ratio, however it produces larger speed ranges in higher gear, which leads to define the speed ratio as follows:

$$\frac{\delta V_{i+1}}{\delta V_i} = K_{step}. \tag{3.40}$$

Inversely, the gear ratio step can be expressed throughout tractive force range as follow:

$$\frac{\delta F_i}{\delta F_{i+1}} = K_{step}. \tag{3.41}$$

As shown in geometric progression method, the ratio step of two adjacent gears was constant. However in the progressive design, the consecutive ratio step C_{step_i} is related to a constant factor k_{factor}:

$$C_{step_{i+1}} = C_{step_i} \times k_{factor}. \tag{3.42}$$

The multiplication of the ratio C_{step_i} together will equate the ratio of first to the last gears, which can be written as follows:

$$\frac{i_{g1}}{i_{g2}} \times \frac{i_{g2}}{i_{g3}} \times \frac{i_{g3}}{i_{g4}} \times ... = \frac{i_L}{i_H} \equiv C_{step_1} \times Cstep_2 \times Cstep_3 \times ...Cstep_{N-1}. \tag{3.43}$$

where i_L and i_H are the low and high gear ratios. By substituting (3.42) into (3.43), then simplifying results in:

$$K_{step}^{N-1} = C_{step_1}^{N-1} \times k_{factor}^{1+2+...N-2}. \tag{3.44}$$

By solving for C_{step_1} results in:

$$C_{step_1} = K_{step} \times k_{factor}^{1-\frac{N}{2}}, N > 2. \tag{3.45}$$

By knowing the value of lower and higher gear ratios, other value of gear ratios can be determined by using the following expression:

$$i_{g2} = \frac{i_{g1}}{C_{step_1}}, i_{g3} = \frac{i_{g2}}{C_{step_2}} = \frac{i_{g1}}{C_{step_1}C_{step_2}}, i_{g_{i+1}} = \frac{i_{gi}}{C_{step_i}} = \frac{i_{g1}}{C_{step_1}C_{step_2}...C_{step_i}}. \tag{3.46}$$

The gear ratios can be defined now if the factor k_{factor} is known. A geometric progression is provided if the $k_{factor} = 1$. Only the progression design is made with k_{factor} less than an unity. A reasonable value of k_{factor} is described as follows:

$$0.8 < k_{factor} < 1.0. \tag{3.47}$$

The two main methodologies have been described, the following section will discuss the results.

3.4.5 Criteria of gear ratio layout

The criteria described in this section are used to qualify how good are the gear ratio are designed. The results will compare two different methods with the standard gear ratio supplied by SMTC. As many parameters are involved in the gear ratio design, this will focus on one case study just for analysis.

Gradeability with a trailer

Gradeability is defined as the highest grade a vehicle can ascend maintaining a particular speed (Akilesh Yamsani 2014). A trailer of 1200 kg was considered including the vehicle mass, where a road grade of over 50% road grade was set to define the vehicle gradeability. The vehicle is uniform and at low speed, consequently this is assumed to be null. The following formula describes the gradeability:

$$Gradeability = \frac{F_{Dive} - F_{roll} - F_{Air}}{M_{vehicle+trailer}}. \tag{3.48}$$

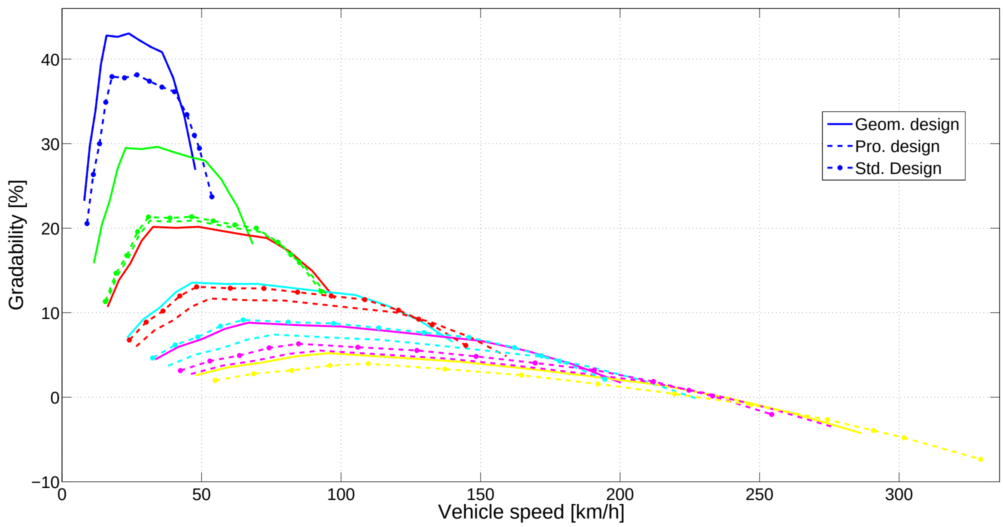

Figure 3.16: Gradeability performance

Acceleration-Traction force

Figure 3.17 demonstrates maximum acceleration with a provided set of gear ratios starting from 1st to 6th, where the Geometric and Progressive ratios are compared with the standard gear ratios. It can be noticed that the acceleration from gear 1 to 6 reduces while the vehicle speed is increasing, alternatively the reserve acceleration will naturally decrease. Similarly, Figure 3.18 represents traction force for different gears.

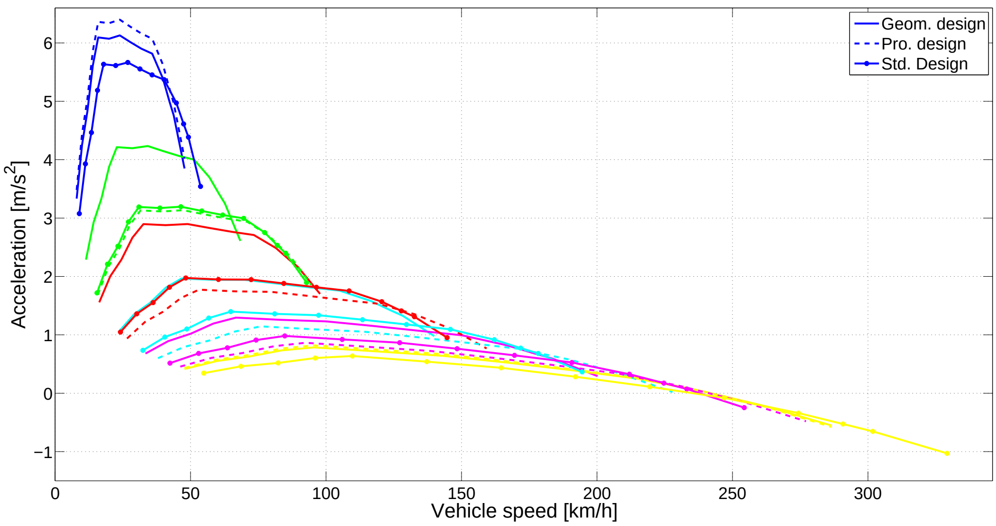

Figure 3.17: Acceleration curves performance

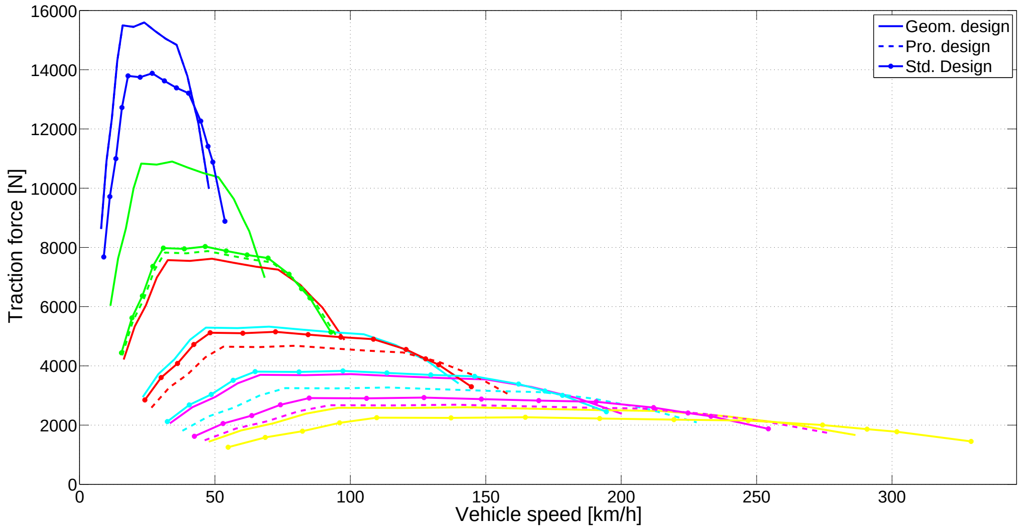

Figure 3.18: Traction curves performance

Gear ratio and ratio step change

Figure 3.19 compares standard gear ratio with Geometric and Progressive designs. It can be noticed that the progressive and standard gear ratios are decreasing similarly. The ratio step is the division of two adjacent ratios, written as follows:

Table 3.3: Compare different methods with standard gear ratio

	i_g1	i_g2	i_g3	i_g4	i_g5	i_g6
Std	13.91	8.04	5.16	3.84	2.93	2.27
Geom	15.62	10.91	7.63	4.33	3.73	2.61
Pro	15.62	7.88	4.69	3.28	2.69	2.61

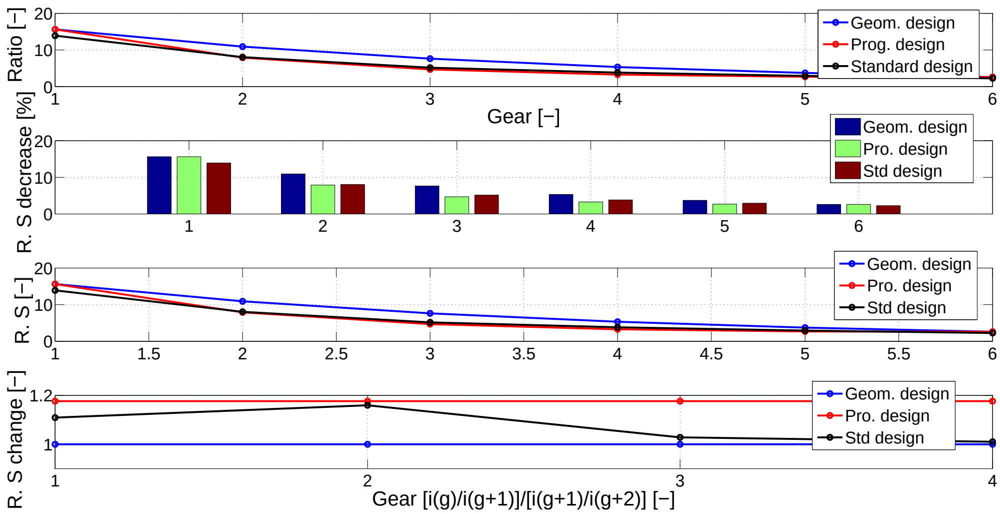

Figure 3.19: Gear ratio, step and mean value

$$\frac{\delta i}{\delta gear} = \frac{i_g}{i_{g_{i+1}}}. \tag{3.49}$$

The bandwidth is defined as the division of two adjacent ratio steps and it is written as follows:

$$\left(\frac{\delta i}{\delta gear}\right)^2 = \frac{i_g/i_{g_{i+1}}}{i_{g_{i+1}}/i_{g_{i+2}}}. \tag{3.50}$$

It would be ideal to have a constant step ratio. However, this cannot be realised because of finite ratio and the usage of double input shaft of Dual Clutch Transmission. The mean value of the ratio step change should be between 1.07 and 1.09, whilst the bandwidth should be less than 0.135 for this particular design.

Table 3.4: Gear ratio design mean value

	Geom. design	*Pro. design*	*Standard design*
Mean ratio	1	1.18	1.08

Traction loss

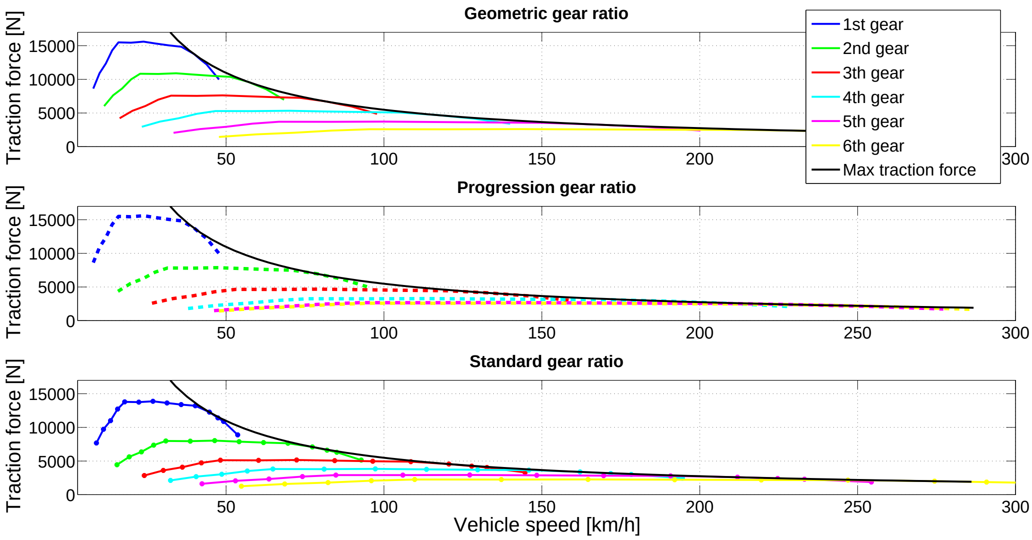

Figure 3.20: Acceleration curves performance

The objective of spacing the gear ratio is to minimise the loss of traction force (i.e intersection between the traction force curve of 1st, 2nd gear and maximum traction force, see Figure 3.20) because of the discontinuous stepping of gears. Traction loss is constant for Geometric design, however for progressive design the traction loss decreases as gear ratio increases.

Saw profile diagram

Saw profile diagram presents the transmission stepping in the velocity/engine-speed diagram, also the range of speed a vehicle can exploits under each gear ratio (see Figure 3.21). It gives a good overview of appropriate configuration of transmission gear ratios. It also allows to identify the earlier upshift possible without stalling the engine and the earlier downshift possible without exceeding the engine red line.

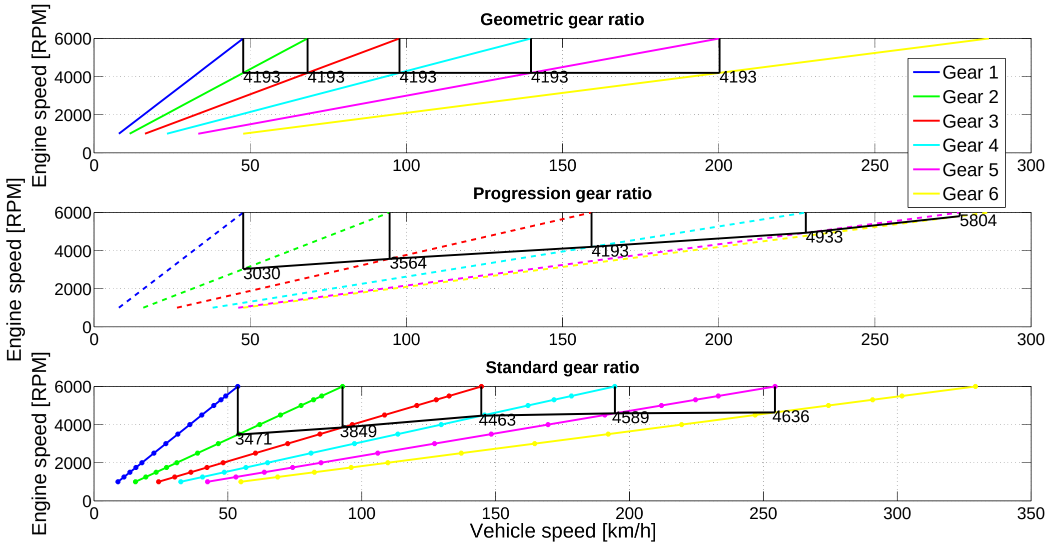

Figure 3.21: Saw curves performance

Fuel consumption

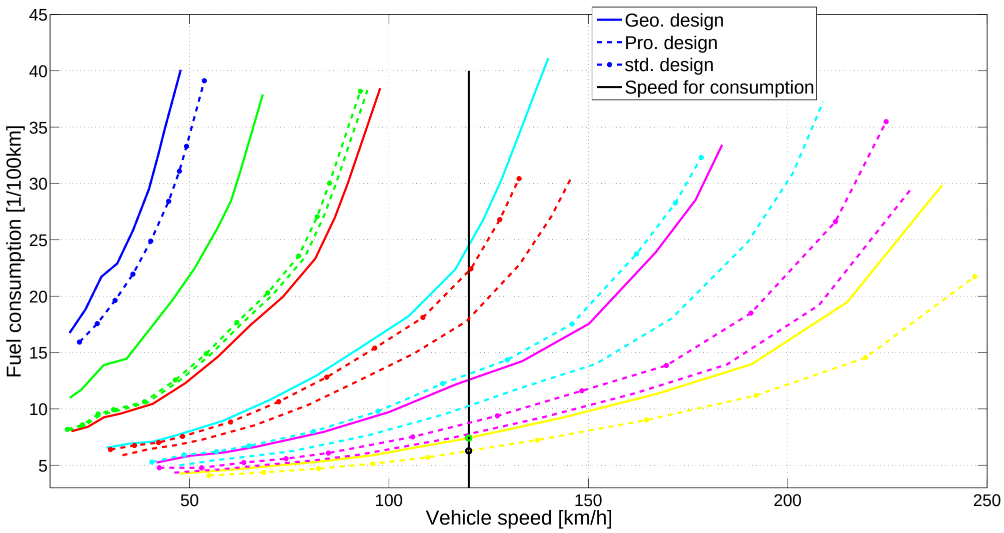

Figure 3.22: Fuel consumption at 120 km/h

Figure 3.22 shows fuel consumption represented by lines of static operation of each gear, and the resulting fuel consumption over the range of vehicle speed. The fuel consumption is calculated as follows:

$$FC = \frac{BSFC \times P_e}{\rho_{fuel} \times v}. \tag{3.51}$$

where ρ_{fuel} denotes fuel density. The fuel consumption criteria is based on the largest gear ratio (6th) at 120 km/h, and it is defined in the following table:

Table 3.5: Fuel consumption

	Geom. design	*Pro. design*	*Standard design*
Fuel consumption ($l/100km$)	7.4	7.4	6.3

This section has described the main criteria of gear ratio. The next step will be to design an algorithm to optimise gear ratio without degrading the vehicle performance, fuel consumption, emissions and comfort.

3.5 Concluding remarks

This chapter has described the powertrain model of the ROEWE 950 vehicle with its validation, and traditional design of gear ratio and gear shift map. This information is then exploited in Chapters 4 and 5 in order to define the problem formulation and develop algorithms for gear ratio and gear shift map optimisation.

Chapter 4

Problem formulation

4.1 Introduction

The optimisation problem formulation is fundamental to the efficient determination of optimal as well as practically realisable solutions. The problem formulation has been described in terms of some parameters and restrictions, where the parameters chosen to define the gear shift map and gear ratio are identified as design variables while restrictions are known as constraint conditions. The optimisation algorithm can then exploit the problem formulation, in order to obtain an appropriate solution. This chapter will present the problem formulation for i) the gear ship map optimisation ii) intermediate gear ratio design for the DCT 6 speed and iii) selection of the gear ratios considering Under-revving excess power. It adopts a traditional approach to problem formulation and includes for each problem the formulation of design variable, constraints, objective functions and boundaries on design variables.

4.2 Gear shift map problem formulation

This section presents the problem formulation for gear shift map optimisation. The role of the gear shift map is to move the engine towards its most efficient regions in terms of both emission and performance. However, the designer of any gear shift map is always constrained by the region that the engine can be placed on the BSFC map. Limitations arise in standard automated gearbox from the availability of only a fixed number of discrete gear ratios that are finite in number. In this thesis a 6 speed SAIC Dual Clutch Transmissions was used to develop the optimised shift map. The standard shift map is composed of 5 gear set including Upshift and Downshift.

4.2.1 Objective formulation

The optimisation algorithm should find the best solution, however the decision as to which criteria to use and the relative importance between criteria should lie with the engineer. This section considers a number of objectives formulation that can help differentiate alternative solutions. The main objectives are expressed and grouped in terms of emissions (Ngo, Hofman, Steinbuch & Serrarens 2013) (Yin et al. 2013), driveability (Le Guen et al. 2011) and durability. The objective formulation presented in this section have either been adopted from published work or designed to provide additional means to differentiate between similar solutions. The formulation was adapted for a minimisation problem, where the lowest values of the objectives represent the best solutions.

Objectives for CO_2 reduction

The objective which relates to emission reduction, adopts a standard formulation given (see Section 3.2.3), in Chapter 3, and is expressed as the sum of CO_2 over the distance travelled over the driving cycle.

The gear utilisation criterion is novel and relates to the means to achieve a low CO_2. It is based on the assumption that vehicles consume less fuel and produce less emissions when they operate on a higher gear. This new criterion aims to quantify the time spent on each gear, hence identify which gear is contributing to low CO_2. Accordingly, this objective function was designed to assist the engineer to quantify the gear usage during the NEDC and identify which gear ratios lead to lower CO_2 emissions. The gear utilisation criterion J_{PGU} is given by the inverse percentage of gear utilisation over a driving cycle. It is described by (Llamas et al. 2010):

$$J_{PGU} = \left(\sum_{u=1}^{6} G_u\%\alpha_u \right)^{-1} \tag{4.1}$$

where the weighting factors α_u (see Table 4.1) are defined in order to favour the time spent on specific gears, with

$$G_u\% = \frac{G_u \times 100}{\sum_{u=1}^{N_g=6} G_u} \tag{4.2}$$

where $G_u\%$ is the percentage of time spent on each gear, and u denotes each gear ratio.

In this thesis, the aim is to promote the use of higher gears, hence the higher the gear, the higher the associated weighting factors α_u (see Table 4.1).

Table 4.1: Normalised constant α_u

u	1	2	3	4	5	6
α_u	1	2	3	5	7	9

In addition taking inspiration from Le Guen et al. (2011), a new cost function was developed to minimise CO_2 by moving the engine operating points, expressed in terms of engine torque, T_e, and engine speed, w_e, towards the left side of the BSFC map. It is realised by minimising the distance (see Figure 4.1) between a reference, or anchor, point $O(w_{ref}, T_{ref})$ on the BSFC map, and the Upshift points for the throttle positions, t_k, of interest. The distance is calculated based on Upshift of each gear set: $g \in [1, 2, 3, 4, 5]$, and throttle positions t_k in 10% increment. The distance d$_{upshifts}$ is expressed as:

$$d_{upshifts} = \sum_{g=1}^{5} \left(\sum_{k=0}^{100} d_{g,t_k} \right) \tag{4.3}$$

where d_{g,t_k} denotes the distance for each Upshift set, and it is expressed as:

$$d_{g,t_k} = U_{g-1,g,t_k}(w_e, T_e) - O(w_{ref}, T_{ref}) \tag{4.4}$$

with $w_{ref} \in [780, 2000]$, $T_{ref} \in [80, 150]$, where $O(w_{ref}, T_{ref})$ and $U_{g-1,g,t_k}(w_e, T_e)$ represent the position of the anchor point fixed on the left edge of the BSFC map and the Upshift between the gears $(g - 1)$ and g, respectively.

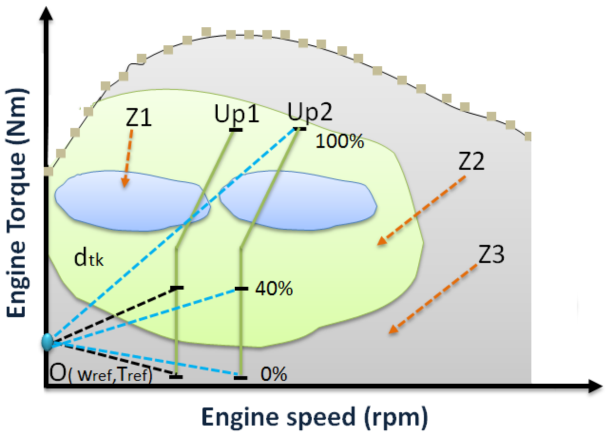

Figure 4.1: The distance (d$_{t_k}$) between the reference point $O(w_{ref}, T_{ref})$, and the Upshift 1 (Up$_1$) and Upshift 2 (Up$_2$) at 0%, 40% and 100% throttle positions, respectively. The grey dotted line represents the engine maximum torque. The engine speed varies from the minimum stable speed, stalling speed, to the maximum engine speed. Z1 represents the zone with the most efficient operating point, Z2 and Z3 are zones with higher fuel consumption

Objectives for performance

The second set of objectives aims to improve driveability. The standard Inverse Reserve Power (IRP) formulation was adopted to characterise the vehicle ability to accelerate (see Section 2.3.2, in Chapter 2):

A new set of criteria aims to simultaneously optimise CO_2 emissions and driveability, inspired from Le Guen et al. (2011), aims to maximise the percentage of time spent on the most efficient Engine Operating Point (EOP). It is achieved by dividing the BSFC map into zones defined based on the range of BSFC values. Three zones were defined based on cross-correlation study (see Section 6.1.1 in Chapter 6) between zones and the main objective function, CO_2 and IRP. The zone thresholds were tuned in order to relate zone 1 to CO_2 emissions as in this thesis, the main focus is based on minimising CO_2 emission. The ranges of BSFC values, [g/K m], for zone$_1$, zone$_2$ and zone$_3$ are $[200, 255[$, $[255, 265[$ and $[265\ max(BSFC)]$, respectively. To express this objective for a minimisation problem, the inverse of the percentage of time the engine spends in each of the three zones is calculated as follows:

$$\begin{cases} J_{z_1} &= \left(\frac{Zone_1 100}{\sum_{k=1}^{3} Zone_k W_k}\right)^{-1} \\ \\ J_{z_2} &= \left(\frac{Zone_2 100}{\sum_{k=1}^{3} Zone_k W_k}\right)^{-1} \\ \\ J_{z_3} &= \left(\frac{Zone_3 100}{\sum_{k=1}^{3} Zone_k W_k}\right)^{-1} \end{cases} \tag{4.5}$$

where k $\in$ [1, 2, 3], and W_k represent the individual weighting for each zones.

Based on the zone definition, J_{z_1} is the most efficient, followed by J_{z_2} and J_{z_3}. The optimisation algorithm will therefore aim to generate solutions corresponding to the engine operating most of the time in the most efficient regions, resulting in the smallest possible values for J_{z_1}.

Objectives for durability

The last criteria aims to improve gearbox durability by minimising the number of gear change in order to prolong gearbox longevity, and as a by-product very short successive up/down-down/up gear changes. It is expressed as sum of the absolute of the difference between successive gear changes:

$$J_{G_{change}} = \sum_{k=1}^{N-1} \left| \dot{dG}(k) \right| \tag{4.6}$$

where $\dot{dG}$ and N denote for successive gear change and maximum number of samples over the NEDC.

In addition to objectives which should be achieved with varying degrees of success, some hard constraints have to be obeyed to create the feasibility shift maps.

4.2.2 Constraint formulation

The constraints are defined as the limit boundaries of unsatisfactory solutions (Long 2014). Firstly, to limit the vehicle speed, upper limit values are imposed on the variables. Secondly, to ensure that the optimised variables represent feasible gear shift map. Such engineering requirements have led the definition of five types of constraints to complement the objective formulation.

Downshift/Upshift Crossing constraints

Two Downshift or two Upshift are not allowed to cross over. This is implemented by calculating the distance between two adjacent Downshift ($\mathrm{D}_{g,g-1,t_k}$, D_{g+1,g,t_k}) or Upshift (U_{g-1,g,t_k}, $\mathrm{U}_{g,g+1,t_k}$) and ensure that the distance is positive. It is expressed as follows:

$$\begin{cases} U_{g-1,g,t_k} - U_{g,g+1,t_k} & > & 0 \\ \\ D_{g,g-1,t_k} - D_{g+1,g,t_k} & > & 0 \end{cases} \tag{4.7}$$

Engine speed constraint

The engine speed should not be less than the minimum stable speed $\mathrm{Min}_{Eng_{speed}}$, nor should it be greater than the maximum allowable speed $\mathrm{Max}_{Eng_{speed}}$:

$$Min_{Eng_{speed}} \leq Eng_{speed} \leq Max_{Eng_{speed}} \tag{4.8}$$

where Eng_{speed} denotes for current engine speed.

Third, minimum hysteresis is required to prevent too frequent successive Downshift and Upshift about the same gears set for a small variation in vehicle speed. Such constraints were incorporated in the design variable formulation, and as a result are never violated (see Section 4.2.3).

Upshift and Downshift shapes

Fourth, the shape of the shift map is also controlled, by observing the percentage of slope, between two adjacent throttle positions ($\mathrm{U}_{g-1,g,t_{k+1}}$, U_{g-1,g,t_k}) of the same Upshift gear. It is given as follows:

$$Up_{Slope_{k+1}} = \frac{U_{g-1,g,t_{k+1}} - U_{g-1,g,t_k}}{U_{g-1,g,t_{k+1}}} 100\%. \tag{4.9}$$

Gear shift speed

Fifth and last constraint is to avoid a shift map with rapid gear change, Up/Down or Down/Up. A conservative value of minimum gear change time was carefully chosen based on the average gear change time of SAIC DCT, which is 400 ms.

4.2.3 Design variables

Design variables represent the free variables to be optimised. They are mapped from the gear shift points that represent the gear shift map. The new mapping presented in this thesis is applicable to any optimisation techniques. It has been designed to enforce the following engineering constraints: i) prevent crossing between Downshift and Upshift ii) maintain a minimum hysteresis between Downshift and Upshift to avoid frequent gear changes for small velocity variations.

The variable mapping expresses the Downshift (VD) and Upshift (VU), from a set of independent variables to a set of relative increments (ΔVD).

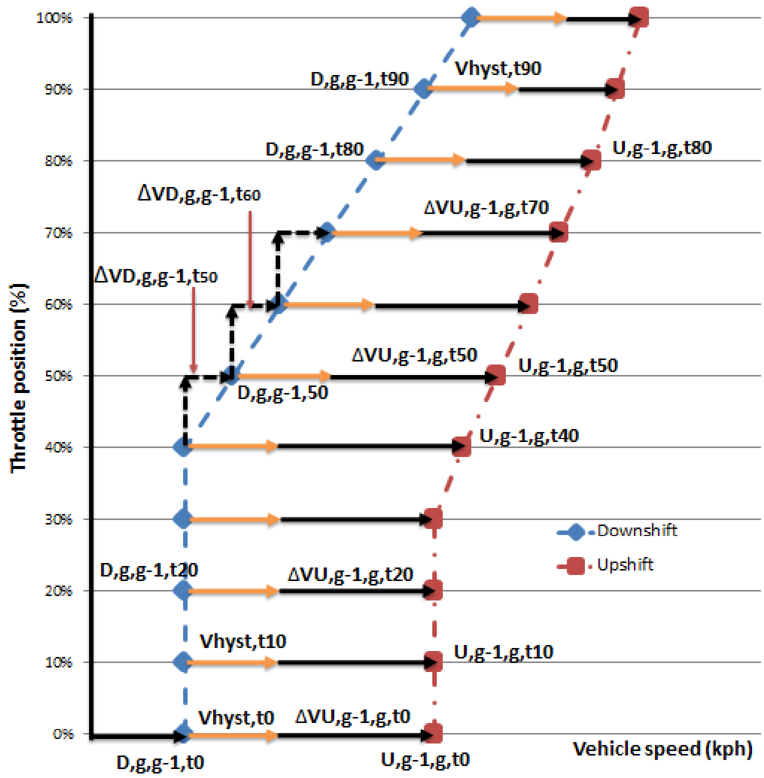

Figure 4.2: Conversion of a Downshift ($\Delta VDw_{g,g-1,t_k}$) and its corresponding Upshift ($\Delta VUp_{g-1,g,t_k}$) into design variables

Figure 4.2 illustrates the mapping of the gear shift map onto design variables. Each variable is expressed in terms of a specific throttle position $t\%$ and a set of consecutive gears $(g, g-1)$, where the subscripts g and $(g-1)$ denote for even gear and odd gear, respectively.

The shape of the Downshift and the determination of each Downshift point at M% throttle position, $D_{g,g-1,t_M}$, is given by successively adding throttle angle dependent increments $\Delta VD_{g-1,g,t_k}$ to the initial Downshift velocity at 0% throttle angle, VD_{g-1,g,t_k}, such that:

$$D_{g,g-1,t_M} = VD_{g,g-1,t_0} + \sum_{k=0}^{M} \Delta VD_{g,g-1,t_k}. \tag{4.10}$$

The corresponding Upshift point at the same M% throttle position, U_{g-1,g,t_M}, is derived by adding to the Downshift point, $D_{g,g-1,t_M}$,a velocity hysteresis, V_{hyst,t_M}, and an additional speed increment, $\Delta VD_{g-1,g,t_k}$, between the Downshift and the Upshift:

$$U_{g-1,g,t_M} = D_{g,g-1,t_M} + V_{hyst,t_M} + \Delta VU_{g-1,g,t_M}. \tag{4.11}$$

The inverse mapping to obtain the design variables from the points on the gear shift map is given by:

$$\Delta VD_{g,g-1,t_M} = D_{g,g-1,t_M} - D_{g,g-1,t_{M-1}}. \tag{4.12}$$

and

$$\Delta VU_{g-1,g,t_M} = U_{g-1,g,t_M} - V_{hyst,t_M} - D_{g,g-1,t_M}. \tag{4.13}$$

Without loss of generality, a throttle angle resolution of 10% was selected, $t_M \in [10, 20, 30, 40, 50, 60, 70, 80, 90]$, which is identical to that implemented on the transmission control unit (TCU). Assuming such a resolution (see Figure 4.2), the 110 shift points (5 gear sets with 11 Downshift $D_{g,g-1,t_k}$ and 11 Upshift U_{g-1,g,t_k} points) are mapped onto 165 free variables comprising 5 gear sets with 1 Downshift point $D_{g,g-1,t_M}$ at 0% throttle position and 10 throttle angle dependent

Downshift increment $\Delta VD_{g,g-1,t_k}$, 11 throttle angle dependent hysteresis V_{hyst,t_M} and 11 speed dependent increments $\Delta VU_{g-1,g,t_M}$.

The benefit of such mapping is that it enforces constraints associated with the relative position of up and down shift (see Section 4.2.3). The drawback is that it increases in the number of design variables to optimise. To reduce the number of design variables the hysteresis V_{hyst,t_M} was taken to be a constant determined based on proprietary requirements (i.e. $V_{hyst,t_0} = V_{hyst,t_{10}} = ... = V_{hyst,t_{100}}$). Such assumption reduces the number of variables by 54. To further reduce the number of design variables the Upshift and Downshift points at 0% and 100% throttle angles were fixed. Their computation is based on proprietary method targeting fuel economy and performance for the 0% and 100% throttle angles respectively. Such an approach required to meet design requirements resulted in a further reduction of the number of variables by 20. The number of design variables to optimise is therefore 91.

To further speed up the algorithm a resolution in terms of velocity increment $\Delta VD_{g,g-1,t_k}$ and $\Delta VU_{g-1,g,t_k}$ equivalent to 1 km/h was found to be suitable using a sensitivity analysis.

4.2.4 Variable bounds

The range and resolution of the design variables were carefully tailored to speed up the algorithm convergence whilst at the same time ensure that the solutions produced were suitable. To guide the algorithm towards practical solutions, the initial population was randomly generated based on a proprietary gear shift map designed using standard techniques. It was found empirically that the best compromise between solution space coverage and generation of practically acceptable solutions was obtained by restricting the change from the original gear shift map to ± 27%.

4.3 Gear ratio problem formulation

This section describes gear ratio problem formulation. The 6 speed SAIC DCT gearbox comprises 6 gear ratios. The first gear should allow the vehicle to start with a trailer under a road grade of 50% gradability.

The 4 intermediates gear ratio (2^{nd},3^{rd}, 4^{th} and 5^{th}) are utilised once the vehicle has started moving. The last gear ratio (6^{th}) in this thesis, is mainly designed for fuel economy and comfort especially for passenger car.

The next subsections describe the intermediate gear ratio problem formulation (see Section 4.3.1), the last gear formulation (see Section 4.3.2).

The first gear ratio design is not considered in this thesis as it is mainly dependant on vehicle gradability, and ability to carry a trailer. It is assumed that it is taken from the proprietary gear shift map.

4.3.1 Intermediate gear

Formulate objective function

The aim of intermediate gears is to allow the vehicle to move from high to low gear or the other way. They also allow to navigate through different zones of BSFC map and access the most efficient area of fuel consumption.

The performance of a set of gear ratio is mainly assessed by spreading the gear ratio on the engine BFSC map, which should guide the engineers to observe where each gear ratio is operating on the BSFC map. Three main objective functions are considered. The first is fuel consumption which is a by-product of CO_2 emissions. The second is IRP which is inversely proportional to CO_2 emissions, which helps the engineers to limit how far the optimiser can minimise CO_2 emissions while still conserving a minimum driveability. The third one is related to the intermediate gear ratio spacing, it is defined as the bandwidth of gear step ratio. The following statement lists the objectives function:

- CO_2 emission (Equation (3.4), see Section 3.2.3, in Chapter 3)
- Engine reserve power (Equation (2.2), see Section 2.3.2, in Chapter 2)
- Gear step change bandwidth (Equation (3.50), see Section 3.4.5, in Chapter 3)

After describing the objective functions. The next task is to outline any engineering constraints on objective functions. They are given in the next section.

Formulate constraints

In order to satisfy a minimum performance when designing the intermediate gears, the following requirement must be taken into account:

- The values of a set of gear ratio starting from the first to the last gear, must be defined in descending order.
- Contrarily to manual transmission, DCT is designed with two input shafts, which leads to geometric restriction. Consequently the mean value of the ratio step should be between 1.07 and 1.09, which represents a limited deviation of a gear set (see Section 3.4.5, Chapter 3).
- The gear step change bandwidth must be below a fixed constant defined by the engineer, a more common value should be less than 0.135 (see Equation (3.50), see Section 3.4.5, Chapter 3).

Design variables

There are four intermediate gear ratios to optimise, starting from G_2 to G_5, as G_1 and G_6 are predefined by gradability and fuel consumption respectively (see Section 3.4.5, in Chapter 3). The gear ratios G_2, G_3, G_4 and G_5 are defined in terms of the following design variables (ψ_a, ψ_b, ψ_c and ψ_d). The optimiser will aim to find the optimal design variables values from which the gear ratios will be reconstructed so that their effect can be simulated within the vehicle model.

$$\begin{cases} G_2 &= & G_1 - \psi_a \\ \\ G_3 &= & G_1 - \psi_a - \psi_b \\ \\ G_4 &= & G_1 - \psi_a - \psi_b - \psi_c \\ \\ G_5 &= & G_1 - \psi_a - \psi_b - \psi_c - \psi_d \end{cases} \tag{4.14}$$

where, ψ_a, ψ_b, ψ_c and ψ_d denote the design variables that relate to gear ratio G_2 to G_5, G_3 to G_5 and G_4 to G_5, respectively. This is achieved adopting the formulation described in (4.14) and by constraining the design variable to be strictly positive.

Design variable bounds

The final task of the formulation is to bound each design variable, by setting the lower and upper bounds of the design variables, such as to keep the solution in the feasible region $\mathbb{R}^n$ (Augusto et al. 2012) and to limit the solution space. A set of gear ratio is defined in descending order, which mean the gear ratio boundaries must follow the same pattern, and is given as:

$$\alpha_\upsilon^L \leq \psi_\upsilon \leq \psi_\upsilon^U, \quad \upsilon = \{a, b, c, d\} \tag{4.15}$$

where, ψ_υ^L and ψ_υ^U represent the lower and upper gear ratio design variables. They have been defined between ± 20% of the original gear ratio of SAIC 6 speed DCT.

4.3.2 Last gear ratio

The use of the last gear on a passenger vehicle is generally encouraged during cruising, when the vehicle is expected to favour fuel economy. As described in Section 3.4.3, in Chapter 3, the three types of design are Under-revving, Optimal and Over-revving. In this thesis, a saloon passenger car is considered, which leads the justification of the adoption of Under-revving design.

Objective functions

Similar competing objectives apply to the gear shift map optimisation and to the gear ratio optimisation. The optimisation of the last gear ratio is mainly dominated by fuel consumption, and the specific objective considered is the vehicle fuel consumption at 120 km/h (see Section 3.4.5, in Chapter 3). The CO_2 emission reduction should however not be at the total detriment of vehicle comfort and driveability. The latter is expressed as the vehicle excess power available for the last gear (see Section 3.4.5, in Chapter 3).

Constraints

The constraints imposed on the last gear ratio, are designed to ensure that the Over-revving corresponds to high performance (greater excess power and fuel consumption), unlikely to Under-revving with better fuel consumption (smaller excess power).

Design variables

The selection of the last gear ratio, considering Under-revving design, is obtained by increasing the last gear ratio of the optimal design (see Section 3.4.3, in Chapter 3). However there are two factors to be considered, where one factor ($i_{Fact,1}$) is for Under-revving, and a second factor $i_{Fact,2}$ for Over-revving. Both factors must be monitored, as the excess power of Under-revving is smaller than excess power of optimal design, contrarily the excess power of Over-revving is greater than excess power of optimal design. Consequently, there are two design variables, $i_{Fact,1}$ greater than 1, and $i_{Fact,2}$ smaller than 1.

Design variable bounds

The boundaries on the factors used to decrease or increase the gear ratio are given as follows:

$$i^L_{Fact,\tau} \leq i_{Fact,\tau} \leq i^U_{Fact,\tau}, \quad \tau = \{1, 2\} \tag{4.16}$$

where, τ are the two boundaries for the optimiser. The boundaries chosen for this thesis are given in the following Table 4.2:

Table 4.2: Under-revving and Over-revving factors bounds

	$i^L_{Fact,\tau}$	$i^U_{Fact,\tau}$
$i_{Fact,\tau}$	12	20

4.4 Handling of the objective functions

This section describes the decision maker to handle multi-objective functions for gear shift map and gear ratio.

4.4.1 Gear shift map with multi-objective functions

In this thesis, the decision maker for gear shift map is based on two principles. The first is a weighted sum combining all objective functions into one scalar. The second is based on Pareto optimal solutions (see Section 2.3.5, in Chapter 2). The two methods are describe as follows:

Weighted sum for gear shift map

The traditional weighted sum method, which combined multiple objective functions into one single scalar (see Section 2.3.5, in Chapter 2) is expressed as follows:

$$Obj_{GSM} = \sum \frac{J_{ob1(i)} W_{GSM_i}}{J_{N1(i)}} \tag{4.17}$$

$i \in [1, ..., 8]$

$J_{ob1} \in \left[J_{CO2}, J_{IRP}, J_{G_j}, J_{G_{ch}}, J_{Dist}, J_{z_1}, J_{z_2}, J_{z_3}\right]$

$J_{N1} \in \left[J_{CO2}(x_0), J_{IRP}(x_0), J_{G_j}(x_0), J_{G_{ch}}(x_0), J_{Dist}(x_0), J_{z_1}(x_0), J_{z_2}(x_0), J_{z_3}(x_0)\right]$

where W_{GSM_i} denotes the weighting associated with individual objectives $J_{ob(i)}$ function. J_{CO2}, J_{IRP}, J_{G_j}, $J_{G_{ch}}$, J_{Dist}, J_{z_1}, J_{z_2}, J_{z_3} denote the objective functions for CO_2, zone 1, IRP, gear change frequency, time spent on each specific gear, distance, zone 1, zone 2 and zone 3 respectively. J_{N1} represents the values for each objective function corresponding to the current manufacturer gear shit map, which is used as a reference for subsequent optimisation (see Section 2.3.5, in Chapter 2). Additionally W_{GSM_i} are positive and must satisfy:

$$\sum_{i=1}^{i=8} W_{GSM_i} = 1, \quad W_{GSM_i} \in (0, 1) \tag{4.18}$$

Modified Pareto for gear shift map

In this thesis, a modified Pareto based on Haas et al. (1998) is applied. It uses objective weighting Pareto ranking to differentiate between non dominated solutions given by:

$$J_{Pare_{rank1}} = 1 + N_{Dominated} + \sum W_{GSM_i} \frac{J_{ob1(i)}/J_{N1}(i)}{Max\left(J_{ob1(i)}/J_{N1}(i)\right)} \tag{4.19}$$

$N_{Dominated}$ represents the number of non-dominated solution.

4.4.2 Gear ratio with multi-objective functions

The methods described above to handle multi-objective, the same principles is also applied to gear ratio. It is given as follows:

Weighted sum for gear ratio

$$Obj_{GR} = \sum \frac{J_{ob2(j)} W_{GR_j}}{J_{N2(j)}} \tag{4.20}$$

$j \in [1, 2 \; and \; 3]$

$J_{ob2} \in [J_{CO2}, J_{IRP}, J_{Bwd}]$

$J_{N2} \in \left[J_{CO2}(x_0), J_{IRP}(x_0), J_{Bwd}(x_0)\right]$

where W_{GR_j} denotes the weighting associated with individual objectives $J_{ob2(i)}$. J_{Bwd} denotes the gear ratio step bandwidth. J_{N2} represents the objective function with the initial gear ratio design variable. It is used to normalise each objective function during optimisation process. Also, W_{GR_i} must be positive and satisfying:

$$\sum_{i=8}^{i=1} W_{GR_i} = 1, \quad W_{GR_i} \in (0, 1) \tag{4.21}$$

Modified Pareto for gear ratio

Similar to Equation (4.19), the same pattern is utilised to define the modified Pareto for gear ratio. It is given as follows:

$$J_{Pare_{rank2}} = 1 + N_{Dominated} + \sum W_{GR_i} \frac{J_{ob2(i)}/J_{N2(i)}}{Max\left(J_{ob2(i)}/J_{N2(i)}\right)} \tag{4.22}$$

4.5 Concluding remarks

This chapter has provided the problem formulation for both shift map and gear ratio optimisations. The problem formulation is the most important stage in optimisation. An identical approach has been adopted for each problem considered: objective and constraints formulation, design variable and bounds formulation. Five objective formulations have been proposed in this thesis to supplement widely accepted formulation. These objectives aim to help users identify the most suitable solutions, typically by observing the performance of engine operating point on the BSFC map, whilst the specific objectives are expressed using various formulations. Additionally, the overall solution of the problem considered involves competing objectives.

The key to success is rooted in the handling of objectives which are presented in Chapter 2. The new design variable formulation is one of the significant contributions of this thesis. It aims to simplify the design process for a gear shift map, also, it allows the user to specify a range of throttle positions and minimum hysteresis in order to guide the optimiser more accurately.

Having formulated the optimisation problem, the next chapter describes various optimisers used to find suitable solutions for either gear shift map, gear ratio or simultaneously weighing the best combination of gear shift map and gear ratio.

Chapter 5

Evolutionary algorithm & swarm intelligence for shift map and gear ratio optimisation

5.1 Introduction

This Chapter presents the main technical contributions of this thesis. It describes the algorithms developed to optimise the gear shift map as well as the gear ratio. The chapter starts with the description of the Multi-Objective Genetic Algorithm (MOGA) modified to accommodate the proposed problem specific operator and a repair mechanism. The second nature inspired algorithm is then presented, namely the Multi-Objective Cuckoo Search (MOCS), which is also modified to accommodate a new local search applied to optimise gear ratio. It presents the different behaviour of the nature inspired techniques implemented in this thesis to justify their selection and their specific features. Finally, it describes the culmination of the work by merging MOGA, MOCS and constrained optimisation, implemented within the MATLAB interior-point algorithm, for the combined gear ratio and gear shift map optimisation.

5.2 Problem specific MOGA

A MOGA was selected to optimise a six speed DCT gear shift map due to its ability to handle competing and changing objectives (see Section 4.2.1 in Chapter 4). Whilst many objectives have been formulated, the two main objectives are to lower the CO_2 whilst keeping the driveability acceptable. To focus the search towards lowering CO_2, a modified Pareto ranking (Haas et al. 1998) was adopted (see Section 4.4.1 , in Chapter 4).

The standard MOGA (Konak et al. 2006) was complemented by a new repair mechanism and a new local search operator, as shown in Figure 5.1 and 5.2. The aim of these improvements is to exploit problem specific features to find better solutions faster. The new repair mechanism was developed to handle minimum reserve power requirements (see Section 5.2.2, in Chapter 4). The new problem specific operator referred as gear early shifting (GES) operator was developed to focus the search towards good regions, in terms of CO_2 emissions, of the solution space (see Section 5.2.1). To prevent the algorithm from becoming trapped in a local minima and producing gear shift with similar characteristics, the GES operator is only applied every N generations, where N is a user tunable parameter.

To avoid unrealistic gear shift map to be accepted, each solution is first checked against the constraints defined in Section 4.2.2. Then the vehicle simulator is run for each candidate solution. If the simulator does not complete the drive cycle simulation, the solution is rejected (see Figure 5.2) as it violates the gear shifting logic and/or is not compliant with the vehicle BSFC map.

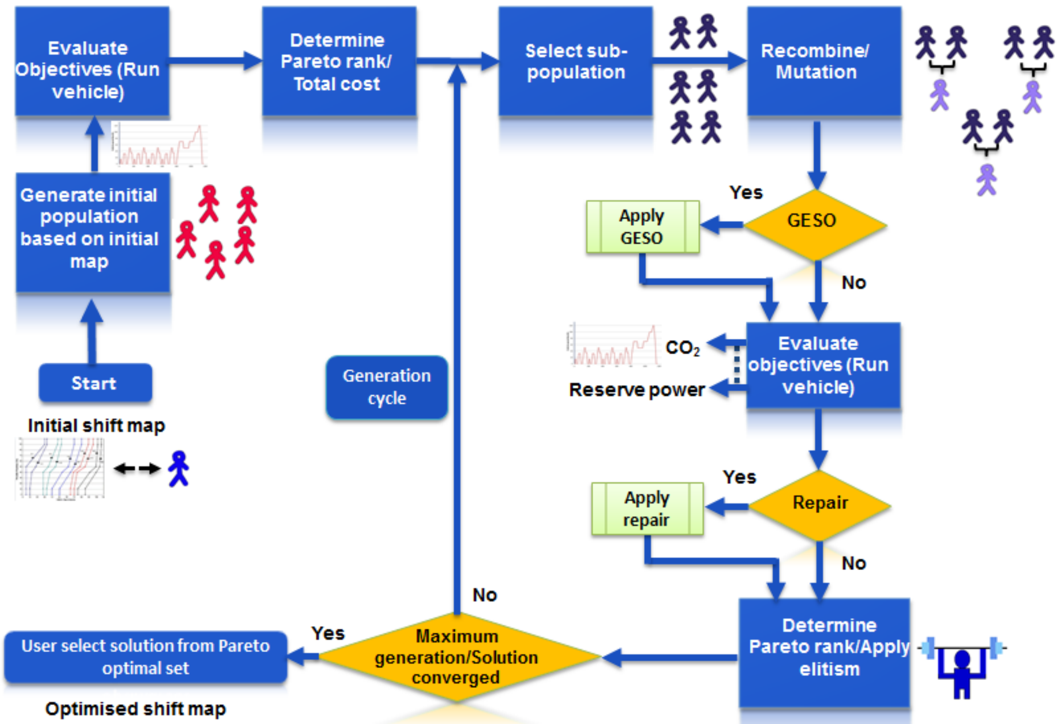

Figure 5.1: Multi-Objective Genetic Algorithm with problem specific (GES) operator and repair mechanism to ensure reserve power constraints are met by the optimised solutions

```
Create N initial solutions
Evaluate objective functions
      Run vehicle model
      Reject infeasible solutions
      Calculate objectives
if Reserve power limit reached then
    Apply Repair mechanism
end if
Determine modified Pareto cost
Calculate fitness
for i = 1 to Max generation do
    Select children for recombination
    Apply recombination & mutation
    if mod(N,3) == 1 then
        Apply GES
    end if
    Evaluate objective functions
      Run vehicle model
      Reject infeasible solutions
      Calculate objectives
    if Reserve power limit reached then
        Apply Repair mechanism
    end if
    Determine modified Pareto cost
    Calculate fitness
    Keep the N best solution
end for
```

Figure 5.2: Multi-Objective Genetic Algorithm with GES and repair mechanism

5.2.1 Local search: gear early shifting (GES) operator

The new GES operator aims to reduce CO_2 emissions by producing early gear shift to reach as quickly as possible the most efficient area of the BSFC map. It is realised by reducing the velocity difference between Upshift and Downshift, where the speed increment $\Delta VU_{g,g-1,t_M}$ are reduced by a ratio $\beta_k \in [0.25, 0.50, 0.75]$ expressed in percentages to form:

$$\begin{cases} \Delta VU_{25g,g-1,t_M} &= \beta_{25}\Delta VU_{g,g-1,t_M} \\ \\ \Delta VU_{50g,g-1,t_M} &= \beta_{50}\Delta VU_{g,g-1,t_M} \\ \\ \Delta VU_{75g,g-1,t_M} &= \beta_{75}\Delta VU_{g,g-1,t_M} \end{cases} \tag{5.1}$$

In this thesis the same set of ratios $\beta_k < 1$ are applied to each gear set and each throttle angle. Investigating randomly generated ratio is considered as further work. Similarly is the investigation of the benefits of using ratios $\beta_k > 1$ to increase the difference between Upshift and Downshift, thereby increasing the hysteresis between up and down shift, resulting in making quick gear changes less likely, but at the cost of higher CO_2.

Parents used by the GES operator are selected based on the following rules. First, N_{CO2} candidate solutions are randomly selected among the $N_{bestCO2}$ individuals in term of CO_2. Then N_{IRP} candidate solutions are randomly selected among $N_{bestIRP}$ individuals in term of IRP. Finally N_{Diff} candidate solutions are selected according to the highest difference in terms of Euclidean distance CO_2 and IRP, between successive point on Pareto set. In this work $N_{bestCO2}$ =$N_{bestIRP}$ = 10, N_{CO2} = N_{IRP} = N_{Diff} =1. Figure 5.3 summarises the algorithm with i_{ind} denoting each individual solution, C and P with subscript CO_2, IRP and Diff denoting the children and parents for the three criteria considered respectively.

Randomly select N_{CO2} amongst $\mathrm{N}_{bestCO2}$ individuals
Randomly select N_{IRP} amongst $\mathrm{N}_{bestIRP}$ individuals
Select N_{Diff} individual
for $i_{ind} = 1$ to $N_{CO2} + N_{IRP} + N_{Diff}$ **do**
    Calculate speed difference $\Delta VU_{g,g-1,t_M}$
    Create 3 new maps per candidate solution to move Upshift towards the Downshift
    for $k = 1$ *to* 3 **do**
        Replace $\Delta VU_{g-1,g,t_M}$ in P by β_k $\Delta VU_{g,g-1,t_M}$ to form C
    end for
end for

Figure 5.3: Local search algorithm: Gear Early Shifting Operator

5.2.2 Solution validation repair mechanism

The main emphasise of MOGA is to reduce CO_2. This can lead to solutions that are on the limit or even inappropriate in terms of reserve power, i.e. ability to accelerate after a gear change. A method called *GeneRepair* operator was proposed by Mitchell et al. (2003), and used to correct invalid tours which may be generated following crossover and mutation in Travelling Salesman Problem. Similarly, a repair mechanism has been devised to detect conditions when the reserve power is insufficient at any time during the drive cycle and automatically adjust the appropriate Upshift to ensure that the minimum requirements in terms of reserve power are met, see Figure 5.4.

Calculate reserve power at each time instant
while Reserve Power $<$ threshold for Upshift gear $VU_{g,g-1,t_k}$ **do**
    Move each affected Upshift gear $VU_{g,g-1,t_k}$ to the right to form $rVU_{g,g-1,t_k}$
        Run vehicle model
        Reject infeasible solutions
        Calculate objectives
    Calculate reserve power at each time instant
    Replace initial solutions by repaired ones
end while

Figure 5.4: Repair mechanism algorithm

5.2.3 Conclusions on problem specific MOGA

This section has presented a MOGA combined with problem specific operator to improve solutions quality and rate of convergence. Additionally, a repair mechanism was developed to insure that solutions produced are practically realisable by enforcing a minimum reserve power constraints. The relative benefits of the proposed modification are evaluated in Chapter 7. The following section describes Cuckoo Search algorithm develop to optimise gear ratio.

5.3 Multi-Objective Cuckoo search

This section, describes Cuckoo Search (CS) algorithm (Yang & Deb 2013) modified for the context of gear ratio optimisation. In addition to the standard Levy Flight operator, it includes Bat, Firefly and Flower Pollination. Theses operators are integrated within the Cuckoo Search to generate new optimised gear ratio. The operator combination aims to improve the performance of the existing Cuckoo Search by exploiting the benefits of other operators.

There are three objectives that are minimised. The most important is the CO_2 followed by IRP and bandwidth. Note that the bandwidth is also formulated as a constraint together with the gear ratio step change (see Section 3.4.5 in Chapter 3).

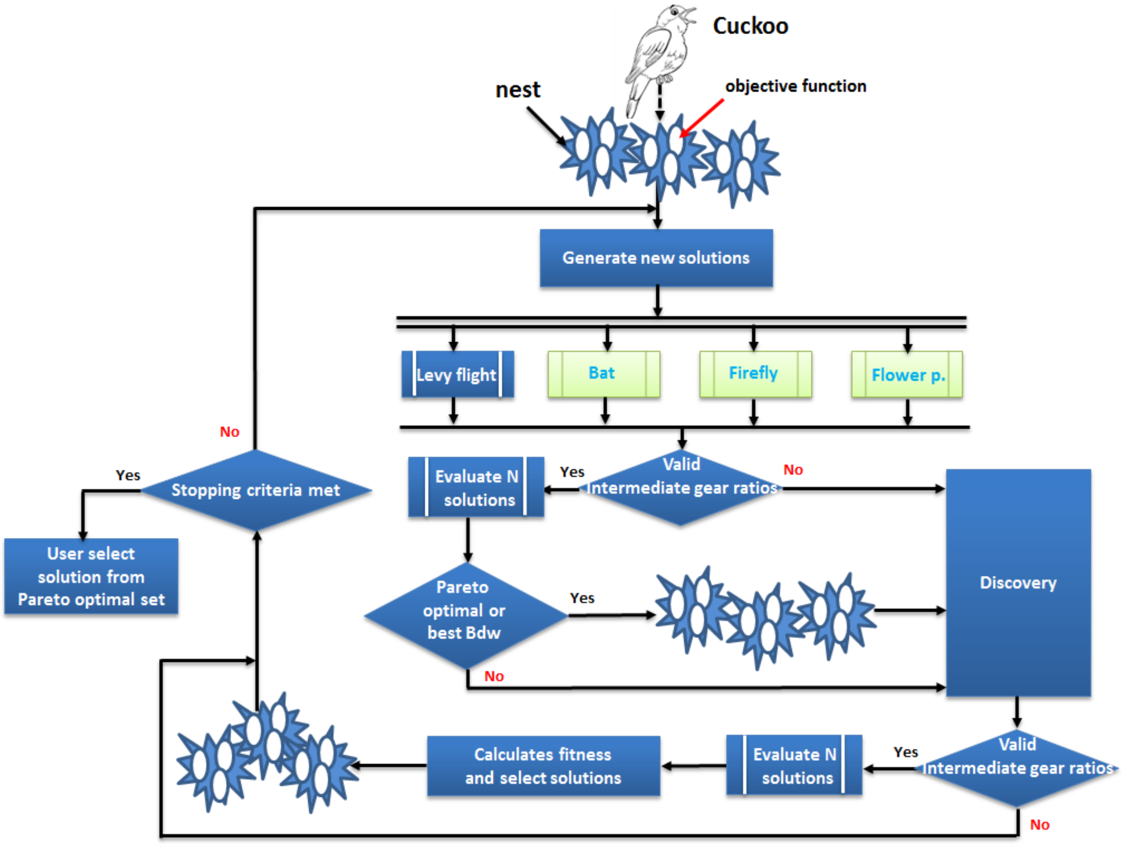

Figure 5.5: Multi-Objective Cuckoo Search with Levy Flight operator supplemented by, Bat, Firefly and Flower Pollination operator for gear ratio optimisation.

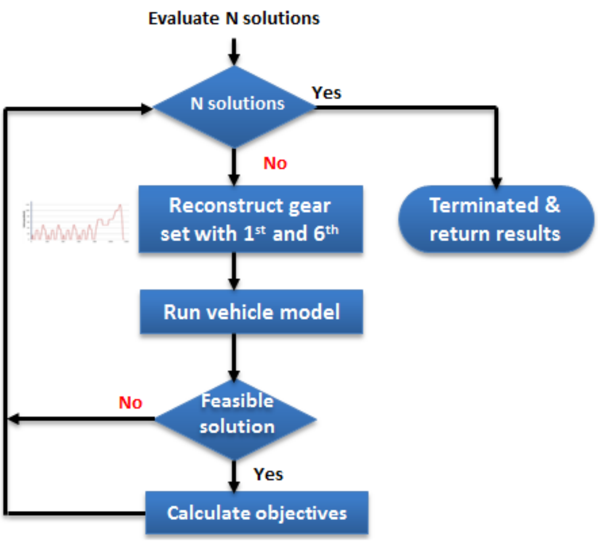

Figure 5.6: Solutions evaluations flowchart in MOCS

In this research, CS has been developed to solve a Multi-Objective Optimisation Problem (MOOP), and uses a modified Pareto rangking to find a set of non-dominated solutions based on 4.19. There are four design variables related to a set of gear ratio to be optimised (see Section 4.3.1 in Chapter 4). The CS for gear ratio optimisation is illustrated in Figures 5.5 and 5.6 and described in Figures 5.7, 5.8. The initialisation stage generates x_i solutions comprising the four design variables (ψ_a, ψ_b, ψ_c and ψ_d) that convert onto 6 gear ratios (see Section 4.3.1). Additionally, considering a MOOP, a Cuckoo can lays multiple eggs (objective functions) in a nest. The main goal is to replace the current value of the objective functions by new solutions in the nest. At each generation, the following tasks are accomplished: (i) Generate new gear set solutions by applying either Levy Fly, Bat, Firefly or Flower Pollination operators. (ii) Reconstruct the gear set, run the vehicle model, evaluate each solutions and calculate the objectives (J_{CO2}, J_{IRP} and J_{Bwd}) for each solutions. (iii) Check if any new solutions i_n are Pareto optimal, then replace the worse solutions, else choose j_n nest randomly and replace them by i_n if J$_{Bwd}$ is better. (vi) New optimised set of gear ratios l_n are generated by abandoning the worse solutions with the probability of $P_a \in [0, 1]$, repeat (ii). (v) Add new solutions created, l_n, to the population, where the modified Pareto cost and fitness of each solutions are calculated. Then classify the solutions in ascending order, finally keep the n host nest with best gear set for the next generation. (vi) Repeat until convergence or until a user defined time limit is reached.

$$x_i = \left[\psi_{a_i}, \psi_{b_i}, \psi_{c_i}, \psi_{d_i}\right] \tag{5.2}$$

Define x_i individual with n_{host} nests ($i = [1, .., n_{host}]$)
Initialise the corresponding cost $J_{CO2}(x_i)$, $J_{IRP}(x_i)$ and $J_{Bwd}(x_i)$
for $Gen_R = 1$ to $Max\ generation$ **do**
  Get cuckoo i_n randomly by local operator:
    Levy flights
    or Bat motion
    or Firefly motion
    or Flower pollenation
  if $Valid\ intermediates\ gears$ **then**
    Evaluate solutions
    Check if Pareto optimal
    if j_n solutions dominate i_n **then**
      Keep solutions of nest j_n for the new population
    else
      Choose a nest j_n randomly among n_{host}
      Replace nest i_n by the new solution set of nest j_n if better J_{Bwd}
    end if
  end if
  Create new solutions of nest l_n by abandoning a fraction of (p_a) of worse nests
  if $Valid\ intermediates\ gears$ **then**
    Evaluate solutions l_n
  end if
  Keep new solutions of nest l_n for the new population
  Determine modified Pareto cost of new population
  Calculate fitness of the new population
  Select and keep n_{host} nests with best solutions
end for

Figure 5.7: Multi-Objective Cuckoo with hybrid operators for gear ratio optimisation

Evaluate objective functions for N nest solution
  Reconstruct gear set from X_i and 1^{st} and 6^{th}
  Run vehicle model
  Reject infeasible solution
  Calculate objectives J_{CO2}, J_{IRP} and J_{Bwd}

Figure 5.8: Multi-Objective Cuckoo with hybrid operators for gear ratio optimisation

5.3.1 Local search component

This subsection describes different operators used within the Cuckoo Search:

Levy Flight

The original Cuckoo search relies on the Levy flight operator to generate new solutions. It is a random walk, where the step size is based on Levy distribution. It was adopted in this work, as Levy flight is efficient in terms of exploring large-scale search space. A new solution x_i^{t+1} is defined as follows:

$$x_i^{t+1} = x_i^t + \theta \oplus Levy(\tau) \tag{5.3}$$

where, α represents the step size scaling factor given as follows:

$$\alpha = \theta_0(x_i^t - x_{cur_{best1}}^t) \tag{5.4}$$

where x_i^t is the current solution, and θ_0 is a constant, whilst the expression in the bracket corresponds to the difference between the current and the best solution in the nest respectively. Generating new solutions from Levy flight is not straightforward, a simple scheme was defined by Yang (2014) can be described as follows:

$$Levy\left(\tau_1\right) = \frac{u}{|v|^{1/\tau_1}} \tag{5.5}$$

where, u and v are obtained from a normal distribution, and it is given as follows:

$$u \sim N(0, \sigma_u^2)\ v \sim N(0, \sigma_v^2) \tag{5.6}$$

with

$$\sigma_u = \frac{\Gamma(1+\lambda)}{\lambda\Gamma((1+\lambda)/2)}\frac{\sin(\pi\lambda/2)}{2^{(\lambda-1)/2}} \tag{5.7}$$

where Γ is the standard Gamma function.

Bat operator

The Bat operator is used in this search, as it has the particularity to use frequency tuning by updating a current solution to obtain a new solutions. The main idea is inspired by echolocation of microbats. A solution is represented by a virtual bat position and its corresponding velocity. It is given by the following expression:

$$Q_i = Q_{min} + (Q_{max} - Q_{min})\beta_{BA} \tag{5.8}$$

where Q_i represents the wavelength. It is defined between a minimum ($Q_{min} = 0$) and maximum ($Q_{max}=2$) range of wavelength. The range of wavelength expressed the travelling range of pulse, which is depending on the frequencies. Consequently, tuning the frequency can impact on exploration and exploitation. $\beta_{BA} \in [0, 1]$ is drawn from a uniform distribution.

$$v_i^{t+1} = v_i^t + (x_i^t - x_{cur_{best2}}^t)Q_i \tag{5.9}$$

$$x_i^{t+1} = x_i^t + v_i^{t+1} \tag{5.10}$$

where, $x_{cur_{best2}}^t$ denotes for current best location (current optimal gear ratio) which has been found so far among the n_{host} virtual bats location. The original Bat algorithm includes a local search, presented by the loudness, in this research loudness is not considered as only Bat algorithm operator is utilised. Also, it is assumed that the pulsation rate is fixed. The interesting particularity of Bat algorithm, it captures the advantage of many algorithm such as the standard of PSO where the frequency controls the space area of swarming particles motions, and Harmony Search(HS) by varying the loudness and pulsation rate. It can be noticed that the updated solution x_i is similar to Arithmetic crossover from GA (Ladkany 2012).

Firefly

The Firefly algorithm (FA) is based on the flashing pattern of fireflies. The operator of Firefly is obtained from the original Fireflies Algorithm. A potential solution of gear ratio is defined as a firefly location. The following assumptions are made to mimic the behaviour of the algorithm:

- All fireflies are unisex, which mean that any firefly can be attracted by any other firefly.
- The attractiveness corresponds to the brightness, and it decreases when the distance increases.
- The objective function is represented by the brightness of a firefly.

The original FA is based on maximisation problem, as the firefly attractiveness simply proportional to the light intensity, which presents the objective function. Therefore, in this search the objective function of each firefly were inverted in order to convert the problem into minimisation problem. The variation of attractiveness β_{ffly} and distance of light intensity r_{ffly} are given as follows:

$$\beta_{ffly} = \beta_{ffly_0} e^{-\gamma_{ffly}.r^2_{ffly}} \tag{5.11}$$

where β_{ffly_0} is the attractiveness at distance $r = 0$.

$$x_i^{t+1} = x_i^t + \beta_{ffly_0} e^{-\gamma_{ffly}.r^2_{ffly,(i,j)}}.(x_i^t - x_j^t) + \alpha_t \mu_i^t \tag{5.12}$$

where x_i is the motion of Firefly i attracted to another, $r^2_{ffly,(i,j)}$, is the distance between any two Fireflies i and j located at x_i and x_j, it is given by the Euclidean distance:

$$r_{ffly,(i,j)} = \sqrt{\sum_{v=a}^{v=d} (x_{i,v} - x_{j,v})^2} \tag{5.13}$$

where, $x_{i,v}$ is the vth component of the gear ratio design variables, which represents the spatial coordinate x_i. Considering gear ratio design variables, the coordinates between two Fireflies are described as follows:

$$r_{ffly,(i,j)} = \sqrt{(x_{i,a} - x_{j,a})^2 + (x_{i,b} - x_{j,b})^2 + (x_{i,c} - x_{j,c})^2 + (x_{i,d} - x_{j,d})^2} \tag{5.14}$$

After describing the formulations, the Firefly operator can be summarised as follows:

for $i = 1 : n_{host}$ **do**
    for $j = 1 : n_{host}$ **do**
        if $-I_i < -I_j$ **then**
            Move firefly i towards j
        end if
    end for
end for

Figure 5.9: Firefly operator for gear ratio optimisation

Figure 5.9 illustrates the core component of the algorithm, where two iterative loops are used to compare each firefly (gear ratio) light intensity (given by the weighted sum of the objective functions, see Section 4.4.2, in Chapter 4), and move any firefly towards the firefly with the strongest light. I_i and I_j denote the light intensity of iterative loop 1 and loop 2 respectively. The advantage of Firefly is to always look forward to move all Firefly toward the current best solution, however the drawback of the algorithm might limit the exploration of different research space. The last component is based on Flower Pollination algorithm which is described in the following section.

Flower pollination

The flower pollination operator is obtained from flower natural reproduction. In nature there are two types of flowers. The first is biotic, where its reproduction is based on transfer of pollen via pollinator such as insects or animals. The second is abiotic, which unlike the biotic, does not necessitate any pollinator as wind and diffusion are the main factor for their pollination. In this search, only the local component was used to create new potential solution of gear ratio. Before describing the Flower Pollination operator, the following two rules are assumed:

- Considering local pollination, abiotic and self-pollination from the neighbourhood flower are used.
- Biotic pollinators can develop flower constancy, which is similar to a reproduction probability that is commensurate to the similarity of two flowers considered.

After defining the assumptions, a new gear ratio design is obtained using the Flower Pollination operator which is given as follows:

$$x_i^{t+1} = x_i^t + \epsilon_{FP}(x_j^t - x_k^t) \tag{5.15}$$

where x_j^t and x_k^t denote pollen from flower 1 (randomly selected gear ratio among the current population) and flower 2 of the same species respectively. This allows to mimic the flower constancy in a restricted neighbourhood. ϵ_{FP} is drawn from a uniform distribution. FA operator is similar to heuristic crossover (Kaya et al. 2011), it has the advantage of directing the search in a promising direction, also it has the particularity to relocate the search when the solutions are clustered. However, it has the drawback of preventing the search space to focus on one direction.

5.3.2 Conclusion

This section has presented a hybrid MOCS algorithm. The hybridization supplemented Levy Flight operator with operators originally developed for Bat, Firefly and Flower Pollination. These operators are arithmetic and heuristic crossover operator, and the combine of these operators can improve the algorithm in term of exploration and exploitation.

The following section describes how MOGA and MOCS are combined together to simultaneously optimise gear ratio and shift map.

5.4 Multi-Objective Genetic Algorithm & Cuckoo Search

The main concept of this hybrid design combining MOGA, cuckoo and constrained optimisation is to exploit the relative strengths as well as solutions previously obtained when considering each problem independently. CS is employed to obtain a set of optimised gear ratio. GA is used to generate a set of optimised gear shift map in favour to low CO_2 emission whilst keeping a good driveability. The following section describes the algorithms combination core.

5.4.1 Optimisation framework

The approach adopted in this work is illustrated in Figure 5.10, where three iterative loops are used to combine the algorithms for gear ratio and gear shift map optimisation. The first iterative loop vary a set of Starter gear ratio including the initial starter gear ratio, which has been defined manually with respect to gradeability (see Section 3.4.5, in Chapter 3). A second iterative loop is then used to select the last gear ratio pre-defined by interior-point algorithm. CS algorithm is integrated in the second iterative loop, where a set of intermediate gear ratios are optimised. The third iterative loop is used to select a set of gear ratio, then applied GA to obtain various optimised shift maps.

```
Define the first gear ratio based on the vehicle gradeability
Define the initial gear ratio
Generate a third first gear by taking the average of the above two gears
Define parameters for gear ratio and gear shift map
for i = 1 : n_StartG do
    Apply interior-point algorithm to optimise the last gear ratio using 4 dif-
    ferent sets of objectives to give 4 possible values for the last gear ratio.
    for j = 1 : n_LastG do
        Select first and last gear ratio
        Define the number of generation
        Apply CS to optimised set of gear ratio
        for l = 1 : n_GearSet do
            Select a set of optimised gear ratio
            Update initial shift map based on optimised gear ratio
            Apply MOGA with repair mechanism and GES
            Nested structure function
                Save gear set
                Save gear ratio
                Save optimised gear shift maps
                Save performance results
        end for
    end for
end for
```

Figure 5.10: Combined gear ratio & shift map optimisation

5.5 Selection mechanism of operators

This section describes and compares an experimental test to generate offspring (solutions) based on various operators defined in this chapter.

The key evolutionary operators can be summarised by *crossover*, *mutation* and *selection* (see Section 2.4, in Chapter 2). The role of crossover is to act as local search within a subspace, and it mainly contributes to the system convergence. Mutation provides a method for global search, and can be defined as randomization approach. Selection method gives a powerful driving force to the algorithm to evolve toward the desired search space.

It is worth pointing out that mutation can take different forms. The generation of new offspring created by the operator of Levy Flight (5.3), Bat (5.10), Firefly (5.12) and Flower pollination (5.15) algorithms are mainly mutation based. These operator use stochastic moves or randomisation method to generation the next offspring.

Levy Flight, Bat and Flower pollination algorithms operators use current best solution among the population to make the next moves. In FA operator, there is no current best solution, however it uses a ranking and selection methods during the update of offspring based on two iterative loops. It can subdivide into multiple subgroups, where each subgroup can potentially swarm around a local mode.

In order to assess each operator abilities of reproducing offspring, an experimental test was set up. The experimental set up consists of generating various offspring based on different crossover operators (direct, intermediate and extended line recombination) from GA, and operators (Levy Flight, Bat, Firefly and Flower pollination) from hybrid MOCS algorithm developed in this thesis. This case study considered the gear ratio with four design variables denoted by ψ_a, ψ_b, ψ_c and ψ_d. Two parents (P1 and P2) are selected from a preliminary test and replicated 3000 times in order to be used by various operators to generate offspring.

Figures 5.11 and 5.12 illustrate the spread of offspring produces by crossover operators from GA and operators from MOCS. In Figure 5.12, it is clear that Levy flight only focus on the two parents to generate offspring. However GA crossover, Bat and Flower pollination algorithm operators generate offspring near both sides of the parents and in between. Bat algorithm operators seem to cover a bit more search space than the last operators. It can be noticed that Levy Flight operators is intensively exploitation. However the operators from GA, Bat and Flower pollination algorithms are exploitation, but they also consider a small

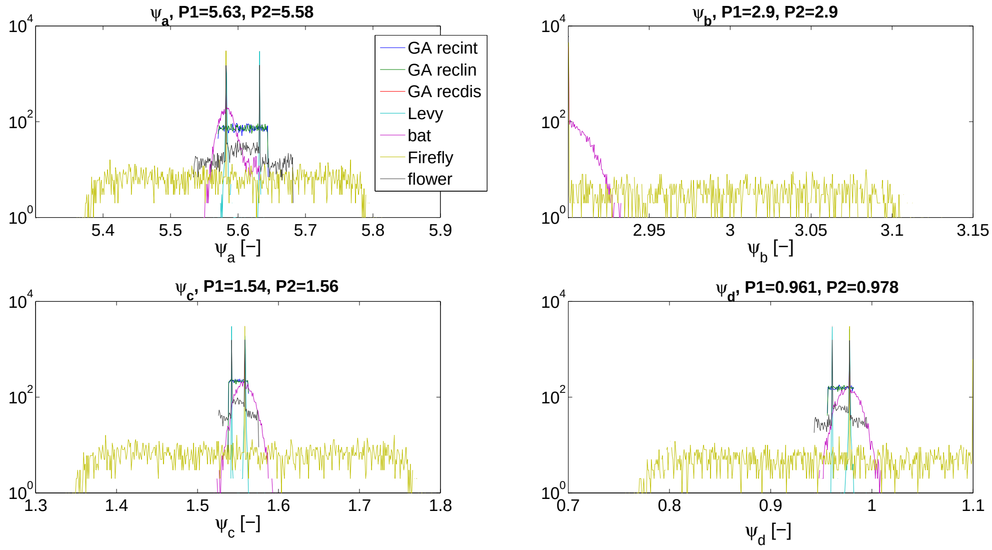

Figure 5.11: Semi-log plot results representing the spread of offspring based on two parents P1 and P2. The offspring are generated using GA crossover operators: direct, intermediate and extended line recombination, also with hybrid MOCS operators: Levy Flight, Bat, Firefly and Flower pollination

range of exploration.

In Figure 5.11, it can be seen that Firefly algorithm outperforms all operators in terms of offspring distribution, as it has the largest range of exploitation distribution. Overall, Firefly algorithm had a promising potential of exploring the search space, additionally it can also act as exploitation.

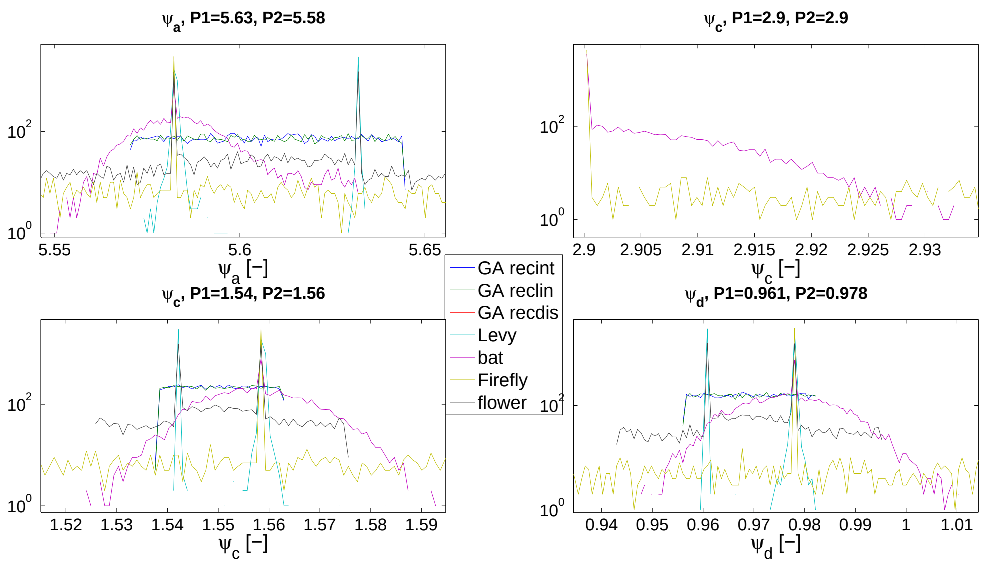

Figure 5.12: Semi-log plot results representing the spread of offspring based on two parents P1 and P2. The offspring are generated using GA crossover operators: direct, intermediate and extended line recombination, also with hybrid MOCS operators: Levy Flight, Bat, Firefly and Flower pollination. This figure illustrates a zooming view around the two parents.

5.6 Concluding remarks

This chapter has described two types of optimisation algorithms: Interior-Point Optimization and nature inspired as well as two methods to handle problems with multiple objective optimisation. A MOGA has been combined with problem specific operator and repair mechanisms to optimise a six speed DCT gear shift map. A standard cuckoo search algorithm has been supplemented with operators inspired from Bat, Firefly and Flower Pollination algorithms to optimise the gear ratio. Finally an iterative algorithm combining constrained and nature inspired optimisation has been developed to determine the best combination of gear ratio and gear shift map.

Having described the operators, algorithms improvements and overall frameworks proposed in this work, the next chapter focuses on the simulation study to demonstrate the expected benefits.

Chapter 6

Simulation settings and parameters selection

6.1 Introduction

This chapter builds on Chapters 4 and 5. Chapter 4 presented the new formulation proposed to solve both the gear ratio and the gear shift map optimisation problems. Chapter 5 described the new optimisation framework exploiting the proposed problem formulations and the problem specific knowledge.

The first section focuses on the objectives formulation and in particular the parameter selection for the new zone definition within the BSFC map and the correlation between the zones and the other objectives.

The second section starts by classifying the solutions obtained according to different objectives to relate objective value to engineering requirements and specific features to differentiate the various solutions. A correlation analysis between CO_2 emission and all the other objectives including the alternative zones parametrisation is performed to identify appropriate zone thresholds. This section concludes with a proposed method to select objective weightings to express their relative importance based on a user classification of a sample of solutions.

6.1.1 Trade-off visualisation and correlation analysis

Figure 6.1 and Figure 6.2 illustrate the correlation between various objective functions. Figure 6.1 shows the group of solutions selected to be analysed later. In Figure 6.2, it can be seen that CO_2 emission is correlated to z1 and a bit to Gj% and Dist, however it is inversely correlated to IRP, Gch and z2. There is no real correlation between CO_2 and z3. Figure 6.2 also shows clearly, the evolution of the group of solution namely Set A, Set B and Set C across various objective functions. They are in general grouped in the same search area. All red dots group have the lowest IRP, but the highest CO_2 alongside Gj% and z1. All green dots group are in most cases in the middle area of various objectives, whilst the magenta dots group are in the lower bottom. Consequently they have the lowest CO_2 emissions and higher IRP alongside Gch and z2.

Both a correlation analysis and visual inspection of the solutions distribution were used to evaluate the relationship between the eight possible objectives considered in this work. The subset of the non-dominated solutions was selected from the solutions obtained using the MOGA described in Section 7.6.5. The two most important criteria, namely CO_2 and IRP were used to select and classify the solutions into three groups denoted by A, B and C (see Figures 6.1 and 6.2). Note that the worse solution in terms of CO_2 of group C, could potentially belong to group B when considering the gear change frequency (Gch), and the time spent on higher gear (Gj%). Figure 6.1 illustrates the outcome of the correlation analysis on a small number of sample solutions, compared to the number used for the correlation study presented in Table 6.1. It can be observed that J_{CO_2} is correlated with J_{z1} , J_{Dist} and time spent on higher gear ($J_{Gj\%}$). By contrast J_{CO_2} and J_{IRP} are non-correlated and can therefore not be met simultaneously. J_{IRP} is correlated with J_{Gch}, and to some extend with J_{z2} and J_{z3}.

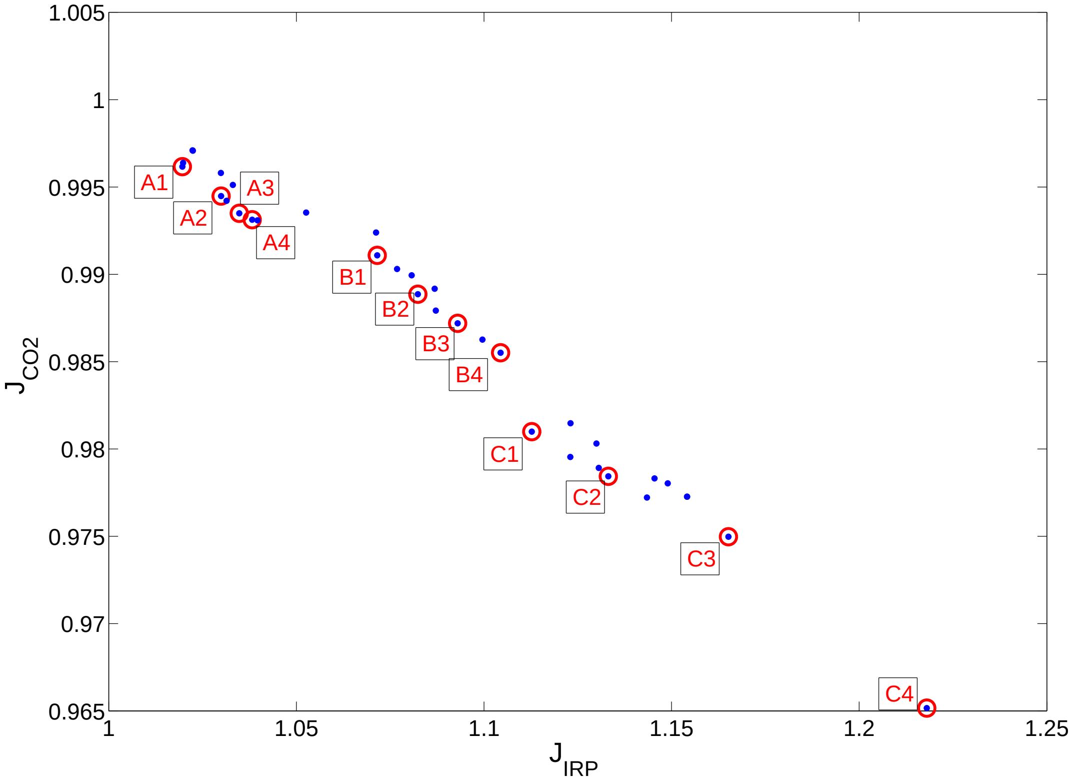

Figure 6.1: Pareto plot representing competing criteria CO_2 emissions versus Inverse Reserve Power (IRP). Three sets of solutions are defined, where each set is comprised of four optimised shift maps. The first set is marked from A1 to A4, the second set is marked from B1 to B4, and finally the third is marked from C1 to C4

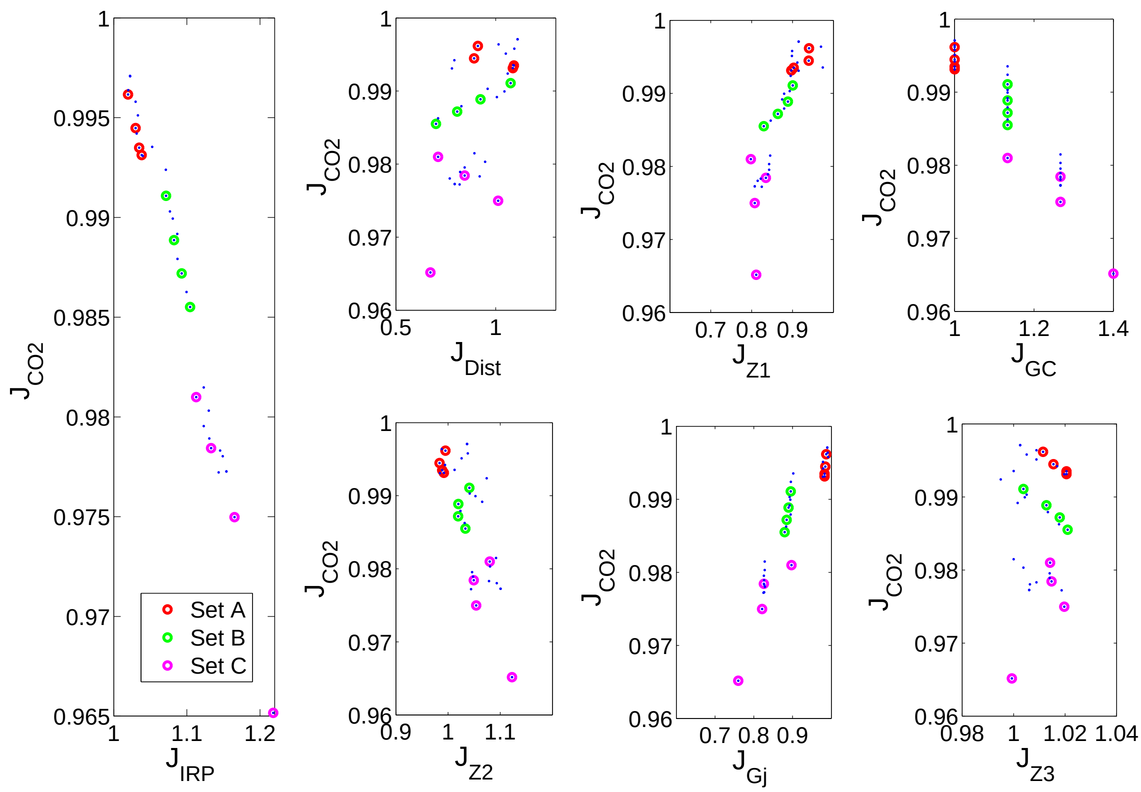

Figure 6.2: Pareto plot representing competing criteria CO_2 emissions versus Inverse Reserve Power (IRP), Distance (Dist), zone 1 (z1), Gear change frequency (Gch), zone 2 (z2), time spent on higher (Gj) and zone 3 (z3). Three sets of solutions are defined, where each set is comprised of four optimised shift maps. The first set is marked red circles, the second set is marked green circles, and finally the third set is marked magenta circles

Table 6.1: Cross correlation results between different objective functions indicating high correlation between J_{CO_2} and BSFC map distance Dist objectives and high non correlation between the group CO_2 Dist and the group IRP Gch confirming the results of Figure 6.2

	J_{CO_2}	J_{dist}	J_{z_1}	J_{IRP}	$J_{G_{ch}}$	J_{z_2}	$J_{G_j\%}$	J_{z_3}
J_{CO_2}	100	62	89	-99	-95	-76	93	-2
J_{dist}	62	100	60	-58	-48	-30	51	-35
J_{z_1}	89	60	100	-89	-80	-77	81	-12
J_{IRP}	-99	-58	-89	100	97	81	-97	-6
$J_{G_{ch}}$	-95	-48	-80	97	100	80	-99	-19
J_{z_2}	-76	-30	-77	81	80	100	-78	-54
$J_{G_{j\%}}$	93	51	81	-97	-99	-78	100	15
J_{z_3}	-2	-35	-12	-6	-19	-54	15	100

Having identified the relative trade off required to be addressed, the next section aims to develop objectives that could capture these trade-offs.

6.1.2 Parameter selection for the new zone objectives

The objectives relating to the zones were designed to attempt to find the most desirable trade off solution by rewarding gear shift map that results in a good percentage of the engine operating points (EOP) in the most efficient region of the BSFC map, i.e. zones 1 and 2. Zone 3 reflects higher fuel consumption characterised by operating the engine at low or very high revolution per minute. Ideally a higher degree of correlation between some of the zones objective and both IRP and CO_2 would be desirable to identify a criteria able to capture both these conflicting requirements. Alternatively the determination of the fuel consumption thresholds should help engineers identify the difference between solutions more clearly.

To address these objectives, three different settings were investigated empirically. Table 6.2 presents three different settings applied to the zones objective function J_{z1}, J_{z2} and J_{z3}. Each setting identifies three zones based on three user selectable fuel consumption thresholds [g/kW]. To identify the most suitable set of thresholds the following investigations were performed:

- The reference and an optimised solution were compared in terms of engine operating point distribution, see Figures 6.3 and 6.3 and associated Table 6.3 and 6.4.
- The objectives representing the different zones formulation were correlated against the other objectives considered in this thesis, see Figure 6.5 and associated Tables 6.5-6.7.

The setting on different zones is to guide the optimiser to favour a shift map with the most desirable EOP (zones 1 and 2). The largest difference between the EOP visualisation on the BSFC maps (see Figures 6.3 and 6.4) can be observed for the setting 2. Similarly the highest difference in terms of cost values is for setting 2 (see Tables 6.3 and 6.4) with setting 2 clearly differentiating solutions, increasing the number of operating points in the most fuel efficient zone: +3 points for zone 1 and +2 points for zone 2.

Table 6.2: Threshold adopted to differentiate the different zones on the BSFC map

	Setting 1 (g/kW)	*Setting* 2 (g/kW)	*Setting* 3 (g/kW)
Zone 1	< 270	< 255	< 252
Zone 2	< 350	< 265	< 268
Zone 3	≥ 350	≥ 265	≥ 268

Figures 6.3 and 6.4 are the EOP of initial shift map and optimised shift map respectively, with three different settings based on Table 6.2. The setting on different zones is to guide the optimiser to favour a shift map with the ideal EOP (zone 1). From Setting 1 to 3, it can be noticed that zones 1 and 2 are gradually decreasing (similar remark can be made from Table 6.3 and 6.4 on the percentage of EOP spent on each zones). The most suitable compromise is represented by

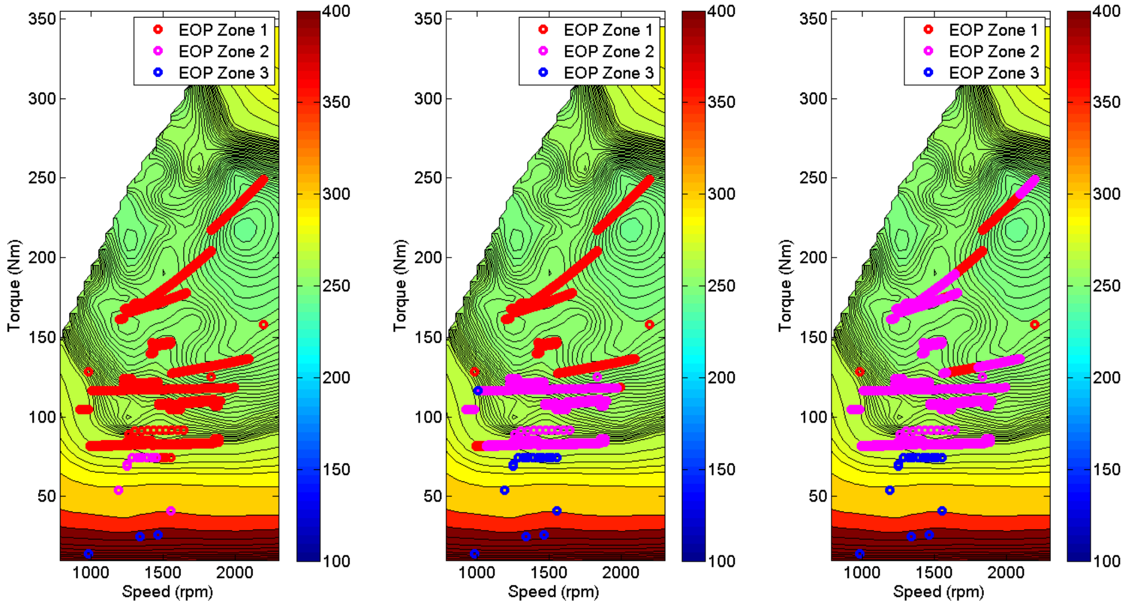

Figure 6.3: EOP of initial gear shift map, where the first is based on setting 1, the second is based on setting 2 and the third is based on setting 3. The red, magenta and blue circles represent the EOP of zone 1, zone 2 and zone 3, respectively.

setting 2, as the EOP of zone 1 is in good balance in comparison to settings 1 and 2.

Table 6.3: Percentage of EOP in zone 1, zone 2 and zone 3 for the initial shift map over the NEDC

	Setting 1	*Setting* 2	*Setting* 3
Zone 1 *EOP* (%)	33	10	4
Zone 2 *EOP* (%)	15	22	29
Zone 3 *EOP* (%)	52	67	67

To evaluate the effect of the zone thresholds selection on the correlation with the other objectives a correlation analysis was performed. The cross-correlation results are based on a set of 26 different shift maps obtained from a Pareto plot of CO_2 versus IRP. Figure 6.5 represents the correlation plot for CO_2, IRP and gear change frequency against the three zones Z1, Z2 and Z3. It can be observed that solutions are grouped in clusters for all three settings. This can help categorises the type of solutions produced. The difference between the groups is more significant in zone 1 for the setting 1 whereas it is more significant in

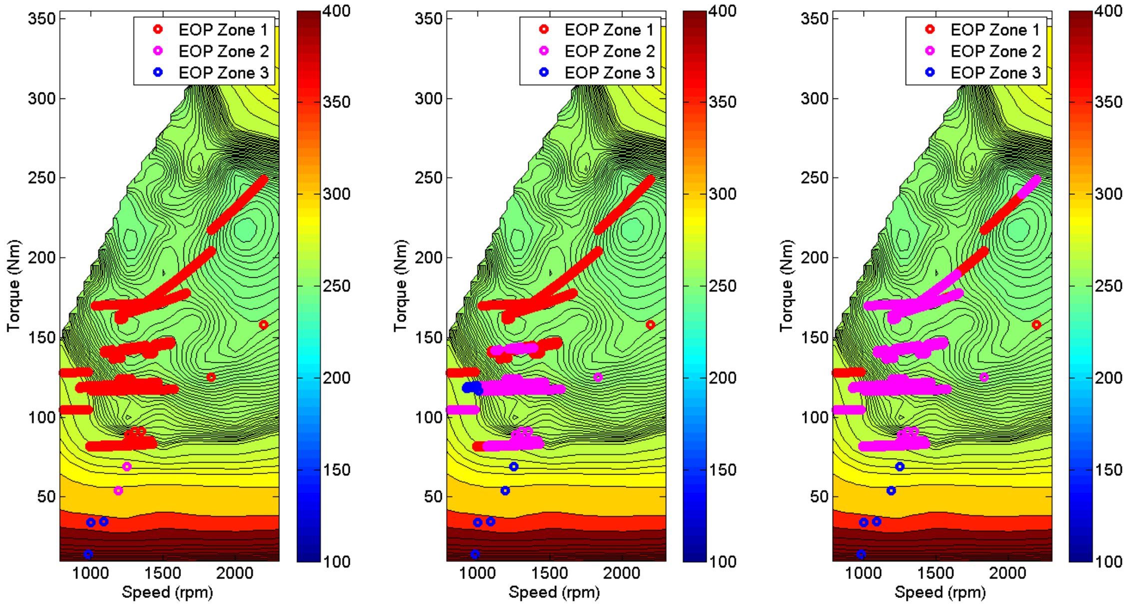

Figure 6.4: EOP of optimised gear shift map, where the first is based on setting 1, the second is based on setting 2 and the third is based on setting 3. The red, magenta and blue circles present the EOP of zone 1, zone 2 and zone 3, respectively.

Table 6.4: Percentage of EOP in zone 1, zone 2 and zone 3 for an optimised shift map over the NEDC

	Setting 1	*Setting* 2	*Setting* 3
Zone 1 *EOP* (%)	34	13	4
Zone 2 *EOP* (%)	14	20	30
Zone 3 *EOP* (%)	52	67	66

zones 2 and 3 for the other two settings. Using setting 2, Zone 2 is proportional to CO2 and inversely proportional to IRP and Gch. The degree of correlation corresponding negative-correlation between zone 1 with CO_2 and IRP respectively increases in magnitude between setting 1 and setting 2.

The following section will describe the influence of different setting on objective functions.

This section plots the cross-correlation between the three different settings (see Table 6.2) on zones (zone 1, zone 2 and zone 3) against CO_2 and IRP. The cross-correlation results are based on a set of 26 different shift maps obtained from a Pareto plot of CO_2 versus IRP.

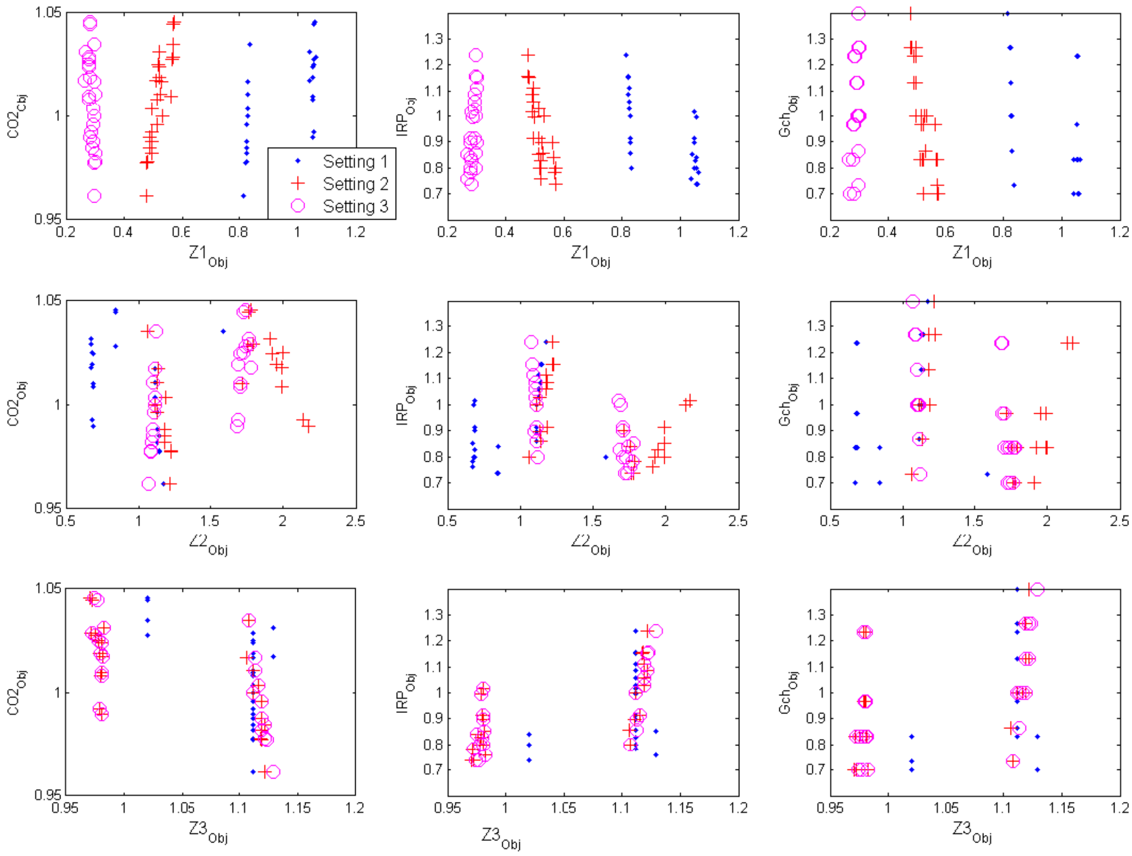

Figure 6.5: Objective functions representing CO_2 and IRP versus zone 1, zone 2 and zone 3. Marker with blue 'point', red 'circle' and magenta 'plus sign' present setting 1, setting 2 and setting 3, respectively.

Figure 6.5 represents the correlation plot of CO_2 and IRP versus zones. Major remarks are based on settings 1 and 3, when most objective functions are proportional in setting 1, they are inversely proportional in setting 3. Setting 2 represents the most appropriate compromise, therefore considering setting 2, it can be noticed that zone 2 is proportional to CO_2 and inversely proportional to IRP and Gch, however zone 2 is partially CO_2, IRP and Gch.

Table 6.5 defines the correlation results of the first setting. Zone 1 is 56% correlated to CO_2, while it is 62% inversely correlated to IRP. Zone 2 is slightly correlated and inversely correlated to CO_2 and IRP.

Table 6.6 defines the correlation results of the second setting. Zone 1 is 86%

Table 6.5: Cross correlation results between different objective functions indicating high correlation between J_{CO_2} and BSFC map distance Dist objectives and high non correlation between the group CO_2 and Dist and the group IRP and Gch. This table is based on setting 1.

	J_{CO_2}	J_{dist}	J_{z_1}	J_{IRP}	$J_{G_{ch}}$	J_{z_2}	$J_{G_j\%}$	J_{z_3}
J_{CO_2}	100	90	56	-98	-96	-32	51	-56
J_{dist}	90	100	54	-89	-89	-35	52	-44
J_{z_1}	56	54	100	-62	-43	-91	-32	-16
J_{IRP}	-98	-89	-62	100	94	42	-41	42
$J_{G_{ch}}$	-96	-89	-43	94	100	21	-64	48
J_{z_2}	-32	-35	-91	42	21	100	53	-22
$J_{G_{j\%}}$	51	52	-32	-41	-64	53	100	-51
J_{z_3}	-56	-44	-16	42	48	-22	-51	100

correlated to CO_2, while it is 80% inversely correlated to IRP. Zone 2 is slightly correlated and inversely correlated to CO_2 and IRP.

Table 6.7 defines the correlation results of the first setting. In setting 1, zone 1 is 56% inversely correlated to CO_2, while it is 62% correlated to IRP. Zone 2 is 59% correlated and 65% inversely correlated to CO_2 and IRP. The last statement finalises and concludes the group for each setting based on the outcome of correlations are presented in Tables 6.5, 6.6 and 6.7.

Table 6.6: Cross correlation results between different objective functions indicating high correlation between J_{CO_2} and BSFC map distance Dist objectives and high non correlation between the group CO_2 and Dist and the group IRP and Gch. This table is based on setting 2.

	J_{CO_2}	J_{dist}	J_{z_1}	J_{IRP}	$J_{G_{ch}}$	J_{z_2}	$J_{G_j}\%$	J_{z_3}
J_{CO_2}	100	90	86	-98	-96	36	51	-59
J_{dis}	90	100	84	-89	-89	35	52	-56
J_{z_1}	86	84	100	-80	-82	15	62	-44
J_{IRP}	-98	-89	-80	100	94	-45	-41	64
$J_{G_{ch}}$	-96	-89	-82	94	100	-22	-64	45
J_{z_2}	36	35	15	-45	-22	100	-52	-95
$J_{G_{j\%}}$	51	52	62	-41	-64	-52	100	30
J_{z_3}	-59	-56	-44	64	45	-95	30	100

Table 6.7: Cross correlation results between different objective functions indicating high correlation between J_{CO_2} and BSFC map distance Dist objectives and high non correlation between the group CO_2 and Dist and the group IRP and Gch. This table is based on setting 3.

	J_{CO_2}	J_{dist}	J_{z_1}	J_{IRP}	$J_{G_{ch}}$	J_{z_2}	$J_{G_j}\%$	J_{z_3}
J_{CO_2}	100	90	-56	-98	-96	59	51	-58
J_{Dist}	90	100	-56	-89	-89	57	52	-56
J_{z_1}	-56	-56	100	62	55	-90	15	87
J_{IRP}	-98	-89	62	100	94	-65	-41	64
$J_{G_{ch}}$	-96	-89	55	94	100	-47	-64	45
J_{z_2}	59	57	-90	-65	-47	100	-29	-100
$J_{G_{j\%}}$	51	52	15	-41	-64	-29	100	30
J_{z_3}	-58	-56	87	64	45	-100	30	100

6.2 Selection of objective weightings

To minimise the number of objective functions and reduce the solution space, the objectives that were correlated, according to cross-correlation of Table 6.6, were grouped together. The first group comprises J_{CO_2}, J_{Dist} and J_{z1} and focuses on emission reduction. The second group comprises J_{IRP}, J_{Gch} and J_{z3} and focuses on driveability at the expense of emission. The last group 3 is durability and currently only considers J_{Gj} based on the assumption that increasing the gear box use through fast and frequent gear changes would reduce its life expectancy.

The groups are implemented through the use of a group weighting combined with individual objective weightings within each group. The cost being normalised against the costs obtained for the current gear shift map, the group weightings are normalised such that their sum equates unity.

The selection of the individual objective weightings is a complex problem in itself. The main objective being to reduce CO_2 emissions, the weightings associated with emissions should therefore be comparatively high. To ensure that the vehicle is enjoyable to drive care should also be taken to ensure that the ability of the vehicle to accelerate after a gear change is not reduced excessively. Based on these general requirements and with the support of the correlation study presented in the previous section, the objectives were ranked empirically in terms of preference (see Table 6.8). The final weighting used in the optimisation is then the ratio between each individual objective weighting and the sum of all the objective weightings.

A MOGA was then used to further refine the determination of the most appropriate objective weighting. Having obtained a set of previously optimised solutions, six of these solutions were examined and ranked empirically from the best to the worse. The MATLAB GA toolbox was then configured to optimise the weight for each group of objective to replicate the proposed ranking. The weightings were initially selected from Table 6.8. Due to time constraints, only a limited amount of simulation could be carried out. It was found that the weightings determined by the GA could only replicate the ranking of 4 out of the 6 solutions selected.

Due to the difficulty in selecting the correct combination of objectives to merge all the conflicting requirement into a single expression, this work favours the use of a modified Pareto ranking. It ranks non dominated solutions according to a weighted sum based on the weightings identified in Table 6.8. Such an approach enables to overcome erroneous choice of objective weightings whilst concentrating on the most promising regions within the solution space.

The next stage in the optimisation procedure is to select the actual ideal solution. Such a choice is challenging as a single car can have many different gear shift maps. These maps are selected based on the user requirement, sport or eco driving, as well as the vehicle environment. The next section aims to identify qualitative features to augment the information given by the objective weightings or if possible identify the objective values that correspond to the most appropriate solutions.

In order to minimise the number of objective functions and ease the multi-objective optimiser to select a solution based on Pareto optimal point, a group of objective functions were defined based on cross-correlation results. According to cross-correlation of Table 6.5, the group of objective function is defined as follows:

- Objective group$_1$ represents emissions: J_{CO_2}, J_{z_1}, J_{dis},
- Objective group$_2$ represents driveability: J_{IRP}, $J_{G_{ch}}$, J_{z_3}
- Objective group$_3$ represents durability: $J_{G_{j\%}}$

Objective group 1 is emissions related, where J_{CO_2} is combined with J_{z_1} and J_{dis} as their correlation values are 90% and 86% respectively. Objective group 2 is driveability related, where J_{IRP} is combined with $J_{G_{ch}}$ and J_{z3} as their correlation values are 94% and 64% respectively. The last objective group 3 is durability related and only considers $J_{G_{j\%}}$.

A weighted sum method is applied to individual objective function to form one scalar as group. The group formulation is given as follows:

$$Group_1 = \frac{J_{CO_2}}{J_{CO2}(x_0)} W_{GSM_1} + \frac{J_{Dist}}{J_{Dist}(x_0)} W_{GSM_2} + \frac{J_{z_1}}{J_{z_1}(x_0)} W_{GSM_3} \tag{6.1}$$

where W_{GSM_1}, W_{GSM_2} and W_{GSM_3} denote the weighted associated with individual objective J_{CO_2}, J_{dis} and J_{z_1} respectively. $J_{CO2}(x_0)$, $J_{Dist}(x_0)$ and $J_{z_1}(x_0)$ are the corresponding objective function with the initial solution, as this allows to normalise the objective function. The solutions selected by the optimiser will strongly depend on the weighting factors, and these weights must be positive, and satisfying:

$$\sum_{L}^{\phi=1} W_\phi = 1, \quad W_\phi \in (0,1) \tag{6.2}$$

where W_ϕ and L denote the weighting ratio and the maximum number of objective function, respectively. Consequently, each individual weighting ratio of group 1 is given as follows:

$$W_{Gr1_d} = \frac{W_{GSM_d}}{\sum_{d=3}^{d=1} W_{GSM_d}} \tag{6.3}$$

where the subscript d denotes each individual objective function.

Group 2 also pursues the same formulation as group 1. It is defined as follows:

$$Group_2 = \frac{J_{IRP}}{J_{IRP}(x_0)} W_{GSM_4} + \frac{J_{G_{ch}}}{J_{G_{ch}}(x_0)} W_{GSM_5} + \frac{J_{z3}}{J_{z3}(x_0)} W_{GSM_6} \tag{6.4}$$

where W_{GSM_4}, W_{GSM_5} and W_{GSM_6} denote the weighted associated with individual objective J_{IRP}, $J_{G_{ch}}$ and J_{z_3} respectively. $J_{IRP}(x_0)$, $J_{G_{ch}}(x_0)$ and $J_{z_3}(x_0)$ are the corresponding objective function with the initial solution, as this allows to normalise the objective function. Each individual weighting ratio follows the same pattern as defined by Equation (6.3).

After defining three different groups as reduced objective functions, a combine multi-group objective function is proposed as follows:

$$Group_{Obj_{Global}} = Group_{Obj_1} W_{Global_1} + Group_{Obj_2} W_{Global_2} + Group_{Obj_3} W_{Global_3} \tag{6.5}$$

where W_{Global_1}, W_{Global_2} and W_{Global_3} denote for individual weighting ratio for multi-group objective function $Group_{Obj_1}$, $Group_{Obj_2}$ and $Group_{Obj_3}$ respectively. Each individual weighting ratio is given as follows:

$$W_{Global_e} = \frac{W_{g_e}}{\sum_{e=3}^{e=1} W_{g_e}} \tag{6.6}$$

where the subscript e denotes each individual group objective function. The weighting in percentage is given in Table 6.8.

Table 6.8: Rank of objective function and weighted sum

Rank	*Objective*	*Weight*	*Coefficient*
1	J_{CO_2}	W_{GSM_1}	500
2	J_{Dist}	W_{GSM_2}	200
3	J_{Z1}	W_{GSM_3}	100
4	J_{IRP}	W_{GSM_4}	70
5	$J_{G_{ch}}$	W_{GSM_5}	60
6	J_{Z3}	W_{GSM_6}	20
7	$J_{G_{j\%}}$	W_{GSM_7}	15
8	J_{Z2}	W_{GSM_8}	5

Table 6.9: Objective functions results of selected solution for optimised weight

Solution	J_{CO_2}	J_{dis}	J_{z_1}	J_{IRP}	$J_{G_{ch}}$	J_{z_3}	$J_{G_{j\%}}$	J_{z_2}	Obj_F	$Rank_{Des}$
1	0.9780	0.7696	0.8148	1.1490	1.2667	1.0063	0.8287	1.0934	1.0230	1
2	0.9872	0.8071	0.8641	1.0930	1.1333	1.0179	0.8847	1.0194	1.0088	6
3	0.9903	0.9596	0.8932	1.0769	1.1333	1.0051	0.8924	1.0414	1.0132	5
4	0.9951	1.0501	0.8983	1.0331	1.0000	1.0089	0.9785	1.0260	1.0056	4
5	0.9962	0.9104	0.9403	1.0196	1.0000	1.0114	0.9867	0.9950	0.9979	3
6	0.9931	1.0855	0.8969	1.0382	1.0000	1.0205	0.9826	0.9920	1.0071	2

GA was run 10 times, with a crossover rate of 0.7. The weight of each objective was selected from Table 6.8 initially, then was randomly changed at each run, therefore the weighted coefficient was always kept higher as it is the main objective targeted. GA has managed to find a coefficient of each weight, however only 4 solutions out of 6 were classified. The coefficients of the group weights are given in Table 6.10:

Table 6.10: Optimised weighting coefficient for $Group_1$, $Group_2$ and $Group_3$

	$Group_1$	$Group_2$	$Group_3$
$Weight$	6400	2300	440

6.3 Solutions classification

To identify features of the solutions found by optimising the gear shift map from a reference gear shift, use is made of solutions belonging to the Pareto optimal set illustrated in Figure 6.1. Three groups (denoted by A, B and C) have been identified based on normalised objective values for both IRP and CO_2.

Group A represents solutions that are most suited for sport mode, providing greater ability to accelerate after a gear change (see Figures 6.6, 6.7, 6.8 and 6.9).

Group B (B1, B2, B3 and B4) represents solutions close to the reference gear shift map, against which all the costs are normalised, with slightly lower CO_2 emissions and similar IRP (see Figures 6.10, 6.11, 6.12 and 6.13).

Group C (C1, C2, C3 and C4) represents solutions that significantly improve CO_2 emissions (see Figures 6.14, 6.15, 6.16 and 6.17).

The features exhibited by these solutions are qualitatively assessed against the shape of the gear shift maps (see Figures 6.6, 6.10 and 6.14), the engine operating point (EOP) (see Figures 6.7, 6.11 and 6.15), the gear changes against time (see Figures 6.8, 6.12 and 6.16), and radar plots of their objective function to visually assess the relative distribution of the objectives (see Figures 6.9, 6.13 and 6.17).

Figure 6.2 illustrates the correlation between various objective formulations. It can be observed that CO_2 emission are correlated to z1 and a bit to Gj and Dist, however it is inversely correlated to IRP, Gch and z2. There is no real correlation between CO_2 and z3. Figure 6.2 also shows clearly, the evolution of the group of solution namely Set A, Set B and Set C across various objective functions. They are in general grouped in the same search area. All red dots group have the lowest IRP, but the highest CO_2 alongside Gj and z1. All green dots group are in most cases in the middle area of various objectives, whilst the magenta dots group are in the lower bottom. Consequently they have the lowest CO_2 emissions and the higher IRP alongside Gch and z2.

Solutions that are on the Pareto optimal set are all optimal, but they favour different criteria. Solutions that exhibit high IRP will result in vehicle exhibiting a higher acceleration.

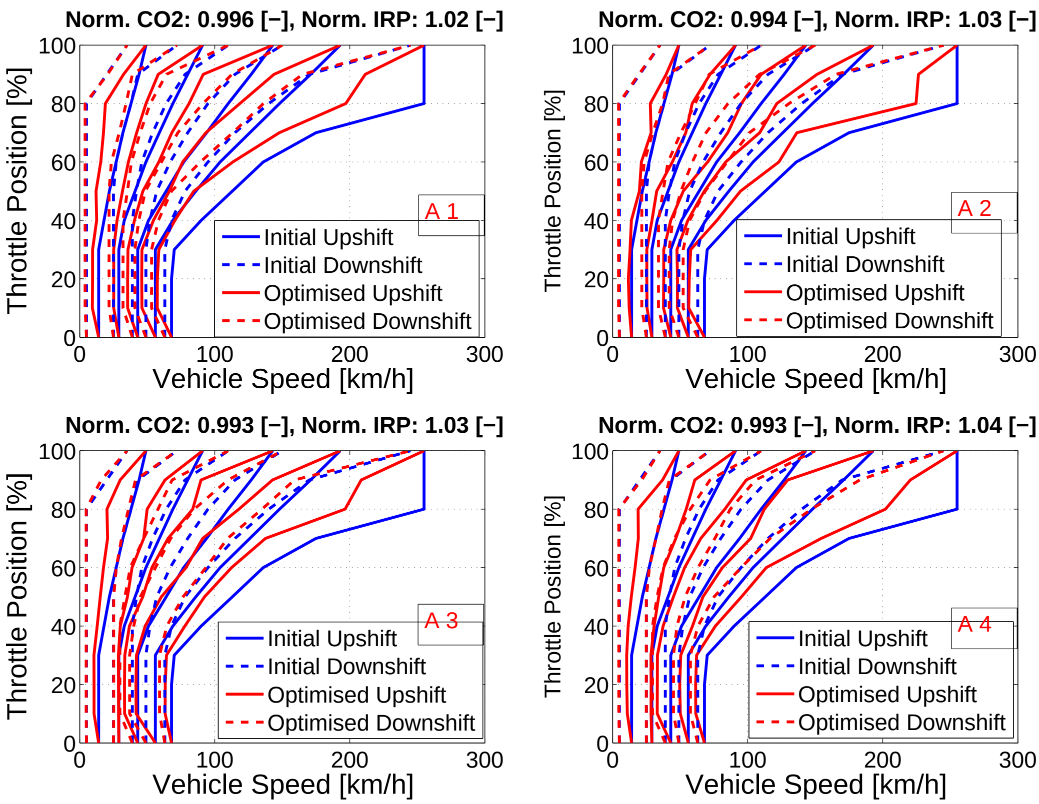

Figure 6.6: Set of Optimised shift map obtained from Pareto optimal solution denoted by A1, A2, A3, and A4, respectively (see Figure 6.1)

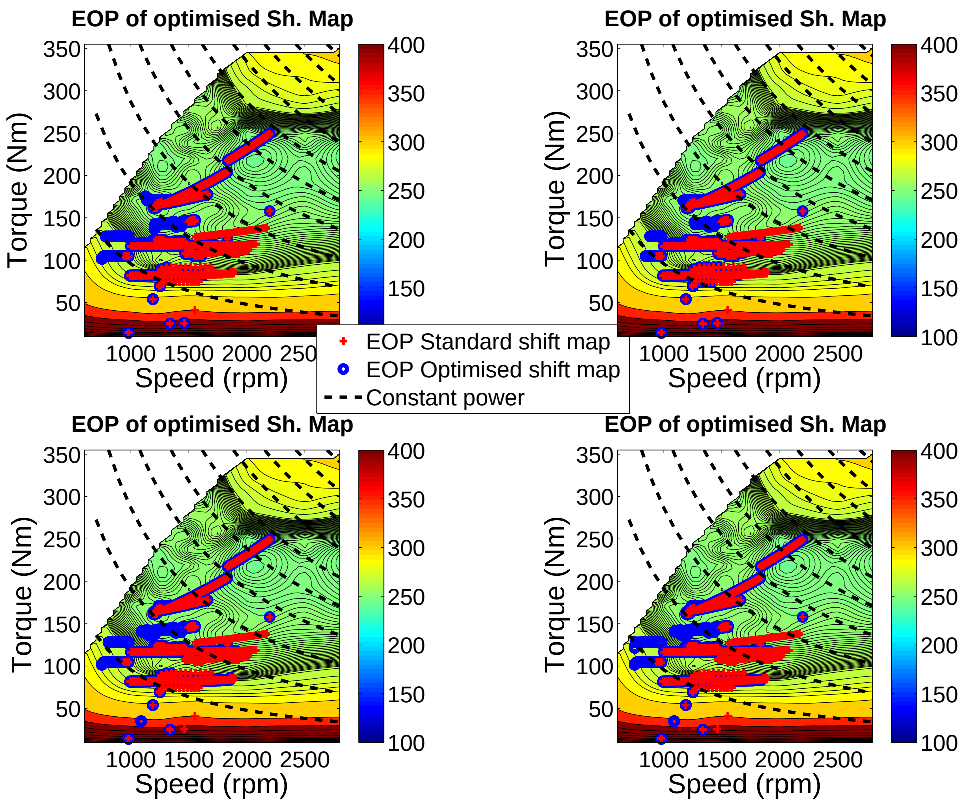

Figure 6.7: Set of Optimised shift map obtained from Pareto optimal solution denoted by A1, A2, A3, and A4, respectively (see Figure 6.1). The NEDC was used to calculate the engine operating point (EOP). The EOP of standard shift map is presented with red mark (+), and optimised shift map presented with blue mark (o).

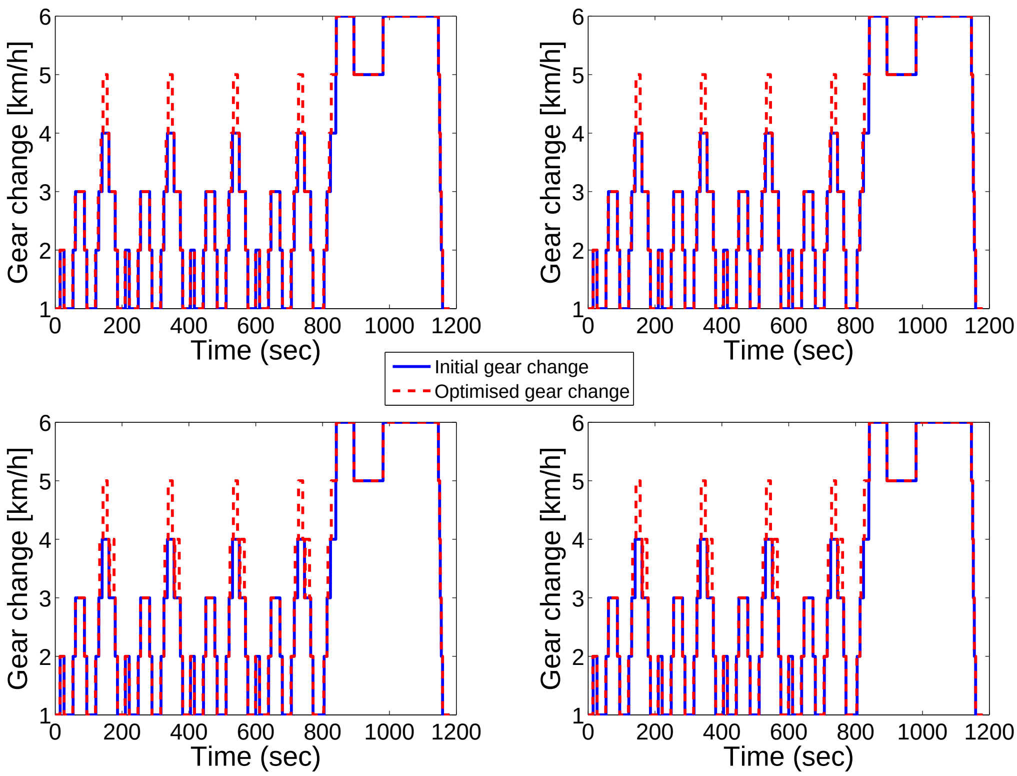

Figure 6.8: Gear change position based on 4 optimised shift maps (A1, A2, A3 and A4 (see Figure 6.1)) compared with initial shift map.

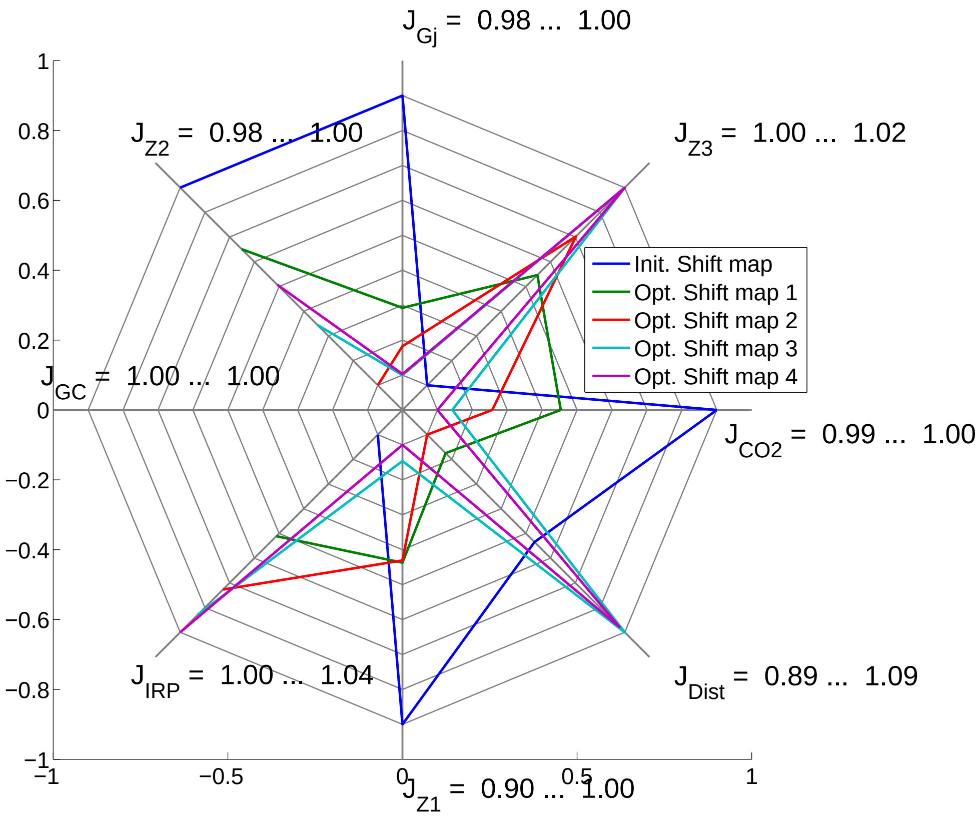

Figure 6.9: Radar plot of objectives functions (CO_2 emissions, IRP, Distances, Gear change frequency, time spent on higher gear, different zone on BSFC map defined as Zone 1, Zone 2, Zone 3) based on 4 optimised shift maps (A1, A2, A3 and A4 (see Figure 6.1)) compared with initial shift map.

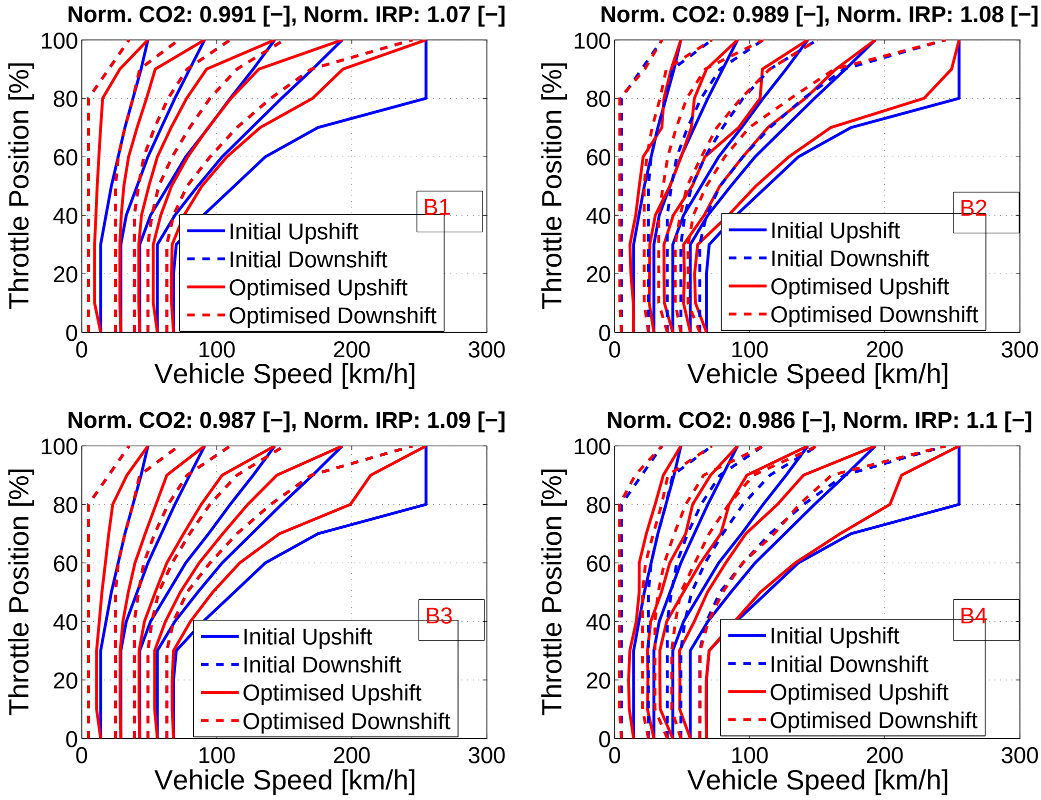

Figure 6.10: Set of Optimised shift map obtained from Pareto optimal solution denoted by B1, B2, B3, and B4, respectively (see Figure 6.1)

Figure6.10, 6.11 and 6.13 illustrate the plot of the second optimal set (B1, B2, B3 and B4 (see Figure 6.1)) shift maps, engine operating point (EOP) and radar plot of their objective function, respectively.

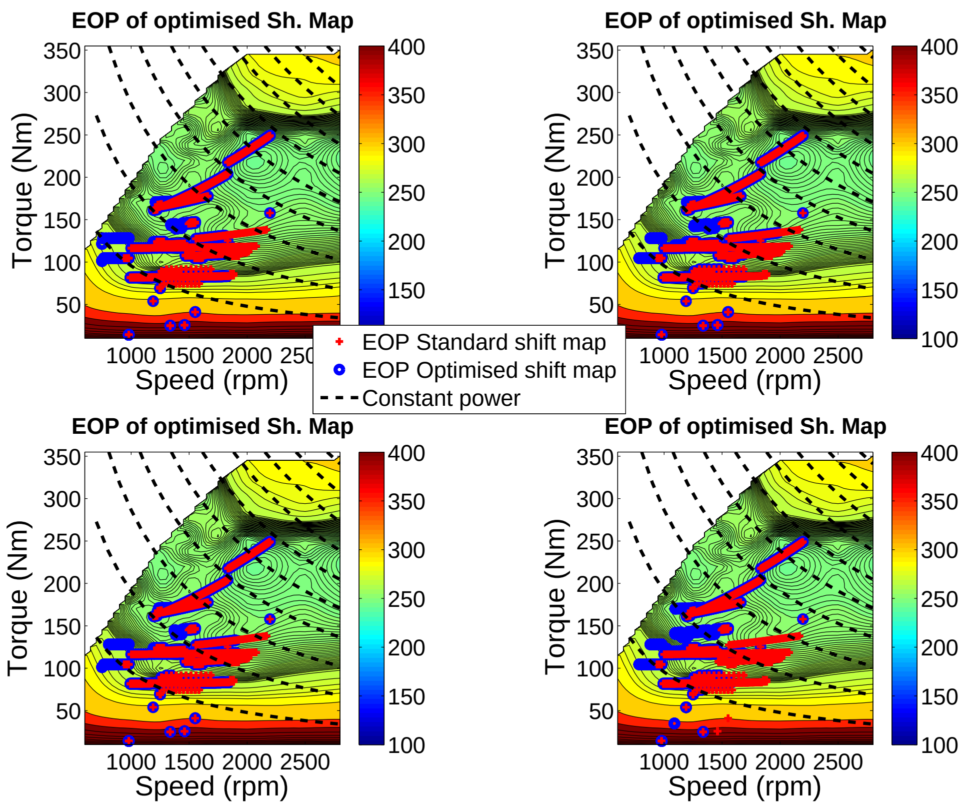

Figure 6.11: Set of Optimised shift map obtained from Pareto optimal solution denoted by B1, B2, B3, and B4 respectively (see Figure 6.1). The NEDC was used to calculate the engine operating point (EOP). The EOP of standard shift map is presented with red marked (+), and optimised shift map presented with blue marked (o).

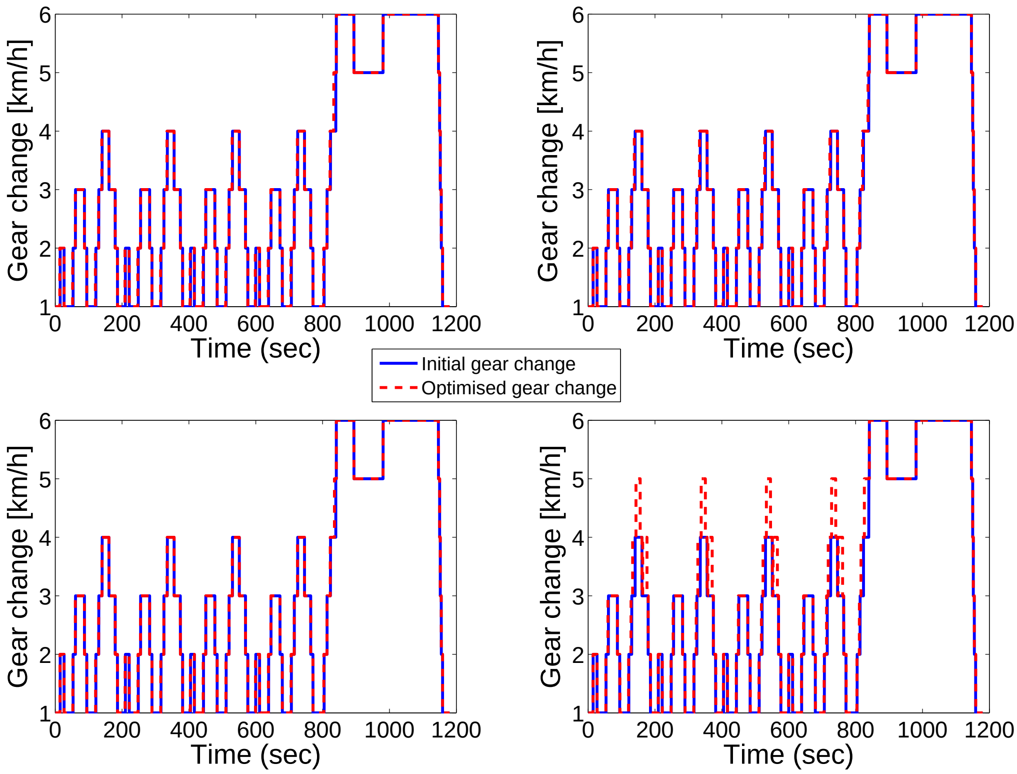

Figure 6.12: Gear change position based on 4 optimised shift maps (B1, B2, B3 and B4 (see Figure 6.1)) compared with initial shift map.

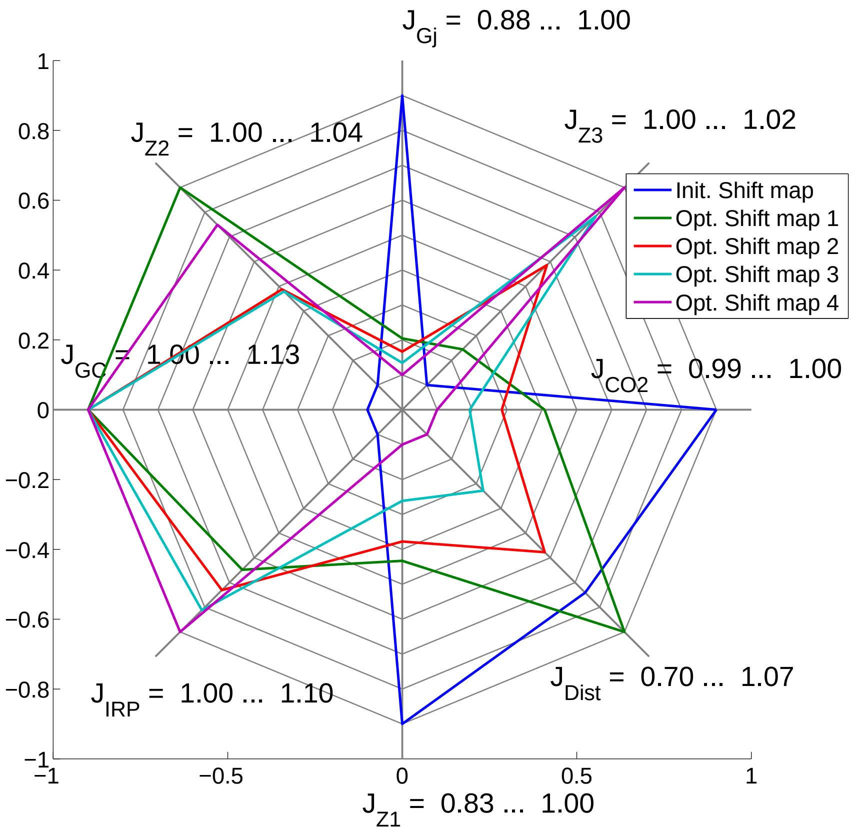

Figure 6.13: Radar plot of objectives functions (CO_2 emissions, IRP, Distances, Gear change frequency, time spent on higher gear, different zone on BSFC map defined as Zone 1, Zone 2, Zone 3) based on 4 optimised shift maps (B1, B2, B3 and B4 (see Figure 6.1)) compared with initial shift map.

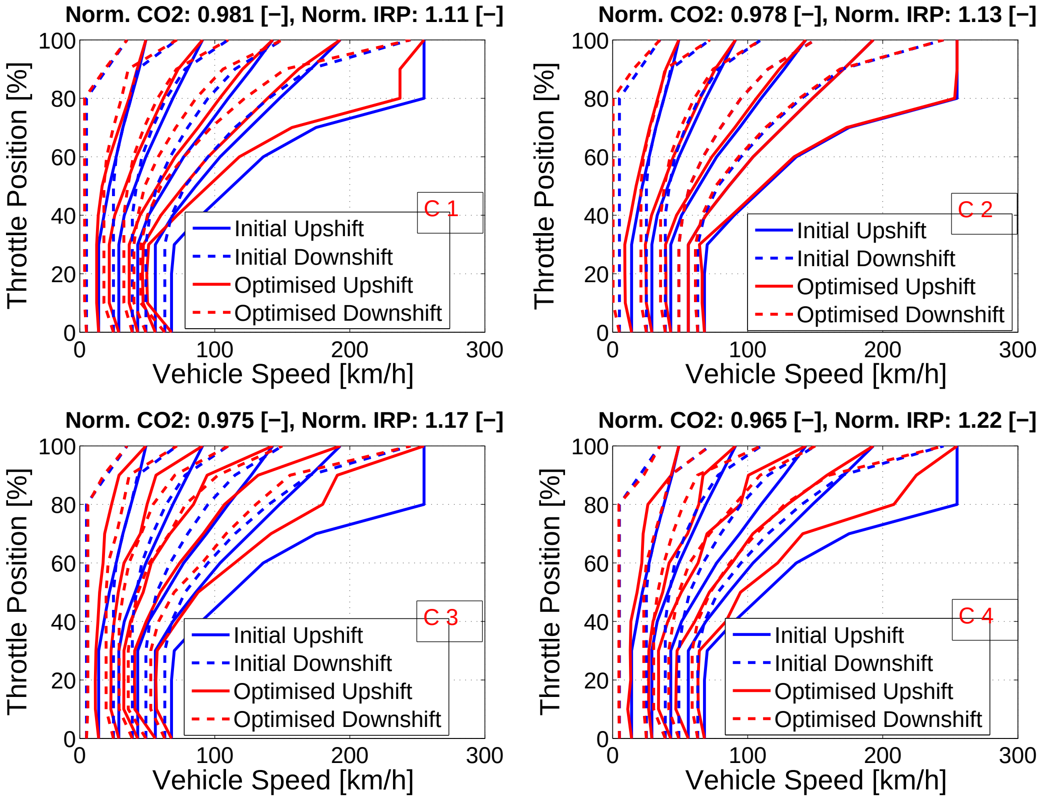

Figure 6.14: Set of Optimised shift map obtained from Pareto optimal solution denoted by C1, C2, C3, and C4 respectively (see Figure 6.1)

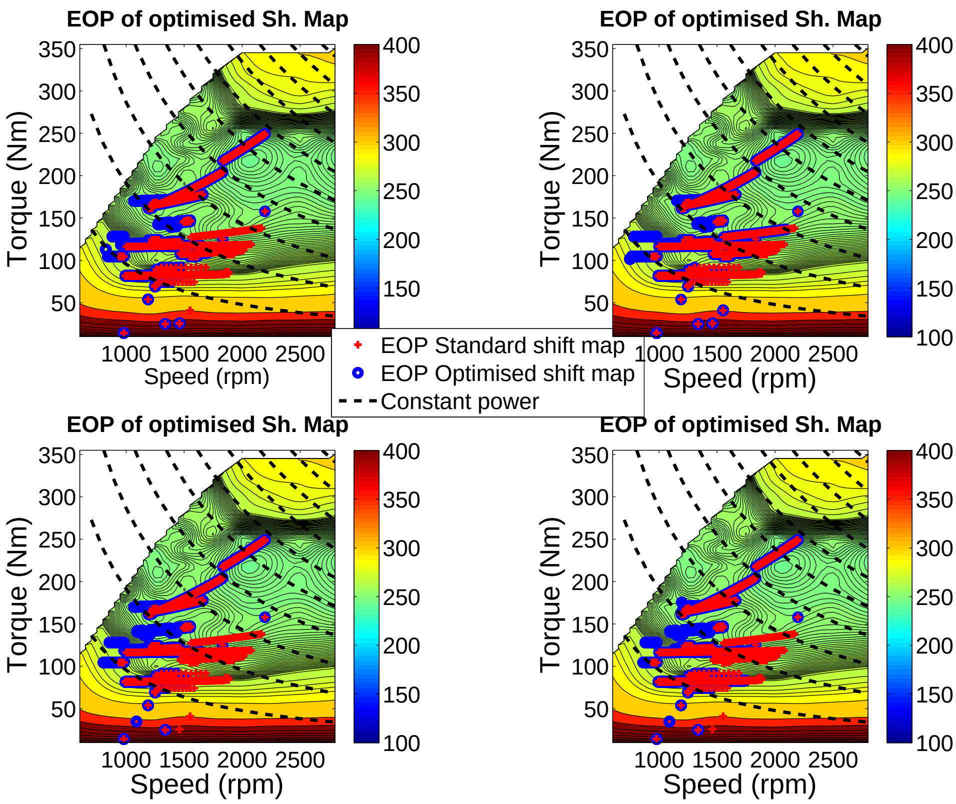

Figure 6.15: Set of Optimised shift map obtained from Pareto optimal solution denoted by C1, C2, C3, and C4 respectively (see Figure 6.1). The NEDC was used to calculate the engine operating point (EOP). The EOP of standard shift map is presented with red mark (+), and optimised shift map presented with blue mark (o).

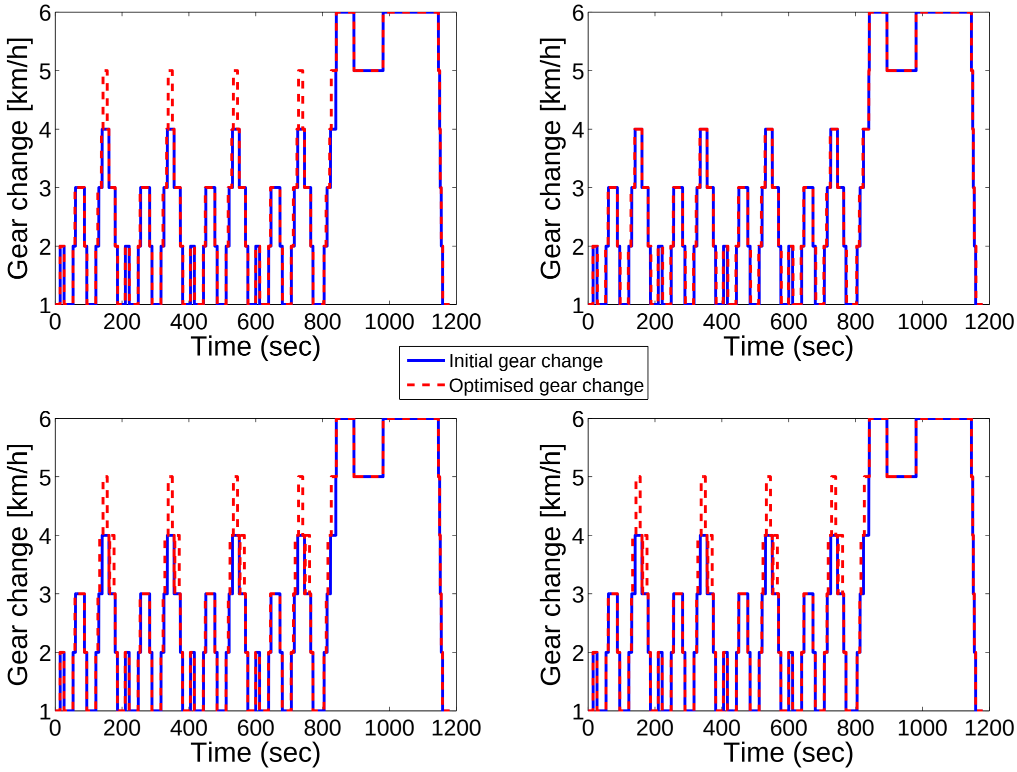

Figure 6.16: Gear change position based on four optimised shift maps (C1, C2, C3 and C4 (see Figure 6.1)) compared with initial shift map.

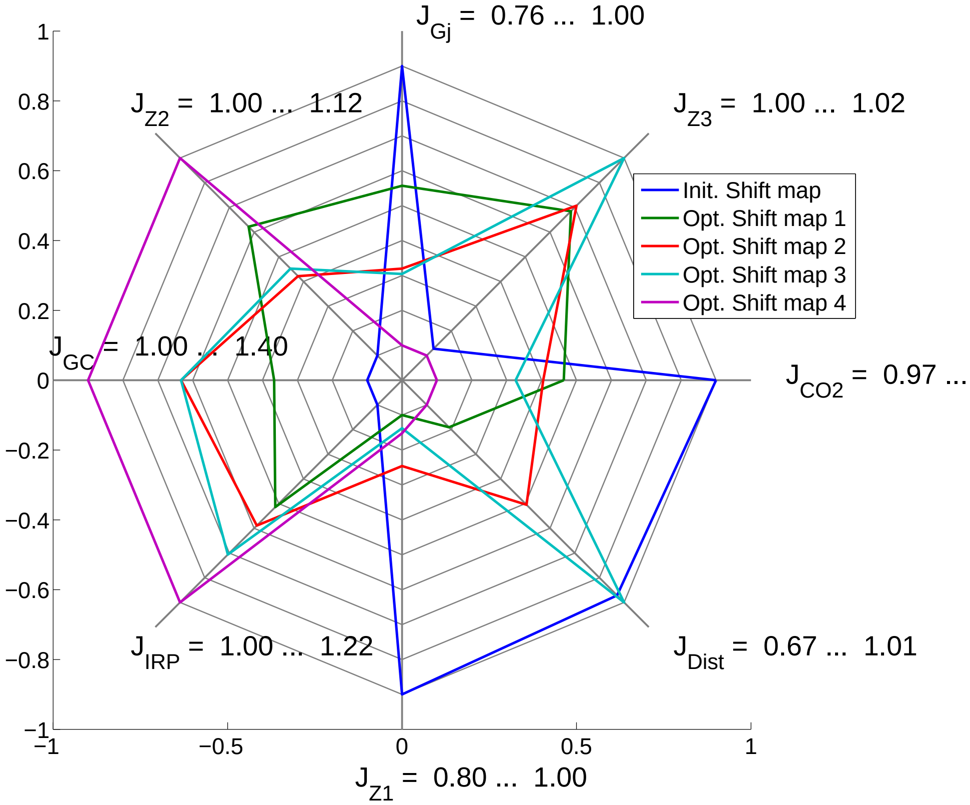

Figure 6.17: Radar plot of objectives functions (CO_2 emissions, IRP, Distances, Gear change frequency, time spent on higher gear, different zone on BSFC map defined as Zone 1, Zone 2, Zone 3) based on four optimised shift maps (C1, C2, C3 and C4 (see Figure 6.1)) compared with initial shift map.

6.4 Concluding remarks

This chapter has identified existing trade-offs in terms of the objectives implemented in this thesis, to evaluate the appropriateness of the optimised solutions produced. A cross correlation study highlighted the degree of correlation between the different objectives and to identify the tuning parameters for the new criteria proposed in this work. The outcome of the correlation study was the division of the objectives into three groups focusing on emissions, driveability and durability, respectively. These tuning parameters for the zones 1-3 were selected to emphasise the difference between solutions that promote an efficient distribution of the engine operating point on the BSFC map and non optimised solutions. z1 promotes better fuel consumption and is correlated with CO_2, Gj% and Dist. The second group, which is not correlated with the first group includes IRP, Gch and z2. To characterise the differences between different solutions, three groups of optimal solutions were selected based on the trade-off between CO_2 and IRP. It was demonstrated that all optimised gear shift maps were shifted to the left in comparison to the original shift map. This resulted in an early shifting and led to reduction in CO_2. The group with the lowest CO_2 emissions have very rapid successive changes for their gear sets 2 and 3, especially at low throttle position. This study has enabled identification of features on the BSFC map as well as gear shift maps to help select solutions which are optimal but also likely to be acceptable in terms of driveability.

Chapter 7

Algorithm performances

7.1 Introduction

Chapter 6 identified the type of solutions that can be obtained from focusing on different objectives as well as features of desirable solutions. Having investigated the formulation of the objectives in the previous chapters, this chapter focuses on the algorithms exploiting such objective formulations. It aims to demonstrate, through simulation studies, the benefits of problem specific features as well as generic algorithm modifications applicable to other optimisation problems. The generic algorithms modifications include the new hybrid Multi-Objective Cuckoo Search (MOCS) which combines Levy Flight function with Firefly, Bat and Flower Pollination operators. The problem specific developments include the gear shift map repair mechanism, the new gear early shifting (GES) operator and the overall optimisation framework for the combined gear shift and gear ratio optimisation. Each contribution is evaluated independently and then in combination against two benchmarks algorithms: the Interior-Point Optimisation and MOGA from MATLAB toolbox. Finally the benefit of the combined MOGA and MOCS to concurrently optimise gear ratio and gear shift map is compared to independent gear ration and gear shift map optimisation.

7.2 Objective handling for algorithm evaluation

The assessment is based on two different multi objective problem formulations. First a Pareto formulation of the objectives that gives a set of equally optimal non dominated solutions is considered, where solutions that favour low CO_2 emission can be selected from the Pareto set post optimisation (see Section 4.4.1, in Chapter 4). Second a weighted sum of the objectives is considered where there is only one optimal solution (see Section 4.4.1, in Chapter 4). Three sets of objectives are considered in the evaluation. The first set (Set1) contains the three objective groupings identified in Section 6.2, denoted Group_1, Group_2 and Group_3.

The second set (Set 2) includes the three main objectives, which are J_{CO_2}, J_{IRP} and $J_{G_j\%}$. The third set (Set 3) includes all the objectives adopted in this thesis which are $\text{J}CO_2$, J_{Dist}, J_{z1}, J_{IRP}, J_{Gch}, J_{z3}, $\text{J}_{Gj\%}$, J_{z2}.

The individual weighting for each objective is based on Table 6.8, while the group weighting is based on the optimised weights determined in Table 6.10 (see Section 6.2, in Chapter 6).

The Pareto based optimisation algorithms evaluated are:

- the MOGA (M_{p1}) based on Haas et al. (1998)

- the MOGA_{Op} (M_{p2}) which is based on M_{p1} but modified to include various operators from the Cuckoo Search Algorithm (see Section 5.3, in Chapter 5)

- the MOGA from the MATLAB toolbox MOGAToolbox (M_{p3})

The Non Pareto based optimisation (weighted sum) algorithms include M_{p1}, M_{p2} as well as:

- Interior-point algorithm (M_{s1}) from the MATLAB toolbox

- GA (M_{s2}) from the MATLAB toolbox

The initial comparison is problem independent and therefore does not include the repair mechanism and GES. Each set up is summarised in a table giving the ideal objective function values achieved at the last generation for each setting. The rate of convergence is illustrated by recording the most suitable objective function at each generation, where the number of generation of each algorithm is set to 30 with a population of 60 individuals. The maximum functions evaluated for interior-point algorithm is set to 2000. Every algorithm used the same initial condition. Pareto based optimisation algorithms use identical initial population whilst weighted sum approaches use a valid solutions of average quality.

7.3 Criteria to evaluate the algorithms performance

This section describes the criteria used in this chapter to evaluate the benefit of the problem specific objectives formulation as well as the proposed algorithms. The objective formulation is evaluated by performing a correlation analysis with existing objectives and observing from a qualitative perspective (e.g. shape of the gear shift map, type of solutions produced) and a quantitative perspective (CO_2 emissions, time spent on higher gears and ability of the vehicle to accelerate after a gear change, expressed as inverse reserve power) the differences between the optimised solutions. The effectiveness of the algorithms is evaluated using:

- the overall most suitable for each objective function

- the mean value and standard deviation of solutions between generation

- the functions evaluated

- the speed of convergence

- the diversity of solution based on Pareto front (Schott 1995) is defined as follows:

$$S_{sprd} = \sqrt{\frac{1}{n-1}\sum_{i=1}^{n}\left(\overline{d} - d_i\right)^2} \tag{7.1}$$

where d_i=$\min_j(\left|f_1^i(\vec{x}) - f_1^j(\vec{x})\right| + \left|f_2^i(\vec{x}) - f_2^j(\vec{x})\right|)$, i,j=1,...n, $\overline{d}$ is the mean of all d_i, and n is the number of Pareto optimal set. If S_{spread} is equal to zero, it means that all members of the Pareto optimal set are equidistantly spaced.

7.4 Repair mechanism effectiveness

One of the major contributions of this work is the solution repair mechanism. It has been designed such that it can be applied to an existing gear shift map or a new solution generated by the optimisation algorithm. It is a convenient tool to rescue solutions, with significant CO_2 saving potential, that would otherwise have been rejected.

To illustrate the benefit of the approach, the vehicle powertrain behaviour is simulated for a previously optimised gear shift with low CO_2 emission. The gear position, the engine operating point and the reserve power are then plotted against time at which the reserve power is below the user defined limit set at 3.2 kW Ngo, Colin Navarrete, Hofman, Steinbuch & Serrarens (2013). The corresponding reserve power and throttle position are identified by green circles and triangles on Figures 7.1, 7.2 and 7.3, respectively.

Plotting the engine operating point on top of the gear shift map, see Figure 7.1, clearly indicates that the lower limit constraints are only infringed for a small region in the gear shift map. Applying the repair mechanism according to the method described in Section 5.2.2, removes the issue associated with the Upshift to 2^{nd} gear by increasing the velocity at which the Upshift occurs for low throttle angles. The ability of the repair mechanism to adjust only a few points in the gear shift map is believed to be very valuable. The same principle could be applied to other criteria and constraints that should be met. The effect of the repaired gear shift map on the vehicle performance assessed against the NEDC was then re-simulated.

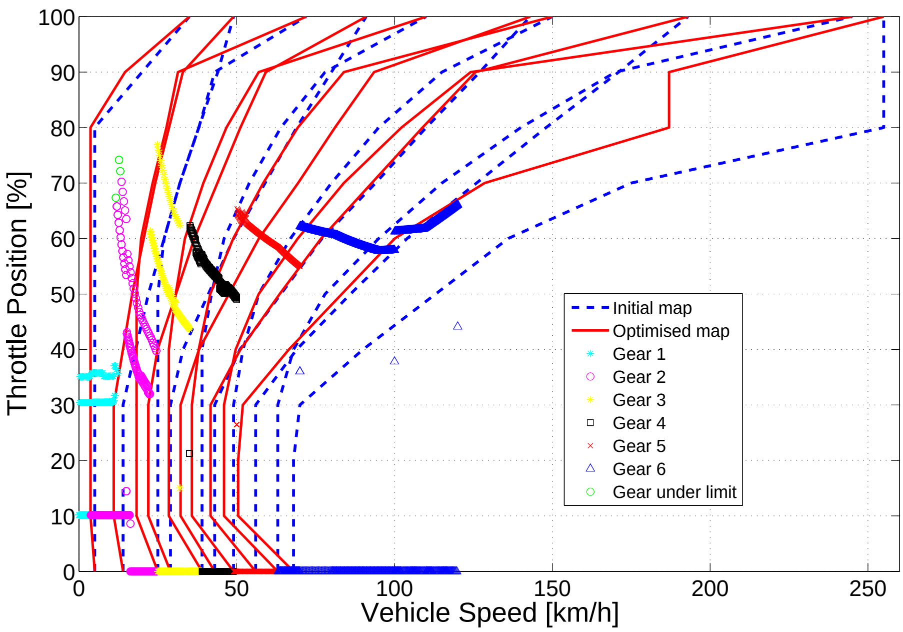

Figure 7.1: Optimised gear shift with reserve power under 3.2 kW

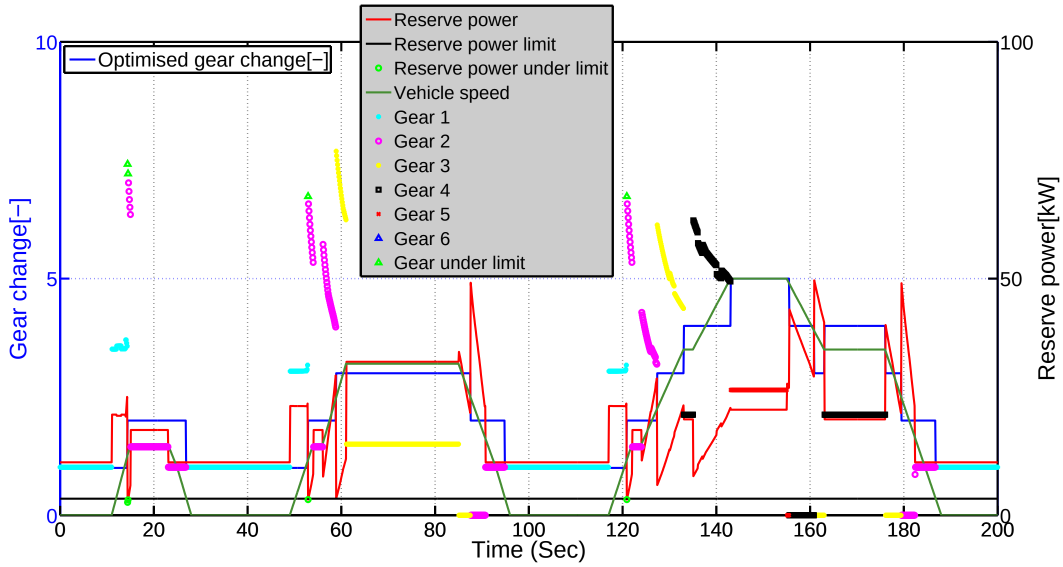

Figure 7.2: Optimised gear shift results over the NEDC with reserve power under 3.2 kW for one period of urban driving cycle

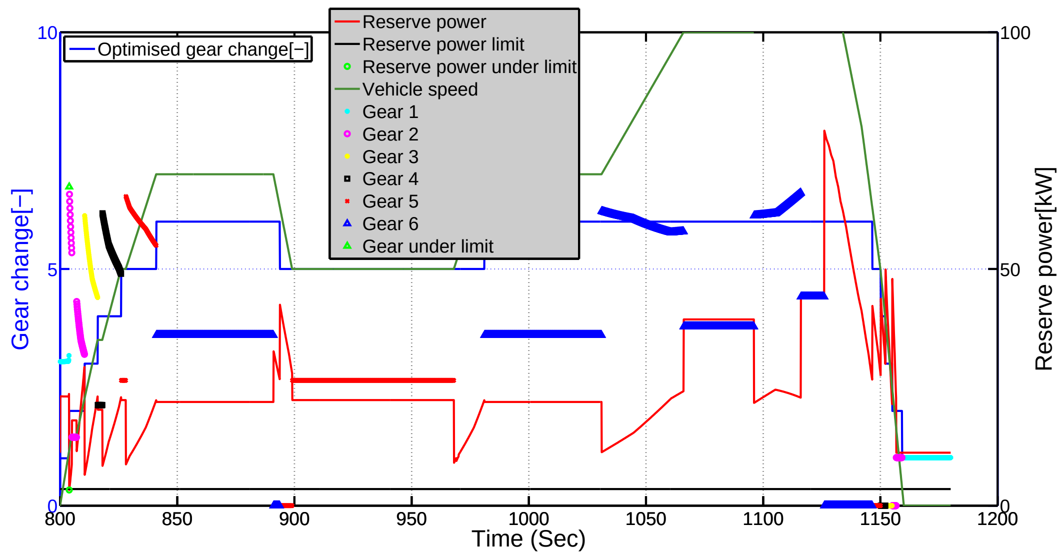

Figure 7.3: Optimised gear shift results over the NEDC with reserve power under 3.2 kW for extra-urban driving cycle

It is clear that, following the application of the gear shift repair mechanism, all the occurrences of reserve power below the limit have been removed. The repaired gear shift map illustrated in Figure 7.4 is only modified for the 2^{nd} gear Upshift. This small modification is able to remove all the occurrences of the reserve power that were under the limit over the whole NEDC, see Figure 7.5 and 7.6. Table 7.1 illustrates the benefit and consequences of applying the repair mechanism to the gear shift map (GSM) illustrated in Figure 7.1 to produce the repaired gear shift map, GSM_r, as illustrated in Figure 7.4.

The application of the repair mechanism results in a slight increase in CO_2 emissions. This increase is unavoidable and results in the necessity to meet the minimum requirement in terms of IRP. Note that similar approaches could be used to design gear shift map for *sport* mode, the only difference being an increase in the minimum reserve power.

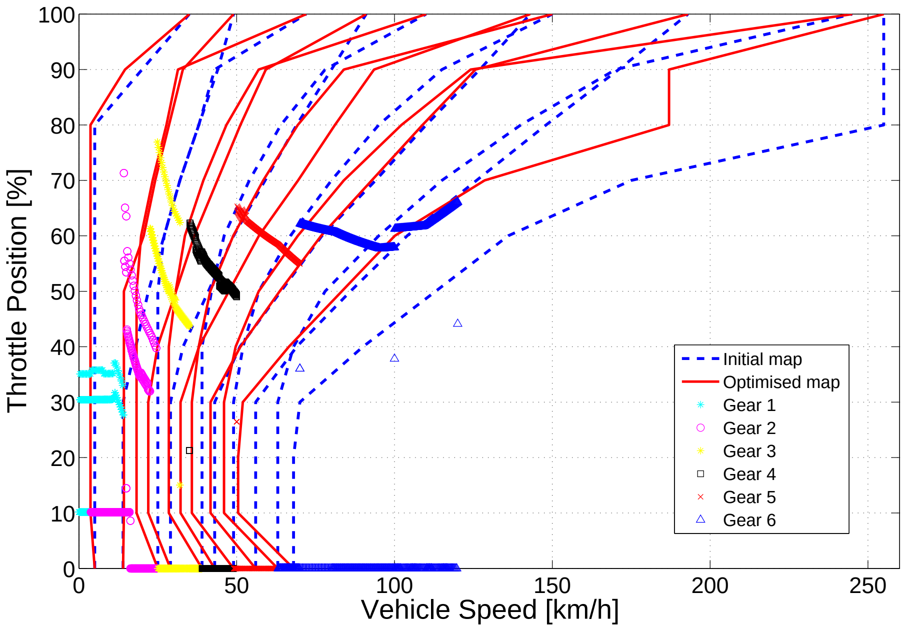

Figure 7.4: Optimised gear shift map repaired to enforce minimum reserve power above 3.2 kW

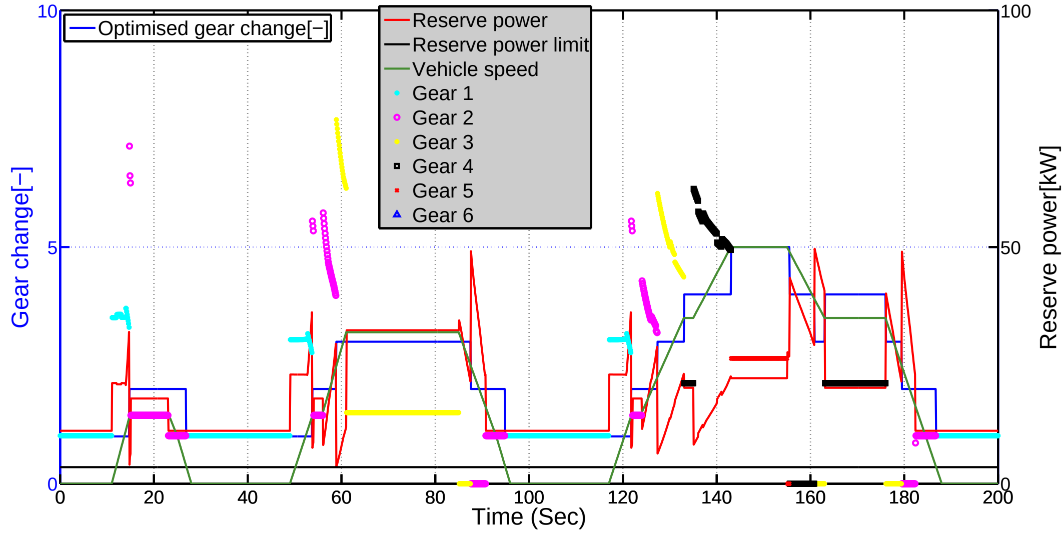

Figure 7.5: Simulation with a repaired gear shift map showing that the minimum reserve power is met at all time over the whole NEDC. This illustration shows one period of urban driving cycle

Table 7.1: Optimised shift map results. GSM is the optimised shift map with reserve power under the limit. GSM_R is the optimised shift map after applying repair mechanism

Solution	J_{CO_2}	J_{Dist}	J_{z_1}	J_{IRP}	$J_{G_{ch}}$	J_{z_3}	$J_{G_j}\%$	J_{z_2}
GSM	0.9773	0.7944	0.8076	1.1541	1.2667	1.0060	0.8267	1.1005
GSM_R	0.9800	0.8031	0.8173	1.1425	1.2667	0.9947	0.8285	1.1348

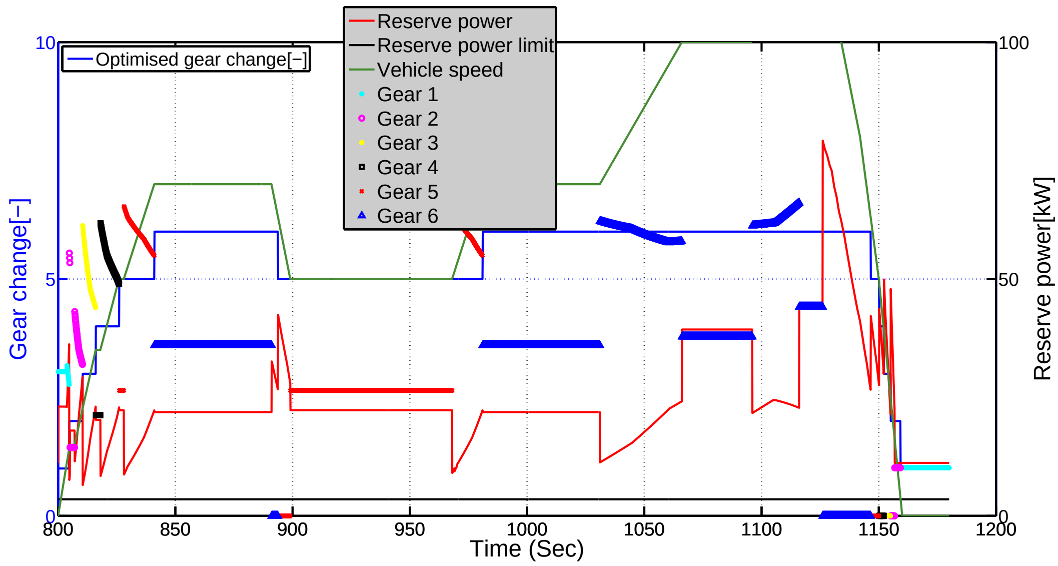

Figure 7.6: Simulation with a repaired gear shift map showing that the minimum reserve power is met at all time over the whole NEDC. This illustration shows one period of extra-urban driving cycle

7.5 Problem specific operator evaluation

Another notable contribution in this thesis is the problem specific GES operator (see Section 5.2.1, in Chapter 5) designed to generate gear shift map with reduced CO_2 emissions. Table 7.2 confirms that the application of the GES operator gives rise to three solutions with improved CO_2 emissions, at the cost, however, of worse IRP.

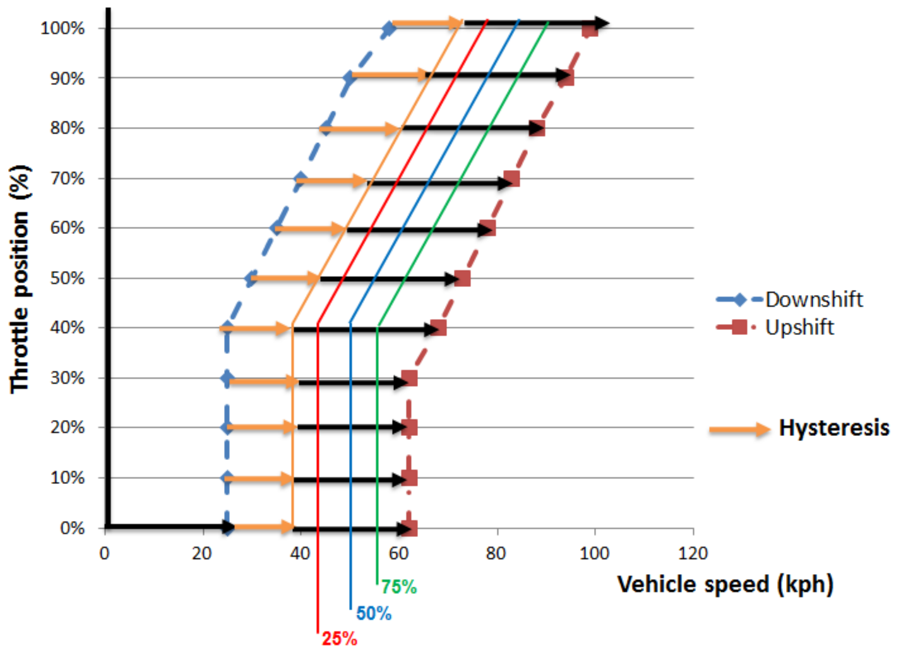

Figure 7.7: Illustration of GES. The full red, blue and green lines denote the three solutions produced by the GES

Table 7.2: Optimised shift map results. GSM$_{GES_{init}}$ is the optimised shift map with . GSM$_{GES_{25\%,\ 50\%\ and\ 75\%}}$ being the optimised shift map after applying the repair mechanism

Solution	J_{CO_2}	J_{Dist}	J_{z_1}	J_{IRP}	$J_{G_{ch}}$	J_{z_3}	$J_{G_j\%}$	J_{z_2}
$GSM_{GES_{init}}$	0.9964	1.0137	0.9697	1.0198	1.0000	1.0089	0.9907	0.9879
$GSM_{GES_{25\%}}$	0.9927	0.7558	0.9150	1.0421	1.0000	1.0198	0.9769	0.9842
$GSM_{GES_{50\%}}$	0.9938	0.8344	0.9283	1.0349	1.0000	1.0169	0.9813	0.9854
$GSM_{GES_{75\%}}$	0.9949	0.9216	0.9469	1.0273	1.0000	1.0153	0.9860	0.9805

The benefit of applying GES has improved the current solution generated by the optimiser by up to 0.37%.

7.6 Algorithm performance evaluation

This section describes the comparison between the algorithms developed in this thesis and benchmarks from the MATLAB toolbox. Following the evaluation of the proposed modifications to generic MOGA and MOCS algorithms, the overall scheme is evaluated in combination with problem specific features developed in this work, namely the repair mechanism and GES.

The overall outcome of the simulation studies is presented in Table 7.3. Tables D.1, . . . , D.21 focusing on each feature evaluation are presented in Appendix D. Each table contains the leading objective value found for each objective considered. The objectives used within the optimisation algorithms were normalized against the initial gear shift map provided by the manufacturer. J_{CO_2} is presented without normalisation in the tables of results to clearly identify the relative merits of the algorithms investigated.

Table 7.3 identifies the most suitable algorithm, which abbreviations are summarised in Table 7.5, and the settings defined in Section 7.2 and identified using the colour coding shown in Table 7.4, for both Pareto and weighted sum objective formulations.

Considering the Pareto case, no repair with GES (green) gives rises to the leading results in terms of CO_2. This is expected as the application of repair increases the J_{CO_2}. M_{p1} and M_{p2} are the most suitable algorithms for J_{CO_2}, J_{Dist}, J_{IRP} and $J_{Gj\%}$ when Pareto ranking is used. Note however that GES may lead to premature convergence and prevent exploration.

J_{z3} reaches a minimum value that is similar, irrespective of each algorithm used. This means that the objective J_{z3} cannot be used to differentiate between alternative solutions. This behaviour can be explained by the drive cycle used to evaluate alternative solutions, where the vehicle is not operating at high speed for significant periods of time.

The ideal algorithm for the weighted sum (W_{Sum}) approach was M_{p7} for most objectives, with the exception of J_{Gch} and J_{z1}, where M_{p6} was better. M_{p7} offered the most suitable performance in terms of J_{Obj}, the latter being used to determine the most suitable solution. Compared to the Pareto based optimisation approach, it can be seen that the selection of the objective weightings is critical to the achievable performance against individual objectives. In general Pareto based optimisation approaches are better at enabling individual objectives to be minimised.

The performance results are provided in more detail in Appendix D. The ideal algorithms with different settings are defined in the following Table 7.3:

Table 7.3: Most suitable algorithm for each objective function

	J_{CO_2}	J_{Dist}	J_{z_1}	J_{IRP}	$J_{G_{ch}}$	J_{z_3}	$J_{G_j\%}$	J_{z_2}	J_{Obj}
Set 1 (Par)	$M_{p1}(2)$	$M_{p2}(1)$	$M_{p4}(2)$	$M_{p1}/M_{p2}(1)$	$M_{p1}(1)$	All(1)	$M_{p1}(1)$	$M_{p2}(1)$	$M_{p2}/M_{p5}(2)$
Set 2 (Par)	$M_{p2}(1)$	$M_{p1}(2)$	$M_{p2}/M_{p4}(3)$	$M_{p1}/M_{p1}(2)$	All $M_{p1}(2)$	All(1)	$M_{p1}(3)$	$M_{p3}(2)$	All(4)
Set 3 (Par)	$M_{p1}(1)$	$M_{p1}(1)$	$M_{p4}(1)$	$M_{p1}(3)$	$M_{p1}(3)$	All(1)	$M_{p4}(2)$	$M_{p1}(3)$	$M_{p1}/M_{p2}/M_{p5}(1)$
Set 1 (W_{Sum})	$M_{p7}(5)$	$M_{p7}(3)$	$M_{p7}(4)$	$M_{p7}(5)$	$M_{p6}/M_{p6}(4)$	$M_{p7}/M_{p7}(2)$	$M_{p7}(6)$	$M_{p6}/M_{p6}(4)$	$M_{p7}(3)$
Set 2 (W_{Sum})	$M_{p7}(3)$	$M_{p7}(4)$	$M_{p7}(6)$	$M_{p7}(6)$	$M_{p6}/M_{p6}(4)$	$M_{p7}(2)$	$M_{p7}(4)$	$M_{p6}/M_{p6}(4)$	$M_{p7}(5)$
Set 3 (W_{Sum})	$M_{p7}(4)$	$M_{p7}(5)$	$M_{p7}(5)$	$M_{p7}(4)$	$M_{p6}/M_{p6}(4)$	$M_{p7}(2)$	$M_{p7}(5)$	$M_{p6}/M_{p6}(4)$	$M_{p7}(6)$

Table 7.4: Colour coding for various setting in algorithms performance assessment

Setting	Colour coding
No Repair mechanism, no GES	Black
Repair mechanism, no GES	Red
No Repair mechanism, GES	Green[1]
Repair mechanism, GES	Blue

[1]Applicable only with Pareto based optimisation algorithms.

Table 7.5: Abbreviation for algorithms investigated

M_{p1}	MOGA original with modified Pareto ranking
M_{p2}	MOGAOp M_{p1} with additional operators from Cuckoo Search
M_{p3}	$MOGA_{Toolbox}$. MOGA from MATLAB optimisation toolbox (gamultiobj)
M_{p4}	M_{p1} with application of GES at each generation
M_{p5}	M_{p2} with application of GES at each generation
M_{p6}	Interior-point algorithm from MATLAB optimisation toolbox
M_{p7}	Single GA from MATLAB optimisation toolbox (ga)

7.6.1 Effect of repair mechanism

Pareto based optimisation

The impact of repair mechanism has limited in some condition the optimiser to reduce further down J_{CO_2}, as it is designed to improve the driveability, however will increase J_{CO_2} as illustrates in Table D.10, in Appendix D.

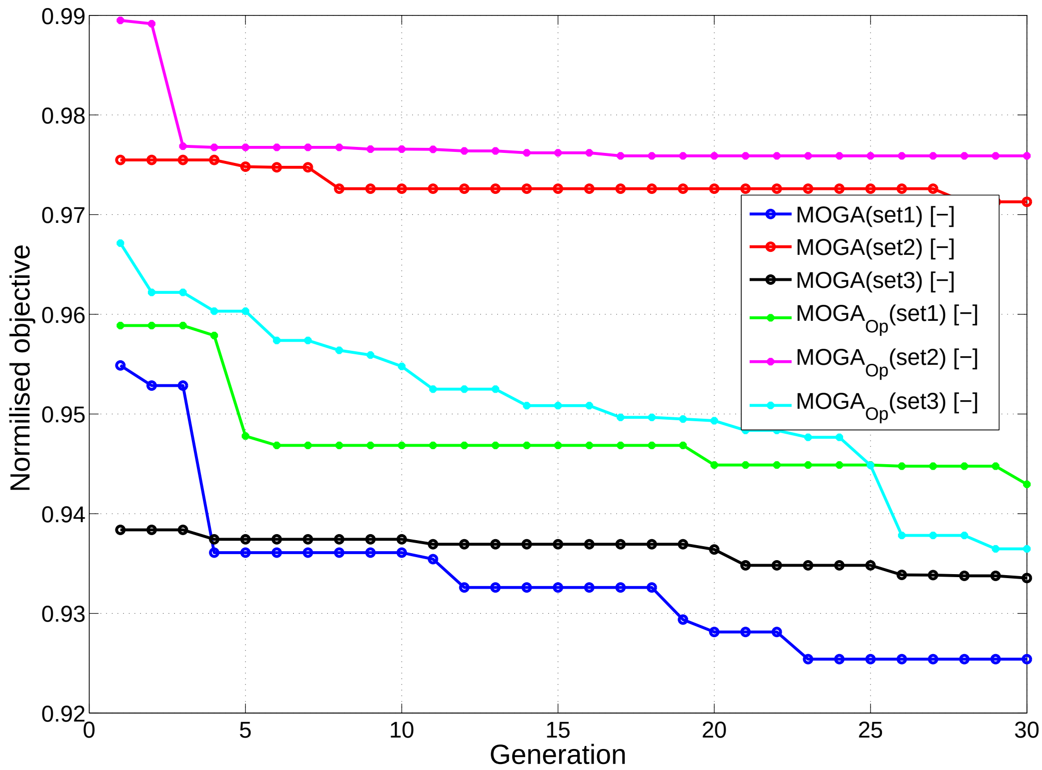

Figure 7.8: Convergence of MOGA and MOGA$_{Op}$ based on Pareto under different objective combinations denoted set 1, set 2, and set 3

7.6.2 Effect of GES operator

Noticed that the application of GES was only implemented MOGA and MOGA$_{Op}$. Additionally, as it was described that GES improve the value of J_{CO_2}, however care need to be taken by applying GES, as it can result to a premature convergence (Pandey et al. 2014). GES was applied in average at every 3 generations, also at each generation in order to highlight the impact of GES. Noticed that GES$_{Ag}$ (M$_{p4}$), GES$_{Ag/Op}$ (M$_{p5}$) are referred to as a more aggressive application of GES, meaning that GES is applied at each generation on MOGA and MOGA$_{Op}$ respectively.

Pareto based optimisation

Tables D.14, Table D.15 and Table D.16 demonstrate the results obtained by applying GES. In general the average of J_{CO_2} has significantly reduce in comparison to non-application of GES, see Table D.17.

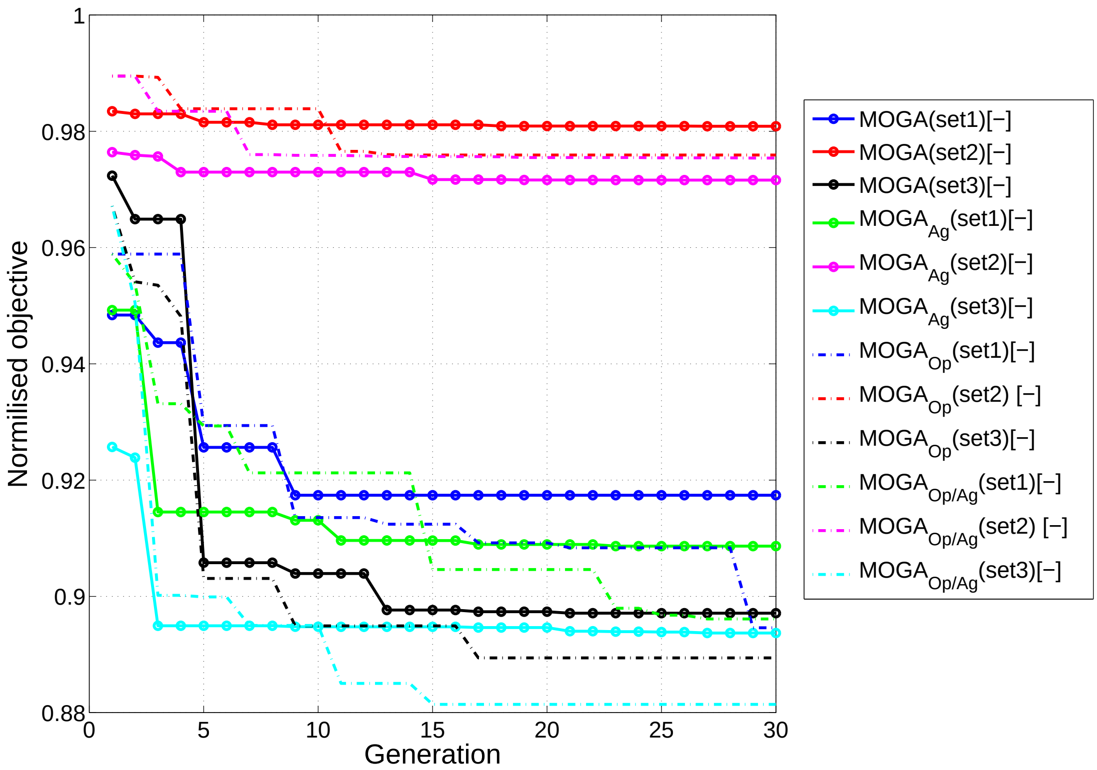

Figure 7.9: Convergence of MOGA, MOGA$_{Ag}$, MOGA$_{Op}$ and MOGA$_{Op/Ag}$ based on Pareto under different objective combinations denoted set 1, set 2, and set 3

Figure 7.9 illustrates the impact of applying GES on the rate of convergence. As expected, it has contributed a higher, faster rate of convergence of fitness values in compared to Figure 7.10 and Figure 7.8. Additionally the application at each generation has also accelerated the rate of convergence.

7.6.3 Effect of objective formulation

The objectives formulation as described in Section 4.2.1, were used as a mean of measure to assess the performance of each optimised shift map. Three different sets were defined (see Section 7.2) as separate objective functions for both Pareto and weighted sum. The first set aims to rely on three group of objectives, namely emissions, driveability and durability. The set 2 is based on the three main objectives uncorrelated, CO_2 emissions, IRP and $G_j\%$ (see Table 6.5, Section 6.1.2, in Chapter 6). Finally, the set 3 was based on all objective functions.

The solutions correspond to the ranked optimisers for CO_2 emissions (see Table 7.3) are defined in Appendix E with their respective objective functions and shift map. The leading solutions are described in Sections E.2 and E.3, and their respective shift map are represented with the minimum hysteresis between Upshift and Downshift. As expected the driveability and gear change frequency are high. On the other hand, the second solution described in Section E.1, despite it low CO_2 emissions, only has a minimum hysteresis at the low throttle position for gear set 2, gear set 3 and gear set 4. Therefore it had a better $G_j\%$ than the two last.

The weighted sum solutions are among the highest CO_2 emissions. The solutions described in Section E.5, is the most suitable from the three solutions. It has a better IRP in compared to Pareto solutions. Solutions presented in Sections E.4 and E.6 are with the minimum in terms of CO_2 emissions, therefore they have improved IRP despite being optimised.

7.6.4 Pareto versus weighted sum approach

The weighted sum method is the simplest technique in optimisation when dealing with more than one objective functions (see Section 4.4.1, in Chapter 4), therefore it is difficult to reflect the user desire when considering the multiple objective function. In this thesis, Pareto outperformed and weighted sum performances were compared under 3 settings (see Section 7.2). It can be noticed that Pareto outperformed the weighted sum in terms of rate of convergence as well as minimum CO_2 emissions (see Figures 7.8, 7.9, 7.10 and 7.11).

7.6.5 MOGA and nature inspired operators

This section describes the performance of algorithms.

Pareto based optimisation

Tables D.1, D.2 and D.3 are the results of Pareto-based optimisation for set 1, set 2 and set 3 respectively. Noticed that J_{CO_2} used in the algorithm was normalized against the initial gear shift map, it is presented without normalisation in the tables of results. This was adopted to assess more easily the potential for CO_2 saving. The MOGA_{Op} gave rise to the ideal J_{CO_2} for set 1 (see Table D.1) but the worse for set 2 (see Table D.2) whilst the MOGA gave the leading J_{IRP} for both set 1 and set 2.

Figure 7.10 represents the rate of convergence of different optimisers, and the correlation between various objective functions respectively. In Figure 7.10, it can be noticed that the convergence of the algorithm depends on the objective formulation, i.e. set is not improving, in terms of the most suitable solution, for many generations, whilst sets 1 and 3 lead to a more regular convergence. MOGA_{Op} is only able to outperform the benchmark MOGA for set 2.

The small population size and use of modified Pareto ranking leads to gaps between solutions on the Pareto set. This initial comparison is not able to demonstrate that it is beneficial to include Cuckoo Search operators within the GA. However, due to time constraints only a few experiments could be run, making the result not statistically significant.

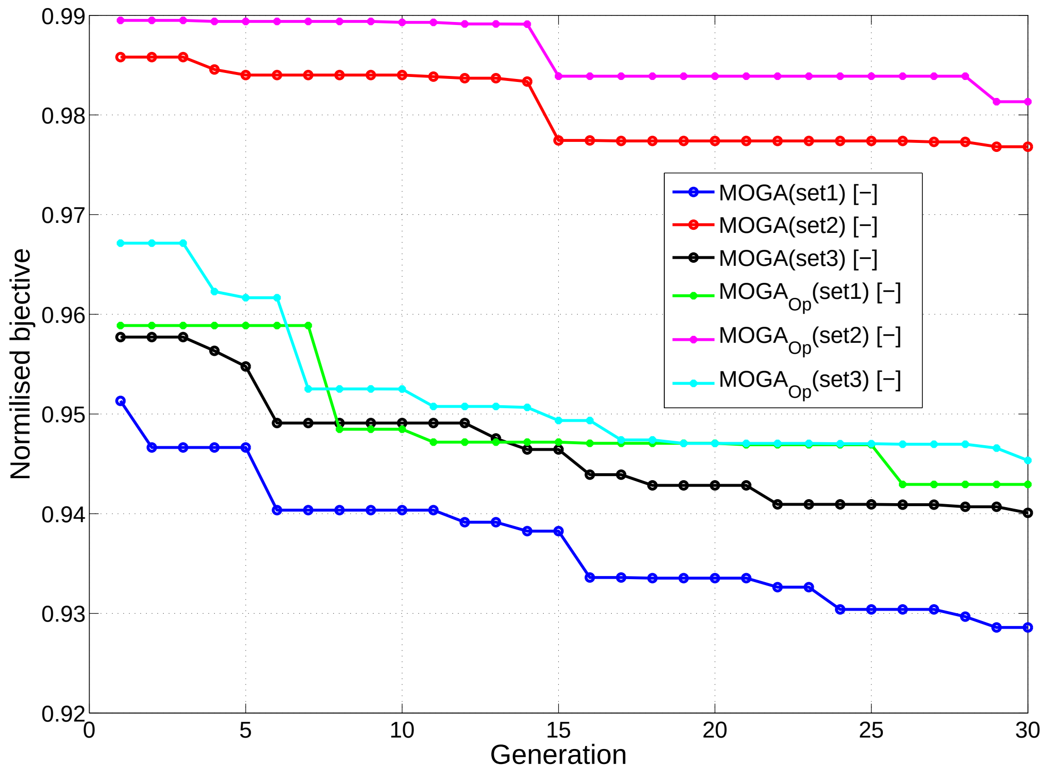

Figure 7.10: Convergence of MOGA and MOGA$_{Op}$ based on Pareto under different objective combinations denoted set 1, set 2, and set 3

Non-Pareto based optimisation

Non-Pareto based optimisation is performed using the interior-point algorithm and GA from MATLAB toolbox.

Tables D.4, D.5 and D.6 illustrate the final solution obtained from interior-point algorithm and GA based on set 1, set 2 and set 3. By contrast to the Pareto based optimisation approach, it can be noticed that J_{CO_2} has not been significantly reduced with average J$_{CO_2}$ around g/km.

Indeed, whilst Pareto based optimisation approach can find solution that excel against any particular objectives, non Pareto base optimisation approaches rely exclusively on the selection of the trade-off between the different objectives.

7.6.6 Algorithms performance with repair mechanism, and GES

Pareto based optimisation

Tables D.18, D.19 and D.20 demonstrate the application of repair mechanism and GES considering set 1, set 2 and set 3 conditions. The application of GES (see Table D.21) in this case, improves the results of convergence rate.

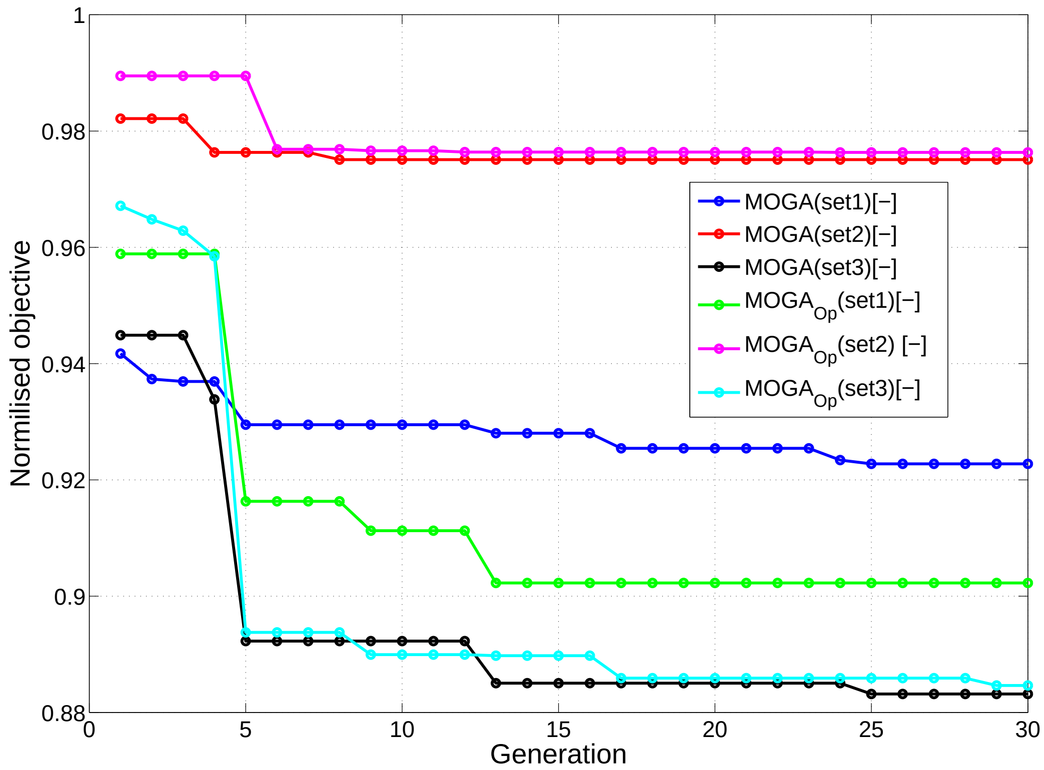

Figure 7.11: Convergence of MOGA and MOGA$_{Op}$ based on Pareto under different objective combinations denoted set 1, set 2, and set 3

This section has described the performance of MOGA, and MOGA$_{Op}$ under different settings with the application of repair mechanism and GES. Additionally, a comparison was made against optimiser benchmark from MATLAB toolbox, MOGA$_{Op}$ considering Pareto, interior-point algorithm and GA considering Non-Pareto. It was highlighted that repair mechanism has improved in average J$_{IRP}$, however increase J_{CO2}. Inversely, GES improves J_{CO_2}, however as a drawback, it can impact on the convergence rate and prevent exploration.

7.7 MOCS

This section describes the MOCS algorithm combined with Levy Flight, Bat, Firefly and Flower Pollination operators. The goal of this section is to verify the performance of each operator for optimising intermediate gear ratio. The comparative assessment of each operator is mainly based on the speed of convergence, which measures the quality of difference solutions. An experiment was realised with a termination condition of 30 generations to assess the performance of difference operators as follows: (i) the operator were individually run. (ii) the operators were randomly selected from generation to generation. (iii) the operators were selected in an ascending order starting from Levy Flight (1), Firefly (2), Bat (3) and Flower pollination (4). Three objective functions were considered in this case, namely: CO_2 emissions, IRP and gear ratio bandwidth (see Section 3.4.5, in Chapter 3). The number of available host nest was fixed to 15. Two sets of weights were considered for this study. Table 7.6 describes the weighted combination for use with the modified Pareto ranking (see Section 4.4.2, in Chapter 4). The Weighting set 1, favours the bandwidth, and Weighting set 2 favours CO_2 emissions.

Table 7.6: Weighting coefficient for gear ratio optimisation. W_{GR_1}, W_{GR_2} and W_{GR_3} denote the weighting coefficient of CO_2, IRP and bandwidth respectively

	W_{GR_1}	W_{GR_2}	W_{GR_3}
Weighting set 1	100	15	300
Weighting set 2	300	15	100

7.7.1 Results based on weighting set 1

The weighting selection of set 1 is justified by the fact that CO_2 emission is prioritised.

The results for each benchmark settings, are described in Tables 7.7 and 7.8.

Table 7.7: Comparative performance of MOCS integrated with Levy Flight, Bat, Firefly, Flower pollination operators separately

	Levy Flight	*Firefly*	*Bat*	*Flower pollination*
functions evaluated	1152	648	1063	1070
Ideal solution	0.51	0.497	0.5029	0.496
Mean value of solution	$1.25e^{-7}$	0	$6.77e^{-8}$	4.76^{-5}
Std of solutions	$2.44e^{-7}$	0	$1.13e^{-7}$	4.58^{-5}
Spread	$2.39e^{-7}$	0	$1.11e^{-7}$	4.48^{-5}

Table 7.8: Comparative performance of MOCS integrated with Levy Flight, Bat, Firefly, Flower pollination operators. The first test is selecting different operators randomly. The second test is selecting gradually different operators

	Random selection	*Order selection*
functions evaluated	1084	1063
Ideal solution	0.499	0.5006
Mean value of solution	5.63^{-4}	7.31^{-7}
Std of solutions	1.034^{-3}	9.54^{-7}
Spread	$1.01e^{-3}$	$9.33e^{-7}$

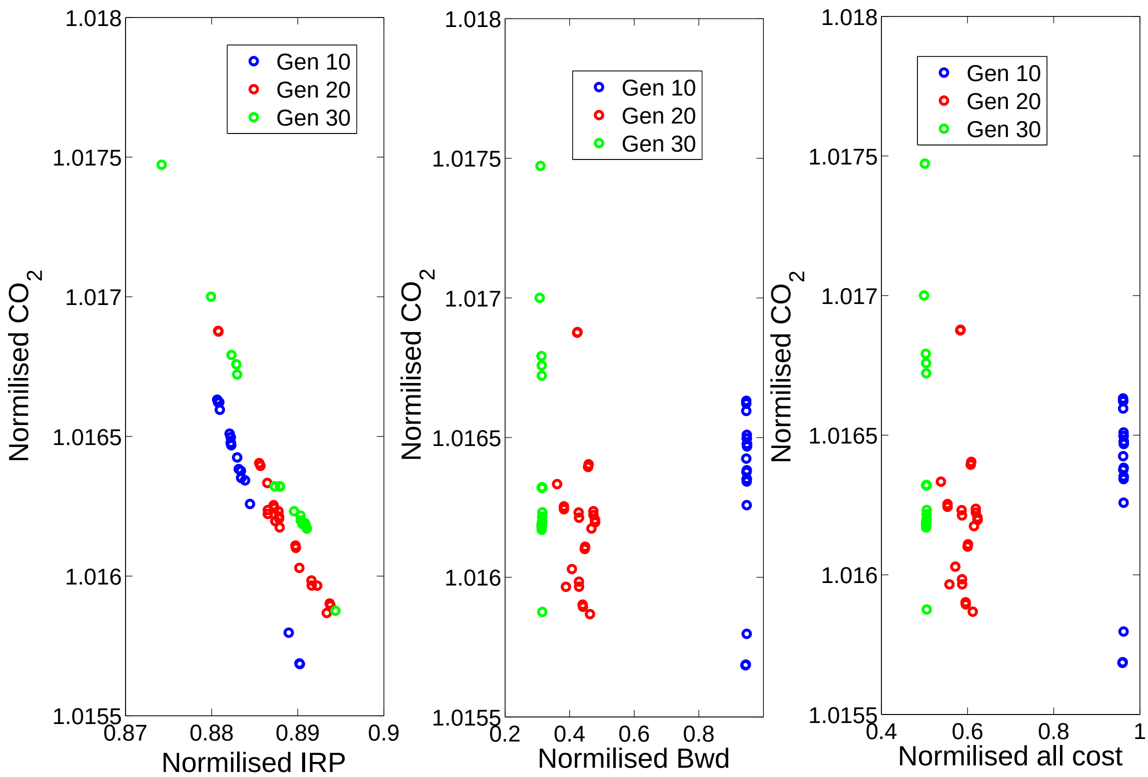

Figure 7.12: Trade-off between CO_2 against IRP, bandwidth and overall weighted combination cost based on random selection of operators: Levy Flight, Firefly, Bat and Flower pollination. The blue, red and green circles denote the solutions trade-off after 10, 20 and 30 generations, respectively.

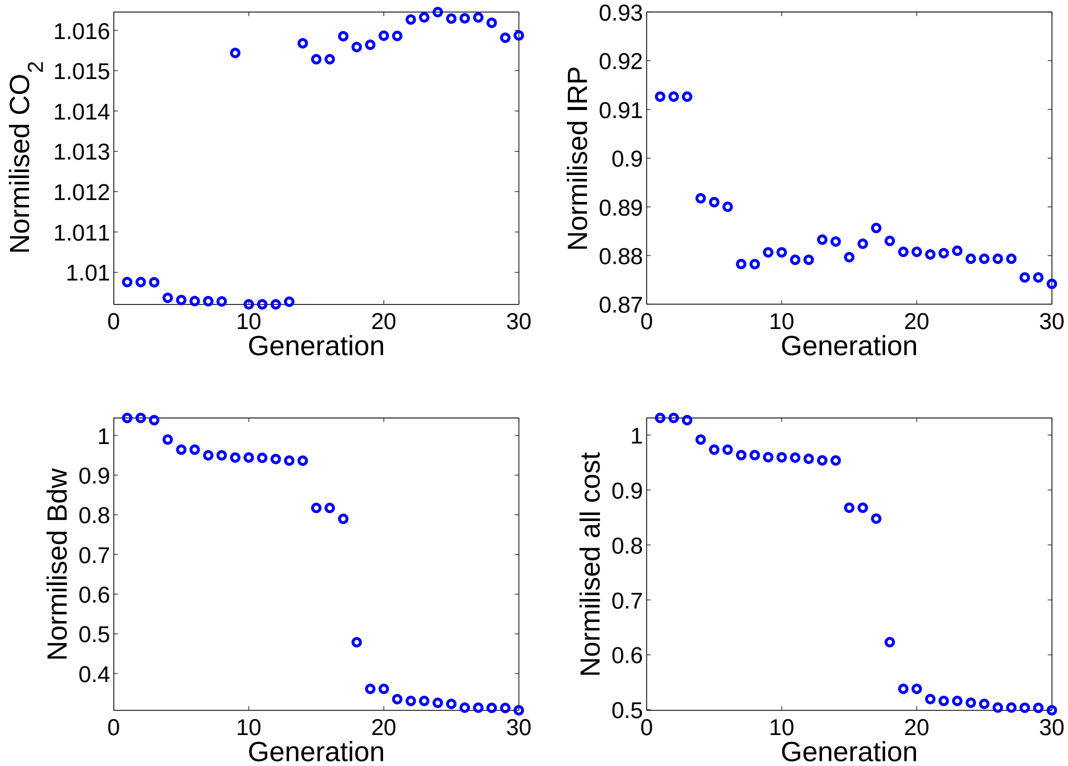

Figure 7.13: Performance of gear ratio optimisation based on random selection of operators: Levy Flight, Firefly, Bat and Flower pollination

Figure 7.12 and Figure 7.13 illustrate the intermediate gear ratio optimisation performance considering randomly selected operators. Figure 7.12 demonstrates the evolution of various objective trade-off against CO_2 emissions. It can be noticed that the CO_2 value is increasing while the IRP, bandwidth and overall cost are decreasing. Figure 7.13 presents the trade-off between CO_2 against IRP, bandwidth and overall weighted combination cost, where the Pareto optimal sets are shown by the blue, red and green circles after 10, 20 and 30 generations respectively.

Similarly, it can be seen from Table 7.7 and Table 7.8, that only random selection managed to maintain a better diversity at the last generation. Thus, it can be concluded that a bigger number of generation is not necessary to optimise the intermediated gear ratio considering the first weighting combination.

7.7.2 Results based on weighting set 2

The second set of weightings puts more emphasis on the gear ratio bandwidth.

Table 7.9: Comparative performance of MOCS integrated with Levy Flight, Bat, Firefly, Flower pollination operators separately

	Levy Flight	*Firefly*	*Bat*	*Flower pollination*
functions evaluated	513	147	444	402
Ideal solution	0.822	0.846	0.822	0.822
$\bar{d}$	0.0091	0.0109	0.0101	0.0112
Std	0.029	0.0297	0.032	0.0363
Spread	0.028	0.0285	0.0307	0.0349

Table 7.10: Comparative performance of MOCS integrated with Levy Flight, Bat, Firefly, Flower pollination operators. The first test is selecting different operators randomly. The second test is selecting gradually different operators

	Random selection	*Order selection*
functions evaluated	423	344
Ideal solution	0.846	0.823
$\bar{d}$	0.0107	0.0108
Std	0.0355	0.0369
Spread	0.034	0.0355

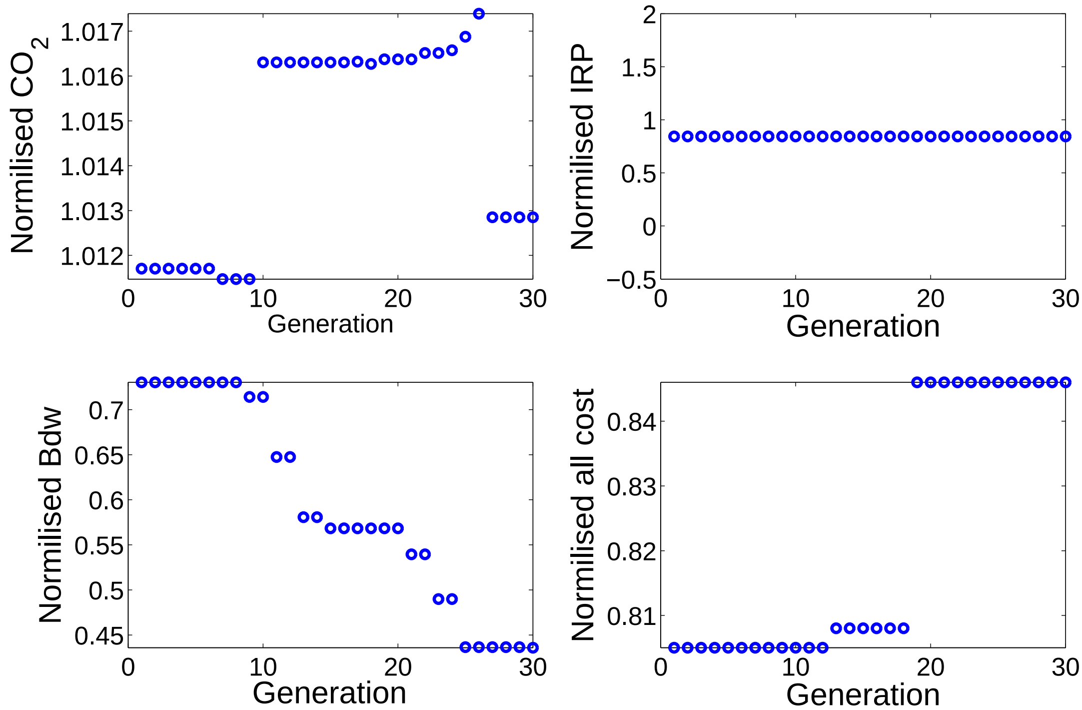

Figure 7.14: Performance of gear ratio optimisation based on Firefly

Figure 7.14 and Figure 7.15 illustrate the intermediate gear ratio optimisation performance considering Firefly of operators. In most case the IRP stays constant, and bandwidth naturally decreasing. However, the overall cost increases from generation to generation. According to Figure 7.15, the spread based on the last generation is well distributed in comparison to most cases noticed in Section 7.7.1.

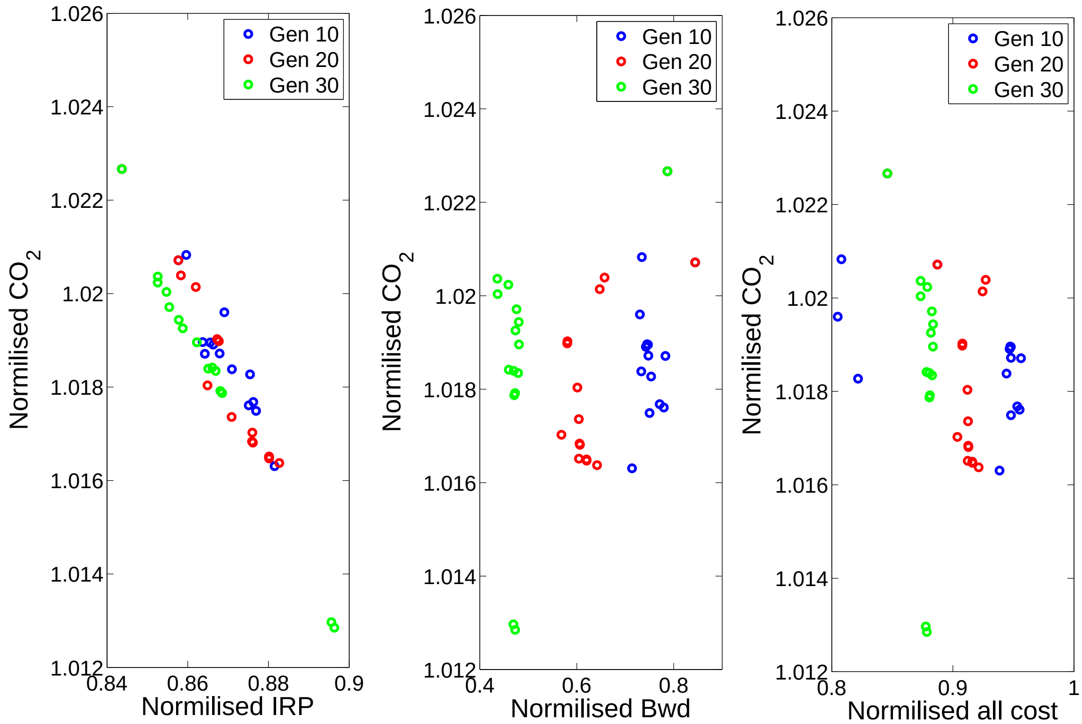

Figure 7.15: Trade-off with Firefly between CO_2 against IRP, bandwidth and overall weighted combination cost. The blue, red and green circles denote for solutions trade-off after 10, 20 and 30 generations respectively

7.8 Combined gear ratio & shift map optimisation

The realisation of combined gear ratio and gear shift map is based on the algorithm described in Figure 5.10 (see Section 5.4.1, in Chapter 5). MOGA, MOCS and interior-point algorithm were combined to obtain a set of gear ratio and optimised gear shift map, as illustrated in Figure 7.16. The set of gear shift and gear ratio combinations contains 15 nests. Each nest is represented by a set of 6 speed gear ratios (G_1,G_2,G_3,G_4,G_5 and G_6). Each nest is then defined with its initial shift map, and 40 optimised shift maps.

For this study, 10 generations were considered for MOCS, and 10 generations for MOGA. Notice that MOCS was setup with random selection of operator at each generation, to encourage diversity amongst the population.

Three different sets of combination are described in the following sub-sections:

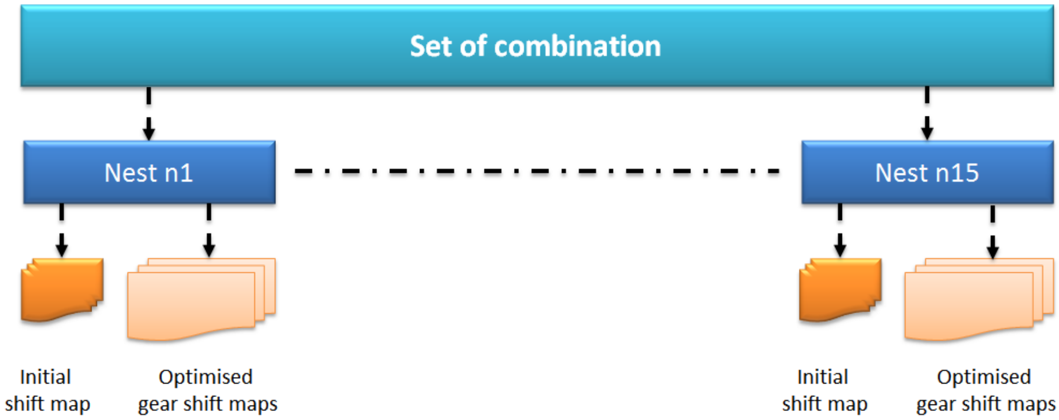

Figure 7.16: Illustration of a set of combination representing, a set of gear ratio, with its initial and optimised gear shift maps respectively

Noticed that within a combined set, not all 15 nest are found to be valid due to constraints. In fact, $comb_{Set1}$ has 15 valid nests, $comb_{Set2}$ has 9 nests valid nests and $comb_{Set3}$ has also 9 valid nests.

Table 7.11: Performance of MOCS integrated with Levy Flight, Bat, Firefly, Flower pollination operators. A random selection of operators is considered in this case. $comb_{Set1}$, $comb_{Set2}$, $comb_{Set3}$ denote the sets of combination 1, 2 and 3 respectively

	$comb_{Set1}$	$comb_{Set2}$	$comb_{Set3}$
$functions\ evaluated$	180	436	485
$Ideal\ solution$	0.7392	0.6994	0.968
$\bar{d}\ value\ of\ solution$	0.0101	0.0023	0.0061
$Std\ of\ solutions$	0.0199	0.0046	0.0119
$Spread$	0.019	0.0044	0.011

Table 7.11 describes the performance of the intermediate gear ratio optimisation based on the combined gear ratio and gear shift map optimisation. It can be seen that the number of function evaluation varies significantly between the first and the last two set of combinations. This can be justified by the complexity of this particular gear set, as the first and last gear ratios are different, meaning

that constraints become more stringent, which can result in a higher function evaluations.

The leading overall objective function is higher compared to the first two.

Table 7.12: Ideal CO_2 emissions for $comb_{Set1}$, $comb_{Set2}$ and $comb_{Set3}$ with their corresponding J_{dis}, J_{z_1}, J_{IRP}, $J_{G_{ch}}$, J_{z_3}, $J_{G_j\%}$, J_{z_2} and Obj_F

	J_{CO_2}	J_{dis}	J_{z_1}	J_{IRP}	$J_{G_{ch}}$	J_{z_3}	$J_{G_j\%}$	J_{z_2}	Obj_F
$comb_{Set1}$	186.18	0.892	0.985	1.47	1.43	1.0	0.934	1.05	0.957
$comb_{Set2}$	186.28	0.9095	0.994	1.49	1.43	1.0	0.69	1.017	0.957
$comb_{Set3}$	186.29	0.814	1.006	1.51	1.43	1.0	0.666	0.983	0.957

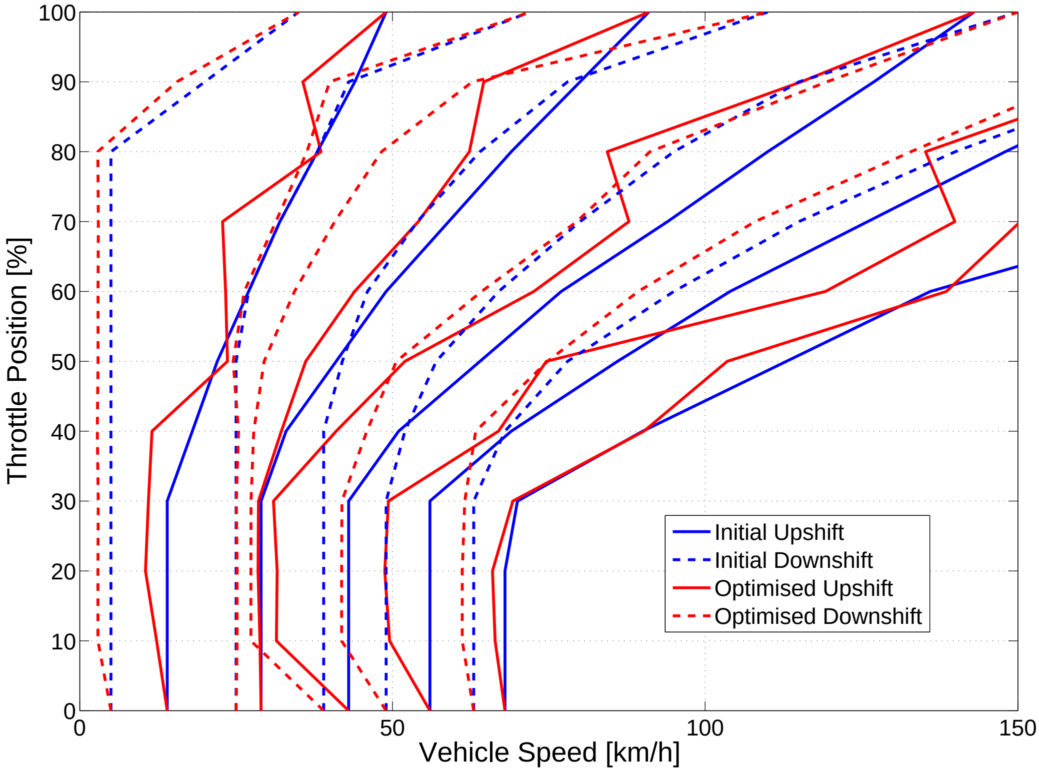

Figure 7.17: Ideal optimised gear shift map in terms of CO_2 based on $comb_{Set1}$

Figure 7.17 represents the optimised gear shift maps in terms of CO_2 from $comb_{Set1}$. It only shows, focuses on the most effective area, between 0 to 70% of throttle position and 0 to 130 km/h. The similarities between these three optimised shift maps $comb_{Set1}$, $comb_{Set2}$ and $comb_{Set3}$ are their very low emissions,

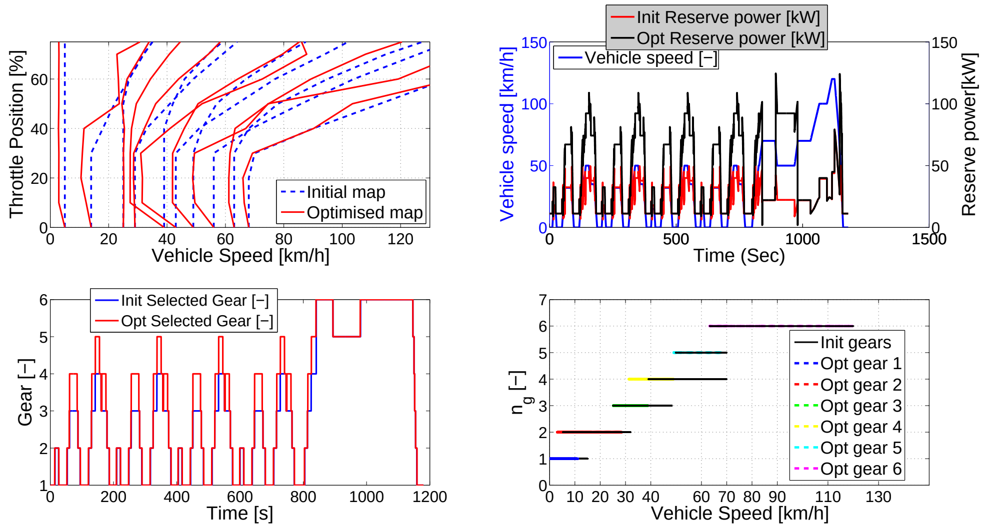

Figure 7.18: Gear shift map results based on $comb_{Set1}$ of the most suitable results. The plots are: optimised gear shift map, reserve power, gear selection and speed range each gear ratio compared to the original shift map

and as expected the IRP has accordingly increased significantly. The advantage of this combined method is rapid convergence, with good results obtained after 10 generations. However the drawback of this method is the rapid degradation of the IRP as it can be seen in Table 7.12, which can consequently affect the driveability.

Figure 7.18 and Figure 7.19 represent the optimised gear shift map results for $comb_{Set1}$, with its corresponding reserve power, gear selection and speed range on each gear ratio in compared to the standard gear shift map (see Section F.1, in Appendix F for $comb_{Set2}$ and $comb_{Set3}$). As expected, the gear 5^{th} usage has increased, which benefit the CO_2 emissions. Therefore, the reserve power has massively increased whilst lowering the CO_2 emissions.

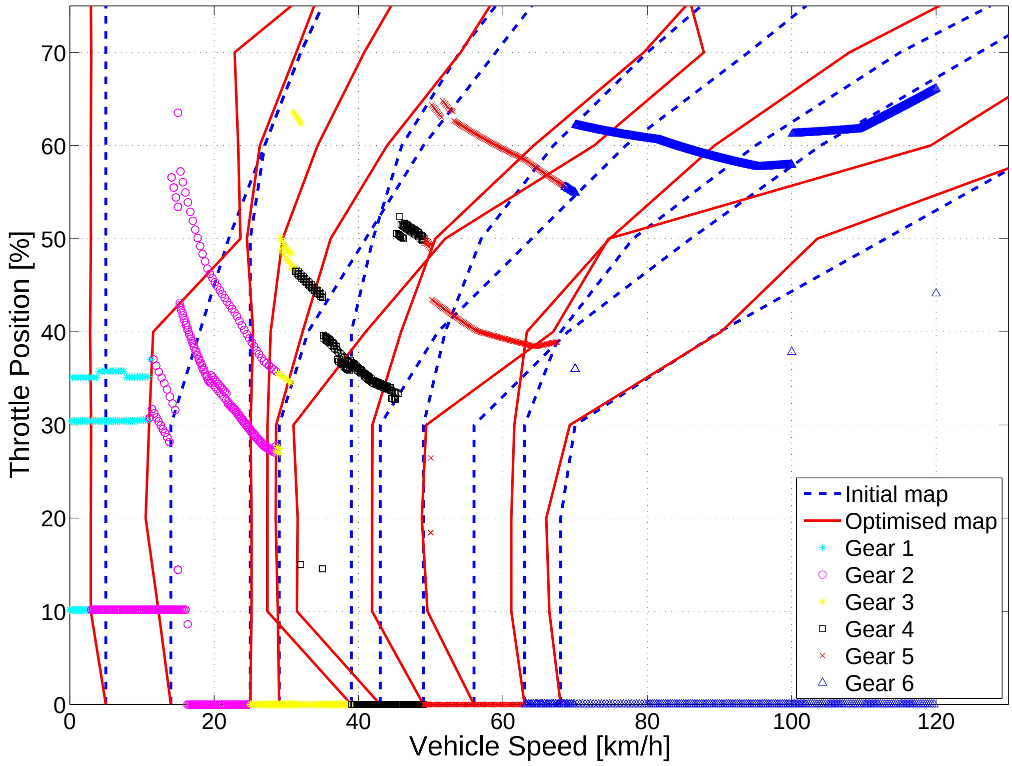

Figure 7.19: Gear shift map results based on $comb_{Set1}$ of the most suitable results. The plot presents the vehicle speed of the NEDC reflected on the shift map.

Table 7.13: Ideal CO_2 emissions for $comb_{Set1}$, $comb_{Set2}$ and $comb_{Set3}$ with their corresponding J_{dis}, J_{z_1}, J_{IRP}, $J_{G_{ch}}$, J_{z_3}, $J_{G_j}\%$, J_{z_2} and Obj_F

	J_{CO_2}	J_{dis}	J_{z_1}	J_{IRP}	$J_{G_{ch}}$	J_{z_3}	$J_{G_j}\%$	J_{z_2}	Obj_F
$comb_{Set1}$	195.9	0.938	1.28	1.08	1.0	1.0	0.296	0.602	0.989
$comb_{Set2}$	193.3	0.901	1.27	1.15	1.13	1.0	0.287	0.61	0.979
$comb_{Set3}$	193.1	0.941	1.27	1.16	1.13	1.0	0.291	0.608	0.978

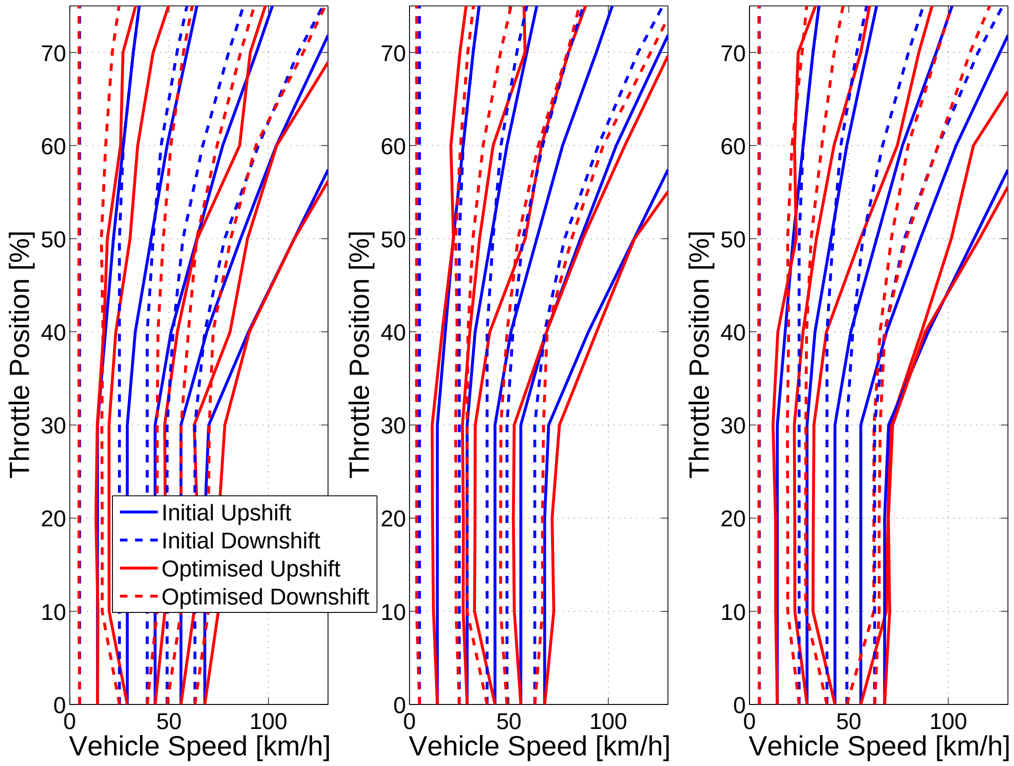

Figure 7.20: Selection of optimised gear shift maps at early generation

Figure 7.20 represents three optimised gear shift maps selected at early generation in order to be compared to the last generation described by Figure 7.17. Table 7.13 represents their objective functions. In terms of CO_2 emissions, the selected solutions from an early generation are similar to the results obtained in Section 7.6. However the leading solutions in terms of CO_2 obtained in the last generation have significantly lower CO_2 values e.g. 186 g/km. The IRP is by contrast significantly increased, expressing a degradation of the driveability as CO_2 decreases (see Table 7.12 and 7.13). Note that the minimum driveability constraints are still met by these solutions, however the overall shape of gear shift map resulting from the combined gear ratio and gear shift map optimisation is not regular. A comparison was also made between the average and ideal CO_2 emissions in terms of shapes of gear shift map. It was found that in the absence of

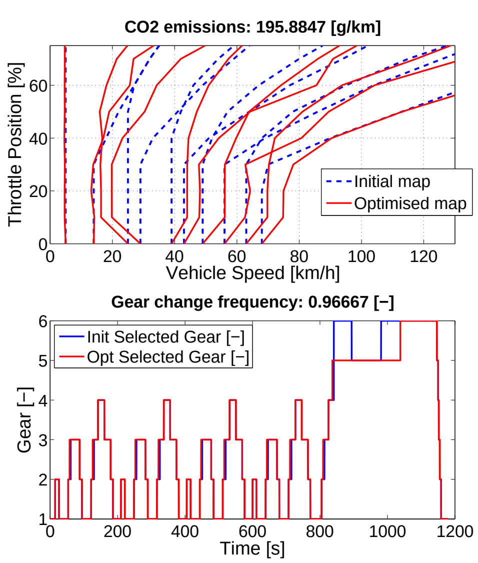

Figure 7.21: Gear shift map results based on $comb_{Set1}$ at the earlier generation. The plots are: optimised gear shift map, reserve power, gear selection and speed range for each gear ratio to the original shift map

stricter constraints on the shape of the gear shift, the optimiser tended to produce irregular gear shift maps that may not be optimal from a practical perspective (see F, Section F.2). The selection of the shape constraints has been identified as an area of further work which requires important inputs from engineers as well as use of a wide variety of driving cycles to ensure that the engine operating points cover the whole gear shift map.

The operating points of combined gear ratio and gear shift map are not similar to the original shift map. This can be explained by the modification of gear ratio. The engine speed vary from 780 RPM to up to 4000 RPM, in compare to the original gear ratio, which vary from 780 RPM to 2400 RPM. It can be noticed that having a wide range of engine speeds and different set of gear ratios benefit the CO_2 emission.

Figure 7.21 and Figure 7.22 represent the optimised gear shift map results for $comb_{Set1}$, with its corresponding reserve power, gear selection and speed range on each gear ratio in compared to the standard gear shift map (see Section F.2, in

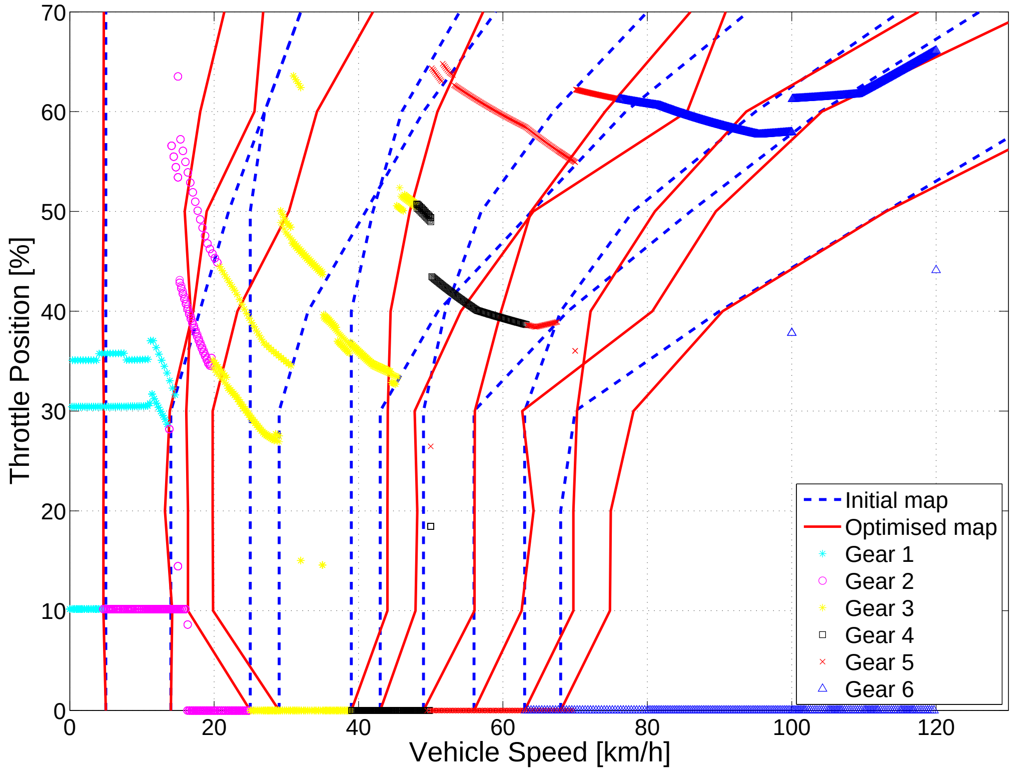

Figure 7.22: Gear shift map results based on $comb_{Set1}$ at the earlier generation. The plot presents the vehicle speed of the NEDC reflected on the shift map.

Appendix F for $comb_{Set2}$ and $comb_{Set3}$). Same remarks can be made as observed in Figure 7.18 and Figure 7.19, except the gear selections are mainly on 4^{th}.

By comparing various objective functions, as seen in Table 7.13 (only optimised gear shift map, see Section 6.1.1, in Chapter 6). It can be noticed that most objective functions are much higher.

7.9 Concluding remarks

This chapter has reported the simulation results for gear shift map and gear ratio. It has illustrated the features of the solutions obtained for individual as well as combined gear shift map and gear ratio optimisation. The chapter started with a demonstration of the working principle of the new problem specific operator and the new repair mechanism. The simulation studies confirmed the ability of the GES operator to improve, in terms of CO_2 existing optimised shift map. The repair mechanism was shown to be able to correct shift maps which exhibits a reserve power below a user defined threshold. Considering the usage of weighted sum to combine a multi-objective function into single objective function. It can be noticed that the final objective function has the same value (see Table 7.12), which makes it difficult to select one without observing various objective functions.

A benchmark study was carried out by comparing the MOGA developed in this thesis against MOGA from MATLAB toolbox considering Pareto ranking and weighted sum. The same conditions were applied in each case, considering integration of repair mechanism and problem specific into MOGA. The ideal compromised set of solutions was Pareto ranking, as it has demonstrated a better diversity among various objective functions. Pareto based optimisation approaches were also able to find solutions with lower CO_2. The evaluation, through simulation, of the new hybrid MOCS to optimised intermediate gear ratio demonstrated that optimising intermediate gear ratio was beneficial to bandwidth but not necessarily to CO_2. The evaluation of the MOGA combined with MOCS to optimise jointly gear shift map and gear ratio demonstrated that such an approach could identify solutions that could significantly reduce CO_2 emissions compared to optimising gear ratio and gear shift map independently.

Chapter 8

Optimised gear shift map experimental results

8.1 Introduction

This chapter details the validation of the shift map developed in this thesis, by testing an optimised gear shift map on a rolling road. This mapping is designed with respect to the engine operating range so that the transmission is in the correct gear at all times e.g. when the driver requires maximal torque. Depending on the prevailing conditions, typically the transmission will select a lower gear moving the engine further into maximum torque producing range (high RPM combined with a wide open throttle). Until recently, these shift maps have been created using a template for the type of engine and vehicle intended and then calibrated by trial and error until adequate performance is achieved according to the ride and drive assessment of a test driver.

A new approach to shift map design is proposed in this thesis, such that the procedure is systematic and automated according to criteria that are selected in an objective function that guides the final definition of the shift map. In Chapter 4, the problem formulation has been described detailing the objective function (see Section 4.2.1). Many variables may be considered, obviously chief among them is CO_2, but also driveability considerations, such as power on demand (acceleration curves), gear shift frequency and other important parameters. In particular a MOGA (see Chapter 5 and Chapter 7) was applied to solve this multi-variable control problem which balances fuel consumption (CO_2 emissions) and driveability. The emissions testing were carried out in SAIC Anting (China) test facilities. The first task was the execution of a series of vehicle tests on a rolling road in controlled conditions in order to establish a baseline average CO_2 figure for the particular vehicle. The next testing phase incorporated the same vehicle but this time with the CO_2 reducing (optimised) shift maps.

In this chapter, a rolling road test result is described and compared with the initial shift map. This chapter is composed as follow: Section 8.2 describes the rolling road parameters, Section 8.4 explains the test results obtained from the initial shift map and optimised shift map. Additionally variability of the simulation model using driver speed input with various optimised shift maps are considered. Finally Section 8.5 concludes this chapter with a discussion.

8.2 Rolling road setting

This section defines the rolling road test procedure, important parameter settings before testing the shift map and an explanation of the test results.

8.2.1 Coastdown test

A coastdown test is a mandatory requirement of the vehicle homologation regulation in order to simulate the vehicle road load during indoor rolling road fuel economy and emission testing (Yasin 1978). The level of driving resistance, such as rolling resistance, vehicle inertia and aerodynamic drag are determined, and adjustment to the rolling road is made as appropriated. The principal properties to maintain during the coastdown test are as follows:

- Tyre rolling resistance:
  This coefficient is related to the tyre design, which determines the effort required to overcome the resistance generated between the road and the tire.

- Vehicle aerodynamic resistance:
  This coefficient is dependant on the vehicle shape. As the vehicle moves, through the atmosphere, an opposite force is generated by the air being deflected by the vehicle. Consequently, the greater the vehicle speed, the higher the resistance.

- Drivetrain and powertrain mechanical resistance:
  This coefficient is concerned with the mechanical friction of the drivetrain. It defines the internal friction that the vehicle has to overcome in order to move the wheels.

In order to determine the data for coastdown adjustment in laboratory testing, the vehicle assigned for this project, ROEWE 950, was taken to a proving ground in Guangde (China), where the environmental conditions (good ambient temperature and humidity) are ideal, and the road is completely flat, straight, and dry for establishing the coastdown properties. The vehicle is driven at 130 km/h, neutral gear position is selected and allowed to coastdown (decelerate) until the vehicle velocity falls below 5 km/h. The vehicle is instrumented to record velocity and distance. The test is repeated several times in order to reduce the effect of measurement error and disturbances.

8.2.2 Test procedures

The testing of emissions and fuel consumption of ROEWE 950 took place on a rolling road (dynamometer) laboratory at the SAIC Anting test and development plant (Shanghai, China). Before the emissions test, vehicles are preconditioned and soaked for at least 6 hours at a test temperature of 20-30C. Emissions are then measured while vehicle is driven according to the New European Driving Cycle (NEDC) speed profile. The entire NEDC consists of four repeated ECE-15 driving cycles of 195s duration each and one extra-urban driving cycle (EUDC) of 400s duration.

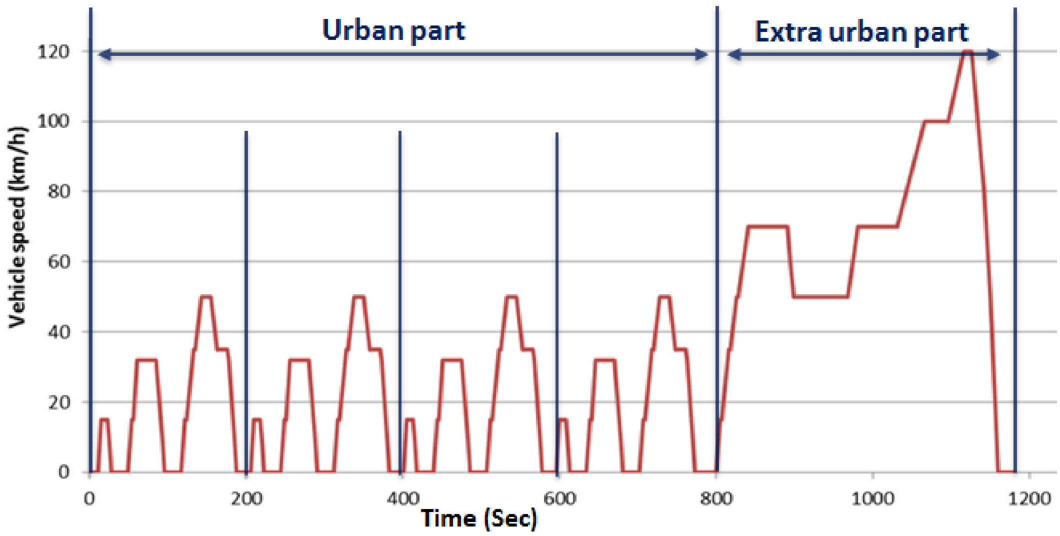

Figure 8.1: The New European Driving cycle (NEDC), based one urban part, composed of four repeated ECE-15 driving cycles, and one extra-urban driving cycle

Additionally, a coastdown must be performed before and after a test, to ensure that the driving resistances of the rolling road are correct. The following data represents an example of coastdown test for this research during a rolling test for gear shift map.

In order to validate the rolling road for fuel and emissions assessment, the coastdown check must be performed against the experimental data obtained from proving ground of Guangde (China). The vehicle speed versus time profile must be adjusted within ± 5 sec, if not, then the driving resistance of the rolling road must be adjusted and a repeat coastdown test performed in order to validate the experimental data (a more detailed coastdown test description can be found in Appendix C).

8.2.3 Explanation of the bag test documentation results

Every test on the rolling road is accompanied by a bag test documentation describing the useful information regarding the particular vehicle used for fuel and emissions, test conditions, fuel type, and the respective emissions test results (see Appendix G). The bag test documentation is composed of four parts as follows:

- Vehicle information & fuel type:

  The first part describes the vehicle details, such as weight (1900 Kg), engine type (gasoline), transmission type (DCT), Driver initial (as it was advised to always use the same driver for all tests), test authorisation number with the date and fuel type (92 RON).

- Test conditions:

  The test conditions section specifies the atmospheric pressure (101.8 kPa), the ambient temperature (24.3 °C, must be maintained), relative humidity (39%).

- Data regarding exhaust analyser:

  An approved analyser is used to assess the concentration of different emissions (CO, NOx, CO_2) in the exhaust gases by inserting a sample probe into the exhaust tailpipe. These samples represent the level of concentration of the various emissions.

- Fuel and emissions results:

  Once the analyser has logged the level of concentration of emissions in the exhaust tailpipe, the results of the emissions are then calculated and printed out.

These documents record all the information of the test conditions with fuel and emissions samples obtained from the rolling road. This information will be used to further assess various optimised shift maps in terms of emissions performance.

8.2.4 Possible sources of error

This sub-section hypothesises possible sources of error, regarding the test phase. It is described as follows:

- The vehicle used for the emissions test was a prototype vehicle, however each test was carried out with the latest Engine Control Unit (ECU) and Transmission Control Unit (TCU) calibration. Additionally, the vehicle was first tested and agreed as valid for rolling road test by calibration engineers, moreover the tyres were also checked.

- It was advised to retain the same driver for all rolling road tests for this research, because of the availability of certified drivers for rolling road testing. However, it was not possible to retain the same driver. While different driver behaviour can affect the final results, it is encouraging to know that all drivers follow the same strict training within SMTC regarding emissions test.

- During the test phases, the vehicle encountered some issues with the start and battery charging system. It was advised to change the vehicle with another prototype vehicle with identical ECU and TCU calibration.

- The laboratory test temperature at Anting test and development plant (Shanghai, China) is maintained at around 25 °C, however the ambient temperature can easily reach 30-35 °C.

- Translation during the test phases. A weekly meeting was held to communicate with SMTC China calibration engineers to discuss testing and any related issues with the rolling road and vehicle. English/Chinese translator was present at the meeting. Additionally, communication with an engineer who does not speak English was assisted by the translator.

8.3 Most suitable selected simulation results for rolling road

This section presents the ideal shift map selected for the rolling road. Table 8.1 illustrates the objective functions of selected gear shift map.

Table 8.1: Best CO_2 emissions for GSM_{Set1}, GSM_{Set2} and GSM_{Set3} with their corresponding J_{dis}, J_{z_1}, J_{IRP}, $J_{G_{ch}}$, J_{z_3}, $J_{G_j}\%$ and J_{z_2}

	J_{CO_2}	J_{dis}	J_{z_1}	J_{IRP}	$J_{G_{ch}}$	J_{z_3}	$J_{G_j}\%$	J_{z_2}
GSM_{Set1}	193.3	0.82	0.812	1.15	1.27	1.01	0.827	1.09
GSM_{Set2}	190.2	0.86	0.803	1.24	1.4	1.01	0.758	1.09
GSM_{Set3}	190.8	0.673	0.811	1.22	1.4	0.999	0.76	1.12

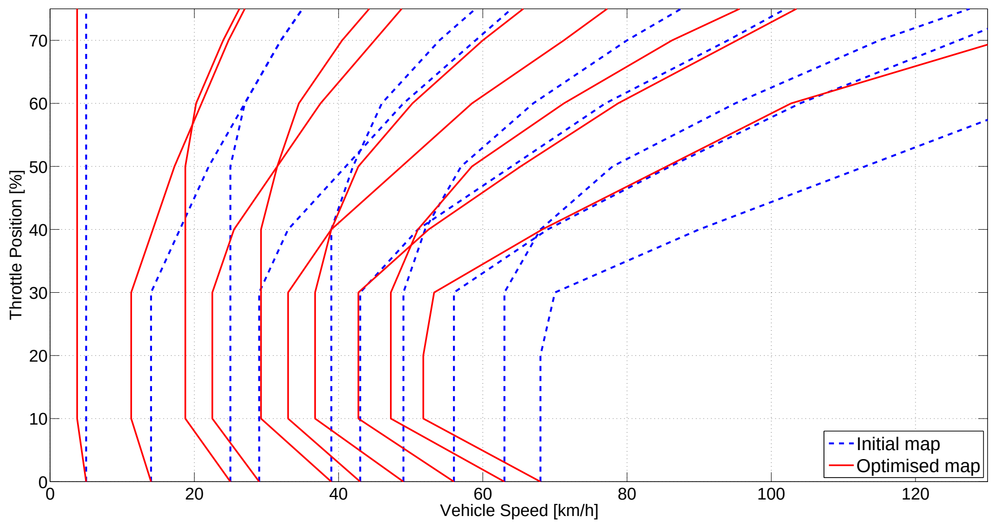

Figure 8.2: Best selected optimised gear shift map 1

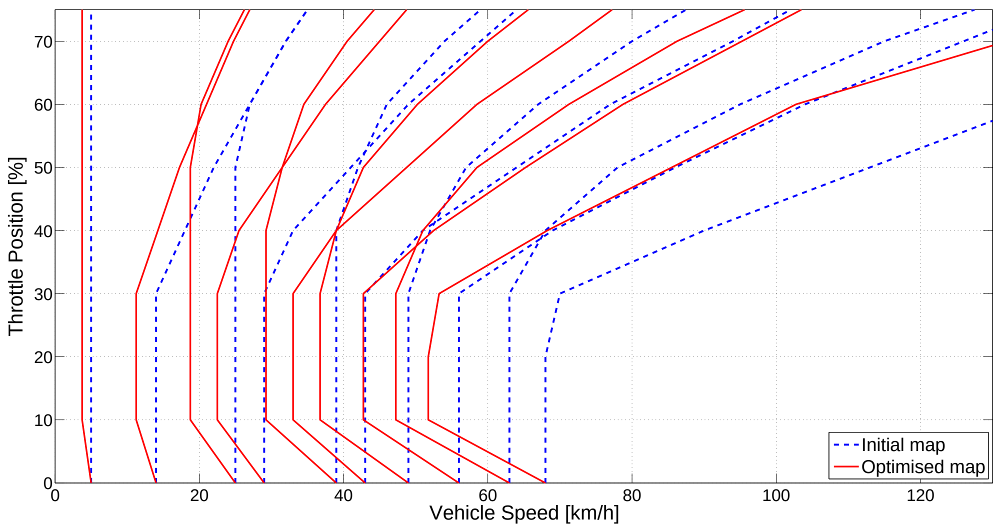

Figure 8.3: Best selected optimised gear shift map 2

Figure 8.2, Figure 8.3 and Figure 8.4 represent satisfactory optimised gear shift map obtained.

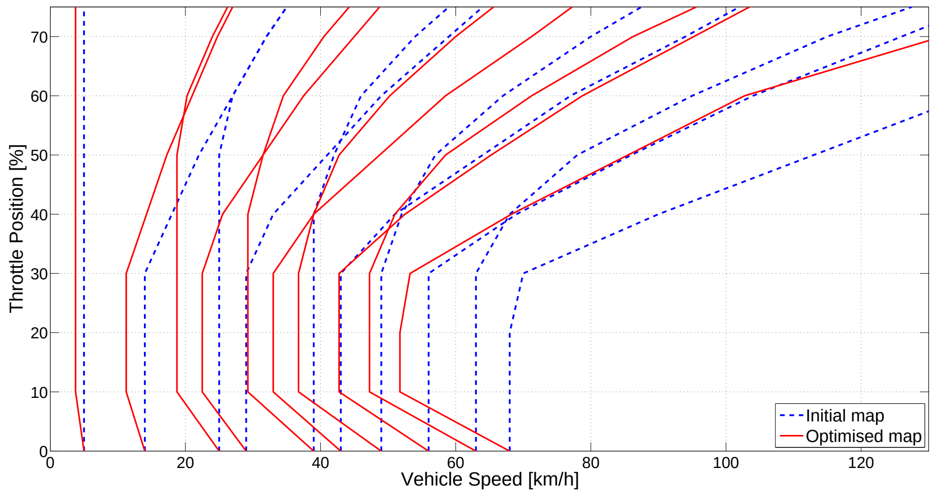

Figure 8.4: Best selected optimised gear shift map 3

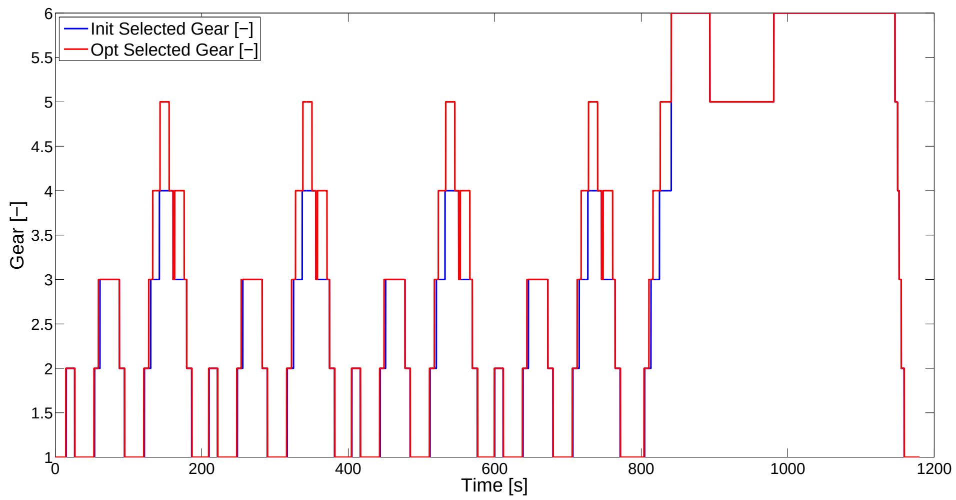

Figure 8.5: Best selected optimised gear shift map 1, gear position

Figure 8.5, Figure 8.6 and Figure 8.7 represent the satisfactory optimised gear shift map and gear position. The gear change frequency has significantly increased for Figure 8.6 and Figure 8.7 as they represent the ideal CO_2 emissions.

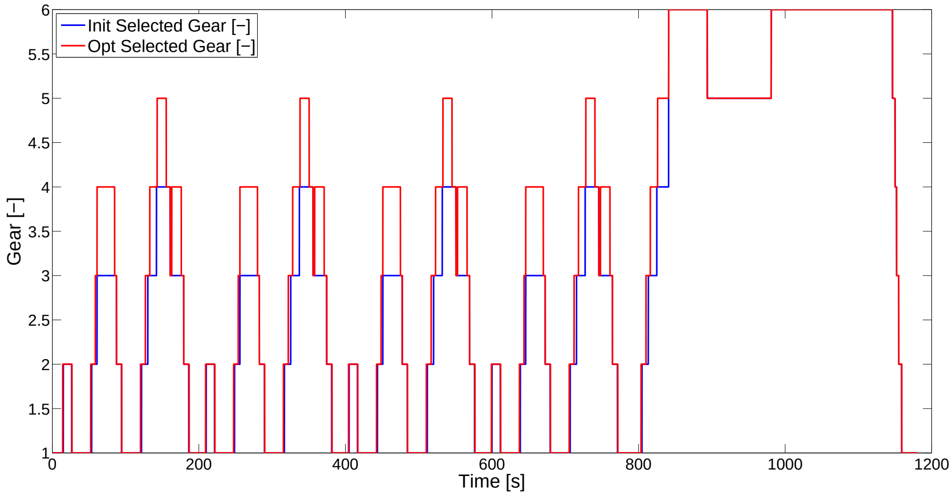

Figure 8.6: Best selected optimised gear shift map 2, gear position

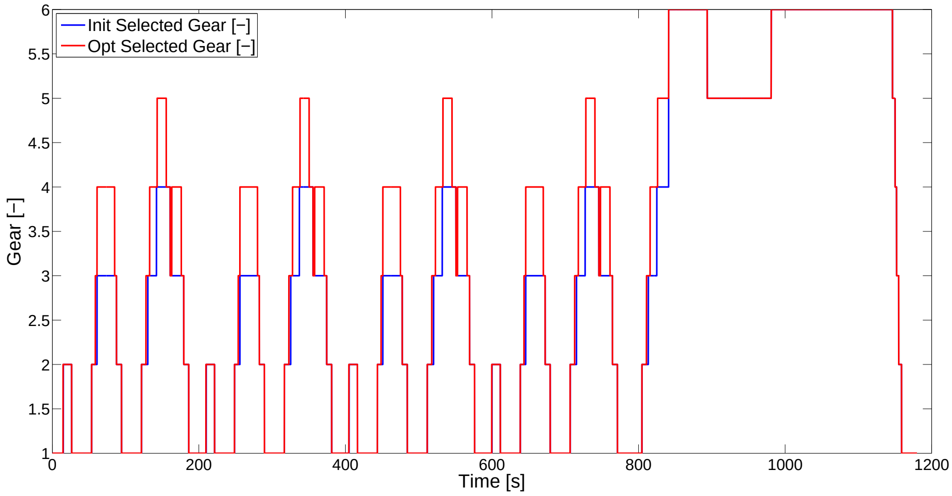

Figure 8.7: Best selected optimised gear shift map 3, gear position

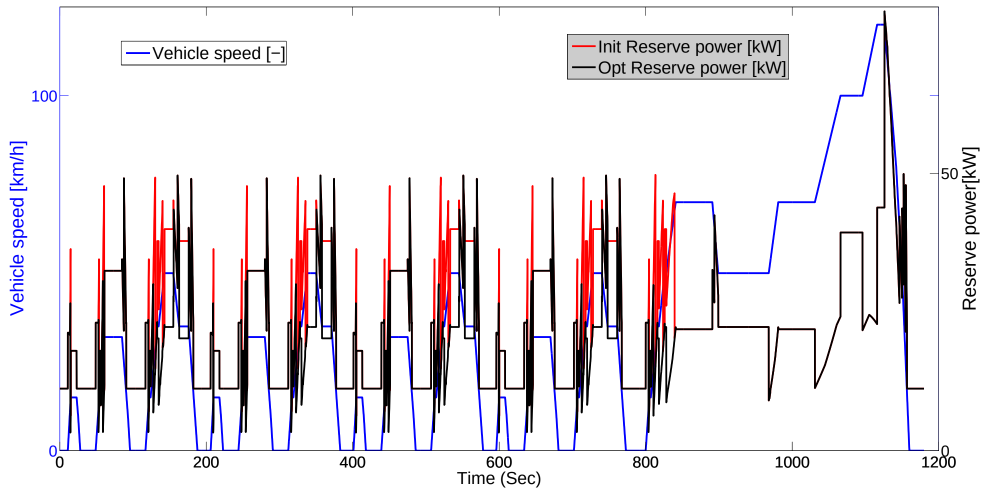

Figure 8.8: Best selected optimised gear shift map 1, reserve power

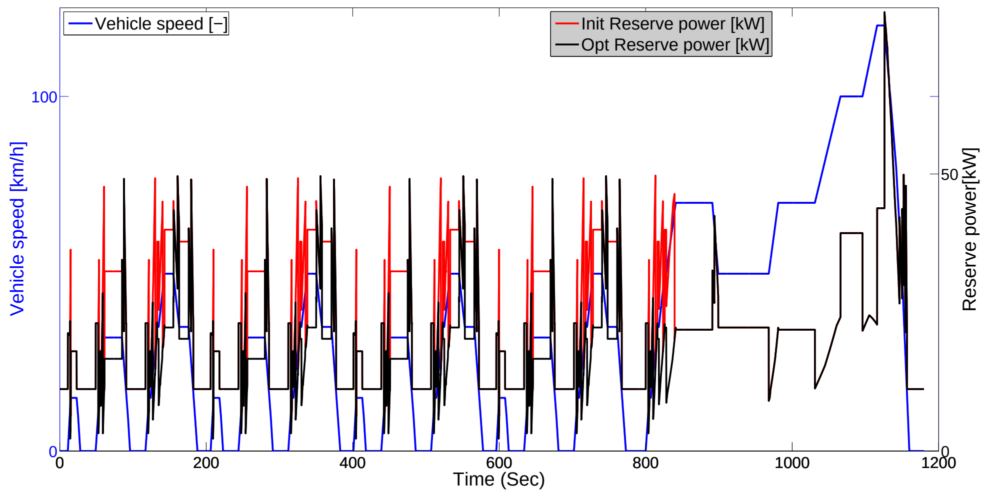

Figure 8.9: Ideal selected optimised gear shift map 2, reserve power

Figure 8.8, Figure 8.9 and Figure 8.10 represent the ideal optimised gear shift map and reserve power. As expected the reserve power of Figure 8.9 and Figure 8.10 are the highest (see Table 8.1).

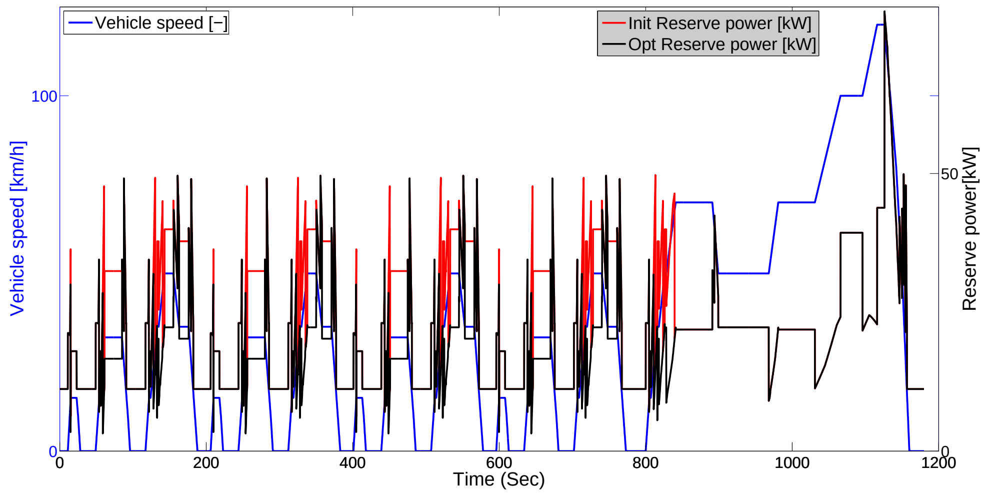

Figure 8.10: Ideal selected optimised gear shift map 3, reserve power

8.4 Test results

This section describes fuel consumption and emissions testing performed for this research. The first section defines the initial shift map test on the rolling road to determine the benchmark CO_2 emissions. Optimise shift map results are then presented and compared with the initial shift map results. Finally, the emissions saving is also reported and concluded.

8.4.1 Benchmark

In this sub-section the test of the initial shift map on the rolling road is described before testing of the optimised shift map. It was agreed to first establish a benchmark CO_2 figure on the rolling road, which will be used to compare the optimised shift map emissions performance. The test conditions for the Benchmark are based on the description given in Section 8.2. Additionally a bag test example documentation can be found in Appendix G. It would have been ideal to repeat the test at least 10 times to establish the benchmark CO_2 figure, however due to limited resources, it was only possible to perform the benchmark test 3 times. Table 8.2 describes the results from three tests with the initial shift map on the rolling road.

Table 8.2: Initial shift map fuel economy (FE) and CO_2 emissions on a rolling road over the NEDC. Three test results are presented in this table generated under the same conditions

	Test 1	Test 2	Test 3
CO_2 (g/km)	196.39	201.69	204.88
F.E (L/100km)	8.42	8.44	8.58

Table 8.3: Initial shift map fuel consumption and emissions on a rolling road over the NEDC. This table shows the average and standard (Std) deviation values for fuel and emissions

	Average value	Std
CO_2 (g/km)	200.98	4.28
F.E (L/100km)	8.4800	0.0872

Table 8.2 shows an overview of fuel consumption and emissions from rolling road test based on the initial shift map. Table 8.3 describes the average value and standard deviation of CO_2 emissions and FE. The average CO_2 listed in this table is 200.98 g/km, however the official figure of ROEWE 950 is 197.7 g/km. The differences can be attributed the fact that the research is based on a prototype vehicle which was still in development phases. The overall objective of this benchmark was to obtain a CO_2 figure in order to compare and quantify the benefit of optimised shift map.

8.4.2 Optimised gear shift map

Having obtained a benchmark CO_2 emission figure, by the method described above, the focus is turned to the optimised shift map. After developing the algorithm to optimise the gear shift map (see Chapters 4 and 5), this section explains the results obtained on the rolling road regarding the optimised shift map. Before loading each gear shift map for the rolling road test, a subjective driveability test was performed on the open road.

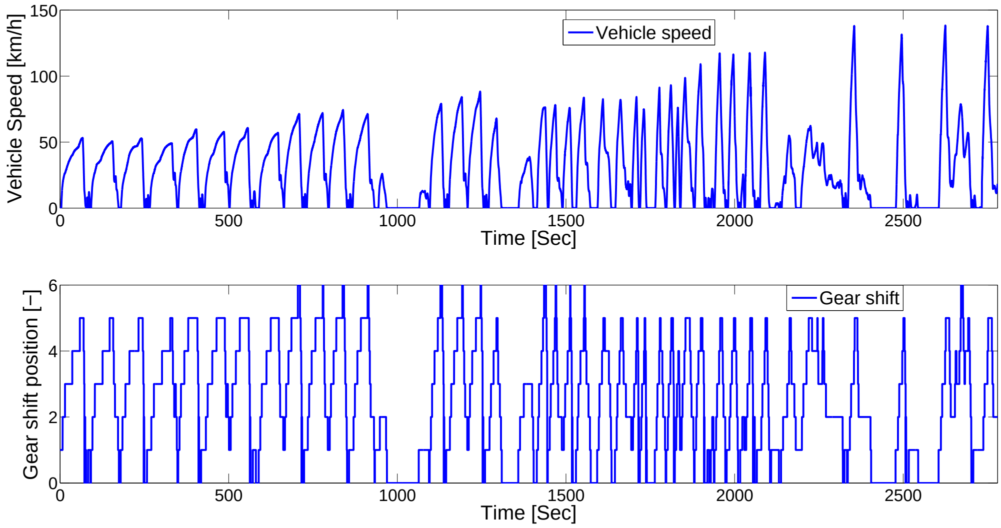

Figure 8.11: Driveability test of Optimised shift map before loading on it in ECU for rolling road test

Every shift map was tested by a calibration engineer before the final test on the rolling road for FE and CO_2 emissions assessment. Figure 8.11 illustrates an example of an optimised shift map assessment in order to verify its driveability. The calibration engineer then filed a report on the shift change at various throttle positions.

Table 8.4: Initial shift map fuel consumption and emissions on a rolling road over the NEDC. Three various test results are presented in this table under the same conditions

	Test 1	Test 2	Test 3	Test 4
CO_2 (g/km)	195.97	198.38	193.42	195.93
F.E (L/100km)	8.2	8.29	8.27	8.42

The percentage change in fuel economy and emissions relative to the optimised shift map on the rolling road are listed in Table 8.6. The average change in CO_2 for the optimised shift map reported in this table is -2.5%. The average change in FE is -2.2%. Clearly the optimised shift map has significantly improved the CO_2 emissions and fuel consumption. The drawback of these tests, is the difficulty of maintaining consistency between various tests, as the standard deviation is 2.02

Table 8.5: Initial shift map fuel consumption and emissions on a rolling road over the NEDC. This table shows the average and standard (Std) deviation values for fuel and emissions

	Average value	Std
CO_2 (g/km)	195.9250	2.0252
F.E (L/100km)	8.2950	0.0918

Table 8.6: Average change fuel economy and emissions for optimised shift map in compared to initial shift map on rolling road

Pollutant & fuel	Percent change (%)
CO_2	-2.5
F.E	-2.2

for CO_2 emissions, this can be explained by the driver input and the prototype vehicle. This is why several tests are required to confirm the results, however considering the average results based on four tests, the method developed in this thesis shows a significant and promising contribution to reducing CO_2 emissions.

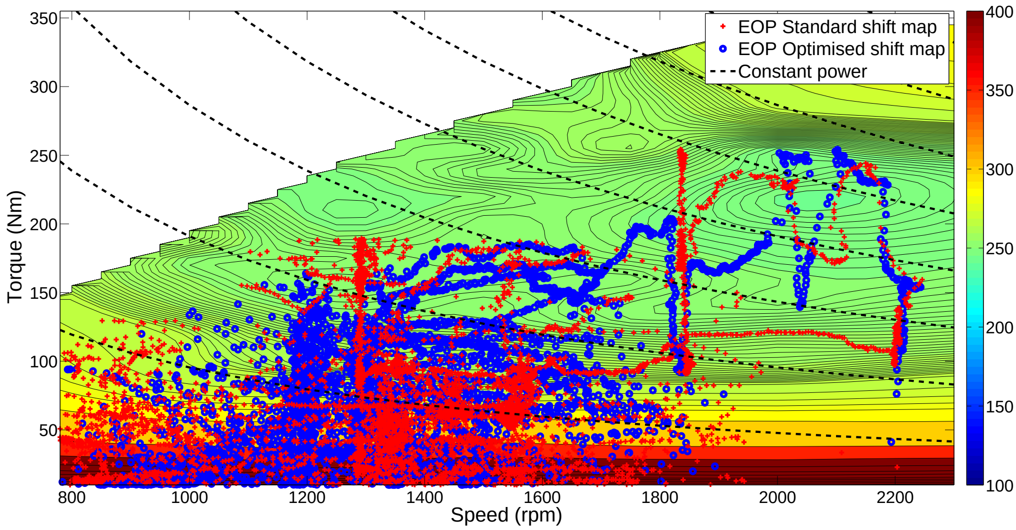

Figure 8.12: Engine operating point of standard shift map and optimised shift map 1 from rolling road

Figures 8.12 and 8.13 illustrate two optimised shift maps in comparison to the initial shift map. Notice that the initial shift map engine speed and torque were

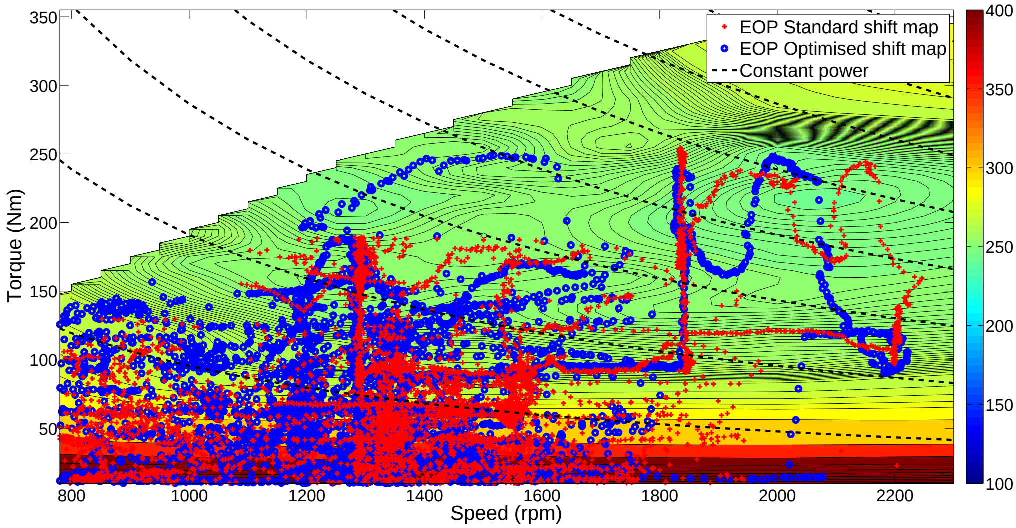

Figure 8.13: Engine operating of standard shift map and optimised shift map 2 from rolling road

not sampled at the same rate, as engine was sampled at 100ms from TCU data acquisition, and torque was sampled at 10ms from ECU data acquisition. Consequently both signals are re-sampled for comparison study. It can be observed that both optimised shift maps have an improved spread of operating points than the initial shift map.

Figures 8.14 and 8.15 demonstrate the engine characteristic of the optimised shift map in terms of maximum torque, actual torque, reserve torque, engine speed and reserve power. Notice that the maximum engine power was estimated using the engine maximum torque data, which has been modelled as a function of engine speed at full throttle position. The figures are similar, but by taking a look at reserve torque and maximum power, the result in Figure 8.14 seems to show more reserve torque than the second in Figure 8.15, at the beginning of the drive cycle. However, later on during the drive cycle, it tends to converge. The most significant factor, in terms of fuel consumption can be attributed to the driver input.

Table 8.7 describes the time spent in each gear with optimised gear shift map

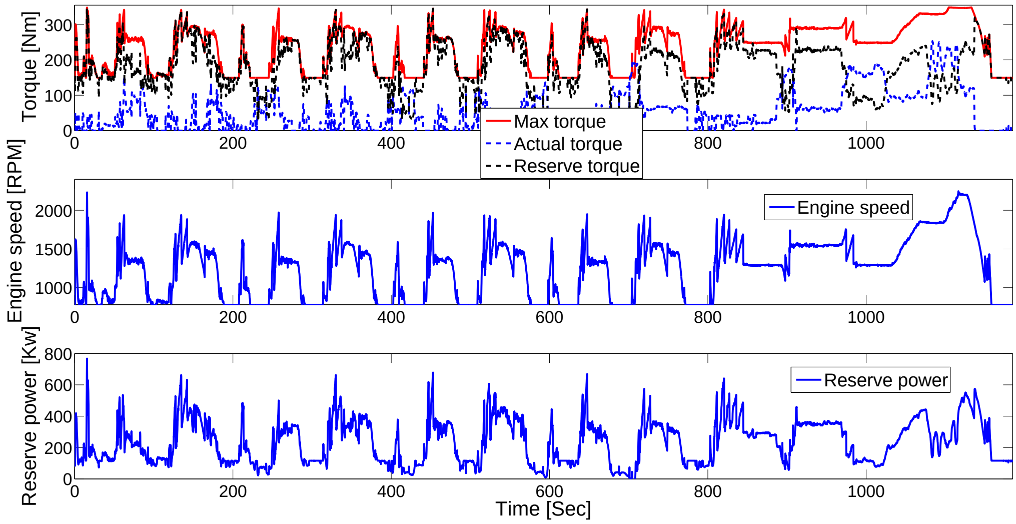

Figure 8.14: This figure illustrates the first optimised shift map, engine maximum torque (estimate), actual torque and reserve torque. Engine speed and estimated reserve power

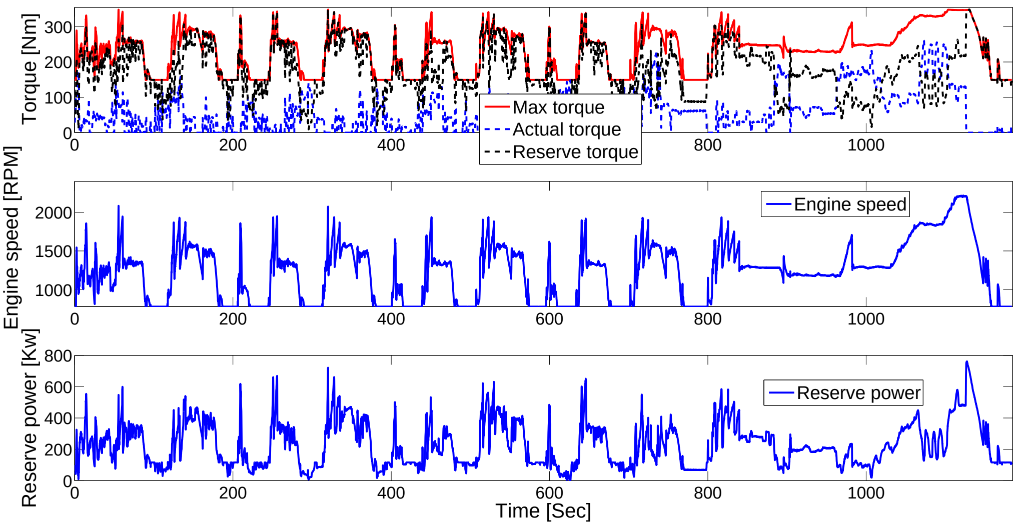

Figure 8.15: This figure illustrates the second optimised shift map, engine maximum torque (estimate), actual torque and reserve torque. Engine speed and estimated reserve power

1 (b) and shift map 2 (c), compared to the initial shift map (a). It is obvious that spending time in higher gears improves fuel economy and CO_2 emissions, as it can be seen that percentage of gear ratio for fifth gear has increased for both optimised shift maps (+10.87% and +10.8%).

Table 8.7: This table illustrates time spent on different gear ratio between optimised gear shift map 1 (b), shift map (c) in comparison to initial gear shift map (a). Additionally with the increase or decrease time spent of each gear ratio for optimised shift map

	Gear 1	Gear 2	Gear 3	Gear 4	Gear 5	Gear 6
a (%)	33.3	11	20.2	14.3	2.3	18.6
b (%)	32.2 (-1.1)	10.9 (-0.1)	20 (-0.2)	4.8 (-9.5)	13.17 (+10.87)	18.8 (+0.2)
c (%)	32 (-1.3)	11 (0)	20 (-0.2)	4.3 (-10)	13.11 (+10.8)	18.9 (+0.3)

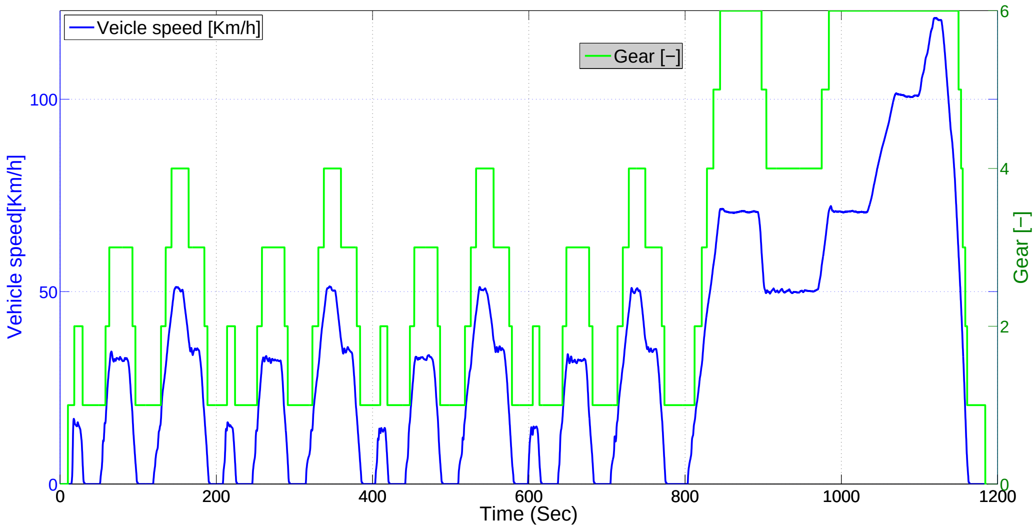

Figure 8.16: Rolling road vehicle speed and gear shift position under initial shift map

Figures 8.16, 8.17 and 8.18 illustrate the initial shift map, and two optimised shift maps gear shift position, as mentioned above, the two optimised shift maps are shifting earlier and maximising the time in fifth gear.

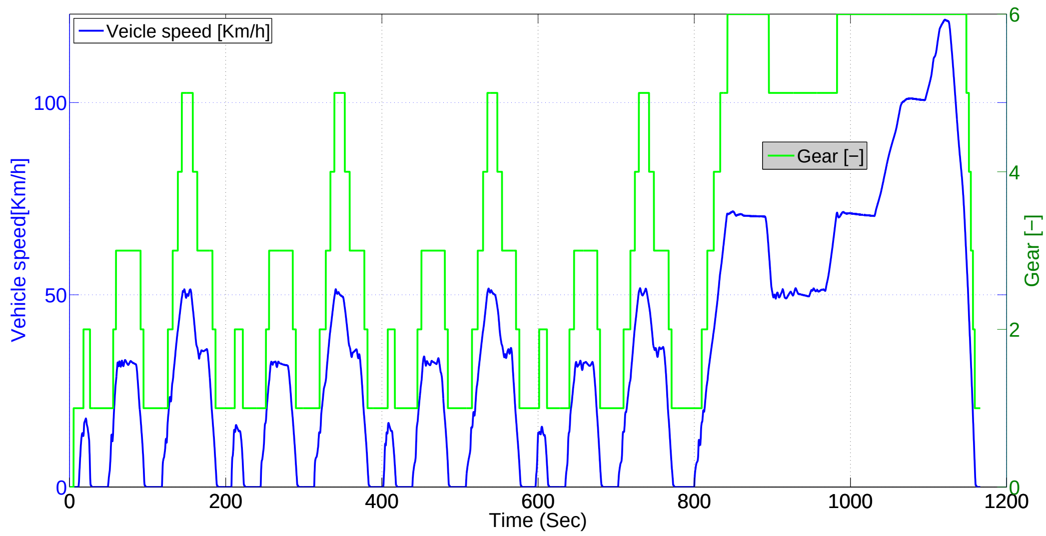

Figure 8.17: Rolling road vehicle speed and gear shift position under optimised shift map 1

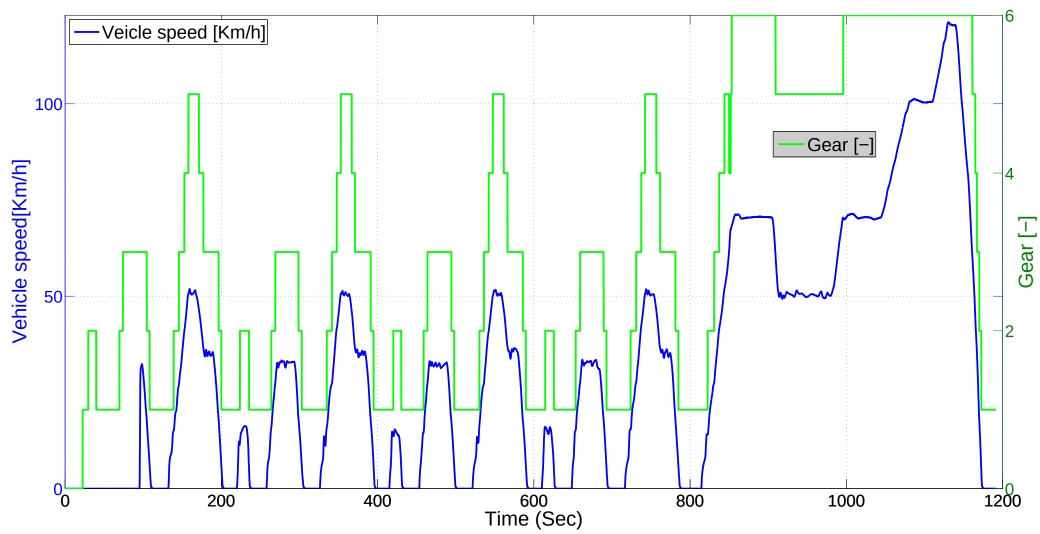

Figure 8.18: Rolling road vehicle speed and gear shift position under optimised shift map 1

8.5 Concluding remarks

This chapter has described the rolling road test of optimised gear shift maps, which has repeatedly demonstrated CO_2 savings, that are predicted in simulation. Additionally, CO_2 emissions were reduced without no perceptible reduction in driveability. The following sub-section described the summary of the testing which has led to reduced CO_2 emissions on the rolling road based on the method developed in this thesis. Additionally, an advise of the testing condition is given for improvement.

8.5.1 Summary of the testing methodology

- A testing methodology was developed, where the vehicle was assessed at first and checked if there are any faults, such as fuel, tyre pressure and general integrity.
- Soak the vehicle for 6 hours (before each test).
- Establish the coastdown check.
- Rolling road test.
- A repeated testing was established to benchmark the CO_2 emissions. These have led to 3 benchmark CO_2 with initial shift map.
- Optimised gear shift map are then loaded and test drive assessment is conducted on road.
- After verification by the calibration engineer, the optimised shift map is then assessed on the rolling.

8.5.2 Improvement

Various rolling road test must be conduct such as to:

- Improve the confidence in the benchmark.
- Improve the confidence in the optimised shift map.
- Test more aggressive CO_2 savings shift maps.

Chapter 9

Discussion, conclusion and further work

This chapter summarises the main contributions from this research on gear shift map and gear ratio optimisation before presenting the conclusions arising from this research and opportunities for further work.

The Conclusion starts with the motivation for the work prior to a description of the novelties and contributions classified in order of importance. This section finished with a quote from the industrial collaborators describing the commercial significance of the work.

The further work section presents opportunities to apply some of the work and opportunities to further develop the methods and software tools developed in this work.

9.1 Conclusion

This research project was prompted by the government initiatives, legislation (Energy Institute 2012) as well as the socio political and customer requirements (Transport 2005) to reduce the use of fossil fuel and significantly reduce vehicles emissions (in particular CO_2). The most significant CO_2 emissions saving at the point of use arises from the adoption of hybrid technologies. However, significant savings can also be achieved via hardware design and software solutions applied to automated manual transmissions. This work has demonstrated that the development of multi objective, nature inspired, optimisation frameworks to optimise both gear shift map and gear ratio could lead to significant CO_2 and fuel consumption savings whilst maintaining vehicle driveability. The culmination of the work on gear shift map optimisation was the experimental validation of the work through rolling road tests performed by the vehicle manufacturer showing a significant 2.5% CO_2 saving compared to the standard vehicle gear shift map. A further CO_2 saving of up to 5.8% was predicted using simulation studies by combining gear ratio and gear shift map optimisation. Note that these significant savings were obtained for gear shift maps that meet the minimum requirement for reserve power, but they also resulted in worsening of the overall reserve power and were characterised by unusual trajectories for the up and down gear shifts.

There are two types of novelties in this thesis: (i) problem specific formulation and methodologies and (ii) improvements of generic optimisation algorithms. The following statements describe them:

- The most significant problem specific contribution in this thesis is the repair mechanism, which can be applied to any gear shift map (see Section 5.2.2, in Chapter 5). The application of the repair mechanism leads to a slight increase in CO_2 emissions (see Table 7.1, in Chapter 7). This increase is unavoidable due to meeting the minimum reserve power requirement set by the designer (see Section 7.4, in Chapter 7). The simulation results in Table D.10, in Appendix D have demonstrated the effect of the repair mechanism.

- The second problem specific contribution is the problem formulations for both gear ratio and gear shift map multi-objective optimisation. These formulations have enabled the efficient and effective development of the overall optimisation strategies developed in this thesis. The gear shift map problem formulation enabled the user to specify the range of throttle position to consider (see Section 4.2.3, Chapter 4). It was designed to enforce the following engineering constraints: i) prevent crossing between Downshift and Upshift ii) maintain a minimum hysteresis between Downshift and Upshift to avoid frequent gear changes for small velocity variations. The number of design variables to optimise was reduced to 90 by reducing the number of control points in the gear shift map using a sensitivity analysis and practical implementation constraints. This resulted in the optimised throttle angle being separated by 10° whilst intermediate throttle angle positions were reconstructed using linear interpolation.

- The intermediates gear ratios were formulated such that the optimiser can focus more efficiently on gear ratio spacing and maintain a continuously decreasing ratio from gear G_2 to G_5 (see Section 4.3.1, Chapter 4).

- The third problem specific contribution is the problem specific GES operator (see Section 5.2, in Chapter 5). It has the ability to improve the existing optimised gear shift map by reducing CO_2 emissions by up to 0.37%. GES decreases the difference between Upshift and Downshift, thereby decreasing the hysteresis between Up and Downshift (with respect to a minimum hysteresis), resulting in making quick gear changes more likely (see Section 7.5, in Chapter 7). Such rapid changes are however acceptable with the use of the proposed SAIC Dual Clutch Transmission gearbox. The GES effect was illustrated in Table 7.3, where the application of GES finished with the lowest CO_2 emissions. Additionally the application at each generations have also accelerated the rate of convergence as demonstrated by comparing

Figure 7.9 and Figure 7.8.

- The fourth problem specific contribution is the implementation of the rate of change constraints to restrict the relative values of the gear shift points compared to their neighbours (see Section 4.2.2, in Chapter 4). It restricts the rate slope of each up/down shift trajectory. It has been shown to be very effective when combined with constrained optimisation such as interior-point algorithm. Note that constraining the shape of the gear shift map may make it more practical to implement but does increase the CO_2 emissions. Therefore the solutions obtained using MOGA and MOCS use fairly large threshold values for possible changes in the rate of change of the up/down shift trajectories, leading to low CO_2 but at the cost of irregular gear shift maps.

- The most significant contribution in terms of algorithm modification applicable to any optimisation problem is the addition to the MOGA used in this work of operators borrowed from other nature inspired optimisation algorithms such as Levy flight, Flower pollination, Bat and Firefly algorithms (see Section 5.3, in Chapter 5). This introduction stems from the observation of the solutions produced by these operators. It was aimed to help focus the search on different regions of the solution space as well as exploit known good solutions to generate new individuals around currently optimal solutions. This hybrid combination has proved successful and was the best performer for gear shift map optimisation. Various experimental tests were carried out to demonstrates the proposed MOGA effectiveness. The outcome of the simulation study was the demonstration that each optimisation algorithm can produce a better solutions than the manufacturers initial map. There is however no win-win situation as gear shift map leading to the best CO_2 savings did exhibit features that may not make them desirable from a practical implementation perspective, such as irregular gear shift map shapes.

- The second most significant contribution in terms of algorithm modification is the development of a hybrid MOCS for gear ratio optimisation. In addition to the standard Levy Flight operator, it includes Bat, Firefly and Flower Pollination. These operators were integrated within the Cuckoo Search to generate new optimised gear ratios.

- Key to any optimisation problem is the ability to ask the appropriate question to the optimiser. These questions are expressed in terms of objectives to be optimised or minimised in the case of this thesis. Three new objective formulations were proposed in this thesis to investigate if the conflicting objectives of achieving low CO_2 and thereby fuel consumption as well as good driveability expressed in terms of reverse power could be achieved simultaneously (see Section 4.2.1, in Chapter 4). These objectives focused on the percentage of time the engine was operating in the specific regions of the BSFC map. Zones 1 and 2 correspond to the two most efficient zone, whilst zones 3 reflects higher fuel consumption characterised by operating the engine at low or very high revolution per minute. It was noticed that zone 3 was proportional to IRP as it represents the highest fuel consumption, therefore zone 3 can reach a minimum level (0.88) during the optimisation process.

- A new criterion, referred to as gear utilisation criterion, was developed to identify the gear usage based on the assumption that maximising the time on higher gear would result in lower fuel consumptions and CO_2 emissions. This criterion gives the designer a quantifiable measure to identify the effect that have the selection of specific gear ratio on the overall CO_2 emission. The designer main task is to decide the most appropriate importance factor for the different criteria developed in order to determine the most suitable trade-off solution. Guiding the algorithm towards the trade-off is achieved by allocating weighting coefficient as defined in Equation (4.1) (see Section 4.2.1, in Chapter 4). To enable the designer a greater flexibility, gear weightings were introduced to identify the specific gears to be targeted. This objective, together with the number of gear changes were found to be particularly useful to identify patterns of gear selection over the NEDC drive cycle for different solutions. These patterns relate to different features in the gear shift map and are strongly correlated to the CO_2 emissions.

- Taking inspiration from Le Guen et al. (2011), a new cost function (Dist) was developed to minimise CO_2 by moving the engine operating points, expressed in terms of engine torque, T_e, and engine speed, w_e, towards the left side of the BSFC map (see Section 4.2.1, in Chapter 4). It is realised by minimising the distance between a reference, or anchor point $O(w_{ref}, T_{ref})$ on the BSFC map, and the Upshift points for the throttle positions, t_k of interest. The problem specific objective aim is to help users identify the most suitable solutions, by observing the performance of the engine operating point on the BSFC map, whilst the specific objectives are expressed using different formulations. It was found that minimising the distances between the reference point ($O(w_{ref}, T_{ref})$), and Upshift points led to a reduction of CO_2 emissions.

- Another objective formulation was designed to maximise the time spent on the higher gear ratios ($G_{j\%}$) (see Section 4.2.1, in Chapter 4). It was noticed that increasing the amount of time spend on high gear ratios, reducing the time spent on lower gears was beneficial to CO_2 emissions.

- The application of the modified Pareto objective formulation based on Haas et al. (1998) for both gear ratio and gear shift map is a contribution for such applications (see Section 5.2, in Chapter 5). It uses objective weighted Pareto ranking to differentiate between non dominated solutions. It has the advantage of focusing the search towards low CO_2 regions without neglecting the other objectives. It has shown to be able to find solutions with lower costs than the standard weighted sum approaches. The combination of a standard MOGA with the modified Pareto objective formulation and the new repair mechanism together with the new local search operator, namely GES. The aim of these modifications were to exploit problem specific features to find improved solutions rapidly. It was shown that GES improved significantly the current solution generated by the optimiser. The application of GES was limited to one at every three generations as it can lead to a premature convergence, as demonstrated in Figure 7.9.

- In addition, the overall combination of both MOGA and MOCS to concurrently optimise gear ratio and gear shift map is novel and has proved extremely successful compared to independent gear ratio and gear shift map optimisation. This combination has led to a significant 5.8% savings in terms of CO_2 emissions.

- This method has resulted in solutions which have been selected for testing first in real life situations to ensure that they offered suitable driveability and then on rolling road. The rolling road tests confirmed that the significant savings found on simulation. On average a saving of 2.5% in terms of CO_2 emissions was achieved.

Considering the research adopted in this thesis, a number of contribution and innovative developments have been made in the field of optimisation applied to gear shift map and gear ratio. The fruits of these contributions were developed to alleviate and support the automotive industry facing strict rules imposed by the government concerning regulation on emissions. Overall the research has been very well received by SAIC motors. The following quote was written by the line manager Chris Woolley:

" *The excellent work conducted during Adama Fofana's time at SMTC UK proved both advantageous and invaluable. His development of control algorithms used for gear shift schedule optimisation, dynamic performance and improved fuel economy proved very successful, these were presented throughout to the Global business and have aided future development in this area. In addition to this the models generated during Adama's time with us are stored in a model library designed and developed my Adama, these models are used today to support product development through simulation.*"

9.2 Further work

The mathematical framework defined to express optimised gear shift maps into design variables may still be improved. An optimisation study should be carried out further to select an appropriate throttle range over various driving cycles. The hysteresis of each throttle position was fixed in order to reduce the number of design variables. However it may be beneficial to investigate throttle specific hysteresis constraints and refined the selection of the hysteresis values adopted in this thesis.

The powertrain model used in this thesis was only validated against the New European Drive Cycle (NEDC). To enable the use of the model to evaluate solutions for other drive cycles, the model should be validated against the World harmonised Light vehicles Test Procedures (WLTP) as well as the road testing carried out by the manufacturer to evaluate the vehicle behaviour from a qualitative perspective. Having validated the simulation model for a range of driving conditions, the optimisation should therefore evaluate the performance of the candidate solutions against the NEDC drive cycle as well as WLTP and the road driving cycle used for driveability tests by the manufacturer.

The effect of the repair mechanism has only been evaluated on simulation. It would be useful to see if such an approach can be used whilst testing the vehicle on the rolling road to perform educated adjustment of the gear shift map in cases when the map tested does not meet acceptable driveability. This is an area which could potentially help reduce calibration costs significantly.

The practical implementation of a gear shift map involves the use of look up table and interpolation between the points on the look up table. Regular shapes are therefore better than irregular gear shift map due to the ease of implementation and the interpolation process. Indeed, care should be taken to prevent sharp and rapid changes that may lead to significant changes in engine RPM for a small variation in throttle angle or up/down shift. It has been shown that it is possible to control the shape of the gear shift map by imposing constraints on the rate of change of the up and down shift trajectory on the gear shift map. This approach, should be further studied to identify a set of appropriate gear specific thresholds to limits the rate of change of the up and down shift trajectories, thereby making them more regular and easier to implement on production vehicle

Due to a limited amount of time, statistical analysis can be improved regarding the selection of the best algorithm, by repeating the simulation undergone for each algorithm under various settings as well as Pareto and weighted sum methods.

An noteworthy characteristic of the Firefly algorithm is its ability to emit light from a long distance. The brightness for the light emitted represents quality of the fitness function for the firefly. It is traditionally proportional to a combined objective function obtained by a weighted sum. Further search could be carried out where, instead of using a combined weighted sum, a modified Pareto function is applied to select a firefly with the brightness depending on the Pareto set as well as the best combination of objectives.

The hybrid MOCS developed for gear ratio optimisation, can have a significant contribution to various fields. The algorithm may still be improved by addition of a performance measure, which can be used to select an operator in order to control the rate of convergence or accurately focus the search direction. Additionally, a fuzzy logic controller could be used to vary the parameters of various operators integrated in the hybrid MOCS.

It may also be worthwhile to investigate a problem formulation to combine gear shift map and gear ratio, and use either MOGA or MOCS to optimise both gear shift and gear ratio simultaneously.

Index

References

Akilesh Yamsani (2014), 'Gradeability for Automobiles', *IOSR Journal of Mechanical and Civil Engineering (IOSR-JMCE)* **11**(2), 35–41.

André, J.-m. & Hugot, M. (2003), 'Impact of the Gearshift Strategy on Emission Measurements', *Artemis 3142 report* (March).

Arora, J. (2011), *Introduction to Optimum Design, Third Edition*, Asoke K. Ghosh, Prentice-Hall of India.

Arora, J., Huang, M. & Hsieh, C. (1994), 'Methods for optimization of nonlinear problems with discrete variables: a review', *Structural optimization* **8**(2-3), 69–85.

Arora, S. & Singh, S. (2013), 'A Conceptual Comparison of Firefly Algorithm, Bat Algorithm and Cuckoo Search', *2013 International Conference on Control, Computing, Communication and Materials, ICCCCM 2013* pp. 1–4.

Augusto, O. B., Bennis, F. & Caro, S. (2012), 'A new method for decision making in multi-objective optimization problems', *Pesquisa Operacional* **32**(2), 331–369.

B. Mashadi, R. B. L. (2012), 'Fuel economy improvement based on a many-gear shifting strategy', *International Journal of Energy and Environment* **3**(4), 577–590.

Baker, J. E. (1987), Reducing bias and inefficiency in the selection algorithm, *in* 'Proceedings of the second international conference on genetic algorithms', pp. 14–21.

Barlow, T., Latham, S., Mccrae, I. & Boulter, P. (2009*a*), 'A reference book of driving cycles for use in the measurement of road vehicle emissions', p. 280.

Barlow, T., Latham, S., Mccrae, I. & Boulter, P. (2009*b*), 'A reference book of driving cycles for use in the measurement of road vehicle emissions', p. 31.

Bennett, A. W. (1872), 'The Origin of Species by means of Natural Selection; or the Preservation of Favoured Races in the Struggle for Life', *Nature* **5**(121), 318–319.

Bielaczyc, P., Woodburn, J. & Szczotka, A. (2014), 'An assessment of regulated emissions and CO_2 emissions from a European light-duty CNG-fueled vehicle in the context of Euro 6 emissions regulations', *Applied Energy* **117**, 134–141.

Binitha, S. & Sathya, S. S. (2012), 'A Survey of Bio inspired Optimization Algorithms', *International Journal of Soft Computing and Engineering (IJSCE)* **2**(2), 137–151.

Broy, M. (2006), Challenges in automotive software engineering, *in* 'Proceedings of the 28th international conference on Software engineering', ACM, pp. 33–42.

Byrd, R. H., Gilbert, J. C. & Nocedal, J. (2000), 'A trust region method based on interior point techniques for nonlinear programming', *Mathematical Programming* **89**(1), 149.

Casavola, a., Prodi, G. & Rocca, G. (2010), 'Efficient gear shifting strategies for green driving policies', *American Control Conference (ACC), 2010* pp. 4331–4336.

Chen, C.-J. & Usman, M. (2001), 'Design optimisation for automotive applications', *International Journal of Vehicle Design* **25**(1-2), 126–141.

Chiandussi, G., Codegone, M., Ferrero, S. & Varesio, F. E. (2012), *Comparison of multi-objective optimization methodologies for engineering applications*, Vol. 63, Elsevier Ltd.

Coello Coello, C. A. (1999), 'A Survey of Constraint Handling Techniques used with Evolutionary Algorithms', *Lania-RI-99-04, Laboratorio Nacional de ...* pp. 1–33.

Colaço, M. & Dulikravich, G. (2011), 'A Survey of Basic Deterministic, Heuristic and Hybrid Methods for Single-Objective Optimization and Response Surface Generation', *Thermal Measurements and Inverse Techniques* pp. 355–405.

Coleman, T. F. & Li, Y. (1996), 'An interior trust region approach for nonlinear minimization subject to bounds', *SIAM Journal on optimization* **6**(2), 418–445.

Deb, K. & Goyal, M. (1996), 'A combined genetic adaptive search (GeneAS) for engineering design', *Computer Science and Informatics* **26**(1), 30–45.

Deb, K. & Saxena, D. K. (2005), 'On Finding Pareto-Optimal Solutions Through Dimensionality Reduction for Certain Large-Dimensional Multi-Objective Optimization Problems EMO for Many Objectives', *Kangal report* **2005011**(2005011), 3353–3360.

Dovgan, E., Tušar, T., Javorski, M. & Filipič, B. (2012), 'Discovering comfortable driving strategies using simulation-based multiobjective optimization', *Informatica* **36**(3).

Energy Institute (2012), 'UK & EU energy initiatives & legislation factsheet', **44**(September 2012), 1–5.

Fister, I., Fister, D. & Yang, X. S. (2013), 'A hybrid bat algorithm', *Elektrotehniski Vestnik/Electrotechnical Review* **80**(1-2), 1–7.

Fletcher, R. & Powell, M. J. D. (1963), 'A Rapidly Convergent Descent Method for Minimization', *The Computer Journal* **6**(2), 163–168.

Fofana, A., Haas, O., Ersanilli, V., Burnham, K., Mahtani, J., Woolley, C. & Vithanage, K. (2016), 'Multi-Objective Genetic Algorithm for automatic transmission gear shift map optimisation', *14-th IFAC Symposium on Control in Transportation Systems, May 18-20, 2016, Istanbul Technical University, Taksim, Istanbul, Turkey* .

Forsgren, A., Gill, P. E. & Wright, M. H. (2002), 'Interior methods for nonlinear optimization', *SIAM review* **44**(4), 525–597.

Fu, J. & Bortolin, G. (2012), 'Gear Shift Optimization for Off-road Construction Vehicles', *Procedia - Social and Behavioral Sciences* **54**(14), 989–998.

Galvagno, E., Velardocchia, M. & Vigliani, a. (2011), 'Dynamic and kinematic model of a dual clutch transmission', *Mechanism and Machine Theory* **46**(6), 794–805.

Gill, P. E., Murray, W., Saunders, M. a. & Wright, M. H. (1981), 'Aspects of mathematical modelling related to optimization', *Applied Mathematical Modelling* **5**(2), 71–83.

Goel, S. & Panchal, V. (2014), 'Performance evaluation of a new modified firefly algorithm', *Reliability, Infocom Technologies and Optimization (ICRITO)(Trends and Future Directions), 2014 3rd International Conference on* pp. 1–6.

Golabi, S., Fesharaki, J. J. & Yazdipoor, M. (2014), 'Gear train optimization based on minimum volume/weight design', *Mechanism and Machine Theory* **73**, 197–217.

Goldberg, D. E. & Deb, K. (1991), 'A comparative analysis of selection schemes used in genetic algorithms', *Foundations of genetic algorithms* **1**, 69–93.

Goldberg, D. E. & Lingle, R. (1985), Alleles, loci, and the traveling salesman problem, *in* 'Proceedings of the first international conference on genetic algorithms and their applications', Lawrence Erlbaum Associates, Publishers, pp. 154–159.

Gopal Dhal, K., Quraishi, I. & Das, S. (2015), 'A Chaotic Lévy flight Approach in Bat and Firefly Algorithm for Gray level image Enhancement', *International Journal of Image, Graphics and Signal Processing* **7**(7), 69–76.

Ha, S.-H. & Jeon, H.-T. (2013), 'Development of intelligent gear-shifting map based on radial basis function neural networks', *International Journal of Fuzzy Logic and Intelligent Systems* **13**(2), 116–123.

Haas, O. C., Burnham, K. J. & Mills, J. a. (1998), 'Optimization of beam orientation in radiotherapy using planar geometry.', *Physics in medicine and biology* **43**(8), 2179–2193.

Halevy, I., Kava, Z. & Seeman, T. (2006), 'Normalization and Other Topics in Multi Objective Optimization', *Optimization* **2**, 89–101.

Henrique, C., Amendola, F., Augusto, M., Alves, L., Politécnica, E., Paulo, D. S. & Paulo, S. (2006), 'Gear shift strategies analysis of the automatic transmission in comparison with the double clutch transmission comparison with the double clutch transmission', *SAE Technical Paper* .

Holland, J. H. (1992), *Adaptation in natural and artificial systems: an introductory analysis with applications to biology, control, and artificial intelligence*, MIT press.

Hu, H., Wang, X. & Shao, Y. (2010), 'Optimization of the shift quality of dual clutch transmission using genetic algorithm', *Proceedings - 2010 6th International Conference on Natural Computation, ICNC 2010* **8**(Icnc), 4152–4156.

Ivarsson, M., Åslund, J. & Nielsen, L. (2013), 'Impacts of AMT Gear-Shifting on Fuel Optimal Look Ahead Control', *SAE International* .

Jebari, K. & Madiafi, M. (2013), 'Selection Methods for Genetic Algorithms.', *International Journal of Emerging Sciences* **3**(4).

Kanagaraj, G., Ponnambalam, S. G. & Jawahar, N. (2013), 'A hybrid cuckoo search and genetic algorithm for reliability-redundancy allocation problems', *Computers and Industrial Engineering* **66**(4), 1115–1124.

Karaboga, D. & Akay, B. (2009), 'A survey: Algorithms simulating bee swarm intelligence', *Artificial Intelligence Review* **31**(1-4), 61–85.

Kasseris, E. P. & Heywood, J. B. (2007), Comparative analysis of automotive powertrain choices for the next 25 years, Technical report.

Kaya, Y., Uyar, M. & Tek\D{j}n, R. (2011), 'A Novel Crossover Operator for Genetic Algorithms: Ring Crossover', p. 5.

Khajehzadeh, M., Taha, M. R., El-shafie, A., Eslami, M. & Branch, A. (2011), 'A Survey on Meta-Heuristic Global Optimization Algorithms 1', **3**(6), 569–578.

Kim, D., Peng, H., Bai, S. & Maguire, J. M. (2007*a*), 'Control of integrated powertrain with electronic throttle and automatic transmission', *IEEE Transactions on Control Systems Technology* **15**(3), 474–482.

Kim, D., Peng, H., Bai, S. & Maguire, J. M. (2007*b*), 'Control of integrated powertrain with electronic throttle and automatic transmission', *IEEE Transactions on Control Systems Technology* **15**(3), 474–482.

Kim, N., Rousseau, A. & Rask, E. (2012), 'Autonomie Model Validation with Test Data for 2010 Toyota Prius', *SAE International* pp. 1–14.

Kirschstein, S., Remelhe, F. & Stolze, B. (2009), 'Efficient transmission application by using modern offline tools', *Proceedings of 8th CTI International Symposium of Innovative Automotive Transmission, Berlin* .

Kirtane, C. (n.d.), 'Gear Shift Schedule Optimization and Drive Line Modeling for Automatic Transmission', pp. 254–260.

Kita, H., Ono, I. & Kobayashi, S. (1999), 'Multi-parental extension of the unimodal normal distribution crossover for real-coded genetic algorithms', *Proceedings of the 1999 Congress on Evolutionary Computation (CEC'99)* pp. 1581–1587.

Konak, A., Coit, D. W. & Smith, A. E. (2006), 'Multi-objective optimization using genetic algorithms: A tutorial', *Reliability Engineering & System Safety* **91**(9), 992–1007.

Kulkarni, M., Shim, T. & Zhang, Y. (2007), 'Shift dynamics and control of dual-clutch transmissions', *Mechanism and Machine Theory* **42**(2), 168–182.

Ladkany, G. S. (2012), 'A Genetic Algorithm with Weighted Average Normally-Distributed Arithmetic Crossover and Twinkling', *Applied Mathematics* **03**(30), 1220–1235.

Le Guen, D., Weck, T., Balihe, A. & Verbeke, B. (2011), 'Definition of Gearshift Pattern: Innovative Optimization Procedures Using System Simulation', *SAE Int. J. Fuels Lubr.* **4**(1), 412–431.

Li, G. & Hu, J. (2010), 'Modeling and analysis of shift schedule for automatic transmission vehicle based on fuzzy neural network', *2010 8th World Congress on Intelligent Control and Automation* pp. 4839–4844.

Lin, Y.-s., Shea, K., Johnson, A., Coultate, J. & Pears, J. (2009), A method and software tool for automated gearbox synthesis, *in* 'ASME 2009 International Design Engineering Technical Conferences and Computers and Information in Engineering Conference', American Society of Mechanical Engineers, pp. 111–121.

Liu, C., Gao, Z. & Zhao, W. (2012), 'A New Path Planning Method Based on Firefly Algorithm', *2012 Fifth International Joint Conference on Computational Sciences and Optimization* pp. 775–778.

Liu, Y., Qin, D., Jiang, H., Liu, C., Zhang, Y. & Lei, Z. (2009), 'Shift schedule optimization for dual clutch transmissions', *5th IEEE Vehicle Power and Propulsion Conference, VPPC '09* **1**, 1071–1078.

Llamas, X., Eriksson, L. & Sundstr, C. (2010), 'Fuel Efficient Speed Profiles for Finite Time Gear Shift with Multi-Phase Optimization', *Vehicular Systems* .

Long, Q. (2014), 'A constraint handling technique for constrained multi-objective genetic algorithm', *Swarm and Evolutionary Computation* **15**, 66–79.

Lourakis, M. I. (2005), 'A brief description of the levenberg-marquardt algorithm implemented by levmar', *Foundation of Research and Technology* **4**, 1–6.

Lucente, G., Montanari, M. & Rossi, C. (2007), 'Modelling of an automated manual transmission system', *IFAC Proceedings Volumes (IFAC-PapersOnline)* **7**(PART 1), 958–963.

Mahlia, T., Tohno, S. & Tezuka, T. (2012), 'A review on fuel economy test procedure for automobiles: Implementation possibilities in Malaysia and lessons for other countries', *Renewable and Sustainable Energy Reviews* **16**(6), 4029–4046.

Mammetti, M., Gallegos, D., Freixas, A. & Muñoz, J. (2013), 'The influence of rolling resistance on fuel consumption in heavy-duty vehicles', *SAE Technical Paper* .

Mani, A. & Patvardhan, C. (2009), 'A novel hybrid constraint handling technique for evolutionary optimization', *2009 IEEE Congress on Evolutionary Computation* pp. 2577–2583.

Martens, D., Baesens, B. & Fawcett, T. (2011), 'Editorial survey: Swarm intelligence for data mining', *Machine Learning* **82**(1), 1–42.

Mashadi, B. & Crolla, D. (2012), Wiley.

Mavrotas, G. (2009), 'Effective implementation of the ϵ-constraint method in Multi-Objective Mathematical Programming problems', *Applied Mathematics and Computation* **213**(2), 455–465.

Mitchell, G. G., ODonoghue, D., Barnes, D. & McCarville, M. (2003), 'GeneRepair-a repair operator for genetic algorithms', *Proc. Genetic and Evolutionary Computation Conference (GECCO) Late Breaking Papers* (1999), 235–239.

Moawad, A. & Rousseau, A. (2014), 'Impact of electric drive vehicle technologies on fuel efficiency to support 2017-2025 cafe regulations', *SAE International Journal of Alternative Powertrains* **3**(2014-01-1084), 163–175.

Nanda, S. J. & Panda, G. (2014), 'A survey on nature inspired metaheuristic algorithms for partitional clustering', *Swarm and Evolutionary computation* **16**, 1–18.

Naunheimer, H., Bertsche, B., Ryborz, J. & Novak, W. (2010), *Automotive transmissions: fundamentals, selection, design and application*.

Newman, K. A. & Dekraker, P. (2016), Modeling the effects of transmission gear count, ratio progression, and final drive ratio on fuel economy and performance using alpha, Technical report.

Ngo, V. D., Colin Navarrete, J. a., Hofman, T., Steinbuch, M. & Serrarens, a. (2013), 'Optimal gear shift strategies for fuel economy and driveability', *Proceedings of the Institution of Mechanical Engineers, Part D: Journal of Automobile Engineering* **227**(10), 1398–1413.

Ngo, V. D., Hofman, T., Steinbuch, M. & Serrarens, a. (2013), 'Gear shift map design methodology for automotive transmissions', *Proceedings of the Institution of Mechanical Engineers, Part D: Journal of Automobile Engineering* **228**(1), 50–72.

Odu, G. O. & Charles-Owaba, O. E. (2013), 'Review of Multi-criteria Optimization Methods Theory and Applications', *IOSR Journal of Engineering* **3**(10), 01–14.

Ortiz-Soto, E., Assanis, D. & Babajimopoulos, a. (2012), 'A comprehensive engine to drive-cycle modelling framework for the fuel economy assessment of advanced engine and combustion technologies', *International Journal of Engine Research* **13**(3), 287–304.

Pandey, H. M., Chaudhary, A. & Mehrotra, D. (2014), 'A comparative review of approaches to prevent premature convergence in GA', *Applied Soft Computing* **24**, 1047–1077.

Pavlyukevich, I. (2007), 'Lévy flights, non-local search and simulated annealing', *Journal of Computational Physics* **226**(2), 1830–1844.

Polyak, B. (2007), 'Newtons method and its use in optimization', *European Journal of Operational Research* **181**(3), 1086–1096.

Qin, G., Ge, A. & Lee, J.-J. (2004), 'Knowledge-based gear-position decision', *IEEE transactions on intelligent transportation systems* **5**(2), 121–125.

Raghuwanshi, M. M. & Kakde, O. (2007), 'Study of Operators adaptability and scale-up study for RAGA', *2007 IEEE Congress on Evolutionary Computation* pp. 2866–2871.

Rajan, A. A. S. & Usmansha, G. S. (2014), 'Optimization & analysis of forging press gear box', *International Journal of Innovative Research and Development—— ISSN 2278–0211* .

Rani, K. A., Malek, M. F. A., Neoh, S. C., Jamlos, F., Affendi, N. A. M., Mohamed, L., Saudin, N. & Rahim, H. A. (2012), 'Hybrid multiobjective optimization using modified cuckoo search algorithm in linear array synthesis', *Antennas and Propagation Conference (LAPC), 2012 Loughborough* pp. 1–4.

Reeves, C. (2010), 'Genetic algorithms', *Handbook of metaheuristics* pp. 109–140.

Robinette, D. (2014), 'A DFSS Approach to Determine Automatic Transmission Gearing Content for Powertrain-Vehicle System Integration', *SAE International Journal of Passenger Cars - Mechanical Systems* **7**(3), 1138–1154.

Salcedo-Sanz, S. (2009), 'A survey of repair methods used as constraint handling techniques in evolutionary algorithms', *Computer Science Review* **3**(3), 175–192.

Santiciolli, F. M., dos Santos Costa, E., Eckert, J. J., Dionísio, H. J., de Alkmin, L. C., Dedini, F. G. et al. (2015), 'Multiobjective gear shifting optimization considering a known driving cycle', *Acta Scientiarum. Technology* **37**(3), 361–369.

Schott, J. R. (1995), 'Fault tolerant design using single and multicriteria genetic algorithm optimization.', *No. AFIT/CI/CIA-95-039. AIR FORCE INST OF TECH WRIGHT-PATTERSON AFB OH* .

Shamekhi, A. H., Bidgoly, A. & Noureiny, E. N. (2014), 'Optimization of the gear ratios in automatic transmission systems using an artificial neural network and a genetic algorithm', *Proceedings of the Institution of Mechanical Engineers, Part D: Journal of Automobile Engineering* **228**(11), 1338–1343.

Shanno, D. F. (1970), 'Conditioning of quasi-Newton methods for function minimization', *Mathematics of Computation* **24**(111), 647–647.

Shariatpanahi, M., Motamedi, A. et al. (2004), 'Neuro-genetic optimization of transmission ratios for automotive performance and emissions', *SAE Technical Paper* .

Singh, J., Singh, J. et al. (2012), 'Selection of gear ratio for smooth gear shifting', *SAE Technical Paper* .

Siskos, P., Capros, P. & De Vita, A. (2015), 'CO_2 and energy efficiency car standards in the EU in the context of a decarbonisation strategy: A model-based policy assessment', *Energy Policy* **84**, 22–34.

Song, M., Oh, J., Kim, J., Kim, Y., Yi, J., Kim, Y. & Kim, H. (2014), 'Development of an electric oil pump control algorithm for an automatic-transmission-based hybrid electric vehicle considering the gear shift characteristics', *Proceedings of the Institution of Mechanical Engineers, Part D: Journal of Automobile Engineering* **228**(1), 21–36.

Sovran, G. & Blaser, D. (2003), 'A Contribution to Understanding Automotive Government / Industry Meeting', *SAE International* (724), 26.

Statnikov, R., Bordetsky, a., Matusov, J., Sobol, I. & Statnikov, a. (2009), 'Definition of the feasible solution set in multicriteria optimization problems with continuous, discrete, and mixed design variables', *Nonlinear Analysis-Theory Methods & Applications* **71**(12), E109–E117.

Taboada, H. A., Espiritu, J. F. & Coit, D. W. (2008), 'Moms-ga: A multi-objective multi-state genetic algorithm for system reliability optimization design problems', *IEEE Transactions on Reliability* **57**(1), 182–191.

Talbi, E.-G. (2009), *Metaheuristics: from design to implementation*, Vol. 74.

Transport, R. (2005), 'Reducing CO_2 Emissions from Cars', *Environment and Road Transport* (August).

Tsutsui, S. & Ghosh, A. (1998), 'A study on the effect of multi-parent recombination in real coded genetic algorithms', *1998 IEEE International Conference on Evolutionary Computation Proceedings. IEEE World Congress on Computational Intelligence (Cat. No.98TH8360)* pp. 828–833.

Tzirakis, E., Pitsas, K., Zannikos, F. & Stournas, S. (2006), 'Vehicle Emissions and Driving Cycles : Comparison of the Athens Driving Cycle (ADC) with Ece-15 and European Driving Cycle (EDC)', *Global NEST Journal* **8**(3), 282–290.

United Nations (2006), 'Economic Commission for Europe (UN/ECE). Uniform provisions concerning the approval of passenger cars powered by an internal combustion engine only, or powered by a hybrid electric power train with regard to the measurement of the emission of carbon dioxide and fuel consumption and/or the measurement of electric energy consumption and electric range, and of categories M1 and N1 vehicles powered by an electric power train only with regard to the measurement of electric energy consumption and electric range. Regulation No 101, E/ECE/324, E/ECE/TRANS/505, Rev.2/ Add.100/Rev.2', (April), 1–79.

US EPA (1999), 'Emission Facts', *US Environmental Protection Agency* (EPA420-F-99-040), 1–4.

Vachhani, V. L., Dabhi, V. K. & Prajapati, H. B. (2015), 'Survey of multi objective evolutionary algorithms', *Circuit, Power and Computing Technologies (ICCPCT), 2015 International Conference* pp. 1–9.

Van Veldhuizen, D. a. & Lamont, G. B. (1998), 'Evolutionary Computation and Convergence to a Pareto Front', *Late Breaking Papers at the Genetic Programming 1998 Conference* pp. 221–228.

Wallington, T. J., Sullivan, J. L. & Hurley, M. D. (2008), 'Emissions of CO_2, CO, NOx, HC, PM, HFC-134a, NO_2 and CH4 from the global light duty vehicle fleet', *Meteorologische Zeitschrift* **17**(2), 109–116.

Wright, A. H. (1990), 'Genetic algorithms for real parameter optimization', *Foundations of Genetic Agorithms* pp. 205–220.

Xi, L. X. L., Xiangyang, X. X. X. & Yanfang, L. Y. L. (2009), 'Simulation of Gear-shift Algorithm for Automatic Transmission Based on MATLAB', *2009 WRI World Congress on Software Engineering* **2**(2).

Xiang, Y., Guo, L., Gao, B. & Chen, H. (2013), 'A study on gear shifting schedule for 2-speed electric vehicle using dynamic programming', *2013 25th Chinese Control and Decision Conference, CCDC 2013* (3), 3805–3809.

Xuexun, G., Chang, F., Fei, C., Jun, Y. & Zheng, Y. (2007), 'Modeling and Simulation Research of Dual Clutch Transmission Based On Fuzzy Control', *SAE Technical Paper* (724).

Yang, X.-S. (2010), 'A new metaheuristic bat-inspired algorithm', *Nature inspired cooperative strategies for optimization (NICSO 2010)* pp. 65–74.

Yang, X.-S. (2011*a*), 'Bat algorithm for multi-objective optimisation', *International Journal of Bio-Inspired Computation* **3**(5), 267–274.

Yang, X.-S. (2011*b*), 'Bat Algorithm for Multiobjective Optimization', *Int. J. Bio-Inspired Comput.* **3**(5), 267–274.

Yang, X.-S. (2012), 'Flower pollination algorithm for global optimization', *International Conference on Unconventional Computing and Natural Computation* pp. 240–249.

Yang, X.-S. (2014), *Nature-inspired optimization algorithms*, Elsevier.

Yang, X. S. & Deb, S. (2009), 'Cuckoo search via Lévy flights', *2009 World Congress on Nature and Biologically Inspired Computing, NABIC 2009 - Proceedings* pp. 210–214.

Yang, X. S. & Deb, S. (2013), 'Multiobjective cuckoo search for design optimization', *Computers and Operations Research* **40**(6), 1616–1624.

Yang, X. S., Karamanoglu, M. & He, X. (2013), 'Multi-objective flower algorithm for optimization', *Procedia Computer Science* **18**, 861–868.

Yao, C., Feng, K. & Hubacek, K. (2015), 'Driving forces of CO_2 emissions in the G20 countries: An index decomposition analysis from 1971 to 2010', *Ecological Informatics* **26**, 93–100.

Yasin, T. P. (1978), 'The analytical basis of automobile coastdown testing', *SAE Technical Paper* .

Ye, Z. Y. Z., Washko, F. W. F. & Lai, M.-C. L. M.-C. (2004), 'Genetic algorithm optimization of fuel economy for PFI engine with VVT-VCR', *Proceedings of the 2004 IEEE International Conference on Control Applications, 2004.* **1**, 364–369.

Yin, X., Wang, W., Chen, X. & Lu, H. (2013), 'Multi-Performance Optimization of the Shift Schedule for Stepped Automatic Transmissions', *SAE International* (2013-01-0488).

Yokota, T., Taguchi, T. & Gen, M. (1998), 'A solution method for optimal weight design problem of the gear using genetic algorithms', *Computers & industrial engineering* **35**(3), 523–526.

Zhou, A., Qu, B.-Y., Li, H., Zhao, S.-Z., Suganthan, P. N., Zhang, Q., H., Z., Shi-Zheng, Suganthan, P. N. & Zhang, Q. (2011), 'Multiobjective evolutionary algorithms: A survey of the state of the art', *Swarm and Evolutionary Computation* **1**(1), 32–49.

Appendix A

Vehicle, Engine & Transmissions specification

Table A.1: Engine: NLE 2.0L

$Power:$	$120KW@6500rpm$
$Torque(Nm)@\ Speed(rpm):$	200
$Torque(Nm)/Litre:$	100
$Engine\ Breathing:$	$Naturally\ aspirated$
$Displacement:$	1995
$Cylinders:$	4
$Compression\ ratio:$	$12.0:1\ TBC$

where the NLE 2.0L is a gasoline type, naturally aspirated, 4 cylinder engine.

Table A.2: Transmission model: DCT 360

$Installation:$	$Transverse$
$Number\ of\ gears:$	$6\ Forward$
$Number\ of\ shafts:$	3
$Max\ torque:$	$350\ Nm$
$Max.\ input\ speed:$	$6800\ mm^{-1}$
$Overall\ length:$	$340\ mm$
$Weight\ (wet):$	$\leq 85\ kg$
$Maximum\ efficiency:$	$\geq 93\ \%$

The DCT (see Table A.2) is designed by Gesellschaft für Industrieforschung (GIF) and manufactured by SAIC Gear Works (SAIC GW).

Table A.3: Vehicle : ROEWE 950 (BP32)

$Kerb\ weight(kg):$	1802
$Gross\ Weight(kg):$	2237
$Trailer\ Weight(kg):$	$N/A\ in\ China$
$CdA(m^2):$	0.318/0.334
$Front\ area(kg):$	2.378/2.384
$Wheel\ Size\ Min:$	$R17$
$Wheel\ Size\ Max:$	$R18$
$Wheel\ base:$	2837
$Width:$	1857

Appendix B

Initial calibration shift map

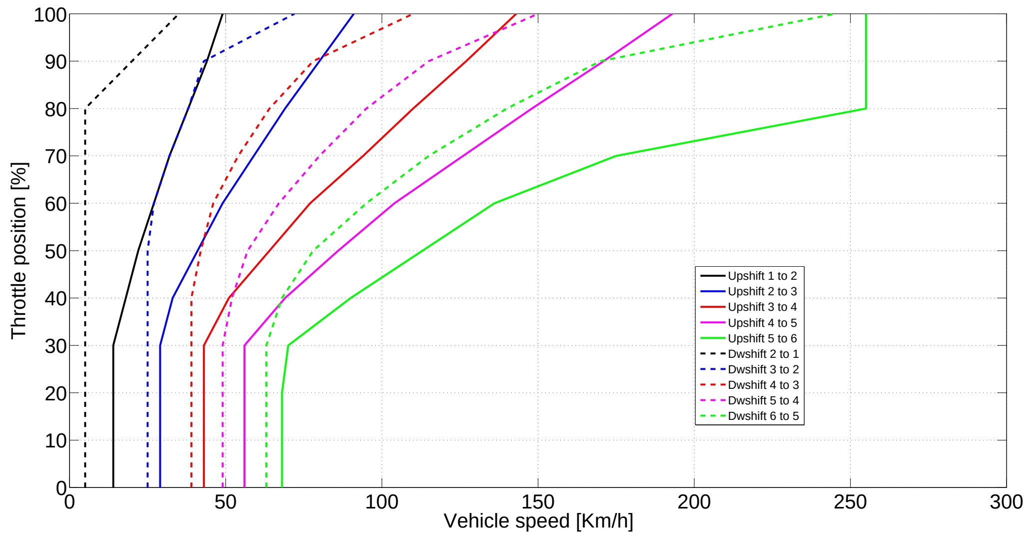

Figure B.1: This figure represents the initial calibration shift map of SAIC 6 speed DCT. The Upshift 1-2, Upshift 2-3, Upshift 3-4, Upshift 4-5 and Upshift 5-6 are represented by solid black, blue, red, magenta and green lines, respectively. The Downshift 2-1, Downshift 3-2, Downshift 4-3, Downshift 5-4 and Downshift 6-5 are described by dotted black, blue, red, magenta and green lines, respectively.

Table B.1: Numerical values (Km/h) of initial calibration Upshift (Up) map of SAIC 6 speed DCT

Throttle position %	$Up\ 1-2$	$Up\ 2-3$	$Up\ 3-4$	$Up\ 4-5$	$Up\ 5-6$
0	14	29	43	56	68
10	14	29	43	56	68
20	14	29	43	56	68
30	14	29	43	56	70
40	18	33	51	69	90
50	22	41	64	86	113
60	27	49	77	104	136
70	32	59	94	126	175
80	38	69	110	148	255
90	44	80	127	171	255
100	49	91	143	193	255

Table B.2: Numerical values (Km/h) of initial calibration Downshift (Dw) map of SAIC 6 speed DCT

Throttle position %	$Dw\ 1-2$	$Dw\ 2-3$	$Dw\ 3-4$	$Dw\ 4-5$	$Dw\ 5-6$
0	5	25	39	49	63
10	5	25	39	49	63
20	5	25	39	49	63
30	5	25	39	49	63
40	5	25	39	52	68
50	5	25	42	57	78
60	5	27	46	67	95
70	5	32	54	80	115
80	5	38	64	95	140
90	20	43	78	115	170
100	35	72	110	150	245

Appendix C

Coastdown test data

1.8m/s 100.11kpa 27.0度 65%RH		
轻载 Target coast down		
测试质量Weight	1753(CVW)+100kg	
轮胎气压	240kPa	
km/h	t (s)	d (m)
130	0	0
125	3.5	124.5
120	7.3	253.4
115	11.3	382.8
110	15.6	518.3
105	20.1	653.9
100	24.9	789.3
95	29.8	923
90	35.1	1057.9
85	40.3	1185.4
80	46	1315.8
75	52.1	1447.2
70	58.6	1577.8
65	65.6	1708.8
60	73.1	1838.5
55	81.4	1971.5
50	90.3	2101.1
45	100.1	2231.3
40	110.6	2355.7
35	121.9	2472.9
30	133.6	2578.6
25	146	2673.4
20	158.9	2754.3
15	172.4	2819.9
10	186.6	2869.5
5	201.1	2900.1

Figure C.1: Vehicle ROEWE 950 coast down data. These data represents vehicle speed, time and distance recorded during vehicle deceleration from 130 km/h to 5 km/h

Actual coast down	
km/h	Input data time (s)
130	0.0
125	3.5
120	7.4
115	11.3
110	15.7
105	20.1
100	25.0
95	29.9
90	35.4
85	40.9
80	47.1
75	53.4
70	60.4
65	67.4
60	75.5
55	83.5
50	92.7
45	101.8
40	112.3
35	122.8
30	134.8
25	146.8
20	160.6
15	174.3
10	190.1
5	205.8

Figure C.2: Actual coastdown test performed on chassis dynamometer of ROEWE 950 for gear shift map fuel and emissions assessment

Boundary		Tolerance(%)
Minimum	Maximum	5
t (s)	t (s)	10
0.00	0.00	
3.33	3.68	
6.94	7.67	
10.74	11.87	
14.82	16.38	
19.10	21.11	
23.66	26.15	
28.31	31.29	
33.35	36.86	
38.29	42.32	
43.70	48.30	
49.50	54.71	
55.67	61.53	
62.32	68.88	
69.45	76.76	
77.33	85.47	
85.79	94.82	
95.10	105.11	
105.07	116.13	
115.81	128.00	
126.92	140.28	
131.40	160.60	
143.01	174.79	
155.16	189.64	
167.94	205.26	
180.99	221.21	

The cost down data must be enter in the green cell. If any of the actual coast down data is outside the target within the boundary -/+ 5, the cell will turn into red, then the actual cost down need to be performed untill the value match the target within the boundary -/+5

	Do not modify
	Dyno results to be filled up

Figure C.3: The actual coastdown on the chassis dynamometer must within ± 5 second against the experimental data obtained from the proven ground

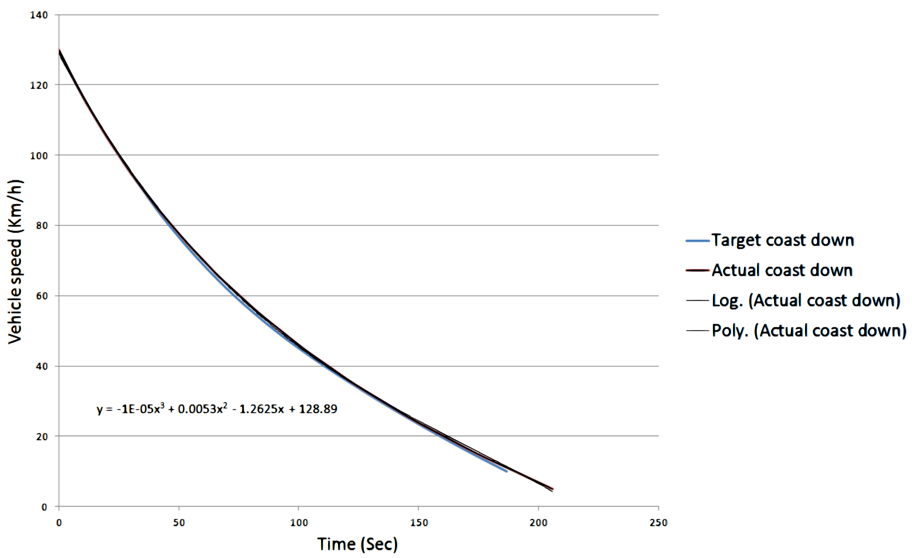

Figure C.4: Target coastdown plot test from chassis dynamometer against experimental test from proven ground

Appendix D

Performance tables of optimisers

D.1 Pareto with no repair and no GES

Table D.1: Most suitable solution upon Pareto optimal set, for each objective function based on set 1, with no repair and no GES

	J_{CO_2}	J_{Dist}	J_{z_1}	J_{IRP}	$J_{G_{ch}}$	J_{z_3}	$J_{G_j}\%$	J_{z_2}	J_{Obj}	S_{sprd}	$\overline{d}$	Std
M_{p1}	193.7	0.92	0.84	0.69	0.56	0.87	0.68	1.07	0.93	0.021	0.0043	0.022
M_{p2}	191.4	0.86	0.82	0.74	0.70	0.87	0.68	1.07	0.94	0.016	0.0031	0.017
M_{p3}	193.9	0.84	0.84	0.96	1.0	0.88	0.64	0.99	0.97	0.014	0.0038	0.015

Table D.2: Most suitable solution upon Pareto optimal set, for each objective function based on set 2, with no repair and no GES

	J_{CO_2}	J_{Dist}	J_{z_1}	J_{IRP}	$J_{G_{ch}}$	J_{z_3}	$J_{G_j}\%$	J_{z_2}	J_{Obj}	S_{sprd}	$\overline{d}$	Std
M_{p1}	191.3	0.89	0.82	0.74	0.70	0.87	0.57	1.06	0.98	0.016	0.0035	0.016
M_{p2}	195.5	0.80	0.85	0.79	0.83	0.88	0.64	0.98	0.98	0.022	0.0043	0.022
M_{p3}	190.9	0.87	0.83	0.95	1.0	0.87	0.64	0.96	0.98	0.017	0.0051	0.017

Table D.3: Most suitable solution upon Pareto optimal set, for each objective function based on set 3, with no repair and no GES

	J_{CO_2}	J_{Dist}	J_{z_1}	J_{IRP}	$J_{G_{ch}}$	J_{z_3}	$J_{G_j}\%$	J_{z_2}	J_{Obj}	S_{sprd}	$\overline{d}$	Std
M_{p1}	191.2	0.82	0.80	0.93	1.07	0.88	0.61	1.11	0.94	0.029	0.0067	0.029
M_{p2}	191.4	0.85	0.79	0.90	0.97	0.88	0.68	1.14	0.95	0.025	0.0065	0.026
M_{p3}	191.0	0.85	0.81	0.94	1.0	0.87	0.64	1.01	0.98	0.024	0.0073	0.025

D.2 Non-Pareto with no repair and no GES

Table D.4: Most suitable solution upon Non-Pareto for each objective function based on set 1

	J_{CO_2}	J_{Dist}	J_{z_1}	J_{IRP}	$J_{G_{ch}}$	J_{z_3}	$J_{G_j}\%$	J_{z_2}	J_{Obj}
M_{p6}	196.8	0.9196	0.8888	1.0365	1.0	1.0038	0.9789	1.048	0.977
M_{p7}	196.48	0.8471	0.8272	0.9833	1.1	0.8843	0.6809	1.96	0.944

Table D.5: Most suitable solution upon Non-Pareto for each objective function based on set 2

	J_{CO_2}	J_{Dist}	J_{z_1}	J_{IRP}	$J_{G_{ch}}$	J_{z_3}	$J_{G_j}\%$	J_{z_2}	J_{Obj}
M_{p6}	196.8	0.9215	0.8888	1.03	1.0	1.0038	0.9789	1.048	1.0
M_{p7}	196.1	0.9406	0.858	0.9974	1.23	0.8843	0.6436	1.89	0.9834

Table D.6: Most suitable solution upon Non-Pareto for each objective function based on set 3

	J_{CO_2}	J_{Dist}	J_{z_1}	J_{IRP}	$J_{G_{ch}}$	J_{z_3}	$J_{G_j}\%$	J_{z_2}	J_{Obj}
M_{p6}	196.8	0.9215	0.88	1.0365	1.0	1.0038	0.9789	1.048	1.0
M_{p7}	196.1	0.9429	0.8586	0.9978	1.23	0.8843	0.6433	1.893	0.9833

Table D.7: Most suitable solution upon Pareto optimal set, for each objective function based on set 1, with repair mechanism and no GES

	J_{CO_2}	J_{Dist}	J_{z_1}	J_{IRP}	$J_{G_{ch}}$	J_{z_3}	$J_{G_j}\%$	J_{z_2}	J_{Obj}	S_{sprd}	$\overline{d}$	Std
M_{p1}	192.5	0.88	0.82	0.69	0.57	0.87	0.60	1.09	0.92	0.012	0.0033	0.012
M_{p2}	193.5	0.86	0.82	0.74	0.70	0.87	0.68	1.07	0.94	0.021	0.0054	0.021
M_{p3}	194.4	0.85	0.84	0.97	1.00	0.87	0.64	0.94	0.96	0.021	0.0056	0.021

D.3 Pareto with repair mechanism and no GES

Table D.8: Most suitable solution upon Pareto optimal set, for each objective function based on set 2, with repair mechanism and no GES

	J_{CO_2}	J_{Dist}	J_{z_1}	J_{IRP}	$J_{G_{ch}}$	J_{z_3}	$J_{G_j}\%$	J_{z_2}	J_{Obj}	S_{sprd}	$\overline{d}$	Std
M_{p1}	191.4	0.89	0.84	0.75	0.7	0.87	0.52	1.09	0.97	0.022	0.0038	0.022
M_{p2}	191.8	0.91	0.84	0.89	0.97	0.87	0.60	1.06	0.97	0.015	0.0027	0.015
M_{p3}	191.9	0.88	0.84	0.95	1.1	0.87	0.57	1.06	0.97	0.019	0.0045	0.019

Table D.9: Most suitable solution upon Pareto optimal set, for each objective function based on set 3, with repair mechanism and no GES

	J_{CO_2}	J_{Dist}	J_{z_1}	J_{IRP}	$J_{G_{ch}}$	J_{z_3}	$J_{G_j}\%$	J_{z_2}	J_{Obj}	S_{sprd}	$\overline{d}$	Std
M_{p1}	191.2	0.79	0.82	0.81	0.73	0.99	0.68	1.05	0.93	0.025	0.0044	0.025
M_{p2}	192.1	0.80	0.82	0.79	0.83	0.87	0.65	1.09	0.94	0.024	0.0079	0.024
M_{p3}	193.4	0.86	0.83	0.95	1.0	0.87	0.57	1.02	0.97	0.028	0.01	0.029

Table D.10: Performance indicator application repair mechanism

	J_{CO_2} g/km	J_{IRP}
Average value with no repair mechanism	192.27	0.8502
Average value with repair mechanism	192.5 (-0.23)	0.840 (+0.010)

D.4 Non-Pareto with repair mechanism and no GES

Table D.11: Best solution upon Non-Pareto for each objective function based on set 1

	J_{CO_2}	J_{Dist}	J_{z_1}	J_{IRP}	$J_{G_{ch}}$	J_{z_3}	$J_{G_j}\%$	J_{z_2}	J_{Obj}
M_{p6}	196.8	0.9196	0.8888	1.0365	1.0	1.0038	0.9789	1.0483	0.97
M_{p7}	197.5	0.8486	0.8866	0.9758	1.1	0.8843	0.7138	1.83	0.95

Table D.12: Most suitable solution upon Non-Pareto for each objective function based on set 2

	J_{CO_2}	J_{Dist}	J_{z_1}	J_{IRP}	$J_{G_{ch}}$	J_{z_3}	$J_{G_j}\%$	J_{z_2}	J_{Obj}
M_{p6}	196.8	0.9215	0.8888	1.03	1.0	1.0038	0.978	1.048	1.0
M_{p7}	192.8	0.889	0.8586	1.06	1.36	0.8902	0.5720	1.81	0.975

Table D.13: Most suitable solution upon Non-Pareto for each objective function based on set 3

	J_{CO_2}	J_{Dist}	J_{z_1}	J_{IRP}	$J_{G_{ch}}$	J_{z_3}	$J_{G_j\%}$	J_{z_2}	J_{Obj}
M_{p6}	196.8	0.9215	0.8888	1.036	1.00	1.0038	0.978	1.048	1.00
M_{p7}	197.57	0.9705	0.8545	0.9361	1.1	0.875	0.6513	2.0332	0.9828

D.5 Pareto with no repair mechanism, with GES

Table D.14: Best solution upon Pareto optimal set, for each objective function based on set 1

	J_{CO_2}	J_{Dist}	J_{z_1}	J_{IRP}	$J_{G_{ch}}$	J_{z_3}	$J_{G_j\%}$	J_{z_2}	J_{Obj}	S_{sprd}	$\overline{d}$	Std
M_{p1}	193.3	0.56	0.79	0.74	0.7	0.87	0.72	1.03	0.92	0.011	0.0033	0.012
M_{p4}	191.6	0.58	0.76	0.74	0.7	0.87	0.61	1.04	0.91	0.0036	0.001	0.0037
M_{p2}	192.6	0.54	0.78	0.69	0.57	0.87	0.65	1.01	0.89	0.0097	0.003	0.0098
M_{p5}	192.6	0.54	0.80	0.80	0.83	0.88	0.72	0.97	0.89	0.016	0.003	0.016

Table D.15: Most suitable solution upon Pareto optimal set, for each objective function based on set 2

	J_{CO_2}	J_{Dist}	J_{z_1}	J_{IRP}	$J_{G_{ch}}$	J_{z_3}	$J_{G_j\%}$	J_{z_2}	J_{Obj}	S_{sprd}	$\overline{d}$	Std
M_{p1}	192.8	0.58	0.81	0.74	0.7	0.87	0.64	1.06	0.98	0.022	0.004	0.022
M_{p4}	190.7	0.59	0.78	0.92	0.97	0.88	0.56	1.05	0.97	0.016	0.003	0.016
M_{p2}	190.6	0.63	0.78	0.81	0.97	0.88	0.60	1.09	0.97	0.012	0.0027	0.012
M_{p5}	190.7	0.71	0.83	0.89	0.97	0.88	0.57	1.02	0.97	0.015	0.0024	0.015

Table D.16: Most suitable solution upon Pareto optimal set, for each objective function based on set 3

	J_{CO_2}	J_{Dist}	J_{z_1}	J_{IRP}	$J_{G_{ch}}$	J_{z_3}	$J_{G_j}\%$	J_{z_2}	J_{Obj}	S_{sprd}	$\overline{d}$	Std
M_{p1}	190.6	0.57	0.79	0.79	0.83	0.88	0.58	0.98	0.89	0.028	0.008	0.029
M_{p4}	191.8	0.61	0.75	0.82	0.97	0.88	0.54	1.89	0.89	0.019	0.0043	0.019
M_{p2}	190.7	0.54	0.76	0.89	0.97	0.88	0.58	1.02	0.89	0.023	0.0088	0.023
M_{p5}	190.6	0.54	0.78	0.87	0.97	0.89	0.58	1.03	0.88	0.025	0.007	0.026

Table D.17: Performance indicator application of GES

	$J_{CO_2}\ g/km$	J_{IRP}
Average value with no GES	192.2703	0.8502
Average value with GES	191.6 (-0.6703)	0.8117 (-0.0385)

D.6 Pareto with repair mechanism and GES

Table D.18: Most suitable solution upon Pareto optimal set, for each objective function based on set 1, with repair mechanism and GES

	J_{CO_2}	J_{Dist}	J_{z_1}	J_{IRP}	$J_{G_{ch}}$	J_{z_3}	$J_{G_j}\%$	J_{z_2}	J_{Obj}	S_{sprd}	$\overline{d}$	Std
M_{p1}	191.32	0.52	0.81	0.74	0.7	0.87	0.68	1.06	0.92	0.017	0.0046	0.017
M_{p2}	193.9	0.47	0.84	0.78	0.83	0.87	0.68	1.06	0.9	0.013	0.0027	0.013

Table D.19: Most suitable solution upon Pareto optimal set, for each objective function based on set 2, with repair mechanism and GES

	J_{CO_2}	J_{Dist}	J_{z_1}	J_{IRP}	$J_{G_{ch}}$	J_{z_3}	$J_{G_j}\%$	J_{z_2}	J_{Obj}	S_{sprd}	$\overline{d}$	Std
M_{p1}	190.9	0.65	0.84	0.85	0.87	0.87	0.58	1.05	0.97	0.01	0.003	0.01
M_{p2}	192.2	0.83	0.84	0.79	0.83	0.87	0.60	1.06	0.97	0.016	0.0026	0.016

Table D.20: Most suitable solution upon Pareto optimal set, for each objective function based on set 3, with repair mechanism and GES

	J_{CO_2}	J_{Dist}	J_{z_1}	J_{IRP}	$J_{G_{ch}}$	J_{z_3}	$J_{G_j}\%$	J_{z_2}	J_{Obj}	S_{sprd}	$\overline{d}$	Std
M_{p1}	190.9	0.47	0.78	0.78	0.83	0.87	0.58	1.06	0.88	0.024	0.01	0.025
M_{p2}	190.7	0.49	0.78	0.79	0.83	0.87	0.57	1.06	0.88	0.031	0.0098	0.03

Table D.21: Performance indicator application of GES

	$J_{CO_2}\ g/km$	J_{IRP}
Average value with no GES	192.2703	0.8502
Average value with GES	191.6052 (-0.6651)	0.8117 (-0.0385)

Appendix E

Leading solution for CO_2 emissions for Pareto and weighting sum

This appendix present the ideal shift map with the minimum CO_2 emissions and their corresponding objective functions.

E.1 Leading Pareto solution for set 1

Table E.1: Leading algorithm for minimum CO_2

	J_{CO_2}	J_{Dist}	J_{z_1}	J_{IRP}	$J_{G_{ch}}$	J_{z_3}	$J_{G_j\%}$	J_{z_2}	J_{Obj}
$M_{p1}(2)$	191.3	0.922	0.851	1.199	1.4	0.995	0.687	1.106	1.008

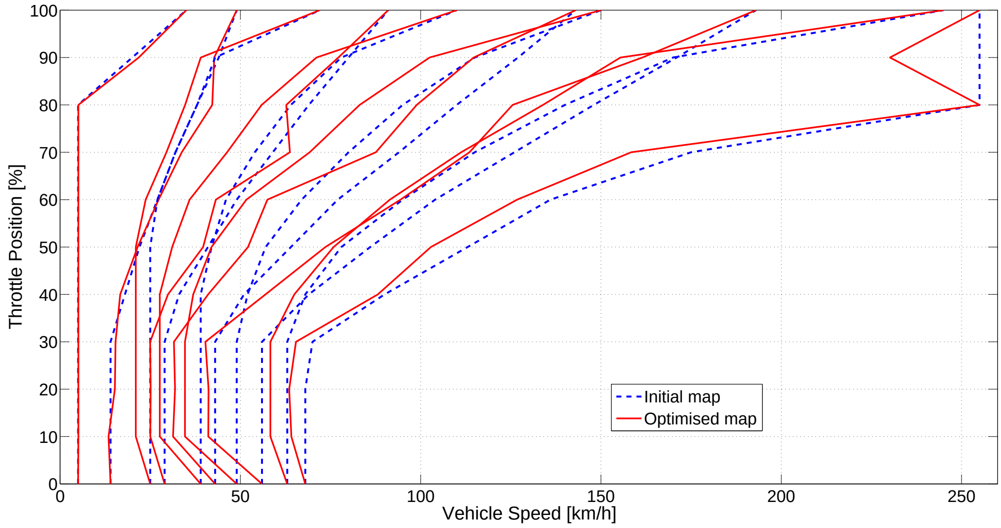

Figure E.1: Leading Pareto shift map for minimum CO_2 emissions under set 1 condition

E.2 Leading Pareto solution for set 2

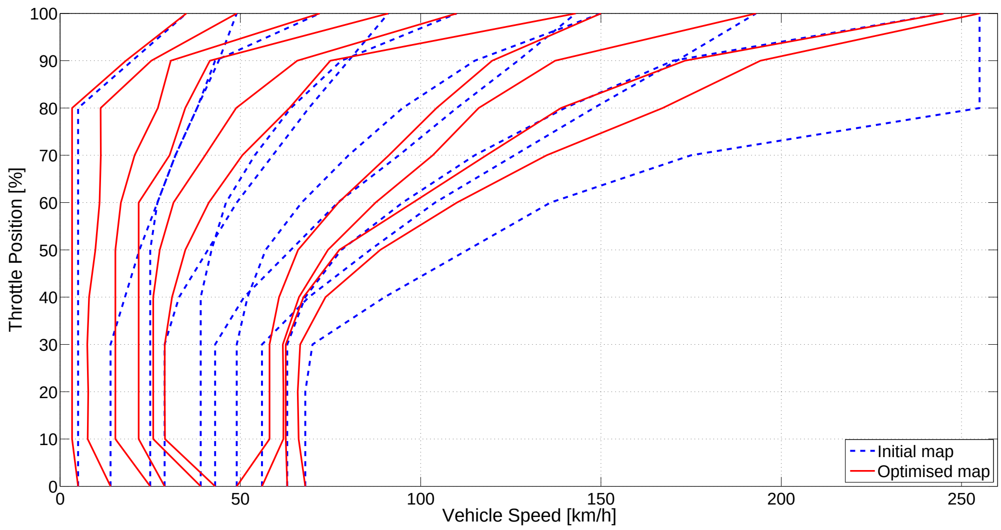

Figure E.2: Leading Pareto shift map for minimum CO_2 emissions under set 2 condition

Table E.2: Leading algorithm for minimum CO_2

	J_{CO_2}	J_{Dist}	J_{z1}	J_{IRP}	$J_{G_{ch}}$	J_{z3}	$J_{G_j\%}$	J_{z2}	J_{Obj}
$M_{p2}(1)$	190.6	0.633	0.779	1.198	1.267	0.995	0.72	1.095	0.986

E.3 Leading Pareto solution for set 3

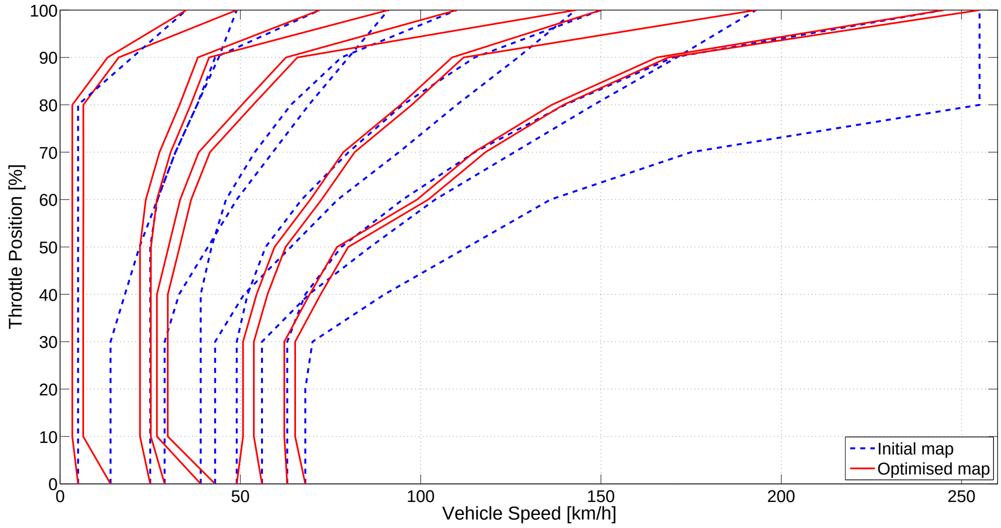

Figure E.3: Leading Pareto shift map for minimum CO_2 emissions under set 3 condition

Table E.3: Leading algorithm for minimum CO_2

	J_{CO_2}	J_{Dist}	J_{z1}	J_{IRP}	$J_{G_{ch}}$	J_{z3}	$J_{G_j\%}$	J_{z2}	J_{Obj}
$M_{p1}(1)$	190.7	0.575	0.799	1.198	1.267	1.025	0.713	1.044	0.899

E.4 Leading weighting sum solution for set 1

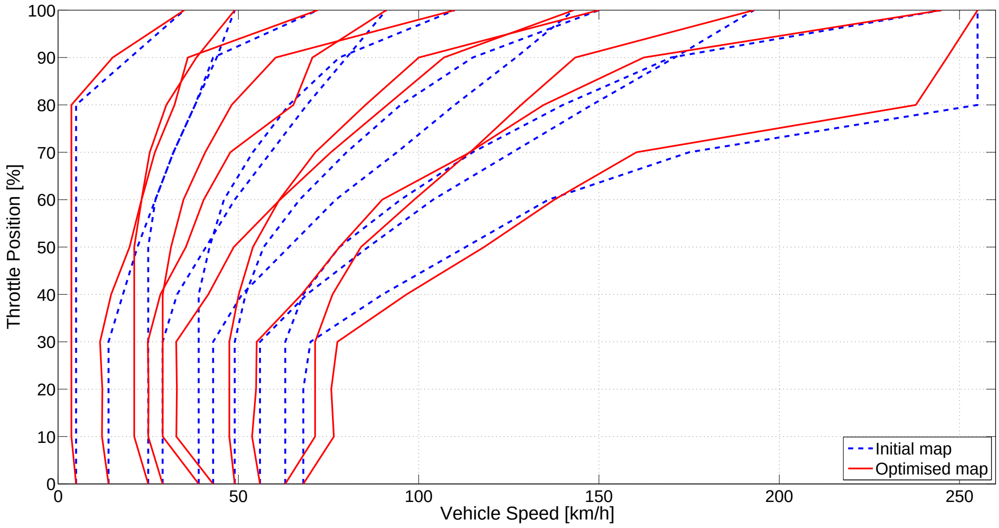

Figure E.4: Leading weighting sum shift map for minimum CO_2 emissions under set 1 condition

Table E.4: Leading algorithm for minimum CO_2

	J_{CO_2}	J_{Dist}	J_{z_1}	J_{IRP}	$J_{G_{ch}}$	J_{z_3}	$J_{G_j\%}$	J_{z_2}	J_{Obj}
$M_{p7}(5)$	196.5	0.847	0.827	0.983	1.1	0.884	0.681	1.969	0.944

E.5 Leading weighting sum solution for set 2

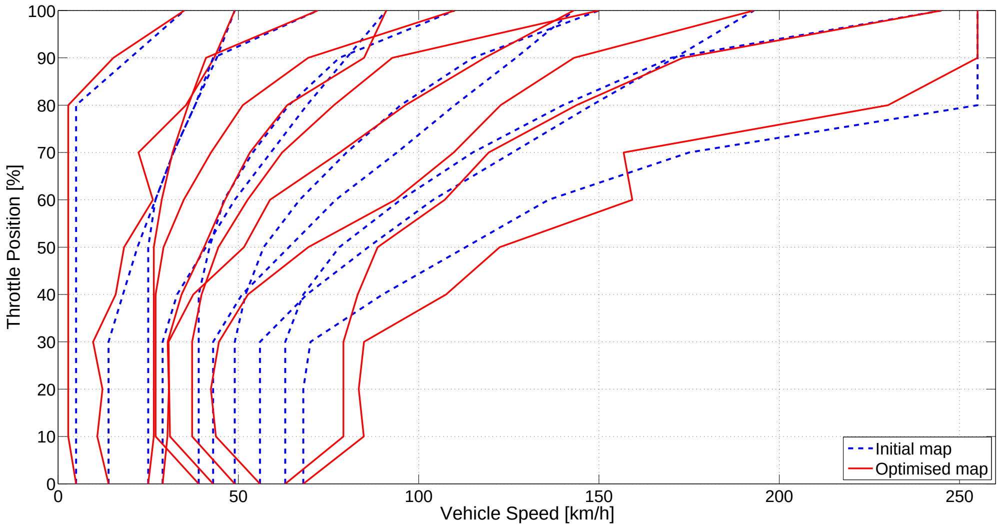

Figure E.5: Leading weighting sum shift map for minimum CO_2 emissions under set 2 condition

Table E.5: Leading algorithm for minimum CO_2

	J_{CO_2}	J_{Dist}	J_{z_1}	J_{IRP}	$J_{G_{ch}}$	J_{z_3}	$J_{G_j\%}$	J_{z_2}	J_{Obj}
$M_{p7}(3)$	192.8	0.889	0.859	1.064	1.367	0.89	0.572	1.815	0.976

E.6 Leading weighting sum solution for set 3

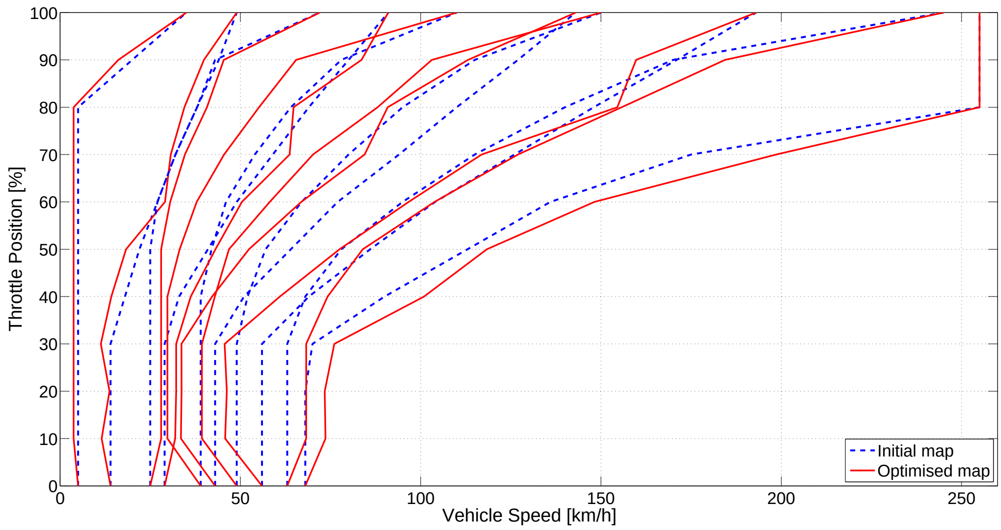

Figure E.6: Leading weighting sum shift map for minimum CO_2 emissions under set 3 condition

Table E.6: Leading algorithm for minimum CO_2

	J_{CO_2}	J_{Dist}	J_{z_1}	J_{IRP}	$J_{G_{ch}}$	J_{z_3}	$J_{G_j\%}$	J_{z_2}	J_{Obj}
$M_{p7}(4)$	196.02	0.943	0.859	0.997	1.23	0.884	0.643	1.89	0.983

Appendix F

Combined gear ratio & shift map optimisation results

F.1 Best combined gear ratio and gear shift map solution

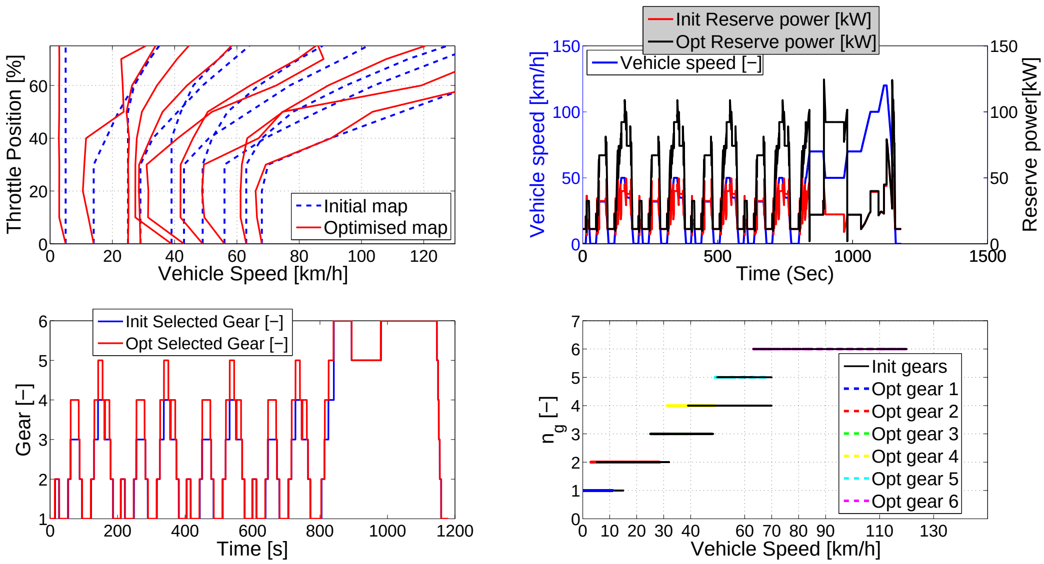

Figure F.1: Gear shift map, engine reserve power, gear selection and operating speed range for each gear ratio for $comb_{Set1}$

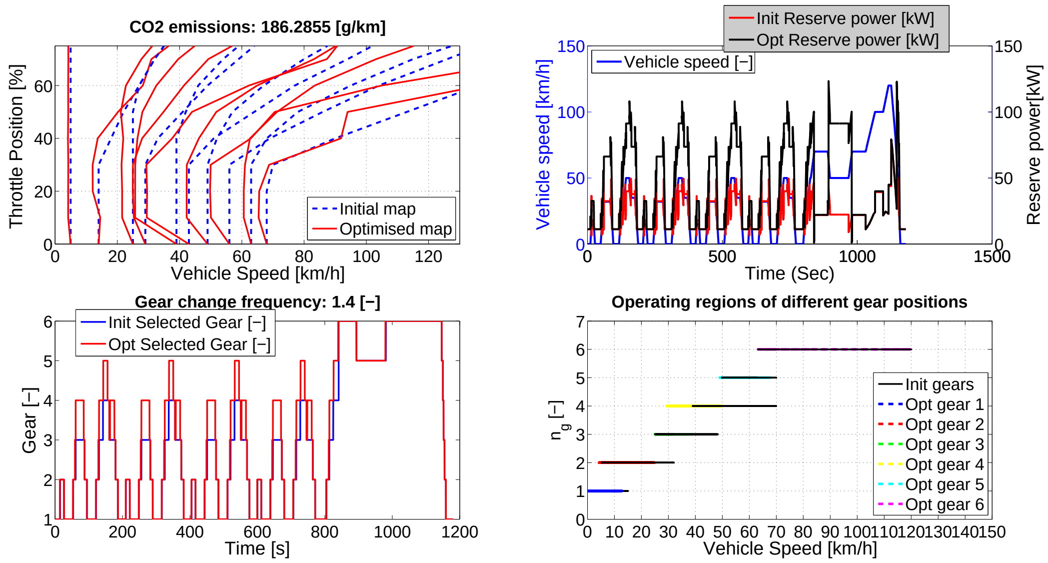

Figure F.2: Gear shift map, engine reserve power, gear selection and operating speed range for each gear ratio for $comb_{Set2}$

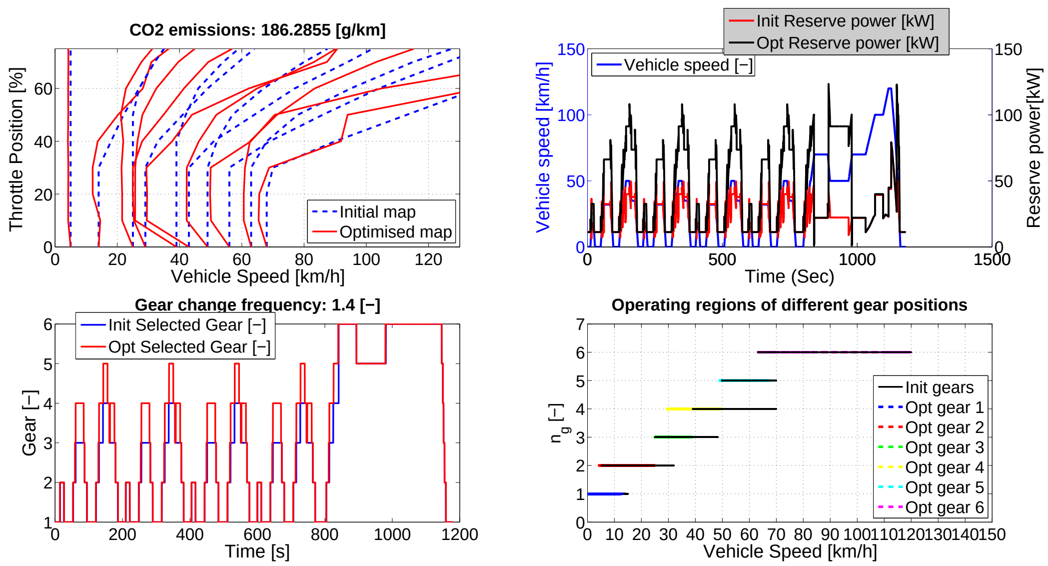

Figure F.3: Gear shift map, engine reserve power, gear selection and operating speed range for each gear ratio for $comb_{Set2}$

F.2 Average combined gear ratio and gear shift map solution

Table F.1: CO_2 emissions for $comb_{Set1}$, $comb_{Set2}$, $comb_{Set3}$ and $comb_{Set4}$ with their corresponding J_{dis}, J_{z_1}, J_{IRP}, $J_{G_{ch}}$, J_{z_3}, $J_{G_j}\%$, J_{z_2} and Obj_F

	J_{CO_2}	J_{dis}	J_{z1}	J_{IRP}	$J_{G_{ch}}$	J_{z3}	$J_{G_j}\%$	J_{z2}	Obj_F
$comb_{Set1}$	195.9	0.937	1.0	1.08	1.0	1.0	0.999	1.00	0.994
$comb_{Set2}$	194.2	0.918	0.78	1.17	1.03	1.0	0.673	1.67	0.986
$comb_{Set3}$	193.3	0.9	0.99	1.15	1.13	1.0	0.938	1.014	0.983
$comb_{Set4}$	193.1	0.94	0.993	1.16	1.13	1.0	0.943	1.011	0.982

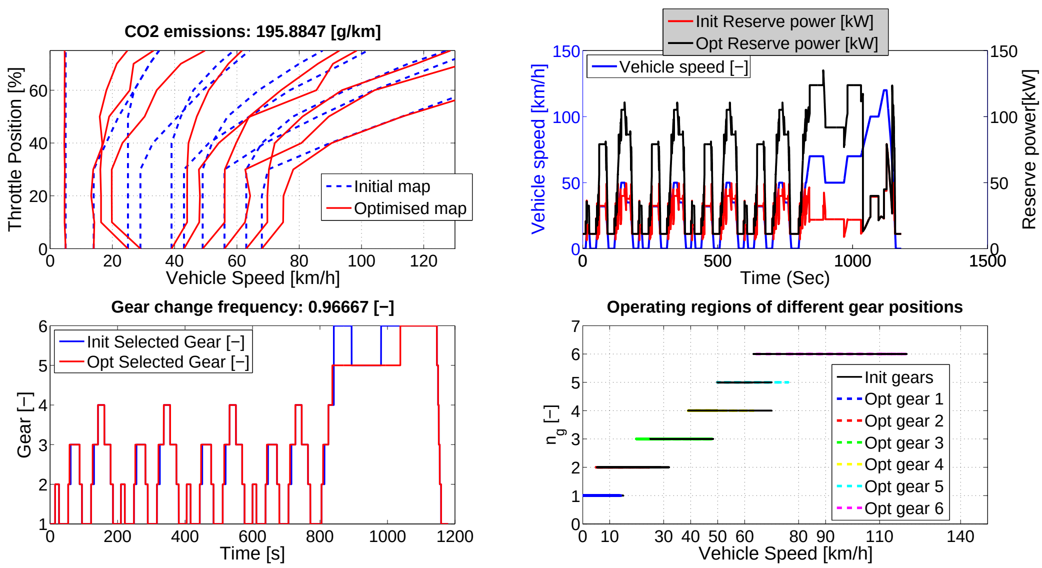

Figure F.4: Gear shift map, engine reserve power, gear selection and operating speed range for each gear ratio for $comb_{Set1}$, $comb_{Set2}$ and $comb_{Set3}$

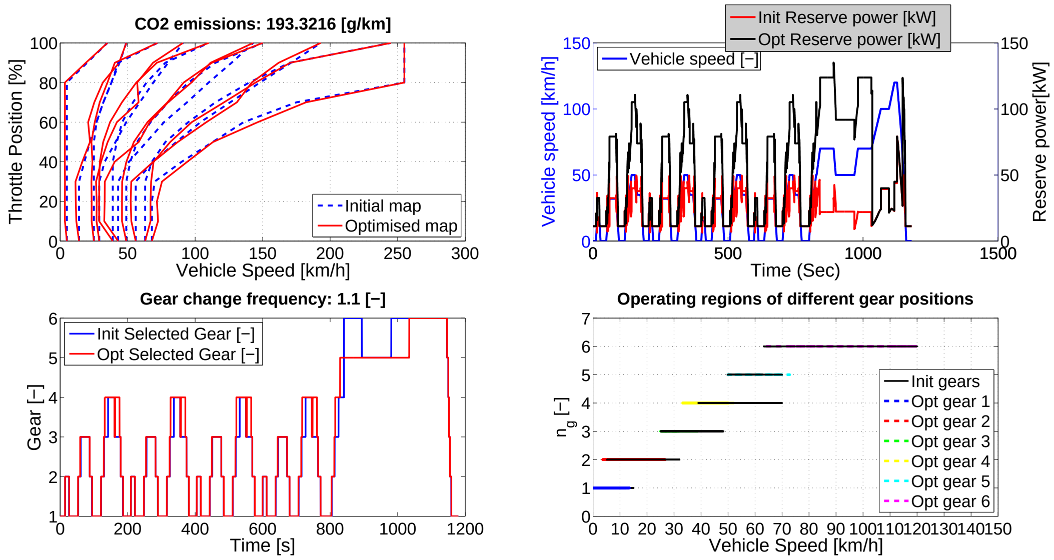

Figure F.5: Gear shift map, engine reserve power, gear selection and operating speed range for each gear ratio for $comb_{Set2}$

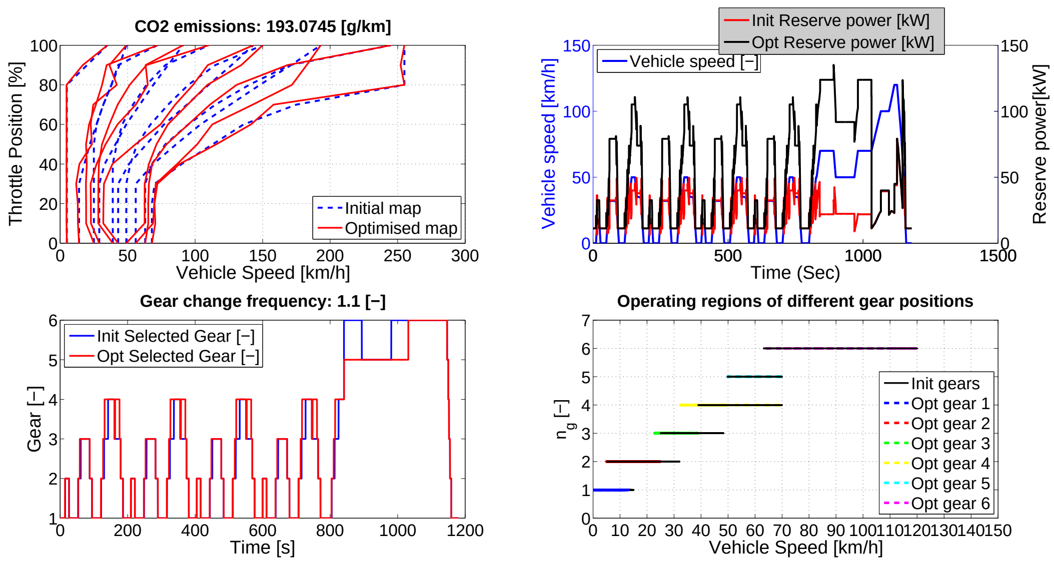

Figure F.6: Gear shift map, engine reserve power, gear selection and operating speed range for each gear ratio for $comb_{Set3}$

Appendix G

Rolling road test bag results

LIGHT DUTY VEHICLE ANALYSIS

06/05/2014	**13:35:37**						
Test......................	MVEG_A_GB18352	CHINA					
CELL ID.................	LightDutyEmission	Test Number..........	20140506_1301_N13SOV0	Vehicle No....................	LSJW36W2DS990582	Fuel...........	STD 92
Displacement (Liter).	2.0000	Model..................	EM140411G	SAIC No.......................	N13SOV014	Density.......	0.7564
Inertia (Kg)............	1902.0000	Transmission(M/A)..	Automatic	Engine No.....................		R-Factor......	0.6000
Request................	TR	Driver..................	QXW	Odo/Sys(KM)................	9005	HWF...........	13.0100
Fuel......................	Gasoline	Engine Family........	Engine Familiy (Gasoline/Di	Tire Pressure (Kpa).........	250.0000	OWF...........	0.0000
Idle (RPM).............	780	Vehicle Year..........	0.0000			CWF...........	88.9000
Operator................	YC	CVS venturi flow....	Phase 1: 0.0000			NHV...........	18491.1992
			Phase 2: 0.0000				

Remarks................	A	B	C
Road Parameter......	155.52	1.730	0.02247
Dyno Parameter......	27.56	1.37	0.02

**** Test Conditions ****

		Phase 1	Phase 2	AVE
Barometer	(Kpa)	101.8	101.8	101.8387
	(mmHg)	763.9	763.8	763.86
Dry bulb Temperatur	(degC)	24.3	24.3	24.25
Relative Humidity	(%)	39.9	41.5	
Specific Humidity	(gH2O/kg Air)	7.4512	7.5271	
Nox humidity correction factor		0.903	0.905	
V-MIX (0 degC)	(CU.ME)	130.6097	67.1885	
Distance	(KM)	3.982	6.914	
Dilution factor		30.3266	14.9986	

Figure G.1: Phase 1

**** Data ****

	EXHAUST SAMPLE	RANGE	BACKGROUND SAMPLE	RANGE	CORRECTED CONC.		*** MASS EMISSION *** (GMS)	(GMS/MI)	(GMS/KM)	Percent	
Phase 1											
HC-FID	25.12	20	2.38	20	22.81	(ppmC)	0.02	0.01	0.46	0.0	(L/100KM)
CO	51.20	2000	-0.36	2000	51.54	(ppm)	0.11	0.04	2.11	0.0	11.0160
Nox-CHME	1.81	10	0.00	10	1.81	(ppm)	0.01	0.00	0.11	0.0	
CO2	0.43	2	0.04	2	0.40	(%)	12.79	5.17	254.63		(KM/L)
CH4	3.81	6	1.81	6	2.06	(ppm)	0.00	0.00	0.05		9.0777
NMHC					20.51	(ppm)	0.02	0.01	0.42		
Phase 2											
HC-FID	3.39	20	2.22	20	1.31	(ppmC)	0.02	0.01	0.01	0.0	(L/100KM)
CO	21.39	50	-0.40	50	21.77	(ppm)	0.11	0.43	0.26	0.0	6.8014
Nox-CHME	0.17	10	0.00	10	0.17	(ppm)	0.11	0.00	0.00	0.2	
CO2	0.89	2	0.04	2	0.85	(%)	12.79	262.09	162.86		(KM/L)
CH4	2.44	6	1.81	6	0.75	(ppm)	0.00	0.01	0.00520		14.7028
NMHC					0.48	(ppm)	0.02	0.00	0.0029		

WEIGHTED	RESULTS	BEFORE ROUNDING	TEST REPORT DATA	EURO IV	Percent	EURO V	Percent
THC	GMS/KM	0.17433	0.17433	0.100	174.3	0.100	174.3
CO	GMS/KM	0.94029	0.94029	1.000	94.0	1.000	94.0
NOX	GMS/KM	0.04224	0.04224	0.080	52.8	0.060	70.4
CO2	GMS/KM	196.39571	196.39571				
THC+NOX	GMS/KM	0.02101	0.02101				
CH4	GMS/KM	0.02101	0.02101				
NMHC	GMS/KM	0.15407	0.15407				
F.E.	L/100KM	8.42602	8.42602				
	KM/L	11.86800	11.86800				

PARTICLE SAMPLING				
Phase 1		Empty		Loaded
Filter ID	1.1		1.2	
Phase 2		Empty		Loaded
Filter ID	2.1		2.2	

Figure G.2: Phase 2